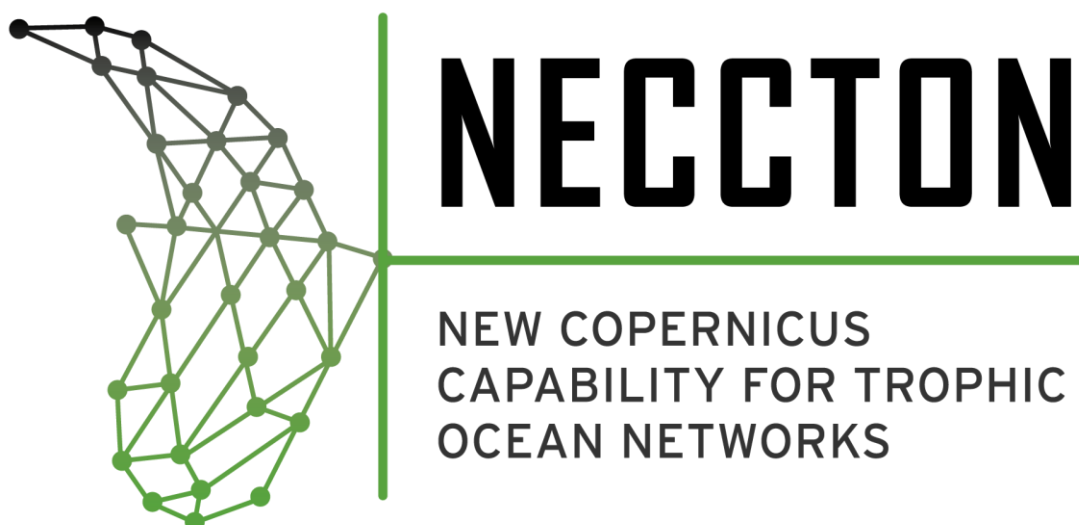


<b>Project</b>	NECCTON No 101081273	<b>Start / Duration</b>	2023-2026
<b>Dissemination</b>	Public	<b>Nature</b>	Report
<b>Date</b>	14/10/2025	<b>Version</b>	1.0



## Deliverable D7.2

### Report on all 16 model coupling developments

<b>Deliverable Contributors:</b>	<b>Name</b>	<b>Organisation</b>	<b>Role / Title</b>
Deliverable Leader	Ute Daewel	Hereon	WP7 Contributor
Contributing Author(s)	Verena Trenkel	Ifremer	WP7 Lead
	Vijith Vijayakumaran	Hereon	WP7 Contributor
	Patrick Lehodey	Mercator-O.	WP7 Contributor
	Martin Huret	Ifremer	WP7 Contributor
	Rebecca Millington	PML	WP7 Contributor
	Helen Powley	PML	WP7 Contributor
	Ken H Andersen	DTU	WP7 Contributor
	Jeroen Steenbeek	EII	WP7 Contributor
	Sergi Pérez-Jorge	IMAR	WP7 Contributor
	Morgane Travers-Trolet	Ifremer	WP7 Contributor
	Thanos Gkanasos	HCMR	WP7 Contributor
	Kostas Tsiaras	HCMR	WP7 Contributor
	Simone Libralato	OGS	WP7 Contributor
	Diego Panzeri	OGS	WP7 Contributor
	Maurizio Ingrosso	OGS	WP7 Contributor
	Sevrine Sailley	PML	WP7 Contributor



This project has received funding from Horizon Europe RIA under Grant Number 101081273

<b>Project</b>	NECCTON No 101081273	<b>Deliverable</b>	D7.2
<b>Dissemination</b>	Public	<b>Nature</b>	Report
<b>Date</b>	14/10/2025	<b>Version</b>	1.0

	Haolin Yu	UoL	WP7 Contributor
	Kenneth A. Rose	UoL	WP7 Contributor
	Marilaure Grégoire	UoL	WP7 Contributor
	Anja Lindenthal	BSH	WP7 Contributor
	Josefine Hahn	BSH	WP7 Contributor
	Laurene Merillet	CLS	WP7 Contributor
	Stefano Ciavatta	MOi	Project lead
Reviewer(s)	Karline Soetaert	NIOZ	Internal Review
	Jason Link	NOAA	External Review
Final review and approval	Stefano Ciavatta	MOi	Project lead

#### Document History:

Release	Date	Reason for Change	Status	Distribution
1.0	14/10/2025	Final version submitted to EC	Submitted	Public
0.1	31/08/2025	Draft submitted for review	In progress	Internal
0.0	31/07/2025	Initial document (table of content)	In progress	Internal

## Preface

This document is the deliverable D7.2 of the Task 7.2 of NECCTON. This includes description of higher trophic level (HTL) models, co-developed by work-package 7, and its coupling to lower trophic level (LTL) models as well as presenting results, validation and calibration of preliminary simulations.

**To cite this document:** Daewel et al (2025). NECCTON: Report on all 16 model coupling developments (D7.2). Zenodo. <https://doi.org/10.5281/zenodo.17193345>

<b>Project</b>	NECCTON No 101081273	<b>Deliverable</b>	D7.2
<b>Dissemination</b>	Public	<b>Nature</b>	Report
<b>Date</b>	14/10/2025	<b>Version</b>	1.0

## TABLE OF CONTENTS

Glossary .....	10
Publishable Summary .....	11
1. Introduction .....	12
1.1 Scope of document.....	12
1.2 Intended audience and reference to user needs .....	12
1.3 Structure of the document .....	12
2. General overview of Model Systems .....	12
2.1 HTL Models in NECCTON.....	12
2.2 Coupling of models of different trophic levels.....	14
3. Model description.....	17
3.1 FEISTY (Leading partner: DTU).....	17
3.2 ECOSPACE (Leading partner: OGS).....	22
3.3 EcoOcean (Leading partner: EII).....	36
3.4 ERSEM-MIZER (Leading partner: PML) .....	43
3.5 SEAPODYM-LMTL (Leading partner: CLS) .....	50
3.6 ECOSMO E2E (Leading partner: HEREON).....	56
3.7 Small Pelagic fish Model (Leading partner: HCMR).....	62
3.8 SS-DBEM (Leading partner: PML) .....	70
3.9 ESD-MED (Leading partner: OGS) .....	75
3.10 NAWH-cetaceans (Leading partner: IMAR) .....	87
3.11 FOIL-DEB (DEB-IBM for anchovy and sardine in the Bay of Biscay) (Leading partner: IFREMER).....	91
3.12 DEB-IBM European Anchovy BS (Leading partner: UoL).....	101
3.13 OSMOSE (Leading partner: IFREMER).....	114
3.14 SEAPODYM-tuna (Leading partner: MOi).....	119
3.15 SEAPODYM-anchovy (Leading partner: MOi) .....	128
3.16 SEAPODYM-Mackerel (Leading partner: CLS).....	134
4. Synthesis .....	150
5. Concluding remarks .....	156
6. References.....	157

<b>Project</b>	NECCTON No 101081273	<b>Deliverable</b>	D7.2
<b>Dissemination</b>	Public	<b>Nature</b>	Report
<b>Date</b>	14/10/2025	<b>Version</b>	1.0

## List of Tables

Table 1. List of HTL models developed in WP7 and LTL models of the CMEMS MFCs to which these models are coupled to. This table is taken from the NECCTON work description. ....	13
Table 2. Functional groups (FGs) represented in the model. Their short name is used in the graphs and in the following text. ....	26
Table 3. Fleets used to describe the fisheries in the model. The fleets result from a combination of gear and size category (based on the LOA) also considering importance for the area and available information on landings, capacity ad effort. ....	27
Table 4. The functional group structure of the EcoOcean model used in NECCTON simulations. ....	38
Table 5. Wet mass ranges for benthic and pelagic ERSEM prey which fish predate on. Fish predation on benthic prey has been added to MIZER as part of NECCTON. Equivalent spherical diameters are given where appropriate in brackets. ....	44
Table 6 Biomass of micronekton groups by biome and province (From Albernhe et al 2024) ....	52
Table 7 Estimates of local mesopelagic fish biomass from the literature and comparison with SEAPODYM-LMTL estimates (CMEMS QUID: LMTL product, 2024). ....	54
Table 8 Outputs from the SEAPODYM-LMTL model. ....	55
Table 9. Fish IBM model basic parameters ....	64
Table 10. Standard outputs of the SEAPODYM model applied to a given species and its fisheries. The ‘dym’ format is a native binary format that can be converted to NetCDF format with R or Python routines. ....	127
Table 11. Description of fisheries targeting anchovy in the Bay of Biscay used in SEAPODYM. PS= purse seine; OTM = midwater otter trawl; PTM = pelagic pair trawl. ....	130
Table 12: Description of fisheries targeting mackerels in the North-East Atlantic. ....	135
Table 13: Age and life stage parameters estimated from bibliography. ....	137
Table 14: Demographic parameters estimated from stock assessment data and previous SEAPODYM studies. ....	138
Table 15: Habitat parameters, estimated from RFID tag data, Eggs and Larvae ICES data, bibliography as well as previous SEAPODYM studies. ....	139
Table 16: Movement and migration parameters, estimated from RBIF data and taken from previous SEAPODYM studies. ....	140
Table 17: Estimated values of the parameters obtained after optimisation. ....	146
Table 18. Pros and cons of the NECCTON higher-trophic-level models ....	152

## List of Figures

Figure 1. List of HTL models described in this report, and their regions of application. ....	14
Figure 2. Sketch of the FEISTY framework. (a) Individual mass balanced allocation of energy of a fish. (b) Population mass balance of a fish functional type. (c) An example of a prey encounter between two functional types where a large fish (blue) eats a smaller prey (purple) when their vertical distributions overlap. (d) Schematic representation of trophic interactions between functional types emerging from the size and vertical interactions. The full model encompasses three resources: small	



<b>Project</b>	NECCTON No 101081273	<b>Deliverable</b>	D7.2
<b>Dissemination</b>	Public	<b>Nature</b>	Report
<b>Date</b>	14/10/2025	<b>Version</b>	1.0

and large mesozooplankton (sand color), a benthic resource (brown), and five functional types: small and large pelagics (pink and cyan), demersal fish (green), mesopelagic fish (purple), and midwater predators (blue). .....	18
Figure 3. Time-series of observed (solid) versus model-based (dashed) catches. Fish catch includes all fishes classified as large pelagic, forage fish (small pelagic) and demersal. Total catch includes all marine organisms including some that were not simulated. The shaded areas are based on the 95% confidence intervals of the catch-only model. From Denderen et al (2024).....	21
Figure 4. Ecospace administrative areas set for fishery allocations. Int=international waters; ter=territorial waters; ITA=Italy; BIH=Bosnia and Hercegovina; HRV=Croatia; MNT=Montenegro; SLO and SVN= Slovenia; 01=3 nautical miles; 02=4 nautical miles; 03=6 nautical miles; 04=up to the midline. ....	30
Figure 5. Ecospace relative predicted effort (for May/2011). ALB=Albania; BIH=Bosnia and Hercegovina; ITA=Italy; MNT=Montenegro. OTB= Bottom otter trawls; PTM= Pelagic pair trawls; PS=Purse seine; TBB= Beam trawls; DRB=dredges; GNX=set nets; LLX= long lines; MIX (seine, traps, small-scale fishery); VL=vessel length.....	31
Figure 6. Ecospace relative predicted effort (for August/2011). HRV=Croatia; SLO and SVN= Slovenia. OTB= Bottom otter trawls; PTM= Pelagic pair trawls; PS=Purse seine; TBB= Beam trawls; DRB=dredges; GNX=set nets; LLX= long lines; MIX (seine, traps, small-scale fishery); VL=vessel length. ....	32
Figure 7. Fitting tested. M01=model 1; PP=fitting by predator/prey setting; PR=fitting by predator setting; w01=relative biomasses weight=1; w20=relative biomasses of stock assessed groups weight=20; S=stepwise fitting; SM= stepwise fitting followed by manual fittings (2-3 number of manual search).....	35
Figure 8 1950-2100 EcoOcean simulation runs to test the impact of different climate scenarios. Panels show the relative temporal change of Total Consumers Biomass (%) by sub-regional oceans under different climate forcing for the period 1950-2100: (A) GFDL RCP2.6; (B) GFDL RCP8.5, (C) IPSL RCP2.6, and (D) IPSL RCP8.5. Figure reproduced with permission from Coll et al. (2020). ....	41
Figure 9 Example output of EcoOcean in the context of Atlantic Meridional Overturning Circulation (AMOC) weakening experiments. The panels reflect relative changes in biomass averaged over 2095-2099 compared to 2016-2020 in % for Total System Biomass (TSB) in the CTL (= no weaking) simulations (a, d), HOS (=weakening) simulations (b, e), and the difference between the two (c, f). (a-c) are for SSP1-2.6 and (d-f) are fore SSP5-8.5. Figure reproduced with permission from Boot et al. (2025). ....	42
Figure 10. Conceptual diagram illustrating two-way coupling between ERSEM and MIZER models... 43	
Figure 11. Impacts on different trophic levels when fish are two-way coupled. Lines show model output from offline FABM-MIZER and ERSEM (blue), original ERSEM-MIZER (yellow) and ERSEM-MIZER with new developments (green). The models were run with the water-column model GOTM, which provided the hydrodynamic forcing. Model runs used coordinates and meteorological inputs for the site Candyfloss, Celtic Sea. ....	47
Figure 12. Mesozooplankton at L4, south of Plymouth. Models were forced by the hydrodynamic water-column model GOTM. Points show observations from the Western Channel Observatory dataset (McEvoy et al. 2023). ....	48

<b>Project</b>	NECCON No 101081273	<b>Deliverable</b>	D7.2
<b>Dissemination</b>	Public	<b>Nature</b>	Report
<b>Date</b>	14/10/2025	<b>Version</b>	1.0

Figure 13. Suspension (top) and deposit feeders (bottom) at L4, south of Plymouth. Models were forced by the hydrodynamic water-column model GOTM. Observations are from the Western Channel Observatory dataset (McEvoy et al. 2023). Points show the mean and error bars the standard deviation of approximately five replicates from each sampling trip.....	48
Figure 14. Fish biomass from two-way coupled ERSEM-MIZER forced by the hydrodynamic model NEMO on the Northwest European shelf. Results are shown from the original model, with demersal fish included, and with demersal fish included minus the original. ....	49
Figure 15 . Map of reference biophysical biomes (by color) and associated provinces by ocean and hemisphere (numbering). Grey areas delineate the domain where the depth of the water column is not sufficient to ensure the existence of the three pelagic layers of SEAPODYM-LMTL. Redrawn from Alberne et al (2024). ....	52
Figure 16. Simplified schematic diagram of the ECOSMO E2E fish and macrobenthos modules, illustrating the energy flow (top) and required inputs for coupling with the LTL model host (bottom). ....	58
Figure 17. Pelagic and demersal fish biomass estimated from International Bottom Trawl survey ICES, 2012; <a href="http://www.ices.dk/Pages/default.aspx">http://www.ices.dk/Pages/default.aspx</a> , last accessed May 2012) and the simulated biomasses of water-column integral of planktivorous fish 1 and benthopiscivorous fish 2 during an annual cycle in the North Sea. (Daewel et al. (2019) sorted the IBT fish data into pelagic and demersal groups. A climatology of the variables from IBT survey for the North Sea is shown here. A 1D water-column integration of GOTM-ECOSMO-E2E for the central North Sea is used here. ....	60
Figure 18. Comparison between simulated distributions of Fish 1 (predominantly planktivorous) and Fish 2 (predominantly benthopiscivorous) with acoustic survey observations of Blue Whiting and Herring in the Norwegian Sea during May–June 2005 (Huse et al., 2015). The model includes a migration scheme for Fish 1. This Figure is adapted from Daewel et al. (2025, in preparation). The modelled fish biomass in the bottom row are given in $gC\ m^{-2}$ . The observed biomass (top row) is given in the Nautical Area Scattering Coefficient (NASC, $m^2\ nmi^{-2}$ ). It is the depth-integrated acoustic backscatter per square nautical mile.....	61
Figure 19. Time series of observed nutrient concentrations ( $\mu mol\ L^{-1}$ ) compared with three model simulations: (1) ECOSMO, which includes only lower trophic levels; (2) ECOSMO E2E, which adds macrobenthos and two fish groups; and (3) ECOSMO E2E with horizontal migration included for Fish 1. The time series is shown for a location in the Norwegian Sea ( $66^{\circ}N$ , $2^{\circ}E$ ).....	61
Figure 20. Average 2000-2020 surface (0-10m) mesozooplankton concentration ( $mgC/m^3$ ). ....	66
Figure 21. Average daily evolution ( $\pm SD$ ) of late larvae growth (mm), against field data. ....	67
Figure 22. Average mean weight (g) – at age against field data (red & blue circles $\pm SD$ ). ....	68
Figure 23. Simulated total Mediterranean anchovy (red line) and sardine (blue line) adults biomass (kt) evolution against biomass estimates from acoustic surveys (dotted lines) for the 2000-2019 period. ....	68
Figure 24. Adult biomass spatial distribution ( $tons/mi^2$ ) averaged over the 2000-2020 period.....	69
Figure 25. SS-DBEM projection for Atlantic horse mackerel ( <i>Trachurus trachurus</i> ) change in abundance under RCP 4.5 (top row) and RCP 8.5 (bottom row). The maps indicate the percentage change in fish biomass. The graphs represent the mean projected abundance (fish per model grid cell) Left column: Medium-term change in percentage: comparison of the 2040-2060 period to the	

<b>Project</b>	NECCTON No 101081273	<b>Deliverable</b>	D7.2
<b>Dissemination</b>	Public	<b>Nature</b>	Report
<b>Date</b>	14/10/2025	<b>Version</b>	1.0

2000-2020 period, no fishing pressure was applied. Middle column: Long-term change in percentage: comparison of the 2080-2100 period to the 2000-2020 period, no fishing pressure was applied. Right Column: mean abundance within the Northeast Atlantic with shaded area indicating the standard deviation within the Northeast Atlantic; MSY 0 (no fishing pressure in black line and grey shade).

Results using ERSEM forcing from past project. ....	73
Figure 26. Plot of the workflow for the ESD-MED .....	79
Figure 27. An example of a 10-fold spatial duplication of the training and test data set. ....	81
Figure 28. example of mean and standard deviation of four models and three different statistics (AIC, $r^2$ , RMSE) for the GAM model of the European hake. Less is better for AIC and RMSE and vice versa for $r^2$ . ....	81
Figure 29: example of the percentage contribution of each approach to the ensemble model for the six species involved. The X-axis shows the name of the model, the Y-axis the percentage contribution (in decimals, e.g. 0.3 = 30%, 0.25=25% etc.).....	82
Figure 30. Example from the GBM model of predicted and observed values for each species. ....	83
Figure 31. Map of spatial distribution of residuals (predicted – observed) for European hake and GBM model. ....	84
Figure 32. Distribution in kg/km <sup>2</sup> for each species for the ensemble model (averaged over the year 1999-2022) .....	85
Figure 33. Map of the distribution of hot spots (legend = G*, Getis ord Gi* index) for each species, derived from the ensemble model and averaged over the year 1999:2022. ....	86
Figure 34. Map of the distribution of number of individuals (legend = N/km <sup>2</sup> ) for European hake (left panel) and Anchovies (right panel), derived from the GLMM model and averaged over the year 1999:2022. Bottom row shows the difference in term of N/km <sup>2</sup> between adults and juveniles (adults – juveniles). ....	86
Figure 35. Schematic representation of the FOIL-DEB model, based on super individuals going through several modules and mortality sources (mechanistic processes are represented in blue), with the required inputs (environmental and observational forcing). ....	93
Figure 36. Model domain of the CROCO configuration to which FOIL-DEB-IBM) is coupled for the anchovy and sardine Bay of Biscay application. ....	98
Figure 37. Calibration of the DEB (left panel) and then the IBM (right panel) modules of the FOIL-DEB model. Anchovy as an example. Left panel: Result of the calibration of the DEB model on size-at-age data of the Bay of Biscay (orange), and validation on data from the gulf of Lion (Mediterranean Sea, red). Predicted growth in the English Channel is also shown (blue). Right panel: Result of the calibration of the IBM model in 0-D. Number of adult per age class (barplots) as well as total abundance (curves) are represented for both model and survey data.....	99
Figure 38. Snapshot of the model result for anchovy, with the location of super individuals (the left panel), and the corresponding biomass density as a NECCTON product (right panel). ....	99
Figure 39. Model structure. ....	104
Figure 40. DEB model calibration of total length for individuals born on June 1st, July 1st, August 1st, and September 1st across 10 regions in two time periods: A–D (1990–1995) and E–H (2012–2017). Black dots represent age-length observations from field surveys in the Turkish EEZ. Grey lines show von Bertalanffy growth curves based on references (1954–2018). ....	108

<b>Project</b>	NECCON No 101081273	<b>Deliverable</b>	D7.2
<b>Dissemination</b>	Public	<b>Nature</b>	Report
<b>Date</b>	14/10/2025	<b>Version</b>	1.0

Figure 41. DEB model calibration showing wet weight for individuals born on June 1st, July 1st, August 1st, and September 1st across 10 regions in two time periods: A–D (1990–1995) and E–H (2012–2017). Black dots represent age-weight estimates derived from field survey length data using a length–weight relationship in the Turkish EEZ. Grey lines show fitted weight curves based on length–weight conversions from von Bertalanffy growth functions in the literature (1954–2018). . 109

Figure 42. DEB model calibration results showing average fecundity by age class for individuals born on June 1st, July 1st, August 1st, and September 1st in two time periods: A–D (1990–1995) and E–H (2012–2017) in different regions. .... 110

Figure 43. Kinesis model calibration of endpoint locations at the final day of a one-year simulation for 1,000 individuals tracking temperature cues (A, C, E, G) and food cues (B, D, F, H) under four artificial scenarios. A-B, overlapping gradients of temperature and food; C-D, opposing gradients of the two cues; E-F, adjacent but non-overlapping optimal regions; G-H, opposite directions of optimal regions..... 111

Figure 44. Kinesis model calibration of movement trajectories for 10 randomly selected individuals tracking temperature cues (A, C, E, G) and food cues (B, D, F, H) under four artificial scenarios. Green triangles mark the starting points; black dots indicate the endpoints. A-B, overlapping gradients of temperature and food; C-D, opposing gradients of the two cues; E-F, adjacent but non-overlapping optimal regions; G-H, opposite directions of optimal regions..... 112

Figure 45. Location of the modelling domain, illustrated by the model cells in brown. The orange line represents the 200m isobath. Inset in the lower left corner: general location in Western Europe. . 117

Figure 46. Preliminary fit of the model for sardine (top) and anchovy (bottom), showing the interannual dynamics of species total biomass summed over the area in tons (left) and the average size at age over the period 2000–2022. OSMOSE is a stochastic model, so 30 replicates were run and summarized through boxplots. Red dots correspond to observations. .... 118

Figure 47. General scheme of SEAPODYM model structure..... 120

Figure 48. Functions used in the definition of spawning habitat and reproduction: (a) Beverton–Holt stock–recruitment function ( $N_b$  =numbers of individuals), (b)thermal function  $f_1$ , (c) prey function  $f_2$ , and(d) predator function  $f_3$ , based on parameters estimated for bigeye tuna (Redrawn from SEAPODYM User’s manual)..... 122

Figure 49. Left: Example of change (skipjack tuna) in thermal preferences function linked to species’ growth: the optimal temperature decreases with increased body size, while standard deviation increases with increased body weight. This effect integrated in the feeding habitat, determines the accessibility to the available biomass of prey. Right: Functional relationships used to determine the natural mortality with shaded area corresponding to the variability allowed locally in relation to the feeding habitat..... 123

Figure 50. Comparison of predicted distributions of tuna total biomass (tonnes  $\text{km}^{-2}$ ) for 1<sup>st</sup> and last decade of the historical time series. Warmer and cooler colours indicate high biomass and low biomass levels, respectively. Total observed catches are shown, with catch proportional to the size of the circles (same scales between decades). Redrawn from Lehodey et al. (in press). .... 125

Figure 51. Example of catch distribution of skipjack tuna in the Pacific Ocean proposed by the fishing tool and validation using only 3 super fisheries (South-East Asia; Western Central Pacific and Eastern Pacific) of the method by comparison with observed catch. .... 126

<b>Project</b>	NECCTON No 101081273	<b>Deliverable</b>	D7.2
<b>Dissemination</b>	Public	<b>Nature</b>	Report
<b>Date</b>	14/10/2025	<b>Version</b>	1.0

Figure 52. Distribution of annual averages of anchovy catch (2013-2018) by the three main fishing gears.....	131
Figure 53. Summary of the population structure for the Biscay anchovy as predicted by SEAPODYM .....	133
Figure 54. Predicted mean distribution of anchovy total biomass in the Bay of Biscay (left: t/km <sup>2</sup> ) and evolution of biomass over time with fishing (black) and in absence of fishing (grey). ....	133
Figure 55: Length at age (left) and weight at length (right) from ICES stock assessment reports. ....	137
Figure 56: Beverton Holt function (recruitment function of stock standing biomass) (left) and abundance at age (right) from stock assessment reports. ....	138
Figure 57: Temperature function of length (from RFID tag data) (left) and egg count function of temperature (right) from ICES Eggs and larvae database.....	139
Figure 58: Velocity at maximal habitat gradient function of body length, from RBIF data. ....	140
Figure 59: Catch and release positions used in the SEAPODYM-TAG optimisation. ....	142
Figure 60: Likelihood values of 10,000 independent configurations as a function of each SEAPODYM-TAG model parameter. Black dots represent arbitrary configurations. The green dot corresponds to the configuration with the lowest likelihood value among all points. Blue and orange dots represent the 50 best configurations, with the orange ones being those with a temperature below 12 degrees. ....	144
Figure 61: Likelihood values function of the parameters of the SEAPODYM-TAG model, conditioned by the value of the other parameters.....	145
Figure 62: Outputs from the SEAPODYM-TAG model.....	147
Figure 63: Observed catch (dotted red line) and predicted (black line) for each of the fisheries with length frequency data (used in the optimisation). ....	149
Figure 64: Observation and prediction from the SEAPODYM TAG model.....	149

<b>Project</b>	NECCON No 101081273	<b>Deliverable</b>	D7.2
<b>Dissemination</b>	Public	<b>Nature</b>	Report
<b>Date</b>	14/10/2025	<b>Version</b>	1.0

## Glossary

Acronym	Meaning
	<b>Physical Model</b>
GOTM	GOTM General Ocean Turbulence Model
HYCOM	Hybrid Coordinate Ocean Model
NEMO	Nucleus for European Modelling of the Ocean
	<b>Coupling Frameworks</b>
FABM	Framework for Aquatic Biogeochemical Models
<b>LTL</b>	<b>Lower Trophic Level models</b>
BAMHBI	Biogeochemical Model for Hypoxic and Benthic Influenced areas
BFM	Biogeochemical Flux Model
ECOSMO	ECOSystem Model
ERGOM	Ecological ReGional Ocean Model
ERSEM	European Regional Seas Ecosystem Model
PISCES	Pelagic Interactions Scheme for Carbon and Ecosystem Studies
SEAPODYM	Spatial Ecosystem and POpulation DYnamics Model
<b>HTL</b>	<b>Higher Trophic Level models</b>
DEB	Dynamic Energy Budget
E2E	End to End
Ecospace	Spatio-temporal ecosystem model of the Ecopath with Ecosim suite
ESD-MED	Ensemble Species Distribution Models - Mediterranean
FEISTY	FishErles Size and functional TYpe model
FOIL-DEB	Fish On-or-Offline IBM with Lagrangian and DEB modules
IBM	Individual Based Model
MIZER	Multi-species dynamic sIZE spectrum modelling in R
NAWH-cetaceans	
OSMOSE	Object-oriented Simulator of Marine EcOSystEms
SPF	Small Pelagic Fish model
SS-DBEM	Size Spectra - Dynamic Bioclimate Envelope Model
	<b>Miscellaneous</b>
AquaMaps	<a href="http://www.aquamaps.org">www.aquamaps.org</a>
FishMIP	Fisheries and Marine Ecosystem Model Intercomparison Project
ISIMIP	The Inter-Sectoral Impact Model Intercomparison Project
MSPACE	<a href="https://www.mccip.org.uk/all-uk/solutions/mspace">https://www.mccip.org.uk/all-uk/solutions/mspace</a>

<b>Project</b>	NECCTON No 101081273	<b>Deliverable</b>	D7.2
<b>Dissemination</b>	Public	<b>Nature</b>	Report
<b>Date</b>	14/10/2025	<b>Version</b>	1.0

## Publishable Summary

The overall objective of NECCTON is to enable the Copernicus Marine Service to deliver products that inform marine biodiversity conservation and food resources management, by fusing ocean ecosystem models and data. Marine higher trophic level products, including those related to marine fish, have, as of now, not been available in the Copernicus portfolio. The outcomes of the higher trophic level (HTL) model developments described in this report aligns with UN Sustainable Development Goal 14 (SDG Life below water: fishes and marine mammals) and support fish-stock assessments for the Common Fisheries Policy Regulation (CFP). This report synthesizes the model developments of HTL model capabilities as described in task 7.2. This includes description of HTL models, coupling to LTL models and presenting results from model evaluation.

In NECCTON, the HTL products are prepared for different Copernicus Marine Service regions by developing a range of models of different complexity and type. The models fall into three categories, marine ecosystem biomass models (FEISTY - Petrik et al 2019, Denderen et al 2021; Ecospace - Libralato and Solidoro 2009; EcoOcean - Coll et al. 2020; MIZER - Bruggeman 2021; E2E - Daewel et al. 2019; SPF - Gkanasos et al., 2021; SEAPODYM-LMTL – Lehodey et al. 2010; 2015), Species Distribution Models (SS-DBEM multi-species - Wilson et al. 2021; ESD-Med species - von Schuckmann et al. 2021; NAWH-cetaceans - Romagosa et al 2019), and Species Population Models (DEB-IBM small pelagics - Bueno-Pardo et al., 2020; Menu et al., 2023; OSMOSE - Morell et al. 2023; SEAPODYM – Lehodey et al 2008; Senina et al 2020). These models were selected to enable an ensemble approach for certain regions and gain insights into the suitability and readiness of various existing modelling approaches to provide operational HTL products for Copernicus Marine Service in the future.

The report shows that NECCTON has advanced the field of marine higher trophic level modelling by better integrating higher and lower trophic levels with improving fishing representations and better representation of spatial and temporal scales. Models now feature improved trophic coupling (including two-way links, consumption constrained to primary/secondary production, benthic–pelagic coupling), finer spatial resolution and movement/migration schemes, and seasonal to decadal variability. For some model spatially dynamic fishing is included, which is a prerequisite for related management scenarios. Functionally, coverage spans small pelagics, demersals, invertebrates, and marine mammals across regions, including the Mediterranean, Black Sea, Atlantic and Arctic Ocean, and Bay of Biscay, yielding outputs from biomass maps to decision-support tools. Together these advances deliver a more integrated, spatially explicit suite of models needed to deliver management relevant products for HTL in the context of Copernicus Marine Service.

<b>Project</b>	NECCTON No 101081273	<b>Deliverable</b>	D7.2
<b>Dissemination</b>	Public	<b>Nature</b>	Report
<b>Date</b>	14/10/2025	<b>Version</b>	1.0

# 1. Introduction

## 1.1 Scope of document

The objective of this document is to provide technical specifications for the 16 HTL models that are applied to provide the five HTL products that are planned to be delivered by NECCTON WP 7 (Trenkel et al. 2023). It will serve as a reference for internal and external users of the products and provide information on model structure, coupling between higher and lower trophic levels models, calibration procedures and exemplary validation of hindcast simulations. In addition, the document provides a guideline for users to contextualize the models and the respective products.

## 1.2 Intended audience and reference to user needs

This document is designed as a guide for the NECCTON partners as well as future users of the new products delivered by WP 7 of NECCTON. WP 7 is working closely with WP1 (Management), WP 2 (Stakeholders) and WP9 (Case studies) to ensure that the model design corresponds to user needs.

## 1.3 Structure of the document

The document is structured as follows. Section 2 provides an overview of the HTL models developed by WP 7 and a general overview of the coupling strategies used for linking HTL and LTL models and products. Section 3 provides a thorough description of each model, including: i) Technical specification of HTL models; ii) Technical details of HTL-LTL coupling, iii) Results from preliminary hindcast simulations for regional applications, iv) Validation of model simulations, v) discussion of model strengths and weaknesses. Section 4 summarizes the models and describes the link to the data products in NECCTON. A summary of possible challenges and expected impacts is given in Section 5.

# 2. General overview of Model Systems

## 2.1 HTL Models in NECCTON

Incorporating HTL (high trophic level) components into operational modelling systems presents a new set of challenges. These components are not only more difficult to model due to their high mobility and variability, they are also linked to more complex stakeholder needs and questions. On the one hand, there is strong demand for species-specific biomass and distribution data, driven by both economic and conservation interests—though not all species attract the same level of attention. On the other hand, HTL components often act as a “missing link” in marine ecosystem models. They represent important transfer processes that feed back into the modelling of LTL (low trophic level) components and inorganic state variables. The latter challenge requires a different type of models that describes fish production on a more concise level e.g. as functional groups or size classes. To cover the diverse requirements for HTL modelling products, in NECCTON, the HTL products are prepared and tested for different Copernicus Marine Service regions using a range of models of different complexity and type. The models fall into three categories, marine ecosystem biomass models (FEISTY



<b>Project</b>	NECCTON No 101081273	<b>Deliverable</b>	D7.2
<b>Dissemination</b>	Public	<b>Nature</b>	Report
<b>Date</b>	14/10/2025	<b>Version</b>	1.0

- Petrik et al 2019, Denderen et al. 2021; Ecospace - Libralato and Solidoro 2009; EcoOcean - Coll et al. 2020; MIZER - Bruggeman 2021; E2E - Daewel et al. 2019; SPF - Gkanasos et al., 2021; SEAPODYM-LMTL – Lehodey et al. 2010; 2015), Species Distribution Models (SS-DBEM multi-species - Wilson et al. 2021; ESD-Med species - von Schuckmann et al. 2021; NAWH-cetaceans - Romagosa et al 2019), and Species Population Models (DEB-IBM small pelagics - Gatti et al., 2017; Bueno-Pardo et al., 2020; Menu et al., 2023; OSMOSE - Shin & Curry 2001; Travers et al., 2009, Morell et al. 2023; SEAPODYM – Lehodey et al 2008; Senina et al 2020). These particular models were selected to enable an ensemble approach for certain regions and gain insights into the suitability and readiness of various existing models to provide operational HTL products in the future.

Table 1. List of HTL models developed in WP7 and LTL models of the CMEMS MFCs to which these models are coupled to. This table is taken from the NECCTON work description.

<b>Group of HTL models</b>	<b>Description of the broad group of models (No., name and reference of the model)</b>	<b>CMEMS domain coupled LTL model</b>	<b>Lead partner</b>
Ecosystem biomass models (EcoBM)	End-to-End systems including key HTL functional groups. One-way bottom-up coupling with LTL models (no movement).		
	1. FEISTY (Petrik et al., 2019; Denderen et al., 2021, Zhao et al 2025)	NWS-ERSEM, IBI-PISCES, BAL-ERGOM, MED-BFM, GLO-PISCES	DTU
	2. Ecospace (EwE) (Libralato & Solidoro, 2009)	MED-Adriatic-BFM	OGS
	3. EcoOcean (Coll et al., 2020)	GLO-PISCES	EII
	Idem above, but two-way coupling with LTL models		
	4. MIZER (Bruggeman et al., 2021)	NWS-ERSEM	PML
	5. SEAPODYM-LMTL (Lehodey et al., 2015)	GLO-PISCES	CLS
	6. E2E (Daewel et al., 2019)	ARC-ECOSMO, BAL-ERGOM	HEREON
Species Distribution models (SpDM)	7. SPF small pelagic fishes (Gkanasos et al., 2021)	MED-ERSEM	HCMR
	Target species distribution based on statistical approach correlating either catch or absence/presence information with an ensemble of environmental variables. Abundance can be derived from bottom-up processes (e.g. size-spectrum)		
	8. SS-DBEM multi-species (Wilson et al., 2021)	GLO-PISCES, NWS-ERSEM	PML
	9. ESD- Med species (Panzeri et al., 2021)	MED	OGS
	10. NAWH-cetaceans (Pérez-Jorge et al., 2020; Romagosa et al., 2019)	GLO/Atl.-PISCES-LMTL	IMAR

<b>Project</b>	NECCON No 101081273	<b>Deliverable</b>	D7.2
<b>Dissemination</b>	Public	<b>Nature</b>	Report
<b>Date</b>	14/10/2025	<b>Version</b>	1.0

Species Population models (SpPM)	Mechanistic approach of one or several target species populations with full Lagrangian movement: One-way coupling (Bottom-up)		
	11. FOIL-DEB (DEB-IBM small pelagics (Gatti et al., 2017; Bueno Pardo et al., 2020))	NWS/Bay of Biscay-ERSEM	IFREMER
	12. DEB-IBM small pelagic (Pethybridge et al., 2013; Gatti et al., 2017)	Black Sea: NEMO-BAMHBI	UoL
	13. OSMOSE small pelagics (Shin & Curry 2001; Travers et al., 2009)	NWS/Bay of Biscay-ERSEM	IFREMER
	Mechanistic approach of several target species populations with Eulerian movement		
	14. SEAPODYM-Tuna (Senina et al., 2020)	GLO-PISCES	MOi
	15. SEAPODYM-Anchovy (Hernandez et al., 2014)	IBI-PISCES	MOi
	16. SEAPODYM-Mackerel (Dragon et al., 2018)	GLO/ N. Atl.-PISCES	CLS

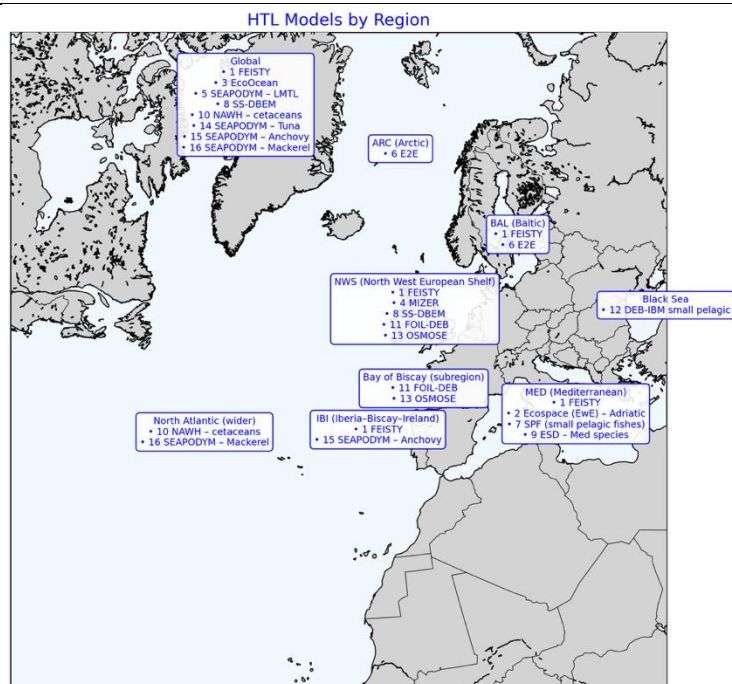


Figure 1. List of HTL models described in this report, and their regions of application.

## 2.2 Coupling of models of different trophic levels

To numerically simulate fish in marine ecosystems, knowledge on the environmental conditions is required, since body growth, metabolic rates, reproduction and migration depends on abiotic variables such as temperature, salinity and oxygen, and biotic variables. Therefore, all HTL models are directly coupled or depending on physical-biogeochemical (LTL) models, which provide spatially and temporally explicit fields of abiotic and biotic state variables. While in Species Distribution models (SpDM) those variables provide the basis to predict indices of habitat and spawning suitability, in mechanistic modelling approaches like Ecosystem biomass models (EcoBM) and Species Population

<b>Project</b>	NECCON No 101081273	<b>Deliverable</b>	D7.2
<b>Dissemination</b>	Public	<b>Nature</b>	Report
<b>Date</b>	14/10/2025	<b>Version</b>	1.0

models (SpPM) the variables modulate physiological rates and are the basis of biomass fluxes. Depending on the modelling approach, the coupling can either be realized one-way, where the physical and biotic LTL state variables are used as forcing for the HTL model, or two-way, where the HTL model components feed-back to the LTL model. The latter leads to modifications in the LTL model components through predation and nutrient re-cycling. Ideally, the coupling to the LTL model should be two-way, which enforces a mass balance between the food consumed by the fish and the mortality losses on the lower trophic levels. However, due to the specific structure of some modelling approaches (e.g. SpDM) and the complexity of two-way coupling, most models utilize a one-way coupling strategy. In all presented cases, the abiotic variables are one-way coupled, as there is no feedback considered from both HTL and LTL model components. For the biotic variables, there are three types of couplings: one-way coupling, production-constrained one-way coupling, and two-way coupling.

### **One-way coupling (“forcing”)**

*Definition:* One-way or unidirectional model coupling refers to “loosely” coupled system where LTL model output, such as phytoplankton and zooplankton biomass, are used to force the HTL model components. As no feedback to the LTL model are considered, the LTL model is independent of the status of the HTL model. In the HTL model, the forcing can be utilized in two different ways.

- i) In mechanistically formulated models (SpPM or EcoBM types), LTL model outputs are integrated in the model formulation and form the basis for estimating fish physiological rates, such as body growth (e.g. plankton biomass as prey fields) or survival (e.g. oxygen). Another coupling method is to define a forcing dependent functional response and relative index, which is then used to constrain certain population mechanisms. Typically, a spawning habitat index can constrain the recruitment of the fish population or a feeding habitat index its spatial distribution;
- ii) In statistically formulated model approaches (SpDM) the forcing is used to define a functional relationship between population indicators like species abundance or spawning habitats and the environmental conditions, which provides spatially and temporally explicit information about the species’ distribution.

There are several advantages of one-way coupling. i) It is easier to code and to parameterize, as complex feedback loops are not considered. The latter also implies that the LTL model does not need to be recalibrated as its dynamics are independent. ii) It typically comes with lower computational costs and runtimes, as the same forcing field can be used offline and for several HTL simulations. iii) Easier coupling between unrelated codes. Not only is tight synchronization between the two codes unnecessary, but this approach also enables coupling across different programming languages and frameworks.

The one-way coupling has an obvious disadvantage, which is probably more relevant in ecosystems with a tight LTL and HTL process coupling and with clear top-down response mechanisms in the food web. The one-way coupling ignores feed-back mechanisms and hence is typically prone to violate basic physical laws, such as energy and mass conservation. This is less problematic for HTL models that include only one species or a subsample of the fish community, but becomes more relevant when the

<b>Project</b>	NECCON No 101081273	<b>Deliverable</b>	D7.2
<b>Dissemination</b>	Public	<b>Nature</b>	Report
<b>Date</b>	14/10/2025	<b>Version</b>	1.0

HTL model component aims at simulating the whole fish community and hence the entire ecosystem mass flow.

### **Production-constrained one-way coupling**

To correct for the violation in mass-conservation, a “production-constrained one-way” coupling can be applied. The simple one-way coupling has the disadvantage that fish may consume more plankton than is lost to mortality in the LTL model. In that case the fish model may therefore create new biomass, i.e. biomass that is not supported by LTL production. The creation of new biomass can be avoided by also passing on the production of plankton (biomass concentration per time) from the LTL in addition to the concentration of plankton. The plankton production would typically be the loss terms that form the closure of the plankton model, either linear or quadratic, i.e.,  $mZ$  or  $mZ^2$ . For this to work, the HTL model must limit fish consumption to not exceed the production of plankton. This procedure does not ensure strict mass balancing (it does not deal with the excretion products, for example), however it ensures that HTL production does not exceed the LTL production.

### **Two-way coupling**

We refer to two-way or bidirectional coupling when the dynamics of the LTL and HTL model components are executed in a tightly synchronized manner, exchanging information/fluxes of matter between both models in run-time. It allows propagation of effects from the LTL model to the HTL and vice versa including effects of predation mortality, egestion, and excretion. While this deals with the mass conservation problem related to the one-way coupling, a few things need to be kept in mind. i) While this is a recommended approach when simulating the whole community, two-way coupling of single species models requires additional consideration of feedback from the remaining fish community. ii) Two-way coupling can (and should) be formulated such that all masses are accounted for, including loss products from the HTL model (egestion and excretion). iii) Since the complex coupling requires a larger set of parameters for the coupling processes, finding the right parameter value sets is a challenge and might require additional model calibration for the LTL model components, e.g. zooplankton predation mortality (see below).

### **Adaptations required when coupling models**

When coupling LTL and HTL models, several model specific adjustments are taken into account. This relates to unit conversion between the different models, averaging, integration and transformation of the transferred state variables (LTL) to meet the needs of the receiving model (HTL), adjustments of specific parameters in the LTL model in case of two-way coupling (e.g. natural zooplankton mortality). Model specific adaptations are explained in the respective section of each model below.

<b>Project</b>	NECCTON No 101081273	<b>Deliverable</b>	D7.2
<b>Dissemination</b>	Public	<b>Nature</b>	Report
<b>Date</b>	14/10/2025	<b>Version</b>	1.0

## 3. Model description

### 3.1 FEISTY (Leading partner: DTU)

#### 3.1.1 Model description

FEISTY (FishErles Size and functional TYpe model) models the entire fish community, both pelagic and demersal, and also includes a simple model of benthic organisms. The FEISTY model is designed to be mechanistic, simple and fast, generally applicable globally, and compatible with biogeochemical model principles. It is based on ordinary differential equations and careful accounting of mass balancing with a production-constrained one-way coupling to the LTL models. FEISTY does not resolve specific fish species but structures the fish community around a few functional types (aka. functional groups or guilds) based on traits of asymptotic size and feeding strategy in the vertical water column (pelagic, demersal, or mesopelagic). This simplification, together with the mechanistic basis, allows for projections into novel environments, e.g., climate change projections.

FEISTY has previously been developed for use in a global environment (Petrik et al. 2019; van Denderen et al. 2021). Within NECCTON it has been implemented as an efficient Fortran library with an R front-end (Zhao et al. 2025). Further, we have derived global fisheries exploitation rates and validated the model (Van Denderen et al. 2024). To be able to couple FEISTY to time-varying forcing from the LTL models, we have also implemented a time-varying input forcing option. Within NECCTON we are testing the hypothesis that we can also model fish communities on a regional scale *without changing model parameters between regions*. The only parameters changed between different couplings to LTL models are the two ecological efficiency parameters that are used to couple the zooplankton and benthic productions to each LTL model.

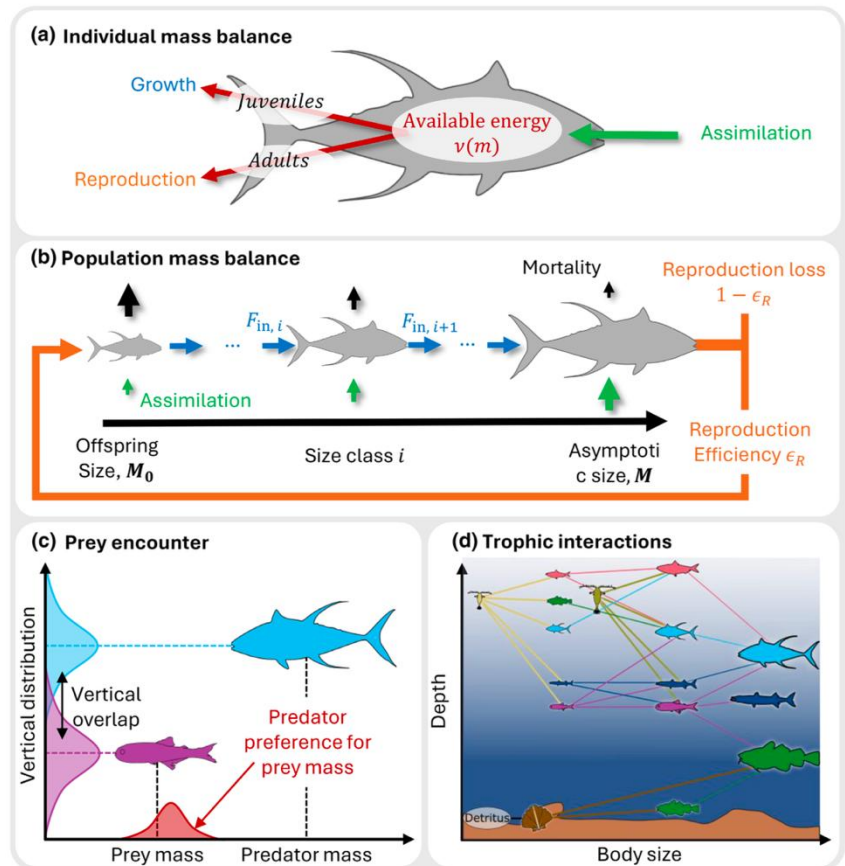
##### 3.1.1.1 Model Formulations: State Variables, Equations, Parameters

The biological basis of FEISTY is described in the publication Zhao et al (2024), with a concise description of all equations and parameters in the vignette for the R-package. Here we will therefore mainly describe the developments that go beyond this description: the time-varying input and the coupling to the LTL models.

First, we provide a brief overview of FEISTY (this is a verbatim copy of the “methods section” in Zhao et al, 2025). For full details, including equations and parameters, please access the vignettes in R after installing the package: `browseVignettes("FEISTY")`.

Project	NECCTON No 101081273	Deliverable	D7.2
Dissemination	Public	Nature	Report
Date	14/10/2025	Version	1.0

Figure 2. Sketch of the FEISTY framework. (a) Individual mass balanced allocation of energy of a fish. (b) Population mass balance of a fish functional type. (c) An example of a prey encounter between two functional types where a large fish (blue) eats a smaller prey (purple) when their vertical distributions overlap. (d) Schematic representation of trophic interactions between functional types emerging from the size and vertical interactions. The full model encompasses three resources: small and large mesozooplankton (sand color), a benthic resource (brown), and five functional types: small and large pelagics (pink and cyan), demersal fish (green), mesopelagic fish (purple), and midwater predators (blue).



FEISTY is similar to other size-based fish models by representing the processes of competition and predator-prey interactions that emerge from larger fish feeding on smaller fish sharing the same habitat. In contrast to most fish food web models, it abstains from representing specific species in favour of grouping species into functional types, i.e., small and large pelagic fish, demersal fish, mesopelagic fish, and midwater predators. The description removes the requirement of having a species-specific representation of density dependence between spawning biomass and recruitment, the traditional “stock-recruitment” relationship used in fisheries science, which was a hindrance to properly representing the influence of the secondary production on the fish community. Ecological processes, e.g., resource competition and mortality, that affect the larval and juvenile stages are here explicitly represented instead of imposing an external carrying capacity on each functional type.

All processes in FEISTY are described at the level of an individual fish that is defined by its body size (mass)  $m$  and is affected by temperature. The core is a mechanistic description of the individual's energy budget (Figure 2 a above). Prey are consumed based on encounter rates, consumed food is assimilated and respired, and the remaining available energy  $v(m)$  is divided between growth and reproduction according to the maturity of the fish.

Individual-level processes are scaled to the population level of each functional type. A functional type is characterized chiefly by its maximum (asymptotic) mass  $M$  and its vertical feeding habitat (Figure 2 b and c).

<b>Project</b>	NECCON No 101081273	<b>Deliverable</b>	D7.2
<b>Dissemination</b>	Public	<b>Nature</b>	Report
<b>Date</b>	14/10/2025	<b>Version</b>	1.0

Fish are spawned at their offspring size (1 mg) and use their available energy to grow through each size class  $i$ . Somatic growth leads to a flux of biomass between size classes  $J(i)$ . Mature fish allocate energy to reproduction and that defines the flux of new offspring that is routed back to the smallest size (Figure 2 b).

The main governing equation is a discretization of the McKendric-von Foerster equation for mass balanced growth. The equation describes the change of biomass in a size class due to the flux between neighbouring size classes and the accumulation and loss of biomass due to somatic growth, reproduction, and mortality:

$$\frac{dB_i}{dt} = J_i - J_{i+1} + (v_i - \rho_i - \mu_i)B_i,$$

with  $B_i$  being the biomass (units of biomass per area) in the  $i$ th size class,  $J_i$  and  $J_{i+1}$  are the fluxes of biomass in and out of the size class  $i$  (units of biomass per area per time),  $\rho_i$  is the biomass-specific reproduction rate (units of per time), and  $\mu_i$  is the biomass-specific mortality rate (units of per time).  $v_i$  represents the biomass-specific energy acquired from predation on the resources or fish (units of per time) after accounting for basal metabolism, which is used for increasing the biomass and for reproduction  $\rho_i$  in the adult size classes.

Fish interact with other size-classes through predation following the principle that big fish eat smaller fish in a shared habitat, such that the feeding preference (dimensionless) between a predator size class  $i$  and a prey size class  $j$  (including mesozooplankton and benthic resource) is:

$$\theta_{i,j} = \theta_{\text{size},i,j} \theta_{\text{vertical},i,j},$$

where,  $\theta_{\text{size}}$  represents the size-based feeding preference and  $\theta_{\text{vertical}}$  represents the vertical (depth) overlap between the predator and prey (Figure 2 c).

Predation fuels growth and reproduction of the predator while also imposing predation mortality on the prey. These feeding interactions, together with the bioenergetic model, define fluxes in and out of size class  $i$ , the available energy for growth, the reproduction rate, and mortality.

### Benthos

Due to the limited access to benthos biomass in the NECCON LTL models, the benthos community is modelled as logistic growth according to time-varying production and limited by a carrying capacity  $K$ :

$$\frac{dR}{dt} = r(t) \left(1 - \frac{R}{K}\right) R - \sum \mu_{R,i} R,$$

where  $r(t)$  is the benthos production given as the detritus flux towards the seabed and  $\mu_{R,i}$  is the mortality by fish eating on the benthos.

#### 3.1.1.2 Model structure and required forcings and inputs; Implementation details

FEISTY is coded in Fortran 90 with an R frontend. It is available as an R package from the github page: <https://github.com/Kenhasteandersen/FEISTY>.

<b>Project</b>	NECCOTON No 101081273	<b>Deliverable</b>	D7.2
<b>Dissemination</b>	Public	<b>Nature</b>	Report
<b>Date</b>	14/10/2025	<b>Version</b>	1.0

### 3.1.1.3 Model specifics to HTL-LTL coupling

FEISTY uses the “production-constrained one-way coupling”. This means that FEISTY is run offline from the LTL model. The forcing required is: the sea floor depth, the temperatures at the surface, at mesopelagic depth, and at the seafloor, the zooplankton concentration, the zooplankton production (mass per time per area), and the detritus flux to the sea floor.

To avoid the creation of new mass in the model, the consumption by the fish predators must not exceed the corresponding zooplankton production ( $P_{R,j}$ , in mass/area/time). If the total consumption by all fish, as calculated by the product of predation mortality on zooplankton and zooplankton biomass ( $\sum_j \mu_{R,j} R_j$ , in mass/area/time) exceeds the zooplankton production, the consumption must be down-regulated.

When consumption of one food item (here the zooplankton resource) is decreased the predator could compensate by eating more of other prey. For simplicity, however, we assume that only the resource consumption is decreased, and the consumption of other prey is not increased to compensate. To follow this assumption, we introduce a down-regulation factor  $f_{dr,j}$ , and henceforth several variable changes. The total consumption of all predators of the resource prey  $j$  is equal to the predation mortality loss of that prey. The predation mortality is updated to:

$$\mu_{p,j} = f_{dr,j} \sum_i \frac{V_i \theta_{i,j}}{E_i + C_{max,i}} C_{max,i} B_i,$$

where  $E_i$  is the total encountered food and  $j$  denotes indices of prey including all resource and fish.  $C_{max,i}$  is the maximum consumption rate of the predator  $i$ . The down-regulation factor  $f_{dr,j}$  is defined as the ratio of the resource production and resource predation loss:

$$f_{dr,j} = \begin{cases} \max \left\{ 1, \frac{P_{R,j}}{\mu_{p,j} R_j} \right\} & \text{where } j \text{ is the resource requiring down regulation} \\ 1 & \text{for other prey} \end{cases}$$

For the other prey whose predation loss do not need down-regulation, the factor is 1 to keep everything unchanged.

The predation loss of a resource prey reflects the consumption of its predators, which requires corresponding updates to maintain mass conservation within the system. We begin by revising the feeding levels of predators. The mass-specific feeding level of a predator  $f_i$  is modified to:

$$f_i = \frac{V_i}{E_i + C_{max,i}} \sum_j f_{dr,j} \theta_{i,j} B_j.$$

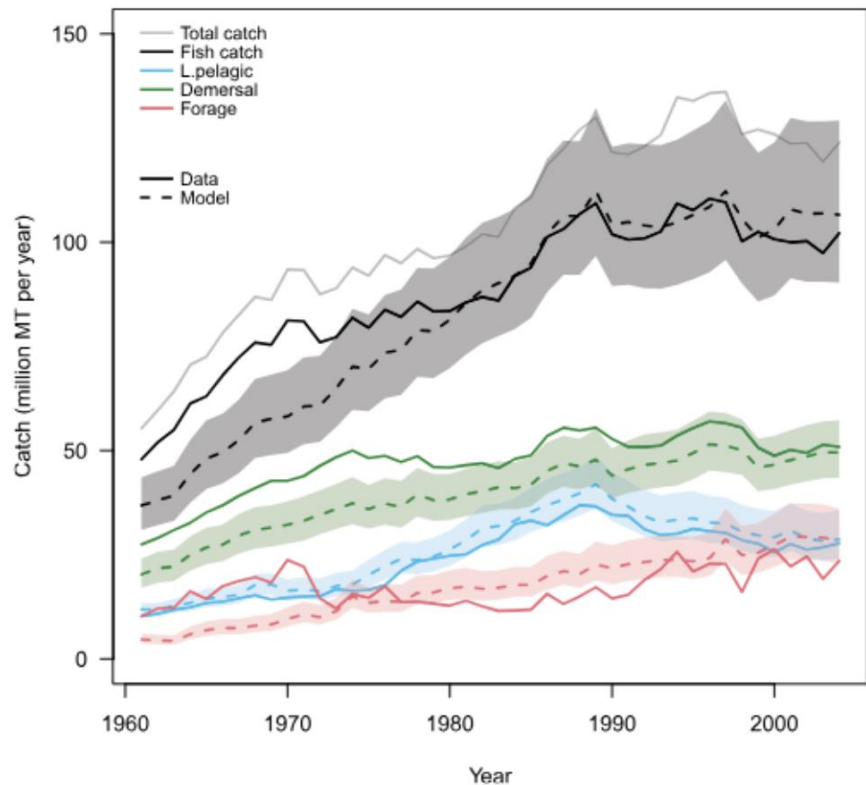
This procedure ensures that new mass is not created in the system. However, it does not ensure perfect mass balance. If the fish predators do not eat all the zooplankton production, there is an “excess” zooplankton production which is not accounted for. Further, as mentioned above, the fish are not allowed to compensate for the reduction in zooplankton consumption by an increase in consumption of other prey. We believe that this latter assumption has a quite small impact.



<b>Project</b>	NECCTON No 101081273	<b>Deliverable</b>	D7.2
<b>Dissemination</b>	Public	<b>Nature</b>	Report
<b>Date</b>	14/10/2025	<b>Version</b>	1.0

### 3.1.2 Validation of global simulation

Figure 3. Time-series of observed (solid) versus model-based (dashed) catches. Fish catch includes all fishes classified as large pelagic, forage fish (small pelagic) and demersal. Total catch includes all marine organisms including some that were not simulated. The shaded areas are based on the 95% confidence intervals of the catch-only model. From Denderen et al (2024).



Hindcast simulations of FEISTY require estimates of the fisheries exploitation rates. In NECCTON we have collated a global data set of fisheries exploitation rates based on observed catches (Denderen et al, 2024). As an independent validation we ran the simple version of FEISTY with just 3 functional groups (small and large pelagic fish, and large demersal fish) and calculated global catches (Figure 3 above). The agreement is remarkably good.

#### 3.1.3 NECCTON Products from the model

FEISTY will produce outputs of total biomass of small and large pelagic fish, demersal fish, and total fish biomass in the units of g wet weight per area. The resolution will be monthly. It will be run on the North-West Atlantic shelf, the Iberia-Biscay-Ireland area, the Baltic Sea, the Mediterranean Sea, and globally.

#### 3.1.4 Discussion of pros and cons of the model

FEISTY is designed to be a light-weight model which can simulate global fish communities with minimal calibration of the LTL model:

##### *Pros of FEISTY:*

- It runs fast (100s of years in seconds for a grid point).
- The Fortran base facilitates a 2-way coupling with FABM. This is, however, not realized in NECCTON but is an obvious potential
- The R frontend makes it easy to use for ecologists
- It simulates the entire fish community

<b>Project</b>	NECCON No 101081273	<b>Deliverable</b>	D7.2
<b>Dissemination</b>	Public	<b>Nature</b>	Report
<b>Date</b>	14/10/2025	<b>Version</b>	1.0

- It is designed with mass balancing in mind. The production-constrained one-way coupling ensures that the fisheries production is limited by the LTL production: no mass is “created” by FEISTY.
- The use of a globally valid parameterization makes it easy to apply to any regional simulation or climate change scenario simulation

The design choices of FEISTY entail some trade-offs:

#### *Cons of FEISTY:*

- The use of functional groups means that FEISTY cannot simulate specific species. For example, it does not provide predictions of cod in the North Sea, but only the total group of large demersal species. This limits the use of FEISTY for species-specific fisheries management.
- FEISTY does not resolve horizontal movement or migrations of fish
- The current offline production-limited coupling means that FEISTY does not provide mortality, detritus, or dissolved organic matter to the LTL model.
- The use of the same set of parameters for all region limits the precision for any specific region.

## **3.2 ECOSPACE (Leading partner: OGS)**

### **3.2.1 Model description**

#### *3.2.1.1 Introduction and biological basis*

Ecospace is an end-to-end food web modeling tool which benefits from the inclusion of spatial or spatial-temporal components. The Ecospace routine, as part of the Ecopath with Ecosim (EwE) suite, inherits settings, parameters, and data from Ecosim (which in turn has inherited some parameter values from Ecopath), and requires defining of additional parameters that explain how the food web and fisheries utilize space (de Mutsert et al., 2024). The EwE suite is reportedly used for analyses of marine ecosystems and trophodynamic and spatial simulations, and has been used globally to quantitatively describe aquatic systems and the ecosystem impacts of fishing and other human activities, such as underwater noise, pollutants and wind farms (Christensen and Pauly, 1993; Colléter et al., 2015; Link and Marshak, 2022). Finally, Ecospace can therefore provide comprehensive assessments of ecosystem productivity, cumulative environmental and human impacts, and multi-sector trade-offs that arise through food-web interactions in scenarios of multiple human activities (Dolan et al., 2016; Holsman et al., 2017).

#### *3.2.1.2 Model Formulations: State Variables, Equations, Parameters*

In NECCON, the EwE modelling approach (Christensen et al. 2008) was applied to the Adriatic Sea. In EwE, food webs are described by means of compartments representing species, an ontogenetic phase of a species or groups of species with ecological significance, thereafter called Functional Groups (FGs). FGs can be defined in different ways also depending on the aim of the model. Initial conditions are used to implement a mass balance approach using the Ecopath routine. Then, changes of FGs biomasses (state variables) in time and time-space are estimated with Ecosim and Ecospace, respectively. Those routines are driven by temporally varying ecosystem drivers that can represent

<b>Project</b>	NECCON No 101081273	<b>Deliverable</b>	D7.2
<b>Dissemination</b>	Public	<b>Nature</b>	Report
<b>Date</b>	14/10/2025	<b>Version</b>	1.0

fishing activities and environmental changes such as primary production and water temperature, or other drivers.

The ecosystem model describes the temporal change of state variables based on the assumptions commonly made in the EwE suite (Christensen et al., 2008). The present model application to the Adriatic Sea adopts 73 state variables (in wet weigh,  $t \cdot km^{-2}$ ) of 66 consumers (Eq. 1), 4 primary producers (Eq. 2) and 3 non-living compartments (Eq. 3) that include fishery discards (in  $t \cdot km^{-2} \cdot y^{-1}$ ).

$$\frac{dB_i(t)}{dt} = \gamma_i * \sum_{j=1}^n Q_{ji}(t) - \sum_{j=1}^n Q_{ij}(t) + I_i - (M_i + e_i) * B_i(t) - \sum_{g=1}^G [F_{ig}^m(t) + F_{ig}^{md}(t)] * B_i(t) \quad (Eq. 1)$$

$$\frac{dB_i(t)}{dt} = PP_i(t) * B_i(t) - \sum_{j=1}^n Q_{ij}(t) + I_i - (M_i + e_i) * B_i(t) \quad (Eq. 2)$$

$$\frac{dD_i(t)}{dt} = \sum_{j=1}^N [\delta_{ji} * (M_j * B_j(t) + u_j \sum_{k=1}^N Q_{kj}(t))] + \sum_{g=1}^G (\delta_{gi} * \sum_{j=1}^N F_{jg}^d(t) * B_i(t)) - \sum_{j=1}^N Q_{ij}(t) \quad (Eq. 3)$$

where  $B_i$  is the biomass of functional group  $i$ ;  $D_i$  is the mass of detritus compartment of group  $i$  (might be used by the scavengers of the food web);  $\gamma_i$  is the growth efficiency ( $\gamma_i = 1 - (r + u)$ ), where  $r$  is the respiration rate and  $u$  the unassimilation of food);  $Q_{ji}$  is the consumption of group  $i$  over all of its preys  $j$ ;  $Q_{ij}$  is the predation on group  $i$  by all of its predators  $j$ ;  $I_i$  is the immigration;  $M_i$  is the non-predatory natural mortality;  $e_i$  is the emigration rate of group  $i$ ;  $F_{ig}$  is the fisheries mortality induced by each gear  $g$  through marketable catches ( $C_{mi} = F_{mi} B_i$ ) and discards ( $C_{di} = F_{di} B_i$ );  $PP_i$  is the primary production rate for autotroph group  $i$ ;  $\delta_{ji}$  is the detritus fate parameter, the flow of detritus produced by a consumer group  $j$  (unassimilated food  $u_i * \sum Q_{ji}$  and natural mortalities  $M_i B_i$ ) to detritus group  $i$ ;  $\delta_{gi}$  is the discard fate parameter, the flow of dead discards by gear  $g$  to detritus group  $i$ . These dynamics are represented in a spatial domain divided into identical grid cells in Ecospace (de Mutsert et al., 2024).

### 3.2.1.3 Model structure and required forcings and inputs; Implementation details

An Ecospace model can be created using the free modeling software suite EwE available at <https://ecopath.org/downloads/>. The software is written in Microsoft Visual Basic .NET and is freely available, although a PRO version is required for using the Spatio Temporal Framework.

Ecospace inherits settings, parameters and data from the Ecosim routine: trophic interaction parameters, biomass of functional groups, as well as fisheries' effort. Furthermore, Ecospace requires additional parameters that define how the food web and fisheries utilize space. In particular dispersal rates are defined for each FG considering the behaviour of species typically with low dispersal (e.g., sessile or benthic infauna; typical dispersal rate  $3 km \cdot year^{-1}$ ), medium dispersal (e.g., coastal resident species; typical dispersal rate  $30 km \cdot year^{-1}$ ), high dispersal (e.g., highly migratory species; typical dispersal rate  $300 km \cdot year^{-1}$ ). Dispersal rates greatly influence Ecospace results, and such typical rates are suggested by developers and experienced users (de Mutsert et al. 2024). Plankton and other transported FG (e.g., suspended organic matter) are advected in Ecospace through an average current field that is given as input. Additional settings define the functional response of each FG to the forcing

<b>Project</b>	NECCON No 101081273	<b>Deliverable</b>	D7.2
<b>Dissemination</b>	Public	<b>Nature</b>	Report
<b>Date</b>	14/10/2025	<b>Version</b>	1.0

functions (e.g., temperature preferences) and geographical factors (e.g., depth preferences). The locations of fisheries harbours and fisheries administrative boundaries are also necessary inputs to increase the model realism.

Environmental variables selected for the Ecospace analysis of the Adriatic Sea were depth, bottom Temperature (T\_bottom), sea surface Temperature (SST), Salinity (SO), dissolved oxygen (O2). Data had a horizontal grid resolution of  $1/24^\circ$  ( $\sim 4.6$  km) and 43 unevenly spaced vertical levels (ranging from the surface down to 800 m in the deeper layers). These environmental variables are typically used in Ecospace to drive the species distributions in relation to FG habitat preferences (niches). In this framework, species have unique responses to these environmental conditions. Ecospace calculates the suitability of each cell for each species: the application of multiple environmental variables in relation with their response functions is calculated in Ecospace as a multiplier factor (Christensen et al., 2014). Each species has a maximum dispersal rate that limits the movement, which is guided by habitat preference, avoidance of predators, availability of preys. Fisheries are also dynamically moving in space considering restrictions (e.g., marine protected areas) and the utility function based on revenues (from fisheries products) and costs (sailing and variable costs). A full description of Ecospace capabilities and limitations are provided in de Mutsert et al. (2024).

#### 3.2.1.4 Model specifics to HTL-LTL coupling

Ecospace can run both as one-way production constrained and a one-way bottom-up coupled model. In Ecospace, all trophic levels, i.e., plankton groups, are simulated simultaneously within the same framework and time steps. This lead the user to implement different possibilities for coupling between HTL-LTL: i) using primary production from LTL (biogeochemical models) to drive the dynamics of phytoplankton (“production constrained one-way coupling”); ii) using the biomasses estimated from phytoplankton, particulate carbon and/or zooplankton functional types in LTL models directly into the Ecospace (using the spatio-temporal framework in a “one-way coupling (forcing)”); iii) using monthly fields obtained from LTL outputs including temperature, salinity, oxygen, currents as forcings in Ecospace model (“one-way coupling (forcing”).

Because LTL state variables for living functional types might have different units (typically  $\text{mgC} \cdot \text{m}^{-3}$ ) than Ecospace ( $\text{tonn wet weight} \cdot \text{km}^{-2}$ ) the coupling requires integration of LTL products over the water column (multiplying the density ( $\text{mgC} \cdot \text{m}^{-3}$ ) by the height of the depth level (m)). Wet weight biomass was obtained by converting the actual biomass expressed in carbon ( $\text{mgC} \cdot \text{m}^{-3}$ ) by multiplying by a conversion factor of 12.5 (Pauly and Christensen, 1995). Moreover, biological resolution between LTL and HTL models can differ, i.e., the functional types in biogeochemical models could be different from the lower trophic levels FGs in Ecospace. Therefore, some aggregation of data from the LTL model is necessary before coupling (see Libralato and Solidoro, 2009).

<b>Project</b>	NECCTON No 101081273	<b>Deliverable</b>	D7.2
<b>Dissemination</b>	Public	<b>Nature</b>	Report
<b>Date</b>	14/10/2025	<b>Version</b>	1.0

### 3.2.2 Application: Hindcast-Simulation

#### 3.2.2.1 Model configuration (*Resolution, Boundary condition, Initial conditions, Model forcing*)

The model using Ecospace is provided for the Adriatic Sea. The Adriatic Sea (central Mediterranean Sea) extends over 138000 km<sup>2</sup> and is characterized by the largest shelf area of the Mediterranean. The Northern and Central parts of the Adriatic Sea are very shallow with a large continental shelf of depths lower than 100 m, with the deepest area located in the Pomo/Jabuka Pit (200-260 m). The southern Adriatic Sea has a relatively narrow continental shelf and a pronounced, steep slope; it reaches a maximum depth of 1223 m. From an administrative perspective, the shores of the northern and central Adriatic (GSA 17) are home to the following countries: Croatia, Bosnia-Herzegovina, Italy and Slovenia. For the southern Adriatic (GSA 18), the countries concerned are Italy, Albania and Montenegro.

Only areas up to a depth of 800 m were considered in the development of the model, as this is the limit at which i) scientific trawl surveys are conducted to monitor demersal species; ii) the limit for most of the exploitation taking place in this area (fishing at depths greater than 1000 m is prohibited in the Mediterranean and only a few vessels are allowed to fish at depths greater than 500 m; FAO, 2023).

A total of 1067 *taxa*, with 405 *taxa* only in the benthic domain, were listed after checking their presence in biomass or catch related databases. Biomass related data come from the international research project ‘MEDiterranean International Trawl Survey’ (MEDITS) (Anonymous, 2017), SOLEMON for the benthic assemblage in the Central North Adriatic Sea, the OBIS Sea Map database for the cetaceans and turtles, for the period 1995-2023. Moreover, after collection of diet data (see dedicated section) further *taxa* were added in the list, when missing from the biomass databases. The species/*taxon* list was aggregated into 73 functional groups (FGs), which describe the basic biological compartments of the food web (Table 2).

The fishing fleets definition was based on knowledge of importance in the area, taking care of features and the main target species that might require separation among fleets. Also, importance in terms of landings and management measures were considered for defining the fleets that were represented in the model as in Table 3.

All data (biomass, parameters, landings and discards, diets) were gathered by species or at the lowest taxonomical level possible and successively data were aggregated according to respective functional groups assignment (see Libralato et al., 2010). Biomasses for several fish and invertebrate species were estimated using data from MEDITS and SOLEMON scientific surveys.

Landing data were obtained from different data sources, both from data calls, official reports and data present on national or institutional repositories. Discards were estimated using the available most recent declared discards in catch data (FDI, DCRF datasets), estimations from scientific surveys (MEDITS and SOLEMON) and discard estimates from field studies of commercial fishing activities (Morello et al., 2005; Raicevich 2008) and stock assessments. The initial conditions (i.e., the Ecopath

<b>Project</b>	NECCTON No 101081273	<b>Deliverable</b>	D7.2
<b>Dissemination</b>	Public	<b>Nature</b>	Report
<b>Date</b>	14/10/2025	<b>Version</b>	1.0

model) were implemented considering data for a reference period of 3 years (2004–2006), that was chosen to facilitate future successive steps of time-dynamic model analysis by means of the Ecosim routine (Christensen et al., 2008). The Ecopath model was manually balanced adopting a top–down approach (Mackinson & Daskalov, 2007) and a pre-balancing analysis (PREBAL, Link, 2010) was carried out to assess the coherence of the input data with the basic thermodynamic laws, rules, and principles of ecosystem ecology at the system level (Heymans et al., 2016; Figure 4).

In Ecospace (and Ecosim) the forcing functions describing the annual oscillation of phytoplankton biomass were retrieved from a set of biogeochemical parameters retrieved from the outcomes of the Deliverable 5.2 (Clark et al., 2025). Particularly, the primary productivity forcing was based on biomass changes of the two-phytoplankton groups (G69\_PDM and G70\_PDF) integrated over 200m depth (Reale et al. 2022). The projections had a tie resolution of 1 month, a horizontal grid resolution of 1/24° (~4.6 km) and 43 unevenly spaced vertical levels (ranging from the surface down to 800 m in the deeper layers).

Environmental variables as well as primary productivity data derived from the biogeochemical model outputs (see Table 4), were coupled in time and space using the spatial-temporal framework (Steenbeek et al., 2016) for simulating years 2004-2023.

Fisheries were allocated to be active in specific “regions” (55) created to represent different administrative areas where the different fisheries are allowed to be active. Regions were created as a combination of territorial waters per country, international waters and distance to coast per country (Figure 4). Fishing effort forcing for Ecosim temporal changes was based on 33 timeseries: 1 from Albania, 1 from Bosnia and Herzegovina, 1 from Montenegro, 6 from Slovenia, 10 from Croatia, and 14 from Italy (Table 5)

In Ecospace, fishing fleets move in 2D in order to follow the centre of gravity of their resources (target species per fishing gear) within the permitted administrative areas, also aiming to reduce the sailing costs and maximising their profits: their movements is in fact, also regulated by the distance to coast in relation to species value. Based on all these variables Ecospace predicts the relative spatial-temporal fishing effort for each fleet (Figure 5 and Figure 6).

Table 2. Functional groups (FGs) represented in the model. Their short name is used in the graphs and in the following text.

<b>FG name</b>	<b>Short name</b>	<b>FG name</b>	<b>Short name</b>
Seabirds	G01_SBR	Hake (age 1)	G38_HKE1
Marine turtles	G02_TTL	Hake (age 2+)	G39_HKE2
Mid-large odontocetes	G03_ODO	Other cephalopods (Slope)	G40_CPXs
Common Bottlenose Dolphin	G04_DBO	Other cephalopods (Shelf)	G41_CPXh
Striped Dolphin	G05_DST	Squids	G42_SQD
Fin whale	G06_FIW	Common cuttlefish	G43_CTC
Rays skates (Slope)	G07_BATs	Musky-Horned octopus	G44_OCM

<b>Project</b>	NECCTON No 101081273	<b>Deliverable</b>	D7.2
<b>Dissemination</b>	Public	<b>Nature</b>	Report
<b>Date</b>	14/10/2025	<b>Version</b>	1.0

Rays skates (Shelf)	G08_BATH	Mantis shrimp (age 0)	G45_MTS0
Sharks (Slope)	G09_SELs	Mantis shrimp (age 1+)	G46_MTS1
Sharks (Shelf)	G10_SELh	Norway lobster (age 0)	G47_NEPO
Blackmouth catshark	G11_SHO	Norway lobster (age 1+)	G48_NEP1
Large pelagic fish	G12_PLS	Blue and Red Shrimp	G49_ARA
Medium pelagic fish	G13_PMS	Red Giant Shrimp	G50_ARS
Demersal piscivorous fish (Slope)	G14_DPSS	Deep-water Rose Shrimp (age 0)	G51_DPS0
Demersal piscivorous fish (Shelf)	G15_DPSh	Deep-water Rose Shrimp (age 1+)	G52_DPS1
Epipelagic fish	G16_EPI	Caramote prawn	G53_TGS
Mesopelagic crustacean feeding	G17_MCF	Decapods_Reptantia (Slope)	G54_REPs
Zooplankton jellyfish feeding fish	G18_ZJF	Decapods_Reptantia (Shelf)	G55_REPh
Demersal fish (Slope)	G19_DEMs	Decapods_Natantia (Slope)	G56_NATs
Demersal fish (Shelf)	G20_DEMh	Decapods_Natantia (Shelf)	G57_NATH
Other flatfishes	G21_FLX	Peracarida (suprabenthos)	G58_PER
Turbot and brill	G22_FTB	Clams	G59_CLM
Gurnads	G23_GUR	Scallops	G60_SCL
Other gadids	G24_GDX	Other Benthic invertebrates	G61_BIX
Other small pelagics	G25_SPX	Seagrasses	G62_SGR
Mackerels	G26_MCK	Seaweeds	G63_SWD
Anglers	G27_LOP	Jellyfish	G64_JLY
Sardine (age 0)	G28_PIL0	Macrozooplankton & Euphasiacea	G65_ZMA
Sardine (age 1+)	G29_PIL1	Mesozooplankton	G66_ZME
Anchovy (age 0)	G30_ANE0	Microzooplankton	G67_ZMI
Anchovy (age 1+)	G31_ANE1	Bacterioplankton	G68_BPL
Solea (age 0)	G32_SOLO	Phytoplankton - diatoms	G69_PDM
Solea (age 1)	G33_SOL1	Phytoplankton - dinoflagellates	G70_PDF
Solea (age 2+)	G34_SOL2	Discards, carrion	G71_DSC
Red mullet (age 0)	G35_MUT0	Suspended detritus	G72_POM
Red mullet (age 1+)	G36_MUT1	Bottom detritus	G73_BT D
Hake (age 0)	G37_HKE0		

Table 3. Fleets used to describe the fisheries in the model. The fleets result from a combination of gear and size category (based on the LOA) also considering importance for the area and available information on landings, capacity and effort.

<b>Fishing gear</b>	<b>Gear code</b>	<b>Vessel length segment (LOA)</b>
Boat dredges	DRB	all vessels (VL-ONE)
Set nets	GNX	all vessels (VL-ONE)
Longlines	LLX	all vessels (VL-ONE)
Small scale fishery, pots, beach seine and other gears	MIX	all vessels (VL-ONE)
Bottom otter trawlers	OTB	smaller than 18 meters (VL—18) between 18 and 24 meters (VL1824) larger than 24 meters (VL24++)

<b>Project</b>	NECCON No 101081273	<b>Deliverable</b>	D7.2
<b>Dissemination</b>	Public	<b>Nature</b>	Report
<b>Date</b>	14/10/2025	<b>Version</b>	1.0

Mid-water pair pelagic trawlers	PTM	smaller than 18 meters (VL—18) between 18 and 24 meters (VL1824) larger than 24 meters (VL24++)
Purse seines	PS	smaller than 18 meters (VL—18) larger than 18 meters (VL18++)
Rapido trawlers	TBB	smaller than 18 meters (VL—18) larger than 18 meters (VL18++)

Table 4. List of Ecosim forcing functions and Ecospace environmental drivers.

Code	role	Variable Name	Time span (monthly)	Resolution	Unit	Source
O2	forcing	Dissolved oxygen	01-2004 to 05-2023	1/24°	mmol O <sub>2</sub> / m <sup>3</sup>	CMEMS
SST	forcing	Sea Surface Temperature	01-2004 to 05-2023	1/24°	°C	CMEMS
bottomT	forcing	Sea Bottom Temperature	01-2004 to 05-2023	1/24°	°C	CMEMS
Depth	forcing	Depth	-	1/24°	m	CMEMS
S	forcing	Salinity	01-2004 to 05-2023	1/24°	PSU	CMEMS
B1	FG: G68_BPL	Pelagic Bacteria	01-1999 to 12-2023	1/24°	mgC/m <sup>3</sup>	Deliverable 5.2 (Clark et al., 2025)
P1	FG: G69_PDM / forcing	Diatoms	01-1999 to 12-2023	1/24°	mgC/m <sup>3</sup>	Deliverable 5.2 (Clark et al., 2025)
P2	FG:	Nano Flagellates	01-1999 to 12-2023	1/24°	mgC/m <sup>3</sup>	Deliverable 5.2 (Clark et al., 2025)
P3	G70_PDF / forcing	Picophytoplankton	01-1999 to 12-2023	1/24°	mgC/m <sup>3</sup>	Deliverable 5.2 (Clark et al., 2025)
P4		Large phytoplankton	01-1999 to 12-2023	1/24°	mgC/m <sup>3</sup>	Deliverable 5.2 (Clark et al., 2025)
Z3	FG:	Carnivorous Mesozooplankton	01-1999 to 12-2023	1/24°	mgC/m <sup>3</sup>	Deliverable 5.2 (Clark et al., 2025)
Z4	G66_ZME	Omnivorous Mesozooplankton	01-1999 to 12-2023	1/24°	mgC/m <sup>3</sup>	Deliverable 5.2 (Clark et al., 2025)
Z5	FG: G67_ZMI	Microzooplankton	01-1999 to 12-2023	1/24°	mgC/m <sup>3</sup>	Deliverable 5.2 (Clark et al., 2025)



<b>Project</b>	NECCTON No 101081273	<b>Deliverable</b>	D7.2
<b>Dissemination</b>	Public	<b>Nature</b>	Report
<b>Date</b>	14/10/2025	<b>Version</b>	1.0

Z6		Heterotrophic Flagellates	01-1999 to 12-2023	1/24°	mgC/m <sup>3</sup>	Deliverable 5.2 (Clark et al., 2025)
R1		Labile Dissolved Organic Matter	01-1999 to 12-2023	1/24°	mgC/m <sup>3</sup>	Deliverable 5.2 (Clark et al., 2025)
R2	FG:	Semi-labile Dissolved Organic Carbon	01-1999 to 12-2023	1/24°	mgC/m <sup>3</sup>	Deliverable 5.2 (Clark et al., 2025)
R6	G72_PO M	Semi-refractory Dissolved Organic Carbon	01-1999 to 12-2023	1/24°	mgC/m <sup>3</sup>	Deliverable 5.2 (Clark et al., 2025)
R7		Particulate Organic Detritus	01-1999 to 12-2023	1/24°	mgC/m <sup>3</sup>	Deliverable 5.2 (Clark et al., 2025)

Table 5. Specification of reference time series data used for simulating the fishing effort of Adriatic fishing fleets (GSA 17 & 18). Fishing fleets: ONE - all fishing gears, DRB – dredge boats, GNX – set nets, LLX – long lines, MIX – mixed and other fishing gears, OTB – otter trawlers, PS – purse seine, PTM – mid-water pair pelagic trawl, TBB – rapido trawl. Fleet length over all (LOA) segments: VL-ONE – all vessel sizes, V--18 – vessel smaller than 18 meters, VL18++ – vessel larger than 18 meters, VL1824 – vessel between 18 and 24 meters, VL24++ – vessel larger than 24 meters. Other abbreviations: GT – gross tonnage, FD – fishing days, N – number of vessels.

Country	Fleet	LOA segment	Value
Albania	ONE	VL-ONE	Total catch index
BiH	ONE	VL-ONE	Total catch index
Croatia	DRB	VL-ONE	Hybrid (GT+FD) (FD equivalent)
Croatia	GNX	VL-ONE	Hybrid (GT+FD) (FD equivalent)
Croatia	LLX	VL-ONE	Hybrid (GT+FD) (FD equivalent)
Croatia	MIX	VL-ONE	Hybrid (GT+FD) (FD equivalent)
Croatia	OTB	VL—18	Hybrid (GT+N+FD) (FD equivalent)
Croatia	OTB	VL1824	Hybrid (GT+N+FD) (FD equivalent)
Croatia	OTB	VL24++	Hybrid (GT+N+FD) (FD equivalent)
Croatia	PS	VL—18	Hybrid (GT+N+FD) (FD equivalent)
Croatia	PS	VL18++	Hybrid (GT+N+FD) (FD equivalent)
Croatia	TBB	VL—18	Hybrid (GT+FD) (FD equivalent)
Italy	DRB	VL-ONE	FishingDays
Italy	GNX	VL-ONE	FishingDays
Italy	LLX	VL-ONE	FishingDays
Italy	MIX	VL-ONE	FishingDays
Italy	OTB	VL—18	FishingDays
Italy	OTB	VL1824	FishingDays
Italy	OTB	VL24++	FishingDays
Italy	PS	VL—18	FishingDays
Italy	PS	VL18++	FishingDays

<b>Project</b>	NECCON No 101081273	<b>Deliverable</b>	D7.2
<b>Dissemination</b>	Public	<b>Nature</b>	Report
<b>Date</b>	14/10/2025	<b>Version</b>	1.0

Italy	PTM	VL—18	Displacement
Italy	PTM	VL1824	Displacement
Italy	PTM	VL24++	Displacement
Italy	TBB	VL—18	EnginePower
Italy	TBB	VL18++	EnginePower
Montenegro	ONE	VL-ONE	Total catch index
Slovenia	GNX	VL-ONE	Vessel number
Slovenia	LLX	VL-ONE	Vessel number
Slovenia	MIX	VL-ONE	Vessel number
Slovenia	OTB	VL-ONE	Displacement
Slovenia	PS	VL-ONE	Displacement
Slovenia	PTM	VL-ONE	Displacement

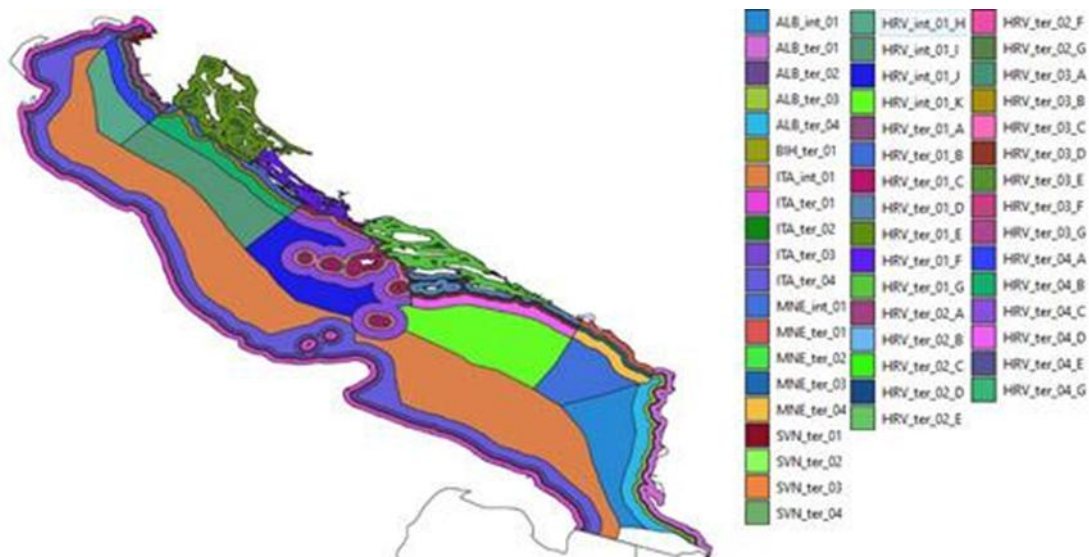


Figure 4. Ecospace administrative areas set for fishery allocations. Int=international waters; ter=territorial waters; ITA=Italy; BIH=Bosnia and Hercegovina; HRV=Croatia; MNT=Montenegro; SLO and SVN= Slovenia; 01=3 nautical miles; 02=4 nautical miles; 03=6 nautical miles; 04=up to the midline.

<b>Project</b>	NECCTON No 101081273	<b>Deliverable</b>	D7.2
<b>Dissemination</b>	Public	<b>Nature</b>	Report
<b>Date</b>	14/10/2025	<b>Version</b>	1.0

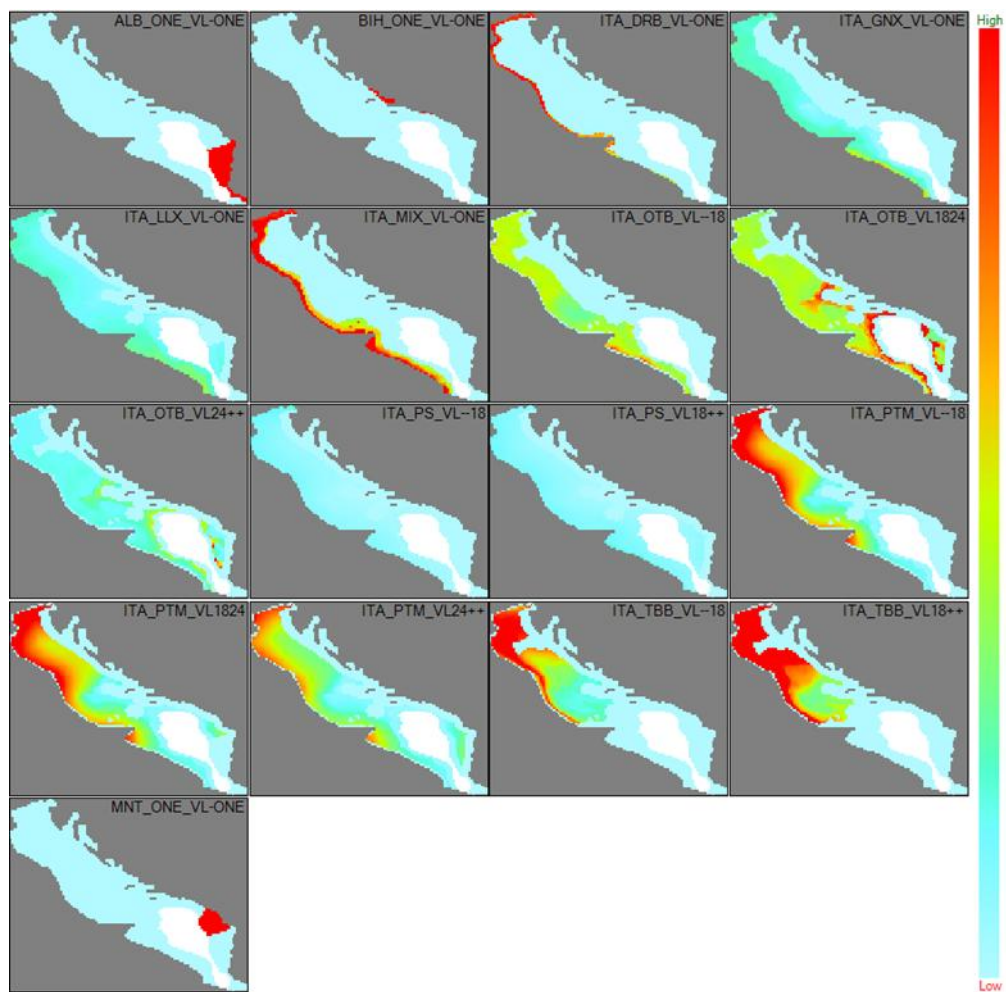


Figure 5. Ecospace relative predicted effort (for May/2011). ALB=Albania; BIH=Bosnia and Hercegovina; ITA=Italy; MNT=Montenegro. OTB= Bottom otter trawls; PTM= Pelagic pair trawls; PS=Purse seine; TBB= Beam trawls; DRB=dredges; GNX=set nets; LLX= long lines; MIX (seine, traps, small-scale fishery); VL=vessel length.

<b>Project</b>	NECCTON No 101081273	<b>Deliverable</b>	D7.2
<b>Dissemination</b>	Public	<b>Nature</b>	Report
<b>Date</b>	14/10/2025	<b>Version</b>	1.0

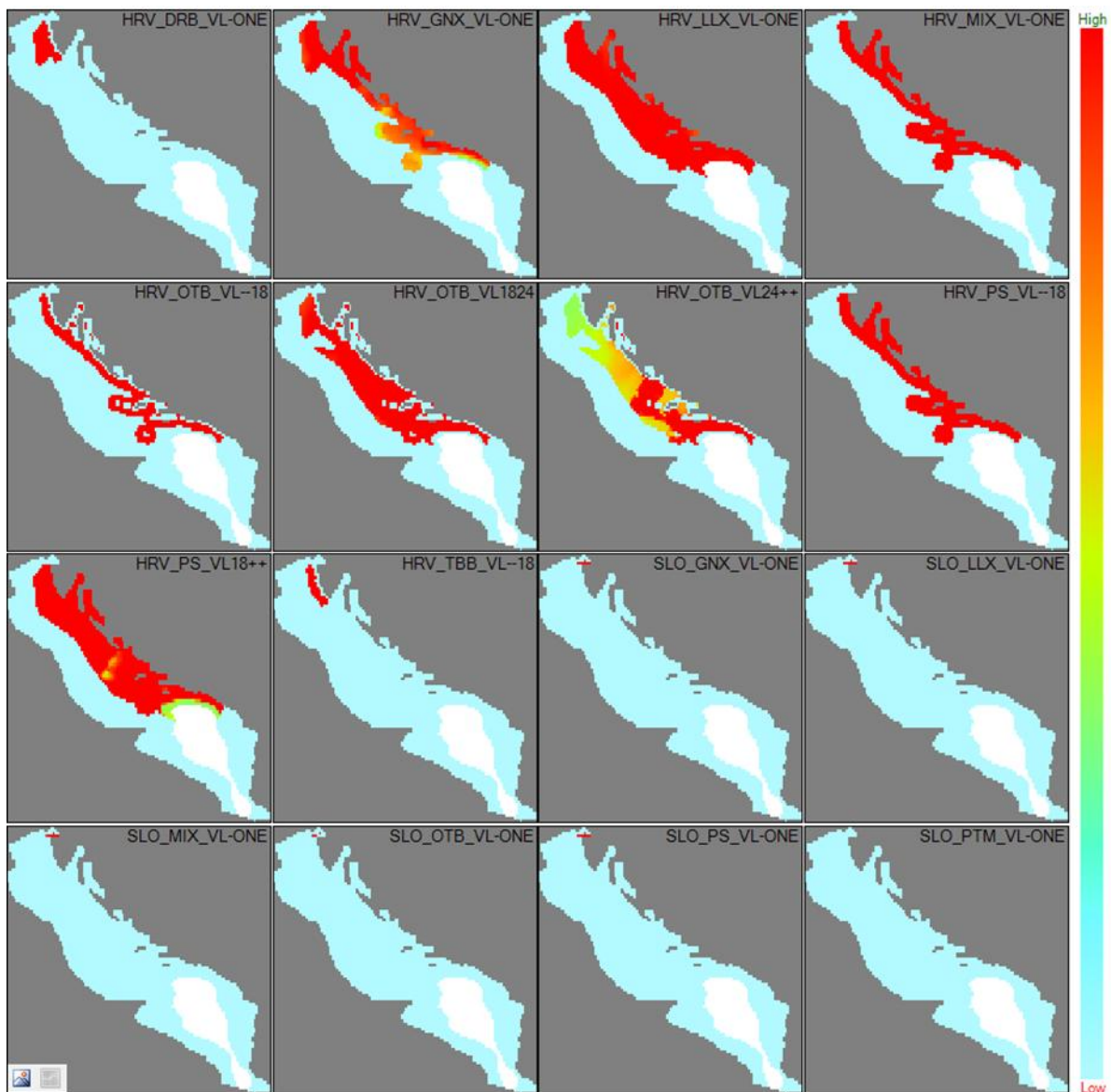


Figure 6. Ecospace relative predicted effort (for August/2011). HRV=Croatia; SLO and SVN= Slovenia. OTB= Bottom otter trawls; PTM= Pelagic pair trawls; PS=Purse seine; TBB= Beam trawls; DRB=dredges; GNX=set nets; LLX= long lines; MIX (seine, traps, small-scale fishery); VL=vessel length.

### 3.2.2.2 Calibration and Validation of hindcast simulations

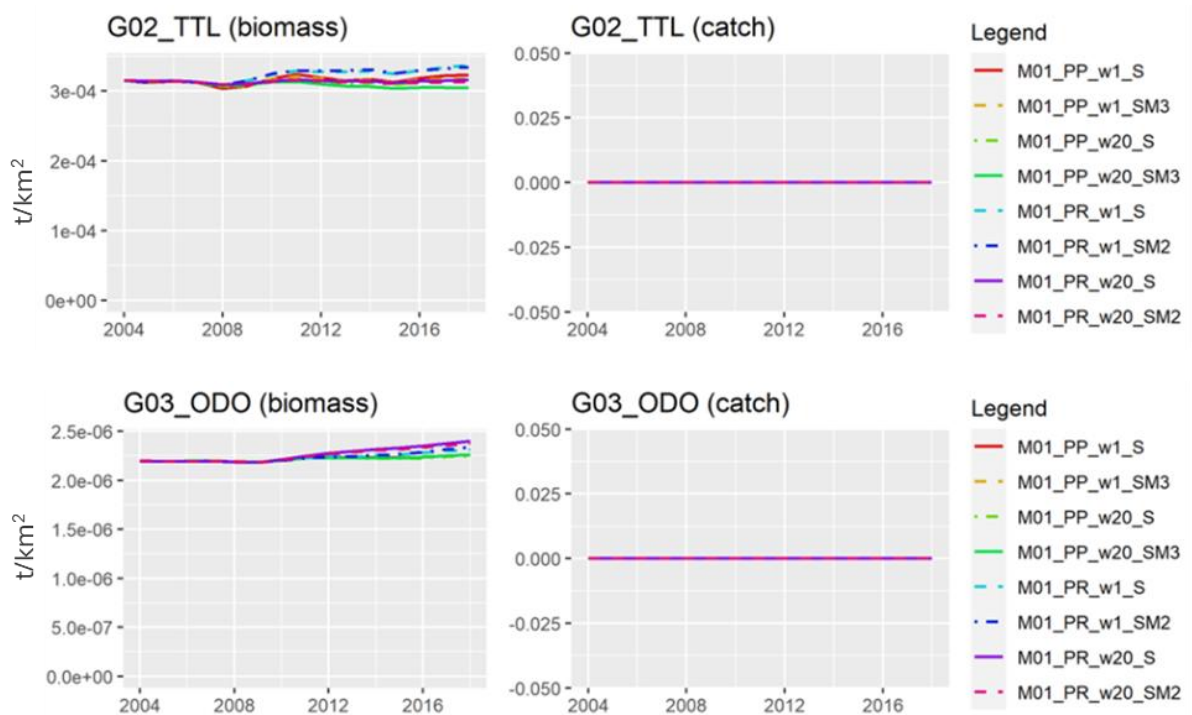
Ecosim temporal changes were driven by primary productivity (one-way coupling) and changes of fishing efforts. The Ecosim model was fitted to time series of biomasses and catches for as many FGs as possible and for the period 2000-2023. Based on the availability of data, 44 and 53 time series of biomass and catches were used respectively. The fitting was performed using different settings: i) fitting by predator (stepwise fitting); ii) fitting by predator/prey (stepwise fitting); iii) fitting using manual settings to estimate the vulnerabilities not considered by the stepwise fitting (see Ricci et al., 2023) (Figure 7).

<b>Project</b>	NECCON No 101081273	<b>Deliverable</b>	D7.2
<b>Dissemination</b>	Public	<b>Nature</b>	Report
<b>Date</b>	14/10/2025	<b>Version</b>	1.0

For Ecospace analysis the best fitted model using predator/prey setting were chosen and two approaches were tested. The first consisted of a sensitivity test, in which the implementation of Fishery Restricted Areas (FRAs) were activated one at a time to assess the ecosystem responses to each restricted area. The second one consisted in the evaluation of the impact of Ecospace management scenarios.

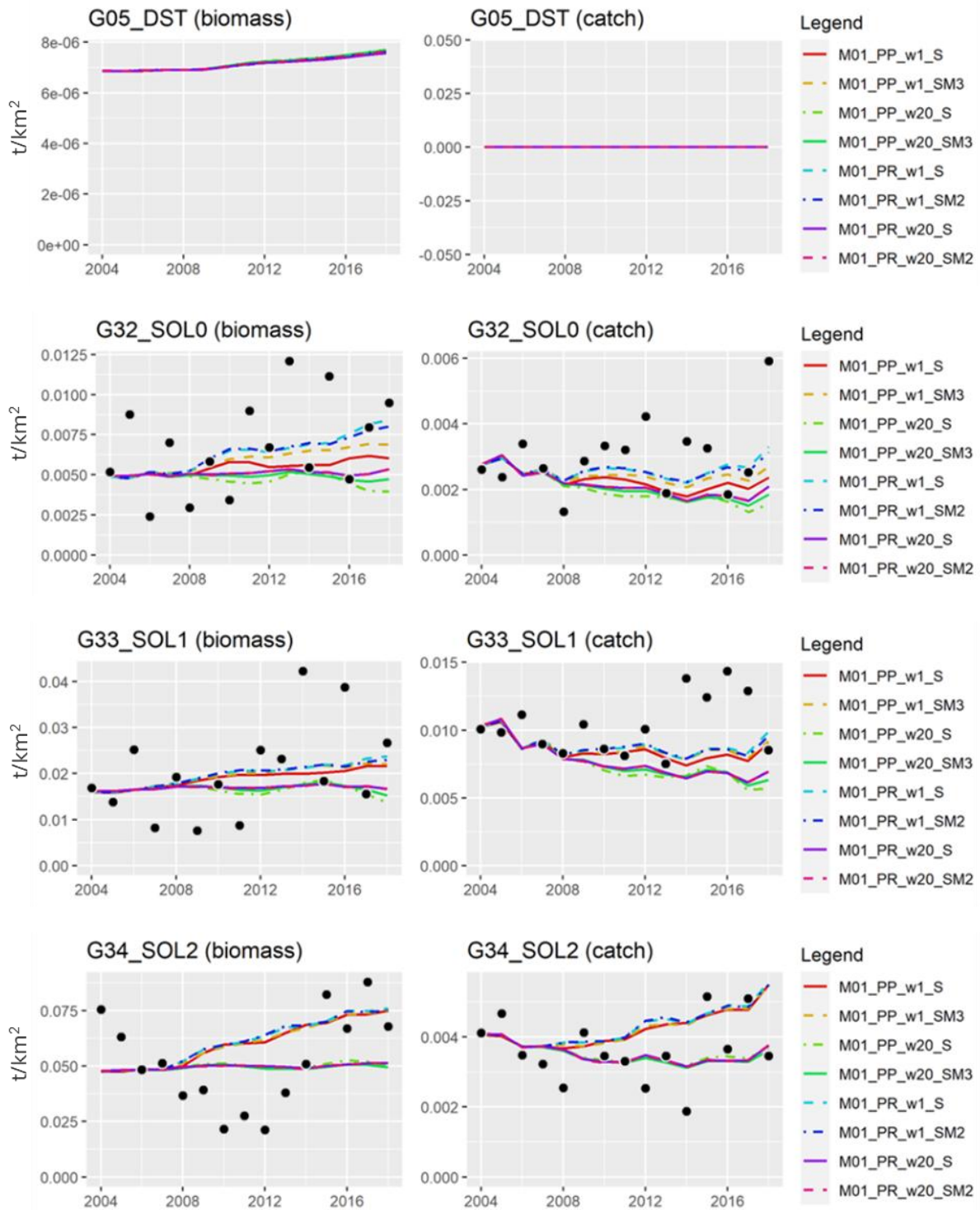
The managed areas include all zones within 3, 4 and 6 nautical miles, the FRA of Pomo, of Bari canyon and North Adriatic sanctuary. FRAs were activated in different time with the spatial-temporal framework (Steenbeek et al., 2016), whilst the effort changes are implemented in Ecosim temporal drivers.

Single regions were set for each fishery restricted area and coastal zone, allowing to assess the changes in biomass at sea of the entire Adriatic domain and also inside each restricted areas and coastal zone. Management fishery restricted areas were dynamically activated/deactivated according to fisheries management regulations in the past decades for best representation of spatio-temporal observed changes.





<b>Project</b>	NECTON No 101081273	<b>Deliverable</b>	D7.2
<b>Dissemination</b>	Public	<b>Nature</b>	Report
<b>Date</b>	14/10/2025	<b>Version</b>	1.0



<b>Project</b>	NECCTON No 101081273	<b>Deliverable</b>	D7.2
<b>Dissemination</b>	Public	<b>Nature</b>	Report
<b>Date</b>	14/10/2025	<b>Version</b>	1.0

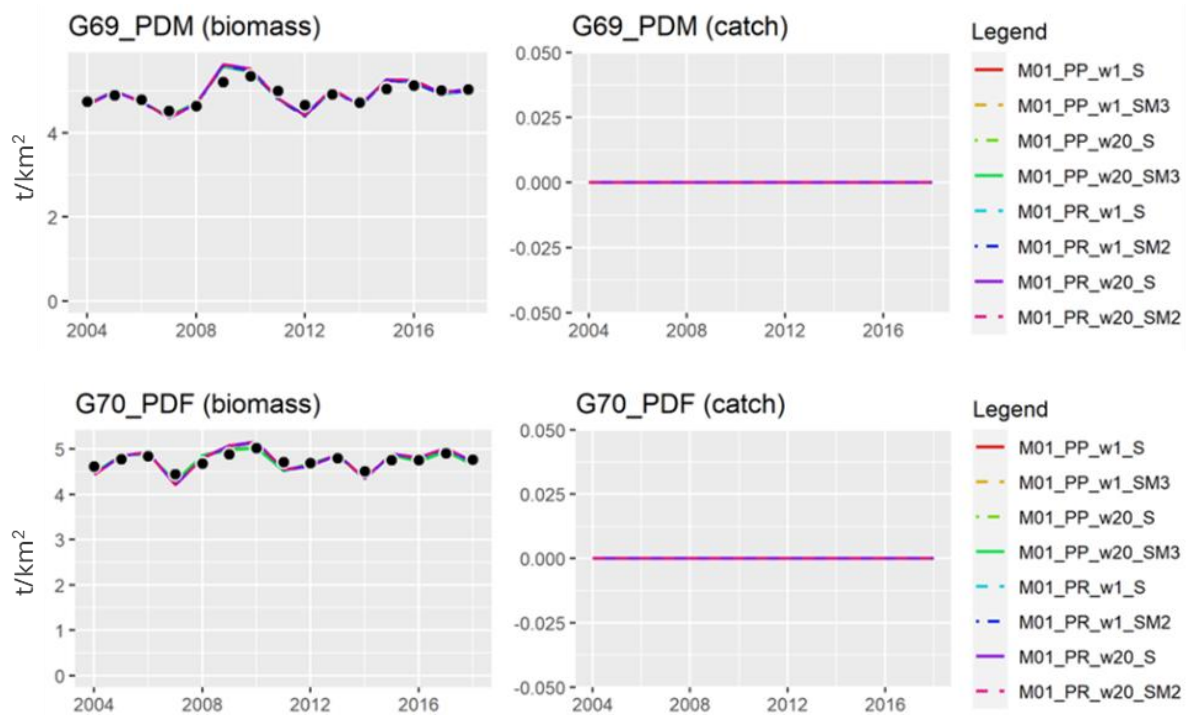


Figure 7. Fitting tested. M01=model 1; PP=fitting by predator/prey setting; PR=fitting by predator setting; w01=relative biomasses weight=1; w20=relative biomasses of stock assessed groups weight=20; S=stepwise fitting; SM= stepwise fitting followed by manual fittings (2-3 number of manual search).

### 3.2.2.3 Results

Ecospace output predicted the temporal-spatial distributions of all 73 functional groups defined in the Ecopath model. Outputs for HTL FGs as the main target species in the Adriatic Sea are reported.

The scenarios implemented allowed i) to assess the ecosystem responses to the implementation of different FRAs were activated one at a time to each restricted area and ii) to evaluate the impacts of management scenarios.

Should be noted that, scenarios were basically devoted to analysing effects of measures on demersal resources; however, HTL FGs were influenced indirectly by management on demersal resources through fishing technical interactions and ecological trophic interactions which are represented in the model.

### 3.2.3 NECCTON Products from the model

The Ecospace approach is used to produce a 2D model of the Adriatic Sea (GSA 17 and GSA 18) for the time period 2000 – 2023. Outputs are provided monthly, at the maximum resolution available (1/24°). Although all 73 FGs are potentially reported, for NECCTON the products that will be considered are specific FGs that can be more accurately fitted to data i.e., small pelagics, some demersal fishes and invertebrates and marine mammals (*Tursiops truncatus*).

<b>Project</b>	NECCTON No 101081273	<b>Deliverable</b>	D7.2
<b>Dissemination</b>	Public	<b>Nature</b>	Report
<b>Date</b>	14/10/2025	<b>Version</b>	1.0

### 3.2.4 Discussion of pros and cons of the model

Building and calibrating spatial and spatial-temporal simulations in Ecospace takes advantage from the previous Ecopath and Ecosim calibration and fitting. The tool facilitates building ecosystem models (from phytoplankton to fish) in which state variables are functional groups (FG) biomasses. One advantage of this structure is the simplification of the food web based on assumptions derived from ecological knowledge and data availability. This permit increased biological resolution for specific target elements however large amount of information is needed to develop and calibrate such a complex model, such as local diet composition (Ecopath), biomass/catches/fishing effort time series (Ecosim) or spatial fishing effort displacement for small scale fishing gear (Ecospace). For instance, this huge amount of required data input slightly limits the flexibility of the approach when one wishes to modify input data.

Ecospace (and Ecosim) derives from an initial condition setting (Ecopath) which assumes mass-balance and often steady state. This can be seen as a limitation, but it is overcome in Ecosim and Ecospace by the use of forcings and input dynamics.

A major limitation is that a real calibration of Ecospace is not feasible and most of the efforts are related to a *a posteriori* comparison of Ecospace outputs with observations to validate/corroborate the results. Moreover, as a limitation, the spatio-temporal framework that facilitates the LTL-HTL coupling in Ecospace is available only in the Pro version of the software.

The Ecospace approach has the advantage of being available with an intuitive graphical user interface, extensive documentation, and a large user community (de Mutsert et al., 2024). The capacity of providing spatial-referenced output facilitates a visual communication of the results, especially in the context of open discussion with managers, decision makers and stakeholders. In fact, this approach represents an effective tool in the context of the EBFM.

## 3.3 EcoOcean (Leading partner: EII)

### 3.3.1 Introduction

Building on the Ecospace modelling approach, EcoOcean v2 is a globally implemented, spatial-temporal marine ecosystem modelling framework designed to simulate the past and future dynamics of marine biodiversity, food-web interactions, and fisheries under climate change and anthropogenic stressors for the global oceans. Building upon its predecessor EcoOcean v1, the v2 system (Coll et al. 2020) significantly enhances ecological realism and responsiveness by incorporating higher taxonomic resolution, dynamic environmental forcing, and improved modelling of ecological processes. It is part of the FishMIP (Tittensor et al. 2018) initiative under ISIMIP and supports scenario testing for marine policy, conservation, and sustainable use of ocean resources.

The EcoOcean model is built on the presumed global biomasses in 1950 needed to deliver the historical fisheries catches and ecosystems that we have today (Christensen et al. 2015) given



<b>Project</b>	NECCTON No 101081273	<b>Deliverable</b>	D7.2
<b>Dissemination</b>	Public	<b>Nature</b>	Report
<b>Date</b>	14/10/2025	<b>Version</b>	1.0

assumptions on the historical evolution of ocean variables and known distributions and intensities of fishing effort. Species distributions and densities are thus an output of the model.

The developers also use EcoOcean as a platform for testing ecological hypotheses.

### 3.3.2 Model Structure

EcoOcean v2 consists of three tightly integrated modules:

#### Biogeochemistry and Primary Production

For EcoOcean v2, inputs were derived from Earth System Models (ESMs), particularly GFDL-ESM2M and IPSL-CMA5-LR, providing time-series of large/small phytoplankton and diazotroph production over the historical (1950–2005) and future (2006–2100) periods, under RCP2.6 and RCP8.5 scenarios.

The oncoming NECCTON simulations will be driven by the Earth System Model data facilitated under NECCTON via one-way coupling of biotic and abiotic components.

For biotic components, EcoOcean resolves primary productivity in three separate functional groups: vertically integrated large and small phytoplankton, and diazotrophs if available. ESM data is used to overwrite the spatial biomasses of corresponding primary producers at the monthly time steps for which ESM data is available. EcoOcean phytoplankton groups not forced by ESM data will be fully managed by the EcoOcean, where nutrient availability can be fluctuated via ESM Net Primary Productivity data (Coll et al. 2020).

For abiotic components, EcoOcean relies on ESM variables such potential seawater temperature (at the 150m from the surface, water column average, and the bottom). For the most recent FishMIP simulations, EcoOcean has been expanded to be able to include salinity, dissolved oxygen and sea ice to affect species distributions. Sea ice concentration can also be incorporated to restrict fisheries in high latitudes.

#### Food-Web Component

At the core lies a spatially explicit version of the Ecopath with Ecosim (EwE) model framework, heavily modified via additional computations to resolve the spatial heterogeneity of functional groups across the global ocean (Coll et al. 2020).

The EcoOcean model contains 55 functional groups that include fish, invertebrates, mammals, seabirds, and plankton. Fish are grouped by size and vertical habitat zonation (see table below).

EcoOcean explicitly accounts for over 3,400 species represented by the functional groups. Although EcoOcean does not explicitly model the species within functional groups, the species composition of functional groups is used to initially distribute the functional groups and to determine how the group may respond to (varying) environmental conditions across the oceans (Coll et al. 2020). Here, the distribution and movement of functional groups are governed by the notions of habitat suitability in

<b>Project</b>	NECCTON No 101081273	<b>Deliverable</b>	D7.2
<b>Dissemination</b>	Public	<b>Nature</b>	Report
<b>Date</b>	14/10/2025	<b>Version</b>	1.0

the Habitat Foraging Capacity Model (HCFM), defined as the ability to feed in a model cell, and the risk of being eaten (de Mutsert et al. 2024).

In EcoOcean, trophic interactions are governed by the Foraging Arena Theory (Ahrens et al. 2012) which introduces predator-prey driven behavioural non-linearity and trophic cascades.

Last, to represent growth rates at latitude, EcoOcean incorporates temperature-adjusted metabolic rates based on long-term temperature averages as obtained from ESM data ( $Q_{10}$ , Coll et al. 2010).

For the oncoming NECCTON simulations, the EcoOcean functional group structure has been expanded with a finer resolution for large pelagic fish, in particular tuna (See Table 4).

Table 4. The functional group structure of the EcoOcean model used in NECCTON simulations.

#	Group name	#	Group name
1	Baleen whales	28	Benthopelagics medium
2	Toothed whales	29	Benthopelagics small
3	Dolphins porpoises	30	Reeffish large
4	Pinnipeds	31	Reeffish medium
5	Birds	32	Reeffish small
6	Penguins	33	Flatfish large
7	Marine turtles	34	Flatfish small medium
8	Sharks large pelagic	35	Cephalopods
9	Sharks large demersal	36	Molluscs (exploitable)
10	Sharks small medium	37	Other molluscs
11	Rays large	38	Lobsters crabs
12	Rays small medium	39	Shrimps
13	Pelagics large	40	Other crustaceans
14	Pelagics large tuna temp.	41	Megabenthos
15	Pelagics large tuna trop.	42	Macrobenthos
16	Pelagics medium	43	Corals
17	Pelagics small	44	Soft corals & sponges
18	Demersals large	45	Meiobenthos
19	Demersals medium	46	Jellyfish
20	Demersals small	47	Large zooplankton
21	Bathypelagics large	48	Mesozooplankton
22	Bathypelagics medium	49	Microzooplankton
23	Bathypelagics small	50	Benthic plants
24	Bathydemersals large	51	Phytoplankton large
25	Bathydemersals medium	52	Phytoplankton small
26	Bathydemersals small	53	Diazotrophs
27	Benthopelagics large	54	Bacteria
		55	Detritus

<b>Project</b>	NECCTON No 101081273	<b>Deliverable</b>	D7.2
<b>Dissemination</b>	Public	<b>Nature</b>	Report
<b>Date</b>	14/10/2025	<b>Version</b>	1.0

## Fisheries Dynamics

Fishing effort is allocated via a gravity model, where profitability dictates spatial fishing intensity (Walters et al. 2000).

EcoOcean represents global fishing via a fleet structure of 14 gear types across 1365 historical fleets. EcoOcean has been calibrated to historical catch data from the Sea Around Us project and prices from Sumaila et al. (2007).

Following the FishMIP protocol 3a (<https://fishmip.org › simulations › isimip3a.html>), EcoOcean allocates nominal fishing effort per Large Marine Ecosystem (LME) for historical \*simulations where LME 0 (the high seas) are subdivided by ocean basin. Within each LME (and LME 0 subdivision) the standard Ecospace fishing effort gravity model plays out. Fishing fleets limited by fuel prices are cost-constrained by a distance from port. Fishing fleets that cannot fish in specific depth zones or over specific bottom types are restricted accordingly (Coll et al. 2020). Additionally, EcoOcean can now incorporate sea ice to restrict fisheries in high latitudes. EcoOcean can also incorporate spatial management tools like MPAs and seasonal closures and fishing effort creep where needed; we yet must decide which mechanisms to incorporate in the NECCTON simulations.

### 3.3.2.1 Key Methodological Enhancements in EcoOcean v2

#### Native Range Constraints

At model initialization, species groups are restricted to their empirically derived native ranges (from Kaschner et al. 2016). This prevents unrealistic distributions at the start of simulations. After initialization, species can migrate freely in response to changing environmental suitability.

#### Cell-Specific Environmental Responses

Cell habitat suitability is computed via the HFCM and unifies the notion of habitat use and environmental sensitivities (Coll et al. 2020). The EcoOcean HFCM is parameterized with functional responses to environmental conditions, per species, corrected for the potential species niches while the environment changes, scaled up to functional group level (Coll et al.).

Species' functional response curves are based on the work of AquaMaps (Kaschner et al. 2016), whereas habitat affinities are obtained from FishBase and SeaLifeBase (Grüss et al. 2019). The per-cell functional responses at the functional group level, corrected for the most likely species composition of a functional group at a given spatial location are then used to scale foraging arena size in a cell, and thus directly affect local growth and consumption rates (Coll et al. 2020).

For the oncoming NECCTON runs, relevant environmental conditions may be expanded, pending data availability.

<b>Project</b>	NECCTON No 101081273	<b>Deliverable</b>	D7.2
<b>Dissemination</b>	Public	<b>Nature</b>	Report
<b>Date</b>	14/10/2025	<b>Version</b>	1.0

### 3.3.2.2 Model Implementation and Simulation Setup

EcoOcean has been implemented in the .NET framework, and the model runs natively on any operating system. EcoOcean simulations typically run for the 1950-2100 period at monthly time steps with a 10-year spin-up period to stabilize ecosystem dynamics. EcoOcean simulations are typically executed on a 1° spatial resolution, although the most recent ISIMIP 3a simulation round included runs at a spatial resolution of 0.25° to assess the impact of grid cell sizes on specifically coastal dynamics. A publication is in preparation.

### 3.3.3 NECCTON Products from the model

The EcoOcean approach will be used to produce a global assessment of the global food web under provided ESM scenarios for the period provided by the ESM. Outputs are provided monthly, at the 1°. Output will be aggregated according to the FishMIP ISIMIP3b protocol, including the explicit representation of large pelagic fish.

There are no preliminary results for the NECCTON EcoOcean runs as Global ESM data only recently became available. For examples of EcoOcean output, please refer to Coll et al. (2020) or Boot et al. (2025).

<b>Project</b>	NECCTON No 101081273	<b>Deliverable</b>	D7.2
<b>Dissemination</b>	Public	<b>Nature</b>	Report
<b>Date</b>	14/10/2025	<b>Version</b>	1.0

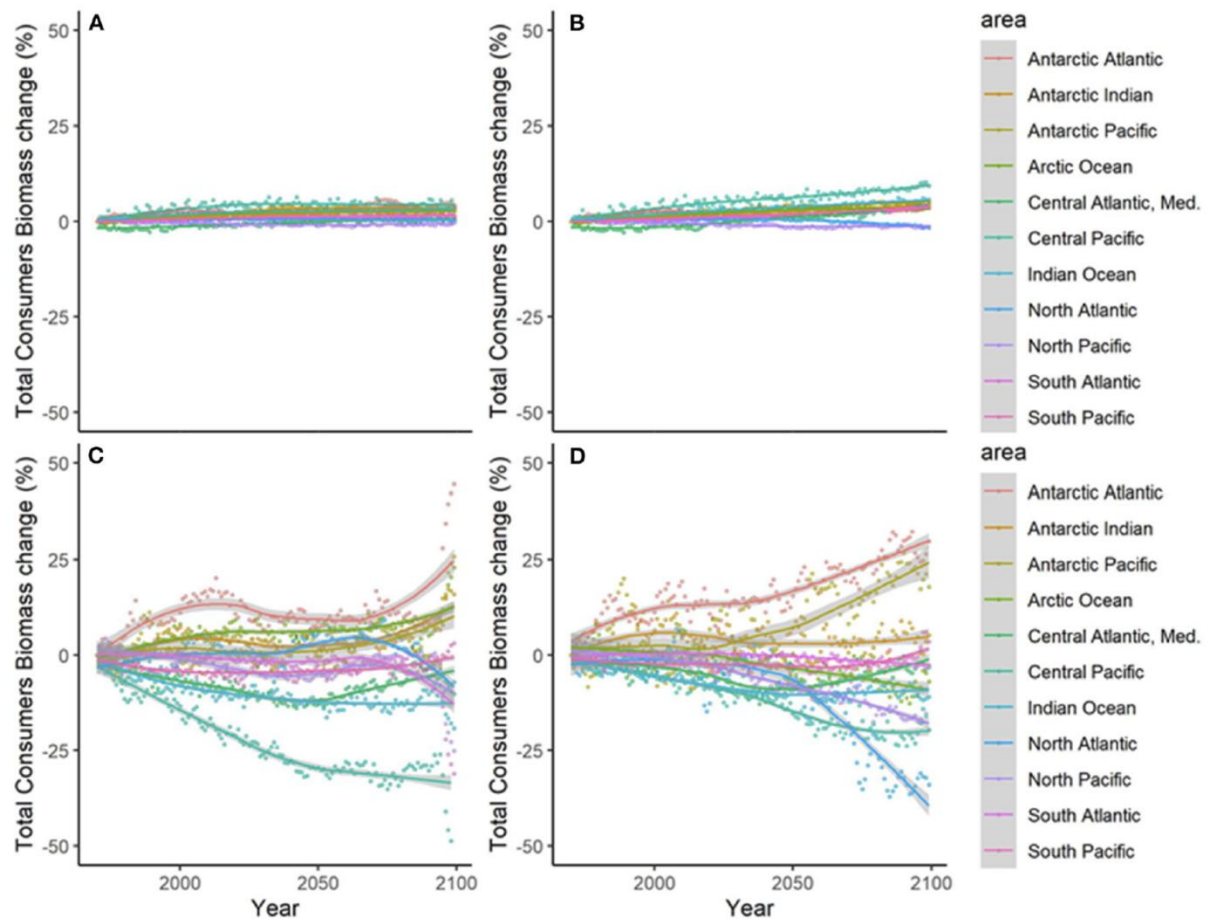


Figure 8 1950-2100 EcoOcean simulation runs to test the impact of different climate scenarios. Panels show the relative temporal change of Total Consumers Biomass (%) by sub-regional oceans under different climate forcing for the period 1950-2100: (A) GFDL RCP2.6; (B) GFDL RCP8.5, (C) IPSL RCP2.6, and (D) IPSL RCP8.5. Figure reproduced with permission from Coll et al. (2020).

<b>Project</b>	NECCTON No 101081273	<b>Deliverable</b>	D7.2
<b>Dissemination</b>	Public	<b>Nature</b>	Report
<b>Date</b>	14/10/2025	<b>Version</b>	1.0

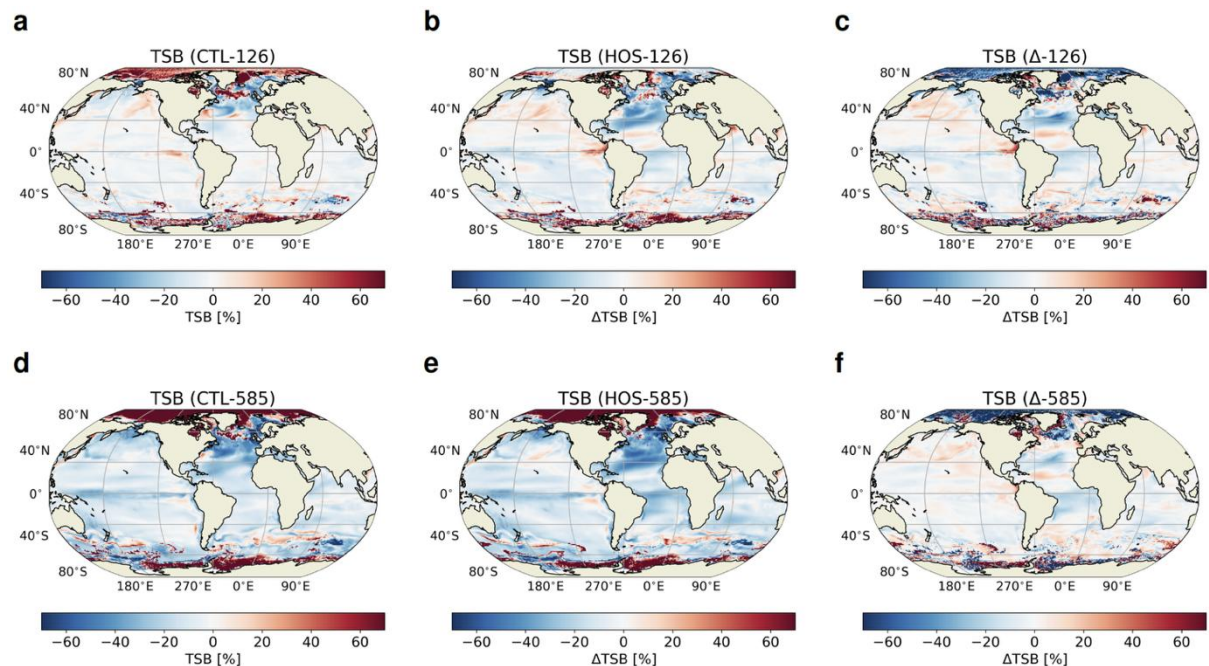


Figure 9 Example output of EcoOcean in the context of Atlantic Meridional Overturning Circulation (AMOC) weakening experiments. The panels reflect relative changes in biomass averaged over 2095-2099 compared to 2016-2020 in % for Total System Biomass (TSB) in the CTL (= no weakening) simulations (a, d), HOS (=weakening) simulations (b, e), and the difference between the two (c, f). (a-c) are for SSP1-2.6 and (d-f) are for SSP5-8.5. Figure reproduced with permission from Boot et al. (2025).

### 3.3.4 Discussion of pros and cons of the model

The main advantage of the EcoOcean MEM is its explicit consideration of the interplay between food web interactions, species movement, changing climate and fishing, which, through trophic cascades, can inform broad-scale climate and cumulative impact studies under complementary and counterfactual scenarios. Especially the newly added spatial validation tools, which will soon be published and will migrate to the EwE approach, have been essential to guide the calibration of the Ecospace model. However, as mentioned in section 3.1.4, comprehensive and [semi]-automated spatiotemporal calibration routines are still lacking in the EwE/EcoOcean family but also for MEMs in general (Steenbeek 2024)

The downside of EcoOcean is its broad scale and food web, making it unsuitable for addressing specific case studies at local scales. Analysis for 1/4° spatial resolution runs have not yet been completed and will reveal how EcoOcean species dynamics will have changed especially in the downscaled and represented in more detail coastal zones. However, for local studies, using a specific model built and calibrated to the local study is a much more sensible approach than using a global MEM such as EcoOcean.

<b>Project</b>	NECCON No 101081273	<b>Deliverable</b>	D7.2
<b>Dissemination</b>	Public	<b>Nature</b>	Report
<b>Date</b>	14/10/2025	<b>Version</b>	1.0

### 3.4 ERSEM-MIZER (Leading partner: PML)

#### 3.4.1 Introduction

ERSEM-MIZER is a two-way coupled model comprised of the lower trophic level model ERSEM (Butenschön et al., 2016) and the community size-structured model of fishes, MIZER (Blanchard et al., 2009; 2012; 2014), mediated by the FABM coupler (Bruggeman & Bolding, 2014). The two-way coupling allows depth-resolved predation on plankton by fish, with the plankton then removed from ERSEM and waste produced by fish excretion and respiration added back into ERSEM at the appropriate depth (Figure 10). Therefore, the model represents a complete food chain from photons to fisheries.

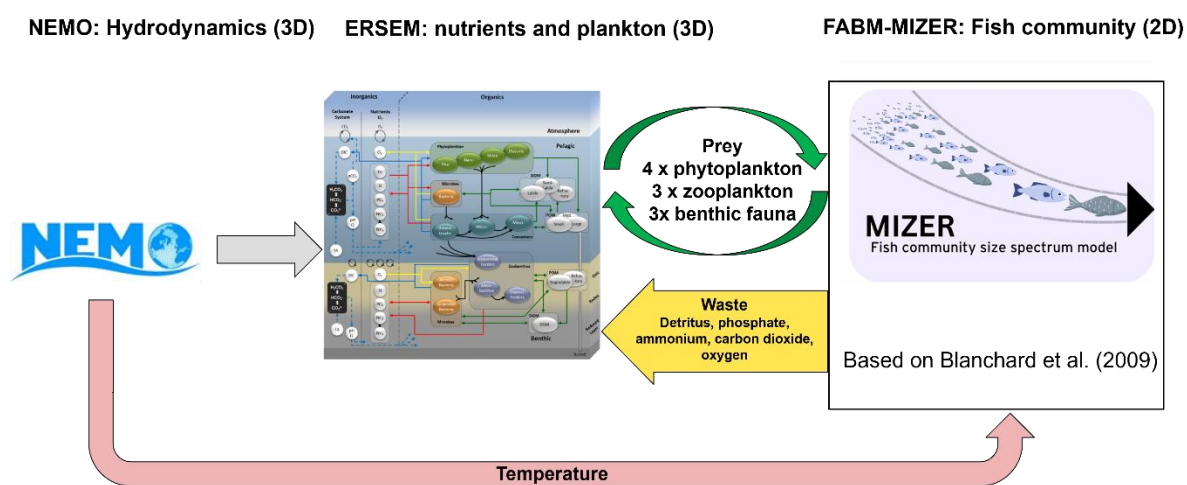


Figure 10. Conceptual diagram illustrating two-way coupling between ERSEM and MIZER models.

Here, we implement the community version of the HTL model MIZER, where fish are represented across a range of size classes, from 1 mg to 1000 kg. Size is considered to be a ‘master’ trait, controlling the rates of physiological processes such as growth and respiration (Andersen et al., 2016; Brown et al., 2004). In MIZER, growth is represented by fish biomass moving to a larger size class. Many ecological processes also scale with size, in particular predation (Dunic & Baum, 2017). Predators are modelled to feed preferentially on prey sizes which are small enough to fit within their mouths, but large enough to maximise the energy gained.

#### *New Developments for NECCON*

FABM-MIZER has previously been set up to allow fishes to feed on plankton and other fishes (Bruggeman 2021; Powley et al. submitted), but not benthic fauna, and therefore fish are missing an important source of food. Consequently, the biomass of total fish was likely under-estimated. For NECCON, ERSEM-MIZER has been developed to include feeding on ERSEM benthic fauna. The benthic fauna within ERSEM are split into three functional groups, based on their feeding method: suspension feeders, deposit feeders and meiofauna. In addition, we have added the potential for variable fishing pressure across the domain, in contrast to previous constant fishing pressure across the whole domain.



<b>Project</b>	NECCTON No 101081273	<b>Deliverable</b>	D7.2
<b>Dissemination</b>	Public	<b>Nature</b>	Report
<b>Date</b>	14/10/2025	<b>Version</b>	1.0

FABM-MIZER will be two-way coupled to the new version of ERSEM developed in NECCTON (WPs 5 and 6). New developments relevant for FABM-MIZER are the addition of mesozooplankton diel vertical migration (DVM) to ERSEM (Clark et al., 2025). As fish are distributed vertically in FABM-MIZER according to the location of their prey, the reduction in predation that mesozooplankton might experience due to DVM is not currently represented when the models are two-way coupled. Other changes to ERSEM as part of NECCTON WP5 will not affect MIZER as directly, such as changes to dissolved organic carbon, the sinking rate of particulate organic matter and inclusion of the spectral light model (Clark et al., 2025).

#### *Model Formulations: State Variables, Equations, Parameters*

In this section we will focus on describing updates to MIZER and changes to ERSEM as a consequence of two-way coupling. A full description of ERSEM can be found in Butenschon et al. (2016) with updates as part of WP5 in NECCTON described in deliverable 5.2 (Clark et al., 2025). Equations for MIZER are extensively described in Blanchard et al. (2009; 2012; 2014) and Scott et al., (2014). Thus here we briefly describe the FABM implementation of MIZER with further details available in Powley et al. (submitted).

FABM-MIZER is run as a 2D depth-integrated model in the same spatial domain and horizontal grid as the NEMO-ERSEM model. All planktonic prey, from picophytoplankton to mesozooplankton are available to fish following their size-structure. Whilst all prey are in theory available to fish, the fish predominantly feed on the larger plankton (diatoms, microphytoplankton, microzooplankton and mesozooplankton) biomasses. In addition, as part of NECCTON, fish can also feed on the benthic fauna. The assigned size classes of pelagic and benthic prey are shown in Table 5. In order to convert between the 3D NEMO-ERSEM outputs and 2D FABM-MIZER it is assumed that fish mirror the vertical distribution of the prey from ERSEM. Fish will respond to the introduction of diel vertical migration of zooplankton by following them to depth during the day. Consequently, the avoidance by mesozooplankton of predation by fish through diel vertical migration is not currently modelled. Depth-resolved feedbacks allow for predation of plankton/benthic fauna by fish and production of waste produced by fish excretion and respiration to be added back into ERSEM (Figure 10).

Table 5. Wet mass ranges for benthic and pelagic ERSEM prey which fish predate on. Fish predation on benthic prey has been added to MIZER as part of NECCTON. Equivalent spherical diameters are given where appropriate in brackets.

<b>Functional group</b>	<b>Pelagic/benthic</b>	<b>Lower size range – Wet mass (g) (ESD <math>\mu\text{m}</math>)</b>	<b>Upper size range – Wet mass (g) (ESD <math>\mu\text{m}</math>)</b>
Meiofauna	Benthic	1e-9	1e-3
Suspension feeders	Benthic	1e-3	1e2
Picophytoplankton	Pelagic	4.188e-15 (0.2)	4.188e-12 (2)
Nanophytoplankton	Pelagic	4.188e-12 (2)	4.188e-9 (20)
Nanozooplankton	Pelagic	4.188e-12 (2)	4.188e-9 (20)
Microphytoplankton	Pelagic	4.188e-9 (20)	4.188e-6 (200)
Microzooplankton	Pelagic	4.188e-9 (20)	4.188e-6 (200)



<b>Project</b>	NECCON No 101081273	<b>Deliverable</b>	D7.2
<b>Dissemination</b>	Public	<b>Nature</b>	Report
<b>Date</b>	14/10/2025	<b>Version</b>	1.0

Diatoms	Pelagic	4.188e-9 (20)	4.188e-6 (200)
Mesozooplankton	Pelagic	4.188e-6 (200)	1e-3

Fish predate on pelagic ERSEM prey and benthic ERSEM prey as well as themselves. Fish are able to feed on the benthos once they reach a threshold size, reflecting that most demersal fish are pelagic during their juvenile stages. It is assumed that the proportion of time that fish spend feeding on the benthos depends on the ratio of pelagic plankton prey to total prey (plankton + benthic) biomass:

$$\sigma = \frac{\sum_{j=1}^7 P_j}{\sum_{j=1}^7 P_j + \sum_{i=1}^3 B_i}$$

where  $P_j$  represents the different pelagic ERSEM prey groups, and  $B_i$  represents the benthic ERSEM prey groups. The preference for feeding on benthic fauna is consequently emergent and avoids adding a fixed feeding preference parameter which would be based on limited data. The flexibility of this method also means that the model can be applied both on- and off-shelf, where benthic fauna biomasses differ by several orders of magnitude, due to vastly different bottom depths. Demersal fishes feed on suspension feeders and meiofauna, which live near or on the surface of the sediment. Fish do not feed on deposit feeders, as most deposit feeders in ERSEM are buried deep in the sediments and therefore not available to fish. Due to the differences in the way demersal fish feed, and differences in units of the benthic fauna, ( $\text{mg m}^{-2}$  vs  $\text{mg m}^{-3}$ ) a lower gamma value, representing the exponent used to calculate the volumetric search rate for a particular size of fish, was applied to the benthic fish. Note feeding on additional benthic groups will need to be added as a consequence of the developments carried out in WP6.

The model is run with 100 size classes of fish ranging from  $10^{-3}$  to  $10^6$  grams of wet mass. The modelled fish are in units of  $\text{mmol C m}^{-2}$  in order to be incorporated into FABM and couple with ERSEM. The original model equations from Blanchard et al., (2009) are in g wet mass and therefore a conversion factor of 0.12 gWM : mmol carbon is applied which assumes 10% of fish WM is carbon (Boudreau & Dickie, 1992). In addition to fish carbon, FABM-MIZER also needs to track phosphorus, nitrogen, silicon and oxygen. It is assumed that fish maintain a constant C:N:P stoichiometry and therefore N and P for fish are not state variables within the model. Instead, they are tracked within the sources and sinks. Fish uptake C, N and P through predation of prey. They produce ammonium, phosphate, carbon dioxide and particulate organic phosphorus and nitrogen, whilst consuming oxygen for respiration, with both the uptake and sources of nutrients fed back into ERSEM. As silicon is not part fish biomass, silicon is immediately egested after ingestion.

Prey capture and ingestion are formulated as a linear functional response without saturation or maximum (cf. Blanchard et al., 2014). Metabolic losses (e.g., maintenance) are implicitly accounted for by using a low efficiency (0.2) for prey-to-biomass conversion, rather than by an explicit standard metabolism loss (cf. Blanchard et al., 2014). Fish recruitment to the smallest size class of fish is relaxed to an expected density calculated by extrapolating the size spectrum of planktonic ERSEM prey, computed at run time using linear regression. If the new expected density is larger than current

<b>Project</b>	NECCON No 101081273	<b>Deliverable</b>	D7.2
<b>Dissemination</b>	Public	<b>Nature</b>	Report
<b>Date</b>	14/10/2025	<b>Version</b>	1.0

density, the current density is relaxed towards the expected density, whilst no relaxation is applied if the density is smaller. In order to achieve mass balance, any excess/supply of carbon/nitrogen/phosphorus needed for recruitment is returned/taken from the detrital particulate organic matter (POM) pool, in this case large POM.

Fishing was implemented by Powley et al., (in review) using a knife-edge approach following (Blanchard et al., 2012; Scott et al., 2014) whereby a constant fishing mortality ( $\text{yr}^{-1}$ ) is applied above a specific size of fish across the entire domain:

$$L = \sum_{i=1}^{100} F w_i \text{ if } w_i > w_{Fmin}$$

Where  $L$  is fish landings ( $\text{gWM m}^{-2} \text{yr}^{-1}$ ),  $F$  is the fishing mortality rate,  $w_i$  is the wet weight of fish and  $w_{Fmin}$  is the minimum weight of fish which are caught. In NECCON, the option of using a spatially varying fishing pressure has been implemented into the code:

$$L = \sum_{i=1}^{100} E_{x,y} w_i Q \text{ if } w_i > w_{Fmin}$$

where  $E_{x,y}$  is the fishing effort in a particular cell and  $Q$  is the effort to mortality ratio, converting the input fishing effort to a mortality rate. Using this method, either fishing effort or a spatially varying mortality rate can be used, in which case  $Q$  would equal 1. This method is similar to the methods used by the FISHMIP models (e.g. DPBM and ZOOMSS [https://github.com/Fish-MIP/Global\\_MEM\\_Model\\_Templates/tree/main](https://github.com/Fish-MIP/Global_MEM_Model_Templates/tree/main)). Tests will be undertaken using the two different fishing regimes.

#### *Model structure and required forcings and inputs; Implementation details*

The code for both the offline model and two-way coupling is written in Fortran and hosted on a public github repository (<https://github.com/pmlmodelling/fabm-mizer/tree/NECCON>). To incorporate the community size-based fish model with FABM, the source and sink terms for each size class of fish are computed, and provided as-is to the hydrodynamic model to be time-integrated using the same solver it uses for all other model variables. The model is built together with NEMO, FABM and ERSEM to produce one executable. As the model is two-way coupled, it uses exactly the same inputs as NEMO-ERSEM. The only additions are the inclusion of fish in the fabm.yaml file and restart files.

#### *Model specifics to HTL-LTL coupling*

##### *Parameters adjustments due to two-way coupling*

Following Powley et al., (in review) mesozooplankton cannibalism was turned off upon two-way coupling as this was considered a top-closure term within ERSEM and the natural mortality rates for mesozooplankton were set to zero. To ensure the survival of the mesozooplankton and consequently to stop fish biomass reducing too much Powley et al., (in review) used different volumetric search rates to those presented by Blanchard et al. (2009). Powley et al., (in review) used a volumetric search rate that was calculated from data from Acuna et al. (2011), adjusted for the size range of fish used in

<b>Project</b>	NECCON No 101081273	<b>Deliverable</b>	D7.2
<b>Dissemination</b>	Public	<b>Nature</b>	Report
<b>Date</b>	14/10/2025	<b>Version</b>	1.0

ERSEM-MIZER model and including data from both searching and filter feeding fish. A substantially lower volumetric search rate was applied for fish feeding on benthic fauna (Blanchard et al., 2009). The addition of predation by fish on benthic fauna also required changes to suspension feeder parameters as there was no explicit top closure term to represent predation by fish. Two changes were made, first an increase in the specific uptake rate which is poorly constrained from literature (Lessin et al. (in prep)). Additionally, large size particulate organic matter was included as a food source. Suspension feeders are already able to feed on medium-size particulate organic matter and based on the size range modelled, should be able to access larger particles too.

### 3.4.2 Application: Hindcast-Simulation

#### 3.4.2.1 Model configuration (Resolution, Boundary condition, Initial conditions, Model forcing)

ERSEM-MIZER is run on the same grid (AMM7; ~7km x 7km) and uses the same lower-trophic level boundary conditions and forcings as in NEMO-ERSEM. Initial conditions for fish are either created using an offline one-way coupled version of the model, run for 50 years using pyfabm and a hybrid python-fortran approach (computationally lightweight), or by spinning up the two-way coupled model on a 5 year repeating cycle, until a quasi-steady state is reached for both fish and ERSEM state variables (computationally expensive). The former uses output from the ERSEM baseline model whilst the later will use the same restart as used in the ERSEM baseline model. There is uncertainty in which method will be used due to initial tests indicating the two-coupled model and offline model produce substantially different results, and therefore the computationally more efficient option of using the offline model may not be sufficient.

Given the computationally expensive nature of running NEMO-ERSEM, initial testing of the developments to two-way coupled ERSEM-MIZER was carried out using a 1D hydrodynamic water column model (GOTM) at 3 different locations on the Northwest European shelf.

#### 3.4.2.2 Results

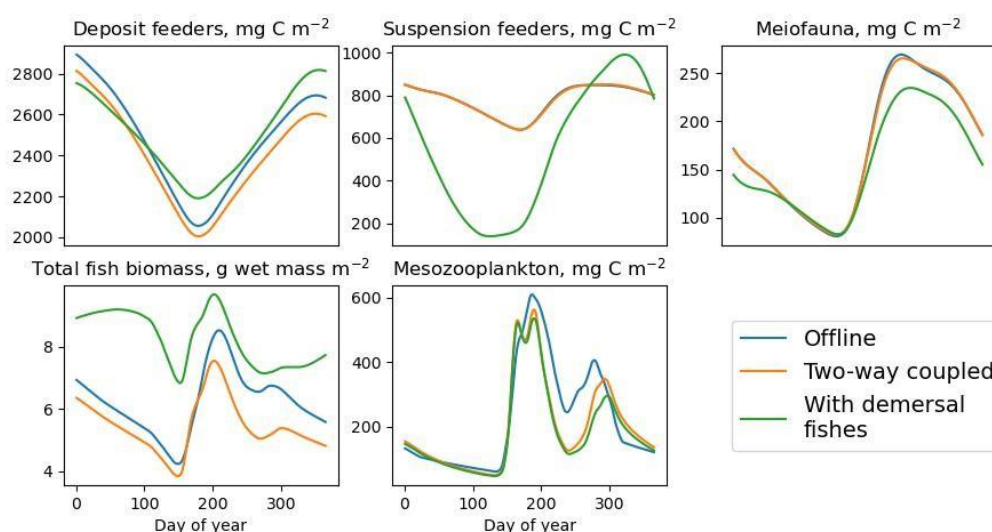


Figure 11. Impacts on different trophic levels when fish are two-way coupled. Lines show model output from offline FABM-MIZER and ERSEM (blue), original ERSEM-MIZER (yellow) and ERSEM-MIZER with new

<b>Project</b>	NECTON No 101081273	<b>Deliverable</b>	D7.2
<b>Dissemination</b>	Public	<b>Nature</b>	Report
<b>Date</b>	14/10/2025	<b>Version</b>	1.0

developments (green). The models were run with the water-column model GOTM, which provided the hydrodynamic forcing. Model runs used coordinates and meteorological inputs for the site Candyfloss, Celtic Sea.

When benthic fauna were included as an additional food source in two-way coupled ERSEM-MIZER, the average fish biomass increased and seasonality of fish biomass was reduced (Figure 11). Suspension feeders were affected by the newly included predation pressure from fish, which resulted in a lower average biomass across the year but with much higher variability across seasons. Deposit feeder biomass, meiofauna and mesozooplankton were largely unchanged with the inclusion of demersal fish.

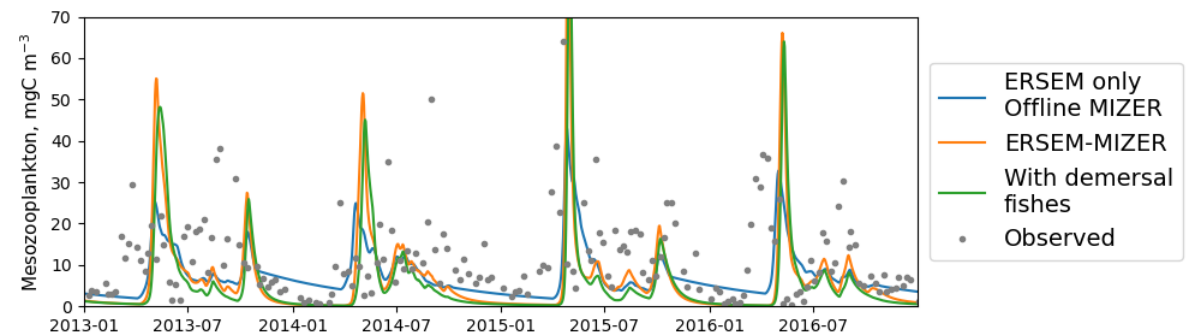


Figure 12. Mesozooplankton at L4, south of Plymouth. Models were forced by the hydrodynamic water-column model GOTM. Points show observations from the Western Channel Observatory dataset (McEvoy et al. 2023).

Previous work has indicated that mesozooplankton are a key variable in two-way coupled models as they experience additional mortality due to predation. We used observations from the Western Channel Observatory to validate our model and found good agreement between model versions and observations (Figure 12).

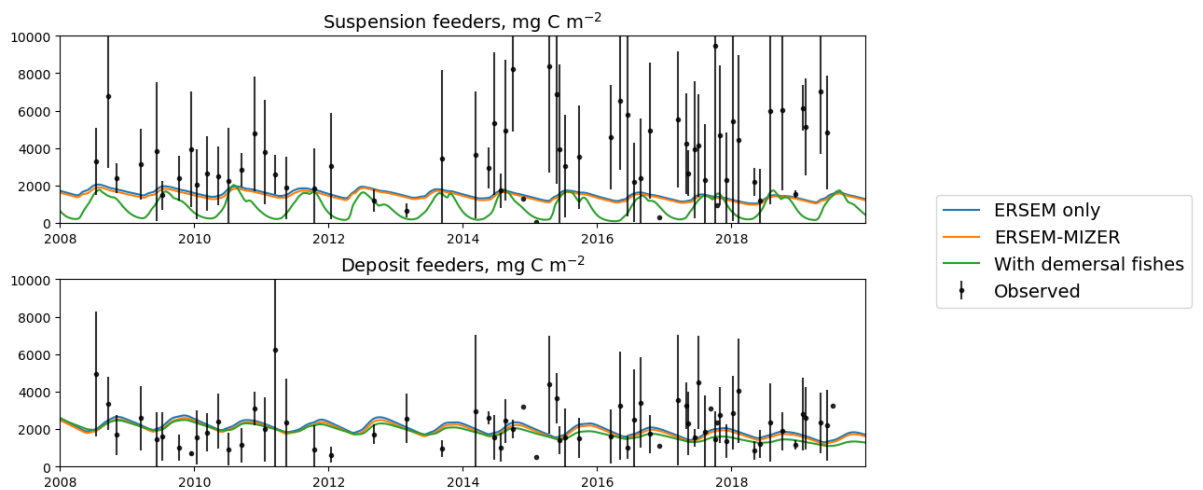


Figure 13. Suspension (top) and deposit feeders (bottom) at L4, south of Plymouth. Models were forced by the hydrodynamic water-column model GOTM. Observations are from the Western Channel Observatory dataset

<b>Project</b>	NECCTON No 101081273	<b>Deliverable</b>	D7.2
<b>Dissemination</b>	Public	<b>Nature</b>	Report
<b>Date</b>	14/10/2025	<b>Version</b>	1.0

(McEvoy et al. 2023). Points show the mean and error bars the standard deviation of approximately five replicates from each sampling trip.

When demersal fish feeding on benthic fauna are included in a two-way coupled model, benthic fauna experience additional mortality due to predation, which means alongside mesozooplankton, benthic fauna will also be a key variable in two-way coupled models. Modelled benthic macrofauna were generally in line with observations, although the average suspension feeder biomass was lower than observed, especially when predation by demersal fish was included (Figure 13). Conclusions cannot be drawn on modelled seasonality, as due to high spatially heterogeneity in the observations, no clear seasonal signal was observed (Lessin et al. (in prep)).

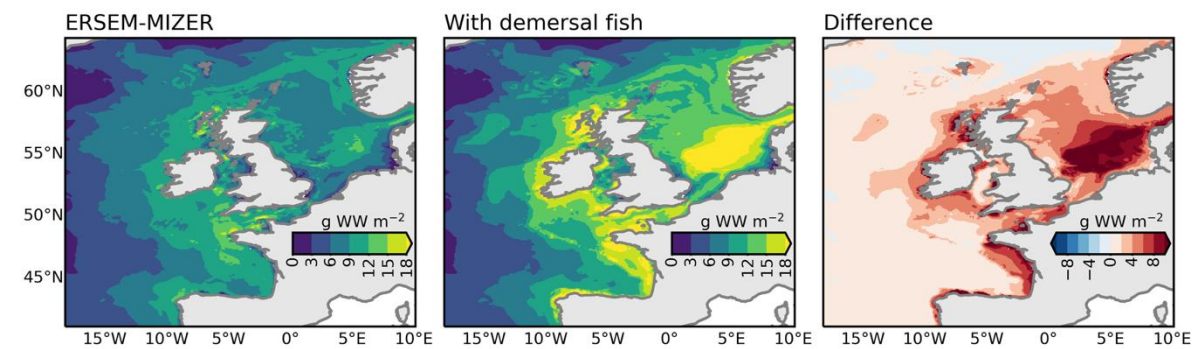


Figure 14. Fish biomass from two-way coupled ERSEM-MIZER forced by the hydrodynamic model NEMO on the Northwest European shelf. Results are shown from the original model, with demersal fish included, and with demersal fish included minus the original.

To test the new developments further, the hydrodynamic model NEMO was used to force two-way coupled ERSEM-MIZER both with and without demersal fish on the Northwest European shelf. The inclusion of demersal fish and the additional food sources they can access led to an increase in fish biomass, which was highest in the central southern North Sea and along the western coasts of France, Spain, Scotland and Ireland (Figure 14).

#### Calibration and Validation of hindcast simulations

Fish landings will be validated against spatial landing data from Gibin et al., (2024) and from ICES (2024). Additional validation will be undertaken on ERSEM state variables.

#### 3.4.3 NECCTON Products from the model

- Small pelagic fish biomass: sum of fish < 100g multiplied by omega (equation page 45) to dictate whether feeding on pelagic plankton biomass
- Unspecified fish biomass: sum of total fish biomass predicted by the model

#### 3.4.4 Discussion of pros and cons of the model

Pros:

- ERSEM-MIZER represents the entire ecosystem from photons to fisheries

<b>Project</b>	NECCOTON No 101081273	<b>Deliverable</b>	D7.2
<b>Dissemination</b>	Public	<b>Nature</b>	Report
<b>Date</b>	14/10/2025	<b>Version</b>	1.0

- Two-way coupling means impact of fish on lower trophic levels is explicitly represented. This means that bottom-up limitation in food availability is properly represented, improving the representation of fish.
- Whole community of fish represented including pelagic planktivores, pelagic piscivores and demersal feeders.

#### Cons:

- Horizontal migration of fish is not included within the model, with fish staying within their 7km grid cell. Consequently, fish biomass in a given cell is entirely dependent on the resource spectrum of the pelagic plankton within that cell. This leads to underprediction of fish biomass/landings in areas where migratory fish are important.
- No inferences on particular species of fish are available from the model. Thus the collapse of fish stocks from climatic and anthropogenic pressures will not be represented as the fish stock may be replaced by another species of fish and thus total biomass may not change.
- Fish recruitment is entirely dependent on the pelagic size spectrum: There is no straightforward relationship between egg production and the biomass in larger (“adult”) size classes – reproductive effort per size class would depend on species composition, which is unknown. Thus it is not possible to calculate a maximum sustainable yield for fisheries management.

### 3.5 SEAPODYM-LMTL (Leading partner: CLS)

#### 3.5.1 Model description

SEAPODYM-LMTL is a numerical model of low and mid-trophic levels of the ocean ecosystem, respectively zooplankton and micronekton groups. It has been described in Lehodey et al. (2010; 2015), Conchon (2016) and used to run Observing System Simulation Experiments (OSSEs) to explore how data sampling could help to estimate the model parameter values and the global biomass of these functional groups (Delpech et al. 2020). It is based on the energy transfer across the food web (Iverson, 1990) with a simplified view of the global marine ecosystem. Phytoplankton production (Net Primary production, NPP) is the source of energy and zooplankton and micronekton are represented by functional groups in three vertical layers: the epipelagic, upper meso- and lower meso-pelagic layers. Temperature and horizontal currents determine the population development (growth, mortality) and the spatial dynamics (Lehodey et al., 2010, 2015). The euphotic depth ( $Z_{eu}$ ) is used to define the vertical layers inhabited by resident and migrant organisms: the epipelagic layer between surface and  $1.5 * Z_{eu}$ , the upper mesopelagic layer between  $1.5$  und  $4.5 * Z_{eu}$ , and the lower mesopelagic layer between  $4.5$  and  $10.5 * Z_{eu}$  (hereafter referred to as L1, L2 and L3 respectively). These definitions have been validated using a large dataset of acoustic data (Lehodey et al., 2015; Conchon et al., 2016).

Temperature and currents are averaged over these three layers. In the following, we use the notation T1, T2, T3 for temperatures averaged in layer 1, 2 and 3 respectively. Unlike the resident functional groups, the migrant micronekton functional groups perform diel vertical migrations and are exposed to different temperature and currents conditions in the vertical layers. This daily vertical migration, which takes place all over the world ocean can be seen as the biggest animal daily migration on Earth

<b>Project</b>	NECCTON No 101081273	<b>Deliverable</b>	D7.2
<b>Dissemination</b>	Public	<b>Nature</b>	Report
<b>Date</b>	14/10/2025	<b>Version</b>	1.0

and notably impacts the ocean carbon cycle by actively exporting carbon below the mixed layer (Bianchi et al., 2013; Pinti et al. 2021). Micronekton also constitute a key intermediate trophic level of the oceanic food web. They feed mostly on zooplankton and are the main prey of marine large predators, some of which are of crucial economic importance (Cf section 3.14: seapodym-tuna application). Despite their pivotal position, knowledge on micronekton remains fragmented with only a few rough estimates of biomasses and a very large range of uncertainty, e.g. between 1 and >10 billion tons globally for migrant mesopelagic organisms (Irigoyen et al., 2014; Proud et al., 2019).

### 3.5.2 Application: Global hindcast simulation of ocean micronekton

#### 3.5.2.1 Model configuration

According to the layers inhabited in the daytime and night-time (nomenclature: Layerday.Layernight), the model simulates three resident and three migrant micronekton functional groups: epipelagic (L1.L1), upper mesopelagic (L2.L2), lower mesopelagic (L3.L3), migrant upper mesopelagic (L2.L1), migrant lower mesopelagic (L3.L2) and highly migrant lower mesopelagic (L3.L1). The model domain is global with a monthly resolution and a spatial resolution of a quarter of a degree. The time series of the simulation extends from January 1998 to December 2019. Prior to vertical averaging, 3D temperature and currents are taken from the FREE-GLORYS ocean simulation, produced by Mercator Ocean International using the ocean general circulation model NEMO (Madec et al., 2008) in a configuration without data assimilation (Lellouche et al., 2021). NPP (mmolC/m<sup>2</sup>/day) is computed with VGPM (Vertical Generalized Production Model, Behrenfeld and Falkowski, 1997), from satellite chlorophyll-a concentration. As there is no reliable satellite chlorophyll data in winter for latitudes above ~ 60° due to sun glint, cloud coverage, and low light levels (e.g. Gregg & Casey, 2007), the dataset has been completed in high latitudes by a biogeochemical product using chlorophyll from PISCES biogeochemical model (Aumont et al., 2015) to avoid gaps in forcing data.

To facilitate the validation and future parameter estimations and data sampling, a method has been developed to characterize large biophysical biomes where homogeneous species communities can be assumed to occur given the same bio-physical environmental conditions. More details on the method and configuration are provided in a publication (Albernhe et al. 2024).

#### 3.5.2.2 Results

The spatial distribution of the reference biophysical biomes shows mostly latitudinal structure with the addition of areas influenced notably by upwelling (Figure 15). The six biophysical biomes can be categorized as follow:

- Biome 1. The tropical biome extends roughly between latitudes 20°N and 20°S in the three oceans. It is characterized by the warmest and most stratified waters associated with relatively low biological production (below 25 mmolC/m<sup>2</sup>/day).
- Biome 2. The subtropical biome is mostly centered around 30°N and 30°S in all basins. It is characterized by warm water temperatures combined with relatively high stratification and production.



<b>Project</b>	NECCTON No 101081273	<b>Deliverable</b>	D7.2
<b>Dissemination</b>	Public	<b>Nature</b>	Report
<b>Date</b>	14/10/2025	<b>Version</b>	1.0

- Biome 3. The eastern boundary coastal upwelling systems display lower epipelagic layer temperature than Biomes 1 and 2, moderate stratification, and is the most productive biome.
- Biome 4. The oceanic mesotrophic systems display an average epipelagic layer temperature as well as a stratification close to Biome 3 but only half of its biological productivity.
- Biome 5. The sub-polar biome is weakly stratified and productive. It covers the cold waters of the Arctic and Southern Oceans, roughly between 40° and 60° in latitudes.
- Biome 6. The polar biome displays the weakest stratification, and the lowest epipelagic layer temperature than any other biomes and extends from latitude 60° to the poles. The NPP is also the lowest of all biomes.

Detailed biomass by group have been computed for each biome and provinces (Table 6). The total biomass of migrant mesopelagic (lower+ upper) biomass is estimated to 0.96 Gt, ie in the lowest range of other estimates. When adding the non-migrant groups, the global biomass reaches 2.82 Gt.

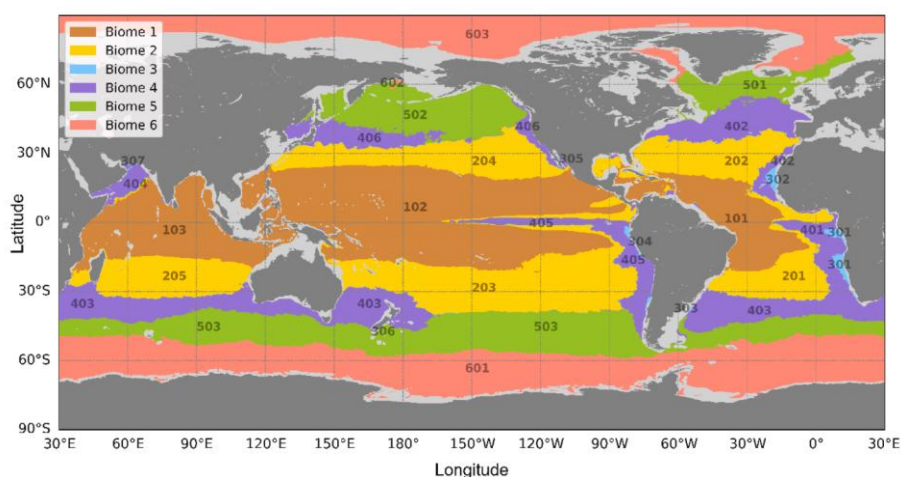


Figure 15 . Map of reference biophysical biomes (by color) and associated provinces by ocean and hemisphere (numbering). Grey areas delineate the domain where the depth of the water column is not sufficient to ensure the existence of the three pelagic layers of SEAPODYM-LMTL. Redrawn from Albernhé et al (2024).

Table 6 Biomass of micronekton groups by biome and province (From Albernhé et al 2024)



<b>Project</b>	NECCON No 101081273	<b>Deliverable</b>	D7.2
<b>Dissemination</b>	Public	<b>Nature</b>	Report
<b>Date</b>	14/10/2025	<b>Version</b>	1.0

Biome	Province	Province's mean surface area in million km <sup>2</sup> (and % of total)	Province's mean migrant biomass (Million tons WW)	Province's mean total biomass (Million tons WW)
1	101	16.8 (5.14%)	29.99	102.19
	102	62.2 (19.08%)	88.26	314.64
	103	21.2 (6.51%)	30.66	111.03
	Sub-total	100.2 (30.73%)	148.90	527.86
2	201	10.3 (3.16%)	36.33	101.27
	202	14.4 (4.41%)	30.03	89.58
	203	33.1 (10.14%)	86.69	253.53
	204	14.9 (4.58%)	50.81	141.88
	205	14.3 (4.40%)	35.87	96.70
	Sub-total	87.0 (26.68%)	239.72	682.96
3	301	0.79 (0.24%)	4.21	15.32
	302	0.46 (0.14%)	1.82	7.45
	303	0.28 (0.08%)	1.39	4.26
	304	0.48 (0.15%)	2.29	8.55
	305	0.17 (0.05%)	0.86	3.01
	306	0.14 (0.04%)	0.46	1.45
	307	0.41 (0.13%)	1.13	3.94
	Sub-total	2.72 (0.84%)	12.16	43.98
4	401	3.05 (0.93%)	15.72	49.46
	402	6.65 (2.04%)	25.68	74.34
	403	20.1 (6.16%)	100.36	262.45
	404	1.90 (0.58%)	4.65	15.80
	405	5.88 (1.80%)	25.85	82.01
	406	6.47 (1.98%)	31.38	92.29
	Sub-total	44.0 (13.51%)	203.64	576.35
5	501	4.60 (1.41%)	21.03	58.96
	502	9.15 (2.80%)	54.39	151.01
	503	39.5 (12.10%)	176.32	455.25
	Sub-total	53.2 (16.31%)	251.74	665.22
6	601	29.5 (9.04%)	81.25	244.33
	602	2.82 (0.87%)	20.24	56.39
	603	6.62 (2.03%)	5.69	26.51
	Sub-total	38.9 (11.93%)	107.17	327.23

### 3.5.2.3 Validation of global simulation

Direct observations of the micronekton rely mainly on trawl sampling, which are costly and complex deep-water operations to perform. The method is known to be subject to biases due to avoidance and poor catchability of some species and the destruction of the more fragile organisms. Net catchability also strongly depends on mesh sizes and trawling speed. Indirect observations through ship-borne acoustic echosounders are a non-destructive alternative approach which presents the advantage of covering large ocean areas (Haris et al., 2021). The model biomass estimate by group is largely controlled by the energy transfer coefficient between the NPP and the micronekton group. These parameters have been calibrated against direct biomass estimates (Lehodey et al 2010; Table 7) and acoustic transects (Lehodey et al 2015).

<b>Project</b>	NECCTON No 101081273	<b>Deliverable</b>	D7.2
<b>Dissemination</b>	Public	<b>Nature</b>	Report
<b>Date</b>	14/10/2025	<b>Version</b>	1.0

Table 7 Estimates of local mesopelagic fish biomass from the literature and comparison with SEAPODYM-LMTL estimates (CMEMS QUID: LMTL product, 2024).

Region Period	Referen ce	Sampling	Method	Range of biomass (m <sup>2</sup> )	Correction (gWW m <sup>-2</sup> )	Model average (gWW m <sup>-2</sup> )
<b>California Current 2010-2012</b>	Davison et al (2015)	35°N- 30°N; 124°W- 118°W	Acoustic model (18 and 38 kHz) with trawling Mesopelagic fish	25– 37 gWW	<b>12-28</b> <sup>(1)</sup>	<b>13.16</b> Average sum of all 5 mesopelagic groups
<b>Northeast Atlantic (Canary) 24 Mar- 2 Jun 2011</b>	Ariza et al (2015)	28°31'N; 15°22'W	Trawling acoustic (120 kHz) as indicator of vertical structure. All migrating organisms in the epipelagic layer	0.2 ±0.06 gC <sup>(2)</sup>	<b>2.4 ±0.7</b>	<b>2.79</b> Average sum in epipelagic layer at night
<b>Western Tropical Pacific Mar -Apr 2010</b>	Suntsov & Domokos (2013)	10°N-17°N 144°E- 147°E	Trawling (IKMT) Night 0-200 m (All mnk) 0.8-1.2 mg m <sup>-3</sup>	0.16-0.24 g WW (night 0- 200 m)	<b>0.8-1.2</b> <sup>(3)</sup>	<b>0.87</b> Sum in epipelagic layer at night
<b>North Atlantic (Azores) 20 Jun–6 Jul 2009</b>	Cook et al (2013)	53°N 35°W	Trawling; data between 0-700 m only are selected. 0.009 g m <sup>-3</sup> in 0- 200 m 0.0045 g m <sup>-3</sup> in 200-700 m	4.05 g WW (0-700 m)	<b>20</b> <sup>(3)</sup>	<b>3.70</b> All groups
<b>Western tropical Pacific Nov-Dec 1998</b>	Hidaka et al (2003)	2°N–20°N 125°–160°E	Trawling; commercial-sized midwater otter trawl 70 m long 0-200 m	St7: 0.212 St15: 0.388 St16: 0.192 gWW	<b>0.57 -1.16</b> <sup>(4)</sup>	<b>1.14</b> Average sum in epipelagic layer at night
<b>East and South off New Zealand (Continental Plateau) Dec 2000- Jan 2001</b>	McClatchie & Dunford (2003)	Mernoo & Snares	Trawling and acoustic (38 kHz) Mesopelagic fish only	13.4-18.2 gWW	<b>13.4-18.2</b>	<b>15.58</b>
		East		0.4 gWW	<b>0.4</b>	<b>11.33</b>
		Campbell		0.3 gWW	<b>0.3</b>	<b>7</b>
<b>Tasman Sea 2004-07</b>	Kloser et al (2009)	148°E- 172°E; 41°S-45°S	Trawling and acoustic (38 and 120 kHz) Mesopelagic fish only	16-29 gWW	<b>16-29</b>	<b>12.79</b> Average of the sum of all 5 mesopelagic groups
<sup>(1)</sup> After removing 2 cruises likely biased by the presence of siphonophores. <sup>(2)</sup> Correction from the authors for sampling efficiency: 14% for gas-bearing animals and 38% and 80% for large and small none-gas-bearing animals, respectively <sup>(3)</sup> Correction for sampling efficiency: 20% (IKMT trawl) <sup>(4)</sup> Correction for sampling efficiency: 33% (commercial-sized midwater otter trawl)						

Acoustic methods provide a proxy for micronekton density along the water column, although the interpretation is challenging and can be biased (Benoit-Bird and Lawson, 2016; Barbin et al., 2024). Nevertheless, detecting shifts or re-organizations in the backscatter intensity vertical structure is a useful tool for identifying ecosystem changes.

The provinces boundaries and their homogeneity within these boundaries have been validated using a database of 394 echo integrated acoustic transects collected between 2006 and 2019 (Albernhe et al 2024). In 93,8% of the cases (N = 1983), the null hypothesis is rejected indicating that the acoustic data distributions are significantly different between the two biophysical biomes crossed by an

<b>Project</b>	NECCTON No 101081273	<b>Deliverable</b>	D7.2
<b>Dissemination</b>	Public	<b>Nature</b>	Report
<b>Date</b>	14/10/2025	<b>Version</b>	1.0

acoustic transect. In 61.76% of all the cases (N = 3639), the variance of acoustic data within a biome is significantly smaller than the variance over a whole transect crossing two biomes.

### 3.5.3 NECCTON products

The model outputs are the biomass distribution of each functional group vertically integrated and expressed in gram of wet weight by square meter (equivalent to metric ton by km<sup>2</sup>), in standard gridded NetCDF format (Table 8).

Table 8 Outputs from the SEAPODYM-LMTL model.

Functional group name	Day layer	Night layer	Notations used	Short name	Unit
Epipelagic micronekton	1	1	D1N1 or 1.1	mnkc_epi	g WW m <sup>-2</sup>
Upper mesopelagic micronekton	2	2	D2N2 or 2.2	mnkc_umeso	
Migrant upper mesopelagic micronekton	2	1	D2N1 or 2.1	mnkc_mumeso	
Lower mesopelagic micronekton	3	3	D3N3 or 3.3	mnkc_lmeso	
Migrant lower mesopelagic micronekton	3	2	D3N2 or 3.2	mnkc_mlmeso	
Highly migrant lower mesopelagic micronekton	3	1	D3N1 or 3.1	mnkc_hmlmeso	

### 3.5.4 Discussion of pros and cons of the model

#### Pros

- Bridges trophic levels: Provides an explicit, mechanistic link from physical–biogeochemical drivers to mid-trophic prey fields that can feed higher-trophic models (e.g., tunas), enabling end-to-end applications.
- Structured functional groups & DVM: Represents micronekton as six functional groups across three pelagic layers, distinguished by diel vertical migration (DVM) behavior—capturing key vertical habitat structure often missing from LTL models.
- Physics-aware transport: Uses advection–diffusion–reaction equations driven by currents, temperature and primary production, so biomass patterns emerge from realistic environmental forcing.
- Parameter optimization with various datasets: Include a robust and computationally efficient method to estimate parameters from biomass estimates or acoustic data.
- Operational readiness: Produced as global gridded fields (e.g., for Copernicus Marine), facilitating downstream use and scenario studies.

<b>Project</b>	NECCON No 101081273	<b>Deliverable</b>	D7.2
<b>Dissemination</b>	Public	<b>Nature</b>	Report
<b>Date</b>	14/10/2025	<b>Version</b>	1.0

## Cons

- Coarse biological simplification: Aggregating diverse taxa and sizes into six functional/DVM groups and three layers risks missing community and size-spectrum nuances, especially regionally.
- Assume large scale temperature-related mortality rates without details in regional / temporal predation pressures locally.
- Strong dependence on forcing quality: Skill can hinge on accuracy of currents, temperature and NPP limiting realism in certain regions/times.
- Acoustic calibration uncertainties: Optimization against acoustics inherits frequency-, taxon- and depth-dependent biases of backscatter, and sparse coverage, which can propagate into biomass estimates.
- Limited near-coastal/topographic fidelity: Currently tuned for open-ocean layers and DVM. It may under-represent shelf, seamount, or boundary-current complexities where behaviors and communities differ.

## 3.6 ECOSMO E2E (Leading partner: HEREON)

### 3.6.1 Model Description

#### 3.6.1.1 Introduction and biological basis Model Formulations

The ECOSMO E2E model (Daewel et al., 2019) integrates biogeochemical and food web processes into a single, fully coupled NPZD-HTL framework to simulate fish and macrobenthos production. It explicitly represents fish and macrobenthos as functional groups. The biogeochemical component includes the three major nutrient cycles (nitrogen, phosphorus, and silica), and equations for oxygen, biogenic opal, detritus, and dissolved organic matter. The model features three phytoplankton (diatoms, flagellates, and cyanobacteria), two zooplankton (herbivore and omnivore), two fish (predominantly planktivorous; predominantly pisci-benthivorous), and one macrobenthos functional group. The fish and macrobenthos are defined by feeding preferences, rather than species-specific traits. This aligns with the widely adopted functional group-based modelling approach for phytoplankton and zooplankton, ensuring consistent feedback across trophic levels (Figure 16). The model was originally implemented in the North Sea and the Baltic Sea and was shown to capture the spatial and seasonal patterns that align with the current knowledge of these ecosystems.

Fish distribution and production are based on vertically integrated prey availability. Fish biomass and production are redistributed at each time step based on prey distribution. Grazing rates for the fish on the vertically integrated prey ( $P_X$ ) is given by  $G_{Fi}(P_X) = \sigma_{Fi,X} \frac{a_{Fi,X} P_X}{r_{Fi} + P_X}$ , where,  $\sigma_{Fi,X}$  is the grazing rate for prey X,  $a_{Fi,X}$  is the feeding preference of fish for prey X,  $r_{Fi}$  is the half saturation coefficient. The total fish consumption is calculated using the vertically integrated prey biomass ( $P_X$ ). This is then redistributed across depth levels in each grid cell based on the actual vertical distribution of prey ( $C_X$ ) as follows,  $R_{Fi(cons)} = P_{Fi} \left( \sum_{X=1}^n G_{Fi}(P_X) \times \frac{C_X}{P_X} + [G_{Fi} C_{MB}]_{z=bottom} \right)$ . Finally, the conservation

<b>Project</b>	NECCON No 101081273	<b>Deliverable</b>	D7.2
<b>Dissemination</b>	Public	<b>Nature</b>	Report
<b>Date</b>	14/10/2025	<b>Version</b>	1.0

equation for fish biomass is as follows,  $\frac{\partial C_{Fi}}{\partial t} + w_m(z) \frac{\partial C_{Fi}}{\partial z} = \gamma_{Fi} R_{Fi(cons)} - m_{Fi} C_{Fi} - \epsilon_{Fi} C_{Fi} - \text{predation loss}$ .

The first term on the RHS of the above equation represents the fish production rate as a product of assimilation efficiency ( $\gamma_{Fi}$ ) and the total consumption ( $R_{Fi(cons)}$ ). The second term on the RHS is the linear fish group mortality rate ( $m_{Fi} C_{Fi}$ ). The third term on the RHS, the Biomass loss due to excretion ( $\epsilon_{Fi} C_{Fi}$ ) is parameterised as a function of temperature (following Gillooly et al., 2001; Clarke & Johnston, 1999) as follows,  $\epsilon_{Fi} = \mu_{Fi} e^{\frac{\theta_{Fi}}{k} \times \frac{T-T_0}{T \times T_0}}$ . Here, T is the temperature in K,  $T_0$  is the reference temperature (273.15 K), k is the Boltzmann factor,  $\mu_{Fi}$  is the fish excretion rate, and  $\theta_{Fi}$  is the temperature control excretion parameter. The second term in the LHS of the equation represents the vertical migration of fish. The vertical migration speed of fish ( $w_m$ ) is determined implicitly by the vertical distribution of fish biomass as a function of the distribution of prey in the water column.

Macrobenthos (MB) is represented as a functional group located in the bottom layer of the model. It feeds on resources available near the seabed, including diatoms and flagellates, micro- and mesozooplankton, detritus, DOM, and organic sediments. The total consumption by MB is the sum of its consumption from each prey type. The grazing rate of macrobenthos on a given prey (X) is calculated using the equation:  $G_{MB}(C_X) = \sigma_{MB,X} \frac{a_{MB,X} C_X}{r_{MB} + F_{MB}}$ . Here,  $F_{MB} = \sum_{X=1}^n a_{MB,X} C_X$  is the total food available.  $\sigma_{MB,X}$  is the grazing rate for prey X,  $a_{MB,X}$  is the feeding preference of MB for prey X,  $r_{MB}$  is the half saturation coefficient.

The total consumption rate of macrobenthos is calculated by adding the consumption rates of all individual prey items:  $R_{MB(cons)} = C_{MB} (\sum_{X=1}^n G_{MB}(C_X))$ .

The macrobenthos production rate is a product of assimilation efficiency ( $\gamma_{MB}$ ) and the total consumption ( $R_{MB(cons)}$ ). The loss due to mortality ( $m_{MB} C_{MB}$ ) and excretion ( $\epsilon_{MB} C_{MB}$ ) are linearly depended on  $C_{MB}$ . The predation loss of MB due to fishes are defined in the fish module. Similarly, the macrobenthos module imposes a predation loss of  $C_{MB} G_{MB}(C_X)$  on prey X. The conservation equation for macrobenthos is given by,

$$\frac{dC_{MB}}{dt} = \left[ \gamma_{MB} C_{MB} \left( \sum_{X=1}^n G_{MB}(C_X) \right) - m_{MB} C_{MB} - \epsilon_{MB} C_{MB} - \text{predation loss} \right]_{z=bottom}$$

As a part of the NECCON project, formulations for macrobenthos and fish were separated from the LTL-ECOSMO code and independent modules were developed in the framework of FABM, with the aim to allow its use in the context of various LTL models. The modules applicability has been demonstrated to be compatible with other lower-trophic-level modelling systems such as the ERSEM and ERGOM (Vijayakumaran et al., 2025). Its modular design enables flexible definition of predation and mortality targets, allowing the model to be easily portable to different marine systems. The module includes fish and macrobenthos functional groups as the two state variables, which are

<b>Project</b>	NECCON No 101081273	<b>Deliverable</b>	D7.2
<b>Dissemination</b>	Public	<b>Nature</b>	Report
<b>Date</b>	14/10/2025	<b>Version</b>	1.0

seamlessly coupled with lower-trophic-level components such as prey (diatoms, flagellates, omnivorous and heterotrophic zooplankton, and detritus), and mortality and excretion targets (detritus, DOM, ammonium, and phosphate). Dissolved oxygen serves as the respiration target. A fish migration algorithm has been developed recently by Daewel et al. (2025, in preparation) for the Norwegian and Barents Seas, making it possible to simulate the horizontal movement of fish groups in response to prey-predation changes.

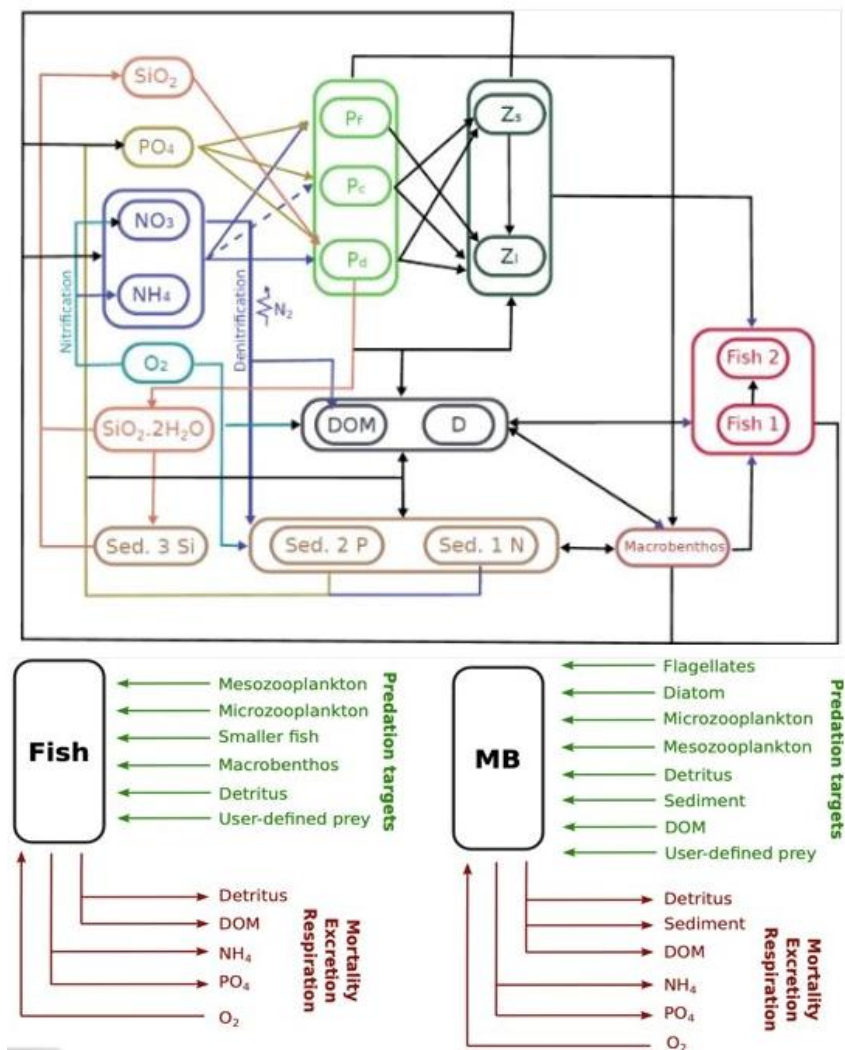


Figure 16. Simplified schematic diagram of the ECOSMO E2E fish and macrobenthos modules, illustrating the energy flow (top) and required inputs for coupling with the LTL model host (bottom).

The parameters used in the macrobenthos and fish modules include: mortality rate, excretion rate, grazing half-saturation constant, temperature sensitivity coefficient, assimilation efficiency, grazing rate on prey items, and feeding preference for prey items. Assimilation efficiency is specified to determine the proportion of ingested food that is incorporated into fish biomass. Grazing is



<b>Project</b>	NECCON No 101081273	<b>Deliverable</b>	D7.2
<b>Dissemination</b>	Public	<b>Nature</b>	Report
<b>Date</b>	14/10/2025	<b>Version</b>	1.0

parameterized through specific ingestion rates and feeding preferences for multiple prey sources, including detritus, macrobenthos, and planktonic or other fish prey. Feeding preferences define the relative allocation of grazing pressure across different prey types, and half-saturation constants regulate the functional response of grazing with respect to prey concentration. Additionally, the model includes a parameter specifying the number of prey types available to the fish group, allowing for explicit representation of trophic interactions within the ecosystem. The model parameters are defined in a fabm.yaml file. A parameterisation toolbox for 1D ECOSMO E2E based on Particle Swarm Optimiser implemented in FABM is available in Nguyen et al., 2024.

#### *3.6.1.2 Model structure and required forcings and inputs*

ECOSMO E2E is written in object-oriented Fortran and is compatible with FABM version 2.0. The model code is available from <https://codebase.helmholtz.cloud/GCOAST/ecosmoe2e>.

#### *3.6.1.3 Model specifics to HTL-LTL coupling*

ECOSMO E2E is a two-way coupled model; all trophic levels are simulated simultaneously within the same framework and time steps. As a result, no unit conversions are needed between model components. Offline coupling is not possible.

The separate modules of fish and macrobenthos can only be used if coupled to a lower trophic level model as it requires the direct coupling to the input and output targets. The whole ecosystem model needs to be coupled to a physical base model to provide information on environmental characteristics. As this is ensured through the coupling via FABM both implementations in 1D and 3D are possible. This also includes that initial and boundary conditions for the relevant state variables are required. Further, the fish module can be used multiple times in the fabm.yaml file to generate multiple fish functional groups.

We suggest to reduce the natural mortality rate for the zooplankton functional groups by 20-25% to account for the additional predation mortality from the HTL model components.

### **3.6.2 Application: Hindcast-Simulation**

#### *3.6.2.1 Model configuration (Resolution, Boundary condition, Initial conditions, Model forcing)*

The model hindcast simulations using ECOSMO-E2E will be provided for the Arctic Ocean and the Baltic Sea. The model set up for the Arctic Ocean is based on NERSC-HYCOM-CICE TOPAZ operational forecasting framework (<https://github.com/nansencenter/NERSC-HYCOM-CICE.git>). The physical model coupled to ecosystem model (based on ECOSMO II lower-trophic level model), used for operational forecast under CMEMS was validated against in situ observations, remotely sensed data and bio-ARGO data (Yumruktepe et al, 2022). The horizontal grid extends from 10°S to the north pole, with the horizontal resolution varying from 1/6 to 1/16 degrees (~11-16 km). The physical fields are initialised from WOA5 climatology and the surface atmospheric forcings are obtained from ERA5 (0.1 degrees, 6 hourly). The hindcast simulation will be performed for 1980–2020 and include two fish functional groups initialised at uniform biomass. The first group is planktivorous, grazing primarily on herbivorous and omnivorous zooplankton; the second is piscivorous and macrobenthivorous, preying

<b>Project</b>	NECCON No 101081273	<b>Deliverable</b>	D7.2
<b>Dissemination</b>	Public	<b>Nature</b>	Report
<b>Date</b>	14/10/2025	<b>Version</b>	1.0

mostly on the planktivores fishes and benthic macrofauna. A migration routine is implemented for the first fish group. The migration is parameterised based on the prey-predation ratio accounting for food availability and competition (Daewel et al., in preparation, 2025).

ECOSMO-E2E is coupled to NEMO-ERGOM modelling system in the Baltic Sea. NEMO (Nucleus for European Modelling of the Ocean) version 4.2.1 is a 3D physical model. The system covers the whole Baltic Sea and part of the North West Shelf to get a good representation of the water exchange at the inflow into the Baltic Sea basin in the Skagerrak. It has a horizontal resolution of 0.017 deg in North-South direction and 0.028 deg in East-West direction, which is about 1 nm. The Model has 56 depth layers. Atmospheric forcing comes from ERA5 reanalysis. ERGOM (Ecological Regional Ocean Model) is an NPZD-model based on nitrogen and phosphorus cycles. It includes three phytoplankton functional groups (diatoms, flagellates and cyanobacteria), one zooplankton group. The hindcast is run for 2018-2020 in 90 seconds time steps and provides daily output.

### 3.6.2.2 Calibration and Validation of hindcast simulations

The figures (Figure 17, Figure 18 and Figure 19) provide details of validation of the ECOSMO E2E model, demonstrating its ability to represent fish biomass and nutrient variability in the North and Norwegian Seas. Detailed validation of the model in the North Sea, and Norwegian Sea are available in Daewel et al., (2019) and Daewel et al., (2025, in preparation), respectively.

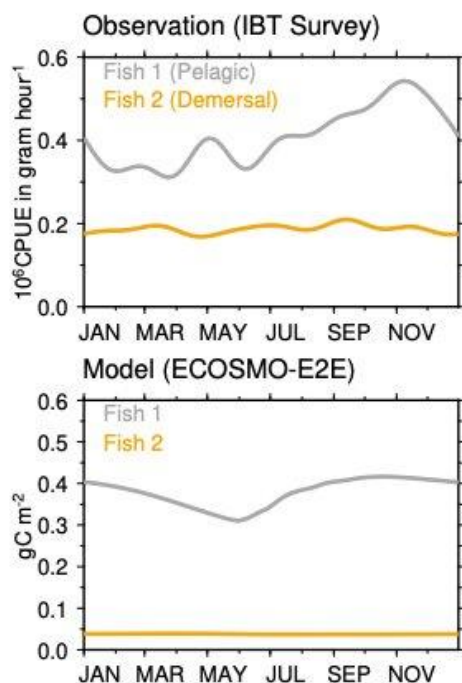


Figure 17. Pelagic and demersal fish biomass estimated from International Bottom Trawl survey ICES, 2012; <http://www.ices.dk/Pages/default.aspx>, last accessed May 2012) and the simulated biomasses of water-column integral of planktivorous fish 1 and benthic-piscivorous fish 2 during an annual cycle in the North Sea. (Daewel et al. (2019) sorted the IBT fish data into pelagic and demersal groups. A climatology of the variables from IBT



<b>Project</b>	NECTON No 101081273	<b>Deliverable</b>	D7.2
<b>Dissemination</b>	Public	<b>Nature</b>	Report
<b>Date</b>	14/10/2025	<b>Version</b>	1.0

survey for the North Sea is shown here. A 1D water-column integration of GOTM-ECOSMO-E2E for the central North Sea is used here.

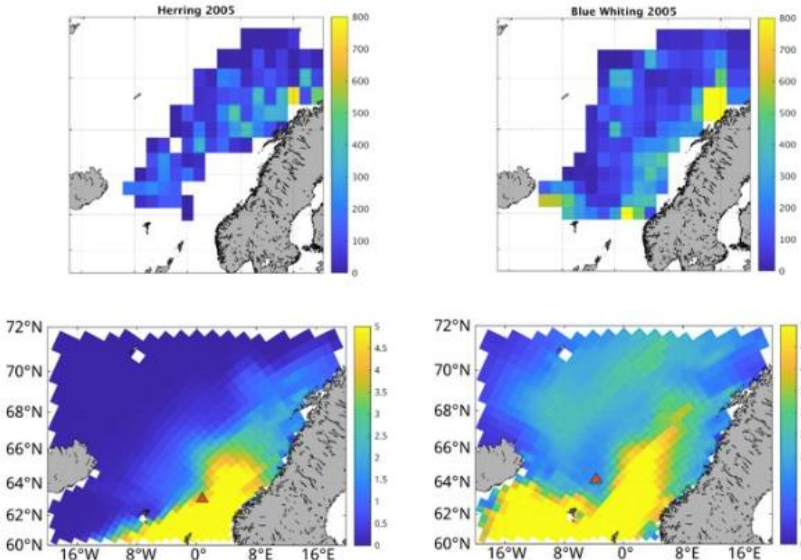


Figure 18. Comparison between simulated distributions of Fish 1 (predominantly planktivorous) and Fish 2 (predominantly benthopiscivorous) with acoustic survey observations of Blue Whiting and Herring in the Norwegian Sea during May–June 2005 (Huse et al., 2015). The model includes a migration scheme for Fish 1. This Figure is adapted from Daewel et al. (2025, in preparation). The modelled fish biomass in the bottom row are given in  $\text{gC m}^{-2}$ . The observed biomass (top row) is given in the Nautical Area Scattering Coefficient (NASC,  $\text{m}^2 \text{nmi}^{-2}$ ). It is the depth-integrated acoustic backscatter per square nautical mile.

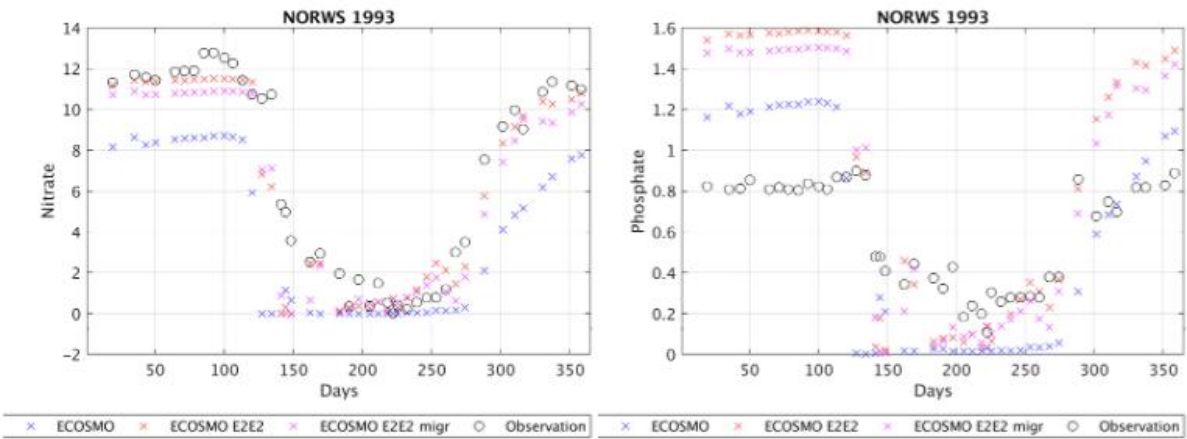


Figure 19. Time series of observed nutrient concentrations ( $\mu\text{mol L}^{-1}$ ) compared with three model simulations: (1) ECOSMO, which includes only lower trophic levels; (2) ECOSMO E2E, which adds macrobenthos and two fish groups; and (3) ECOSMO E2E with horizontal migration included for Fish 1. The time series is shown for a location in the Norwegian Sea ( $66^\circ\text{N}$ ,  $2^\circ\text{E}$ ).

### 3.6.3 NECTON Products from the model

The ECOSMO-E2E system will be used to produce monthly hindcasts of two fish functional groups, planktivorous and pisci-benthivorous, from 1991 to 2020 in the Arctic Ocean. Outputs are provided on a high-resolution ( $\sim 12 \text{ km}$ ) stereographic grid and at 16 fixed depths (0, 10, 20, 30, 40, 50, 60, 70, 80, 90, 100, 125, 150, 175, 200 m, and bottom) at monthly resolution.

<b>Project</b>	NECCTON No 101081273	<b>Deliverable</b>	D7.2
<b>Dissemination</b>	Public	<b>Nature</b>	Report
<b>Date</b>	14/10/2025	<b>Version</b>	1.0

Similarly, Baltic Sea hindcasts will be available for 3 years, with ~1 nm spatial resolution at daily and monthly intervals for 56 depth layers.

### 3.6.4 Discussion of pros and cons of the model

#### Pros

- Two-way coupling with lower-trophic-level models enables both top-down and bottom-up feedback, and provides more realistic ecosystem behavior.
- Written in Fortran and built on the FABM framework, allowing integration with various BGC models (e.g., ERSEM, ERGOM, ECOSMO).
- Modular design supports the inclusion of multiple fish functional groups.
- Contains few model parameters, making it easier to tune.
- Incorporates a simple migration scheme, allowing fish to move towards prey and away from predators.
- Suitable for regional and global applications.

#### Cons

- Biological simplification: Grouping fish into a few functional categories can be difficult and arbitrary.
- Juvenile and adult stages of the same species may belong to different functional groups, creating ambiguity.
- Mismatch with observation data, which often reports on species or size classes, not broad groups used in the model.

## 3.7 Small Pelagic fish Model (Leading partner: HCMR)

### 3.7.1 Model description

HCMR has developed a 3D full-life-cycle, individual based model (IBM) for anchovy and sardine, on-line coupled to an existing hydrodynamic/biogeochemical low-trophic level model, currently operational on Mediterranean basin scale (Korres et al., 2007; Kalaroni *et al.*, 2020), as part of the POSEIDON forecast system ([www.poseidon.hcmr.gr](http://www.poseidon.hcmr.gr)). The hydrodynamic model is based on Princeton Ocean Model (POM; Blumberg and Mellor, 1983), while the biogeochemical model is based on European Regional Seas Ecosystem Model (ERSEM, Baretta *et al.* 1995), appropriately adapted to the characteristics of the specific ecosystem.

The 3-D IBM was developed for the Mediterranean Sea ecosystem, aiming to describe the full life cycle of anchovy and sardine (from egg to adult), their spatial distribution and their important energetic features. The small pelagic fish model has been previously implemented in the North Aegean Sea for anchovy (Politikos et al., 2015) and as a multispecies model for anchovy and sardine (Gkanasos et al., 2021).

<b>Project</b>	NECCOTON No 101081273	<b>Deliverable</b>	D7.2
<b>Dissemination</b>	Public	<b>Nature</b>	Report
<b>Date</b>	14/10/2025	<b>Version</b>	1.0

### 3.7.1.1 Introduction and biological basis

#### Model Formulations: State Variables, Equations, Parameters

The anchovy lifespan is divided into seven stages and the sardine lifespan into eight stages. These include the embryonic stage, the early and late larval stages, the juvenile stage and the adult life stages, which include three age classes for anchovy and four for sardine.

#### Bioenergetics

Fish growth is calculated with a Wisconsin-type bioenergetics model, taking into account all important processes, such as consumption, respiration, egestion, excretion, specific dynamic action and reproduction. The somatic growth is regulated through the equation:

$$\frac{1}{W_{SI}} \cdot \frac{dW_{SI}}{dt} = [C - (R + EG + SDA + EX + E_{buffer})] \cdot \frac{CAL_z}{CAL_f}$$

where  $W_{SI}$  corresponds to fish wet weight (g),  $C$  to consumption,  $R$  to respiration,  $EG$  to egestion,  $SDA$  to specific dynamic action,  $EX$  to excretion,  $E_{buffer}$  to the energy allocated to reproduction,  $CAL_z$  to the caloric equivalent of zooplankton and  $CAL_f$  to the caloric equivalent of fish (Gkanasos et al., 2021). All growth model parameters were obtained from the literature. The consumption half-saturation parameter for each fish age-class has been tuned to obtain a best fit with the available growth data.

#### Movement

Egg and early larval stages are considered as passive tracers, with their movement being mainly controlled by the advection from ocean currents. They are assumed to remain in the upper 30 meters of the water column, with vertical movement due to buoyancy not considered for simplicity. Late larvae, juveniles and adult stages are assumed to perform diurnal vertical migration between the surface layer (0-30m) during the night and the sub-surface layer (>30m) during the day. Their vertical distribution in the water column is assumed to follow the distribution of available prey (zooplankton). In the horizontal, fish are assumed to move towards areas with higher food availability, following also some habitat restrictions, related with bathymetry (see Politikos et al., 2015 for more details).

#### Population dynamics

The species population ( $N$ ) is regulated from reproduction, as well as natural ( $M$ ) and fishing ( $F$ ) mortalities:

$$\frac{dN}{dt} = - (M + F) \times N$$

Fishing mortality is applied only on the adult stages with the fishing grounds mainly coinciding with the Mediterranean Sea continental shelf. The natural mortalities are adopted from the literature and are stage specific for both species. For the juvenile stages the adopted natural mortality is based on stock assessment estimates and it has been treated as a calibrated parameter in order to achieve a best fit with the field biomass estimates. Finally, for fish found in unfavourable conditions, a cumulative weight loss of more than 30% of the body weight is assumed to cause mortality due to starvation. In Table 9 the main fish IBM model parameters are shown.

<b>Project</b>	NECCON No 101081273	<b>Deliverable</b>	D7.2
<b>Dissemination</b>	Public	<b>Nature</b>	Report
<b>Date</b>	14/10/2025	<b>Version</b>	1.0

Table 9. Fish IBM model basic parameters

<b>Parameter</b>	<b>Anchovy</b>	<b>Sardine</b>
Length range (mm):		
Early larvae	4-11	5-13
Late larvae	11-42	13-50
Juvenile	42-100	50-105
Adult Stage, age-1	5 <sup>th</sup> March – 4 <sup>th</sup> March (year+1)	1 <sup>st</sup> September – 31 <sup>th</sup> August (year+1)
Adult Stage, age-2	5 <sup>th</sup> March – 4 <sup>th</sup> March (year+1)	1 <sup>st</sup> September – 31 <sup>th</sup> August (year+1)
Adult Stage, age-3	5 <sup>st</sup> March – 1 <sup>st</sup> December	1 <sup>st</sup> September – 31 <sup>th</sup> August (year+1)
Adult Stage, age-4	-	1 <sup>st</sup> September – 30 <sup>th</sup> April (year+1)
Length at maturity (mm)	100	105
Egg energy	0.66	1.11
Daily specific fecundity (eggs g-1)	46	20.1
Batch Energy (g prey per g fish per day)	0.012	0.0086
Spawning period SST threshold	Start: SST >15°C End: October	Start: SST <16°C End: mid-April
Optimum temperatures for consumption	22.7 (early larvae) 21.9 (late larvae)	15.1 (early larvae) 15.2 (late larvae)

<b>Project</b>	NECCTON No 101081273	<b>Deliverable</b>	D7.2
<b>Dissemination</b>	Public	<b>Nature</b>	Report
<b>Date</b>	14/10/2025	<b>Version</b>	1.0

	17.1 juveniles 18.4 adults	16.85 juveniles 18.4adults
Half saturation parameters for consumption (g prey m <sup>-3</sup> )	0.3 (early larvae) 0.12 (late larvae) 0.13 (juveniles) 0.1 (adults age 1) 0.085 (adults age 1-4)	0.3 (early larvae) 0.1 (late larvae) 0.15 (juveniles) 0.045 (adults age 1) 0.029 (adults age 2) 0.023 (adults age 3,4)
Natural mortalities (dimensionless)	0.4, embryos 0.2, early larvae 0.065, late larvae 0.0195, juveniles 0.0021, 0.0018, 0.0017, 0.0017 adults ages 1-4	0.4, embryos 0.2, early larvae 0.065, late larvae 0.004, juveniles 0.0021, 0.0018, 0.0017, 0.0017 adults ages 1-4
Adults fishing mortalities (dimensionless)	0.0016	0.0017

### 3.7.1.2 Model structure and required forcings and inputs; Implementation details

The model code is written in Fortran77 and runs on a linux environment, using Intel Fortran (ifort) compiler, mpi and parallel-netcdf libraries. The coupled hydrodynamic-biogeochemical (LTL) model runs on multiple cores, using a parallel (domain decomposition) version of POM (Jordi and Wang, 2012).

### 3.7.1.3 Model specifics to HTL-LTL coupling

The LTL and the fish IBM models are two-way coupled, with both anchovy and sardine consuming zooplankton. Early larvae consume microzooplankton, late larvae consume both micro and mesozooplankton at equal preferences, while juveniles and adults only consume mesozooplankton. The zooplankton biomass consumed by the fish is removed from the LTL model, while fish byproducts

<b>Project</b>	NECCON No 101081273	<b>Deliverable</b>	D7.2
<b>Dissemination</b>	Public	<b>Nature</b>	Report
<b>Date</b>	14/10/2025	<b>Version</b>	1.0

are channelled back to the organic particulate (detritus) matter pool of the model and fluxes due to excretion as dissolved organic matter.

Due to the different units of the fish (g wet weight) and the LTL (mgC/m<sup>3</sup>, mmol N, P/m<sup>3</sup>) models, the fish biomass is translated to carbon, nitrogen and phosphorus average concentrations in the water column of the LTL grid cell. A conversion factor from fish gram ww to mgC is used (6.8mg C to mg wet weight), based on the carbon content of anchovy dry weight (Czamanski et al., 2011), assuming that dry weight corresponds to 32% of the wet weight (Politikos et al, 2015).

In the older version of the model, the LTL and fish IBM models were on-line coupled, with fluxes being calculated and applied on each model time-step. In the present model version, the LTL model is parallelized (domain decomposition) and thus, fluxes with the fish IBM model are not applied on each time step, but on a daily basis.

### 3.7.2 Application: Hindcast-Simulation

#### 3.7.2.1 Model configuration (Resolution, Boundary condition, Initial conditions, Model forcing)

The atmospheric forcing used for the needs of the simulations were obtained from ECMWF – ERA5 (Hersbach et al., 2020) with 0.25° x 0.25° resolution. The coupled LTL model has a 1°/10 x 1°/10 resolution. The river discharge and nutrients inputs were based on Ludwig et al. (2009) dataset. The LTL model open boundary (Gibraltar) conditions were obtained from existing climatologies for temperature/salinity (MODB) and dissolved inorganic nutrients (MEDATLAS). The hindcast model simulation has been initialized from Kalaroni et al. (2020) model output.

The average 2000-2020, surface (0-10m), mesozooplankton concentration is displayed in Figure 20. The areas that show the highest concentrations, are those influenced by major Mediterranean rivers (i.e. Po, Rhone, Axios, Evros, Ebro, Nile), as well as areas receiving lateral nutrient inputs from the Atlantic (Alboran Sea) and Black Sea (North Aegean).

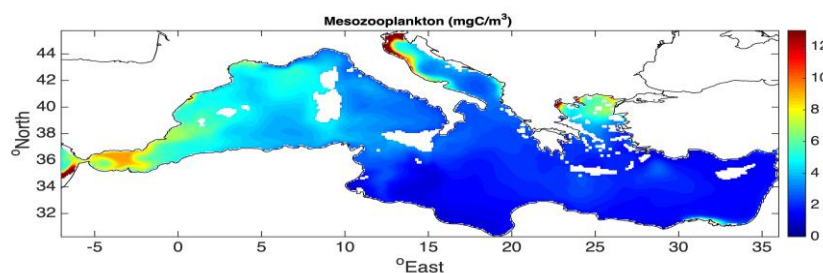


Figure 20. Average 2000-2020 surface (0-10m) mesozooplankton concentration (mgC/m<sup>3</sup>).

The small pelagic fish model was initialized on 1<sup>st</sup> January 2000 with biomasses in accordance with historical data from GFCM reports, the MEDIAS project and related publications (e.g. Leonori et al., 2021). An initial number of 1000 Super Individuals (SIs) was assigned for each age, from the juvenile to adult-2 stage of each species, with reference weights per age. The SIs were initially placed in areas

<b>Project</b>	NECCTON No 101081273	<b>Deliverable</b>	D7.2
<b>Dissemination</b>	Public	<b>Nature</b>	Report
<b>Date</b>	14/10/2025	<b>Version</b>	1.0

adjacent to the species main habitats in the Mediterranean (Alboran Sea, Catalan Sea, the Gulf of Lion, the Ligurian and Tyrrhenian Seas, the Adriatic Sea, the Southern Sicily Sea and the North Aegean Sea).

Age dependent natural mortality rates (applying on all stages) and fishing mortality values (applying only on the adult stages) for the different species habitats in the Mediterranean, were derived from the literature (GFCM\_WGSASP\_2017 & 2021). In order to fill data gaps for specific GSAs and achieve faster model tuning, these were averaged for the entire Mediterranean and are shown in Table 9.

### 3.7.2.2 Results

The consumption half-saturation parameter for each fish age-class has been tuned to obtain a best fit with the available growth data. The anchovy and sardine larval growth was fitted against data on the daily evolution of larval length. As shown in Figure 21, the simulated mean (2000-2020) larval length evolution is found in good agreement with the data, particularly for sardine.

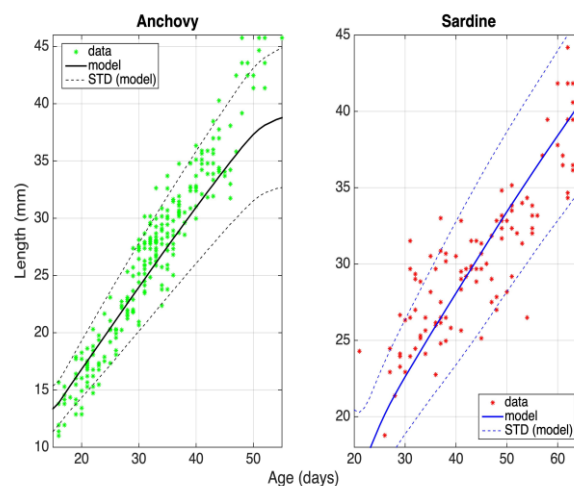


Figure 21. Average daily evolution ( $\pm$ SD) of late larvae growth (mm), against field data.

The growth rate of the juvenile and adult stages was also tuned to obtain a best fit with available weight-at-age data, averaged from all GSAs. With the exception of the sardine adults of age 4 & 5 where a model overestimation may be noticed (within the  $\pm$ SD range), the mean weight evolution is accurately represented in the model (Figure 22).

<b>Project</b>	NECCTON No 101081273	<b>Deliverable</b>	D7.2
<b>Dissemination</b>	Public	<b>Nature</b>	Report
<b>Date</b>	14/10/2025	<b>Version</b>	1.0

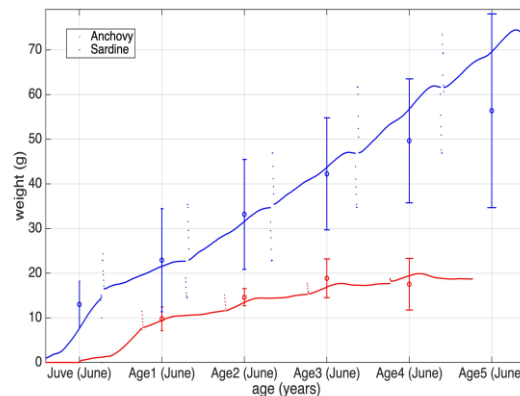


Figure 22. Average mean weight (g) – at age against field data (red & blue circles  $\pm$ SD).

The simulated anchovy and sardine biomass interannual variability was validated using biomass estimates from acoustic surveys, collected during the Medias project (Leonori et al., 2021). The average simulated species stocks (634 and 339kt for anchovy and sardine respectively) are close to the data (578 and 371kt for anchovy and sardine respectively). The observed sardine stock inter-annual variability was reproduced by the model relatively more successfully ( $r^2=0.4$ ), as compared to anchovy ( $r^2=0.25$ ). This may be partly attributed to the lack of data for the year 2003, creating a significant variability increase, mainly for anchovy and less for sardine (Figure 23).

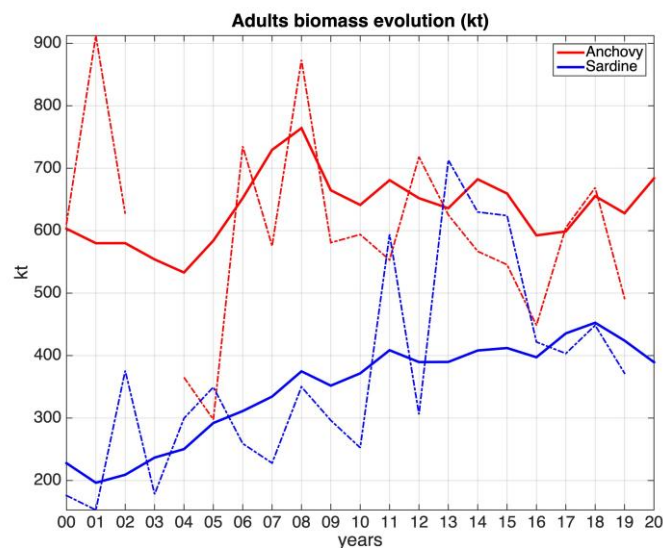


Figure 23. Simulated total Mediterranean anchovy (red line) and sardine (blue line) adults biomass (kt) evolution against biomass estimates from acoustic surveys (dotted lines) for the 2000-2019 period.



<b>Project</b>	NECCTON No 101081273	<b>Deliverable</b>	D7.2
<b>Dissemination</b>	Public	<b>Nature</b>	Report
<b>Date</b>	14/10/2025	<b>Version</b>	1.0

Spatially, the model reproduces fish concentrations in the main known habitats of anchovy and sardine, which include the Alboran Sea, the Catalan Sea, the Gulf of Lion, the Ligurian and Tyrrhenian Seas, the Adriatic Sea, the Southern Sicily Sea and the North Aegean Sea (Figure 24).

Although both species stocks are well represented cumulatively for the Mediterranean Sea, there are deviations from the reference biomasses in certain habitats. Most probably, these deviations arise from the use of basin-average natural and fishing mortality values, unevenly affecting the different stocks.

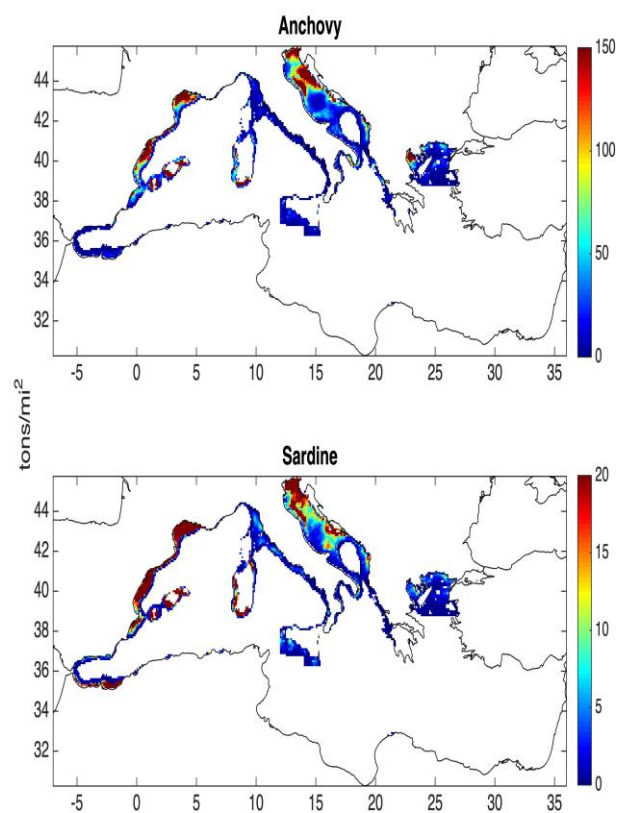


Figure 24. Adult biomass spatial distribution (tons/mi<sup>2</sup>) averaged over the 2000-2020 period.

The largest anchovy concentration is simulated in the Adriatic Sea, followed (in descending order) by the Catalan Sea, the Gulf of Lion, the North Aegean Sea, the Alboran Sea, the Ligurian and Tyrrhenian Seas. The largest sardine stock is simulated again in the Adriatic, followed by the Catalan Sea, the Gulf of Lion, the Alboran, the Ligurian and Tyrrhenian and the North Aegean Seas.

<b>Project</b>	NECCTON No 101081273	<b>Deliverable</b>	D7.2
<b>Dissemination</b>	Public	<b>Nature</b>	Report
<b>Date</b>	14/10/2025	<b>Version</b>	1.0

### 3.7.3 NECCTON Products from the model

HCMR will provide monthly maps of  $1^{\circ}/10 \times 1^{\circ}/10$  resolution in NetCDF format of:

- Adult's biomass spatial distribution (g m<sup>-2</sup>)
- Adult's average weight (g)

### 3.7.4 Discussion of pros and cons of the model

The Individual Based small pelagic fish Model, two-way coupled to a hydrodynamic-biogeochemical (POM-ERSEM) model developed for the needs of NECCTON project, is a complex tool, used for the study of anchovy, sardine and the ecology of the Mediterranean Sea. The model simulated the most important features of both anchovy and sardine (e.g bioenergetic functions and population dynamics). Moreover, it provides the feedback of fish stocks on the ecosystem, allowing for the study of phenomena such as species competition due to resource depletion.

The model is highly customizable; therefore, it can be tuned so that it accurately reproduces the peculiarities of each species, originating from differences in ecology among regions. Moreover, the IBM small pelagic fish model can include more species, thus even better describing the interspecies dynamics.

On the downside, the IBM model has a demanding tuning process, especially when long-term simulations are required. Given its two-way coupling, it is also a heavy, physical memory consuming model, which runs relatively slowly, making long-term (e.g. climate) simulations time consuming.

## 3.8 SS-DBEM (Leading partner: PML)

### 3.8.1 Model description

#### 3.8.1.1 Introduction and biological basis

The SS-DBEM (Fernandes et al., 2013) is an advanced, process-based, mechanistic niche model that uses principles from habitat suitability and population dynamics. The model is further constrained by a set of mechanistic physiological equations that limit the habitat suitability component of the model, resolving key limitations of correlative habitat suitability models. The SS-DBEM projects the impact of changes in the environment (e.g. warming, deoxygenation) and human activity (fishing pressure) on the abundance and or biomass of (the) modelled species, and is run in a multi-species framework to allow for competition for basal resources between species to be considered in their effect on individual species biomass. This can be further explored within the size structure of individual species considering also the effect of temperature on the slope of individual species size-spectrum.

#### 3.8.1.2 Model Formulations: State Variables, Equations, Parameters

The SS-DBEM (Fernandes et al., 2013; Fernandes et al., 2020) is a combined mechanistic-statistical approach that has been applied to a large number of marine species globally and is one of the models participating in the Fisheries model inter-comparison programme (FISHMIP; Tittensor et al., 2018; Lotze et al., 2019). The model projects changes in species distribution and biomass while explicitly

<b>Project</b>	NECCON No 101081273	<b>Deliverable</b>	D7.2
<b>Dissemination</b>	Public	<b>Nature</b>	Report
<b>Date</b>	14/10/2025	<b>Version</b>	1.0

considering known mechanisms of population dynamics and dispersal (both larval and adult), as well as eco-physiological changes caused by changing ocean conditions (Cheung et al., 2011). Present distributions of selected species in the SS-DBEM are first estimated using the Sea Around Us database method (Close et al., 2006). Then, the suitability of each species to different environmental conditions is defined using its model-inferred environmental preference profile (see Cheung et al., 2008a; 2009 for more details). The model can then be driven by ocean model outputs (datasets) to evaluate the impact of recent (Queirós et al., 2018) or future (Sailley et al., 2025; Wilson et al., 2021) changes in fish populations.

Within the SS-DBEM, fishing scenarios are defined relative to each species' maximum sustainable yield (MSY). We define MSY as the highest average theoretical equilibrium catch that can be taken continuously from a stock under average environmental conditions (Hilborn and Walters, 1992). Assuming a simple logistic population growth function and under equilibrium conditions, MSY can be defined as:

MSY = [Equation]

where  $\text{intR}$  is the intrinsic rate of population increase and [Equation] is the biomass at a species' carrying capacity (Schaefer, 1954; Sparre and Venema, 1998). In this model, the  $\text{intR}$  for each species is calculated based on natural mortality (Pauly, 1980; Cheung et al., 2008b).

### 3.8.1.3 Model structure and required forcings and inputs; Implementation details

Variables from the LTL levels are used to provide the environmental forcings for the model. The variable used are: bottom and surface temperature, salinity, oxygen, pH, currents, primary production and mixing depth layer.

Information on habitat, distribution and life parameters were sourced from the SeaAroundUs project, SeaLifeBase, and FishBase as appropriate.

### 3.8.1.4 Model specifics to HTL-LTL coupling

The SS-DBEM is one-way coupled, also referred to as offline coupling. This means the LTL model is only used as a forcing, without any feedback between the models.

## 3.8.2 Application: Hindcast-Simulation

### 3.8.2.1 Model configuration (Resolution, Boundary condition, Initial conditions, Model forcing)

The model outputs are on a 0.5 by 0.5 degree grid meaning it is composed of squares that are roughly 50 by 50 kilometres. The spatial domain covered by the SS-DBEM outputs is determined by the spatial domain of the biogeochemical model used to provide the environmental variables needed to force the model. The model is built to be used globally. Consequently, it can be run globally and regionally without any need for adjustments. The model outputs are expressed as an annual value that represent the potential abundance of fish within each grid square of the model

<b>Project</b>	NECCON No 101081273	<b>Deliverable</b>	D7.2
<b>Dissemination</b>	Public	<b>Nature</b>	Report
<b>Date</b>	14/10/2025	<b>Version</b>	1.0

The outputs from climate models are used to drive the SS-DBEM, which projects changes in fish species distribution and biomass while explicitly considering known mechanisms of population dynamics and dispersal (both larval and adult), as well as eco-physiological changes caused by changing ocean conditions (Cheung et al., 2011; Fernandes et al., 2013; Fernandes et al., 2020). The SS-DBEM is a combined mechanistic-statistical approach that has been applied to a large number of marine species globally and is one of the models participating in the Fisheries model inter-comparison program (FISHMIP; Tittensor et al., 2018; Lotze et al., 2019).

Initial distributions of selected species in the SS-DBEM are first estimated using the Sea Around Us database method (Close et al., 2006). Using data primarily derived from FishBase ([www.fishbase.org](http://www.fishbase.org)) and SeaLifeBase ([www.seaaroundus.org](http://www.seaaroundus.org)), it determines distribution based on (see Close et al., 2006 for more details on the method):

- presence
- latitudinal range
- range limiting polygons
- depth range
- habitat preference
- the effect of “equatorial submergence”

Then, the suitability of each species to different environmental conditions (e.g. temperature, salinity, oxygen concentration, bathymetry; is defined using its model-inferred environmental preference profile (see Cheung et al., 2008a; 2009 for more details), which create seed populations. The model is initialized with these seed populations using the estimated present distribution and then driven by ocean model outputs to evaluate the impact of recent (Queirós et al., 2018) or future (Fernandes et al., 2016) changes in environmental conditions on fish populations distribution. Combining ocean dynamics (e.g. advection) with mortality, growth, and dispersal processes, the model projects future patterns in distribution and biomass (see Cheung et al., 2008, 2009, for more details) with the carrying capacity of each species being dependent on the environmental conditions and limited by primary production. The Size Spectra component of the SS-DBEM accounts for resource by comparing the biomass that can be supported in any given area (based on primary production and the derived size spectrum) to the energy demand of the species that are predicted to be present in the area. Energy is distributed to species in proportion to their energy demand and their growth rate (see Fernandes et al., 2013 for details). Because the model accounts for both environmental preference and population dynamics, any changes in environmental conditions will result in changes in life history (e.g. growth, migration), carrying capacity, and, consequently on the abundance and distribution of species.

The SS-DBEM fisheries model was initiated with seed populations for each species in 1990 and run until 2099. As mentioned, the model calculated biomass of fish each year after migration, reproduction and death (both natural and through fishing) were taken into account. Trial experiments in our study showed that the model reaches a stable state in under 10 years when run with constant conditions. We therefore treated the first 10 years of a model run as spin-up and only report changes between 2000 and 2099. The model was run on a global configuration, where all of the world’s oceans are represented, to overcome any boundary condition issues. It is worth noting that the model is

<b>Project</b>	NECCTON No 101081273	<b>Deliverable</b>	D7.2
<b>Dissemination</b>	Public	<b>Nature</b>	Report
<b>Date</b>	14/10/2025	<b>Version</b>	1.0

capable to run 100s of species globally (see Cheung et al., 2019) and as such does not need specific parameterization for this regional application with the species selected and the forcing being the only change.

### 3.8.2.2 Results

Figure 25 shows the kind of results that can be expected from the SS-DBEM: maps of distribution of fish species at different year, comparison of the distribution to show population movement and temporal trends for a specific region.

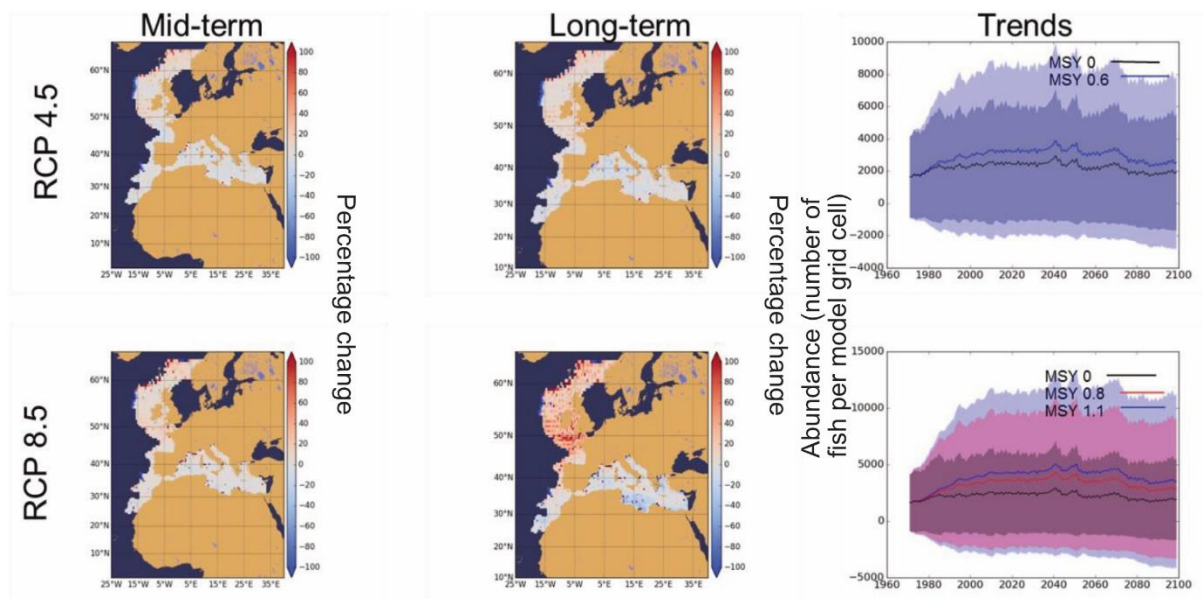


Figure 25. SS-DBEM projection for Atlantic horse mackerel (*Trachurus trachurus*) change in abundance under RCP 4.5 (top row) and RCP 8.5 (bottom row). The maps indicate the percentage change in fish biomass. The graphs represent the mean projected abundance (fish per model grid cell) Left column: Medium-term change in percentage: comparison of the 2040-2060 period to the 2000-2020 period, no fishing pressure was applied. Middle column: Long-term change in percentage: comparison of the 2080-2100 period to the 2000-2020 period, no fishing pressure was applied. Right Column: mean abundance within the Northeast Atlantic with shaded area indicating the standard deviation within the Northeast Atlantic; MSY 0 (no fishing pressure in black line and grey shade). Results using ERSEM forcing from past project.

### 3.8.2.3 Calibration and Validation of hindcast simulations

Previous validation exercises (Fernandes et al., 2020; MSPACE report annex 1) showed that the model could reproduce trends in survey data for the period 1970-2000. For the biogeochemical models that provide the environmental variables to the SS-DBEM this correspond to the historical period, that is the atmospheric forcing is provided by data rather than by atmospheric model. There is a known sensitivity of the SS-DBEM to the model used to provide the forcing. This is due to the LTL model sensibility to climate and the resulting change in trends for the forcing variables. This means that decrease in projected HTL biomass might happen with a different intensity in timing.

### 3.8.3 NECCTON Products from the model

The SS-DBEM will deliver for the global Tuna results and the Northeast Atlantic pelagic fish.

<b>Project</b>	NECCON No 101081273	<b>Deliverable</b>	D7.2
<b>Dissemination</b>	Public	<b>Nature</b>	Report
<b>Date</b>	14/10/2025	<b>Version</b>	1.0

The provisional list of species is as follows:

Atlantic pelagic: mackerel (*Scomber scombrus*), herring (*Clupea harengus*), turbot (*Scophthalmus maximus*), dab (*Limanda limanda*), blue whiting (*Micromesistius poutassou*), capelin (*Mallotus villosus*), Atlantic horse mackerel (*Trachurus trachurus*), European Sprat (*Sprattus sprattus*), atlantic halibut (*Hippoglossus hippoglossus*), European seabass (*Dicentrarchus labrax*), Atlantic salmon (*Salmo salar*), meagre (*Argyrosomus regius*), gilt-head seabream (*Sparus auratus*), sardine (*Sardina pilchardus*), anchovie (*Engraulis encrasicolus*)

Global tuna: bluefin tuna (*Thunnus thynnus*), albacore tuna (*Thunnus alalunga*), yellowfin tuna (*Thunnus albacares*), bigeye tuna (*Thunnus obesus*), frigate tuna (*Auxis thazard*), kawakawa (*Euthynnus affinis*), skipjack tuna (*Katsuwommus pelagis*)

### 3.8.4 Discussion of pros and cons of the model

The Dynamic Bioclimate Envelop Model modelling approach has a number of inherent assumptions and uncertainties that may affect the performance of the model (RD.3). Firstly, the model is based on the assumption that the current predicted species distributions depict the environmental preferences of the species and are in equilibrium. Secondly, the underlying biological hypothesis, represented by the model structure and input parameters, may be uncertain. Moreover, the models did not consider the potential for phenotypic and evolutionary adaptations of the species.

Theoretical and empirical data were used to model trophic interactions. The modelling approach does not incorporate the full range or complexity of interactions among species, but avoids the difficulties of formalising transient and complex species-specific predatory interactions at large-scales. It also requires no assumptions about the extent to which species-specific trophic interactions that are currently observed will persist in the future. Furthermore, at the system level, size-based processes account for much of the variation in prey choice and trophic structure.

<b>Project</b>	NECCOTON No 101081273	<b>Deliverable</b>	D7.2
<b>Dissemination</b>	Public	<b>Nature</b>	Report
<b>Date</b>	14/10/2025	<b>Version</b>	1.0

### 3.9 ESD-MED (Leading partner: OGS)

#### 3.9.1 Model description

The ensemble of species distribution models for the Mediterranean Sea (ESD-MED) was developed for demersal and pelagic fishes, to assess and understand the best distribution over time and space (Panzeri et al., 2024). Survey data from MEDITS (Mediterranean International Trawl Survey; Spedicato et al., 2019) and Essential Oceanographic variables ( EoVs) from the Copernicus Marine Service dataset (CMS) were used, from 1994/1999 to 2022 (Von Schuckmann et al., 2021). The different approaches were applied to individual species: demersal species European hake, red mullet, deep-water shrimp and red giant shrimp, as well as to two pelagic species such as European anchovy and sardine. All models used the index of kilograms per square kilometer (kg/km<sup>2</sup>) or number of individuals per square kilometer (N/km<sup>2</sup>) and bottom layer variables such as bottom temperature or oxygen content. The fitted models were evaluated in a framework that includes spatial training and test datasets to assess the best model for each class. The final prediction results (extrapolation in a Copernicus grid) are weighted between the different models according to their performance (Panzeri et al., 2021). To determine the optimal distribution of adults and juveniles of the studied species, we used only GLMM (which shows best performance; Panzeri et al., 2024) to create a single-species model that includes a term to assess spatial interaction and dependence (the presence of a stage determines the presence/density of the same and other stages, in our case juveniles and adults). In this case, we used the number of individuals per square kilometer (N/km<sup>2</sup>) from the MEDITS survey, which also records individuals per length (size).

For the results of both approaches (density/abundance distribution of species), eSDM and GLMM, we analysed the hot spots with the Getis or Gi\* statistic to highlight the areas with high aggregation (positive values hot spots, negative values cold spot) across time and space (Panzeri et al., 2024).

##### 3.9.1.1 Introduction and biological basis

##### 3.9.1.2 Model Formulations: State Variables, Equations, Parameters

The ESD-Med is an ensemble that includes different approaches, i.e. parametric and semi-parametric approaches (such as GLMM, Generalized Linear Mixed Models, and GAM, Generalized Additive Model) and machine learning methods (such as Random Forest RF or Gradient Boosted Method, GBM).

#### GAMs

GAMs are flexible extensions of Generalized Linear Models (GLMs). The key difference is that GAMs allow the relationship between the response variable and the predictors to be non-linear, estimating these relationships using "smoothing" functions instead of simple linear coefficients (Panzeri et al., 2024). They're excellent for capturing complex patterns in data without having to specify the exact form of the non-linearity beforehand.

#### General Equation:

The general form of a GAM is:

$$g(E[Y]) = \beta_0 + f_1(X_1) + f_2(X_2) + f_p(X_p)$$



<b>Project</b>	NECCON No 101081273	<b>Deliverable</b>	D7.2
<b>Dissemination</b>	Public	<b>Nature</b>	Report
<b>Date</b>	14/10/2025	<b>Version</b>	1.0

Where:

Y: Response variable (e.g., species presence/absence, abundance).

$E[Y]$ : Expected value of the response variable.

$g()$ : Link function, which connects the mean of the response to the linear predictor (e.g., logit for binary data, log for counts).

$B_0$ : Intercept.

$f_i(X_i)$ : Are the smoothing functions (non-linear) for each predictor ( $X_i$ ). These functions are estimated from the data and capture complex relationships that would otherwise be modeled linearly.

### GLMMs

GLMMs extend GLMs by including random effects in addition to fixed effects. They are crucial when data exhibit a hierarchical or grouped structure (e.g., repeated observations at the same site, species nested within sites, or multiple samples in the same year; e.g., Thorson et al., 2025). Random effects model the variability between groups not accounted for by the fixed predictors.

#### General Equation:

The general form of a GLMM can be seen as:

$$g(E[Y]) = \beta_0 + \beta_1 X_1 + \beta_p X_p + \alpha$$

Where:

Y: Response variable for observation in group.

$E[Y]$ : Expected value of the response.

$g()$ : Link function.

$B_0$ : intercept

$B_1(X_1)+B_2(X_2)+B_p(X_p)$  : linear predictor

*beta*: Represents the fixed effects part, where the *betas* are constant coefficients across the entire population.

*alpha*: Represents the random effect for group. This term varies randomly among groups (e.g., among sampling sites) and is usually assumed to follow a normal distribution with a mean of zero and a certain variance (see also Anderson et al., 2022 ).

### Random Forest (RF)

Random Forest is a non-parametric ensemble learning algorithm that combines the predictions from many individual "decision trees" (Catucci et al., 2025). It's highly robust against overfitting and can handle nonlinear relationships and complex interactions between predictors well.

#### Conceptual Operation:

Instead of a single equation, Random Forest relies on an algorithm:

1. Bagging (Bootstrap Aggregating): To build each tree, a random subsample with replacement (bootstrap sample) is drawn from the original dataset. This ensures that each tree sees a slightly different data set.

<b>Project</b>	NECCON No 101081273	<b>Deliverable</b>	D7.2
<b>Dissemination</b>	Public	<b>Nature</b>	Report
<b>Date</b>	14/10/2025	<b>Version</b>	1.0

2. **Random Feature Subspace:** At each node of every decision tree, a random subset of predictors is selected from which to choose the best split. This decorrelates the trees, making the "forest" more robust.
3. **Tree Construction:** Each tree is grown to its maximum depth (it's not pruned), minimizing error (e.g., MSE for regression, Gini impurity for classification).
4. **Combining Predictions Regression:** The final prediction is the average of the predictions from all individual trees.

Classification: The final prediction is the majority vote class from the trees.

There isn't a clear equation like for linear models, but the idea is:

$$Y_{RF}(x) = \frac{1}{B} * \sum_{b=1}^B T_b(x)$$

Where:

$Y_{rf}(x)$ : The final prediction from the Random Forest for a given input  $x$ .

$B$ : The total number of trees in the forest.

$T_b(x)$ : The prediction of the single decision tree  $b$  for the same input  $x$ . Each is a decision tree built on a bootstrap subsample of the original data and with a random subset of features available at each node split.

## GBM

The Gradient Boosted Machine (GBM) equation isn't a single formula that directly fits data like in generalized linear models. Instead, it's an iterative equation that describes the sequential process of building the model by adding the contributions of "weak learners" (typically decision trees; Panzeri et al., 2024). The core idea is that each new tree aims to reduce the errors (or more precisely, the "pseudo-residuals") of the model built in the previous steps.

The final model  $F_M(x)$  after  $M$  iterations (i.e., after adding  $M$  trees) is given by the sum of the contributions from all trees, along with an initial baseline prediction:

$$F_M(x) = F_0(x) + \sum_{m=1}^M v * h_m(x)$$

- For regression (e.g., predicting a continuous value), is typically a constant, often the mean of the training data's response values.
- For binary classification (e.g., predicting a 0/1 probability), is typically the log-odds of the positive class:
- This is the cumulative sum of contributions from each weak tree added in every iteration.
  - Represents the  $m$ -th weak tree (often a decision tree with limited depth, e.g., 4-8 levels) that is fitted in iteration  $m$ . This tree is trained not on the original response variable  $y$ , but on the pseudo-residuals (or the negative gradient) of the  $F_{m-1}(x)$  model from the previous iteration. The goal of  $h_m(x)$  is to correct the errors that  $F_{m-1}(x)$  made.

<b>Project</b>	NECCTON No 101081273	<b>Deliverable</b>	D7.2
<b>Dissemination</b>	Public	<b>Nature</b>	Report
<b>Date</b>	14/10/2025	<b>Version</b>	1.0

- $\nu$  (nu): This is the learning rate (or "shrinkage"). It's a small value between 0 and 1 (e.g., 0.01, 0.1). Introducing  $\nu$  reduces the contribution of each individual tree, making the learning process slower and more gradual. This helps to prevent overfitting and improves the model's generalization ability. A smaller  $\nu$  usually requires a larger number of trees ( $M$ ).

### *3.9.1.3 Model structure and required forcings and inputs; Implementation details*

The workflow for the application of the ESD-MED is shown in Figure 26. Basically after testing the explanatory LTL variables for correlations, the set considered useful to explain the distribution of a species is used for each approach of the ensemble (GLMM, GAM, RF and GBM). Starting from the application with all the explanatory variables the training and testing is done successively by reducing the number of explanatory variables in order to obtain the best model for each approach with the most limited number of explanatory variables (Panzeri et al., 2021). The best model for each approach is used to make prediction over the grid for each approach. Such results are then weighted to obtain the ESD-MED results.

<b>Project</b>	NECCTON No 101081273	<b>Deliverable</b>	D7.2
<b>Dissemination</b>	Public	<b>Nature</b>	Report
<b>Date</b>	14/10/2025	<b>Version</b>	1.0

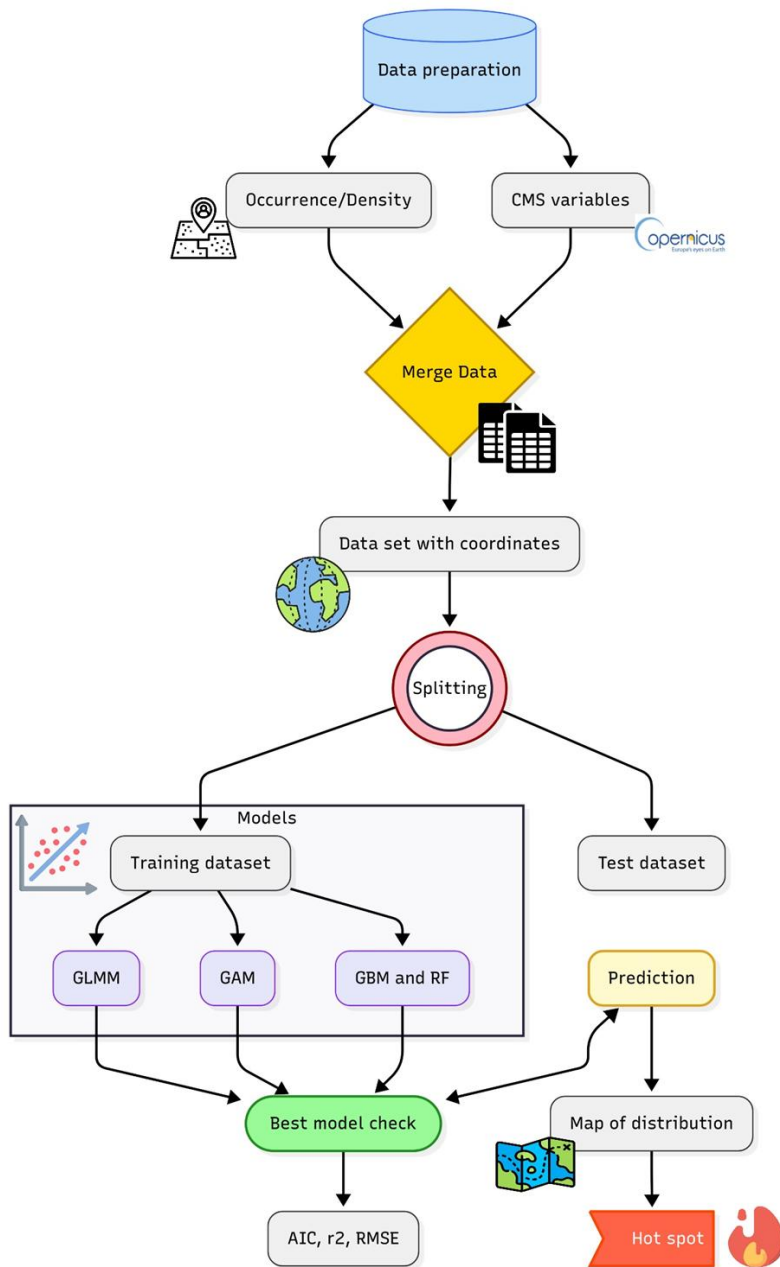


Figure 26. Plot of the workflow for the ESD-MED

<b>Project</b>	NECCON No 101081273	<b>Deliverable</b>	D7.2
<b>Dissemination</b>	Public	<b>Nature</b>	Report
<b>Date</b>	14/10/2025	<b>Version</b>	1.0

#### 3.9.1.4 Model specifics to HTL-LTL coupling

The model used is a one-way offline coupling of physical and biogeochemical variables coming from LTL modelling approaches. The occurrence/density of the species is statistically correlated with the Copernicus Marine Service variables obtained from reanalysis. The LTL variables are used without conversion as the statistical models found eventual factors or functions that connect with occurrence or density of the species. Notably since the LTL-HTL coupling is purely statistical and the densities of HTL species are typically only 2D different aggregation of 3D LTL variables can be used such as vertical integration, average by depth strata, maximum or minimum value, surface or bottom values. These choices are made considering the ecology of the species under analysis and their known living habitat (Von Schuckmann et al., 2021).

### 3.9.2 Application: Hindcast-Simulation

#### 3.9.2.1 Model configuration (Resolution, Boundary condition, Initial conditions, Model forcing)

The model simulations for ESD-MED are carried out for the Mediterranean Sea. The model is coupled to CMS variables with a one-way offline coupling and was validated using observations in a training and testing protocol (Panzeri et al., 2021). The prediction of the best model was performed on the Copernicus grid with a horizontal resolution of  $1/24^\circ$  degrees ( $\sim 4$  km). The temporal resolution of the MEDITS data ranges from 1994 or 1999 to 2022, with samples distributed mainly in summer. The final prediction on the CMS grid ranges from the same years of the MEDITS data (1994 or 1999) to 2022, distributed over the month of July.

The CMS variables used are:

- Surface temperature (sst, C°) from 1994 to 2022, resolution  $1/24^\circ$
- Bottom temperature (tmp\_bot, C°) from 1994 to 2022, resolution  $1/24^\circ$
- Bottom Salinity (PSU) from 1994 to 2022, resolution  $1/24^\circ$
- Bottom Oxygen (mmol/m3) from 1999 to 2022, resolution  $1/24^\circ$
- Integrated chlorophyll (mg/m2) from 1999 to 2022, resolution  $1/24^\circ$
- Bottom particulate organic carbon (mg/m3) from 1999 to 2022, resolution  $1/24^\circ$

#### 3.9.2.2 Calibration and Validation of hindcast simulations

To determine the best model (from a set of possible models) we followed the procedure developed in Panzeri et al., (2021; 2024): we checked the covariates for collinearity and selected variables that were not highly correlated (e.g. VIF  $\leq 3$  and Pearson correlation  $\leq 0.5$ ). We fitted different model combinations by using a spatial block with stepwise approach where each model was subjected to spatial k-fold cross-validation; thus, it was fitted to a spatial training dataset created by randomly selecting 75% of the data. The remaining 25% of the datasets were used to test the best fit of the model. Training and testing were repeated with 10-fold cross-validation (see Figure 27), with data selected at random without replacement.

<b>Project</b>	NECTON No 101081273	<b>Deliverable</b>	D7.2
<b>Dissemination</b>	Public	<b>Nature</b>	Report
<b>Date</b>	14/10/2025	<b>Version</b>	1.0

The best model for each approach is evaluated based on the best performance between training and test dataset by diagnostics such as AIC (Akaike Information Criteria) for the training dataset and  $r^2$  and RMSE for prediction on the test dataset (see Figure 28). A good trade-off between the different diagnostics is evaluated by the user and the best model is used for fitting and prediction (on a spatial and temporal grid with the same covariates) to obtain a graphical representation (map of distribution and hotspots) for each species and approach. The ensemble model is evaluated using the RMSE for each approach and the final prediction for the ESD-MED (ensemble of SDM for index of  $\text{kg}/\text{km}^2$ ) is weighted by the percentage contribution of each approach (e.g. GAM 45 %, RF 35 %, GBM 10 %, GLMM 10 %, see Figure 29).

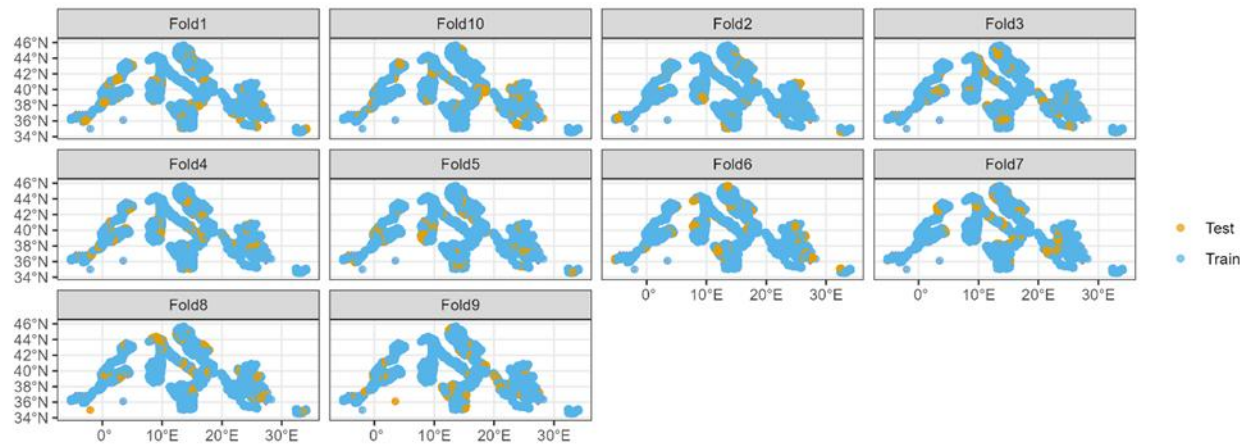


Figure 27. An example of a 10-fold spatial duplication of the training and test data set.

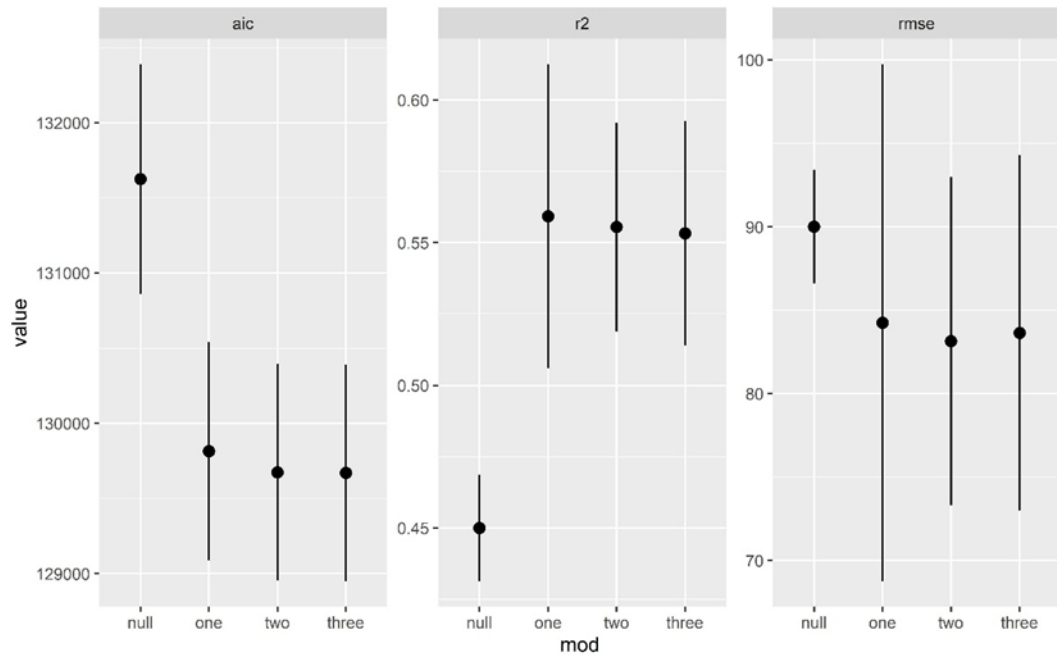


Figure 28. example of mean and standard deviation of four models and three different statistics (AIC,  $r^2$ , RMSE) for the GAM model of the European hake. Less is better for AIC and RMSE and vice versa for  $r^2$ .

<b>Project</b>	NECCTON No 101081273	<b>Deliverable</b>	D7.2
<b>Dissemination</b>	Public	<b>Nature</b>	Report
<b>Date</b>	14/10/2025	<b>Version</b>	1.0

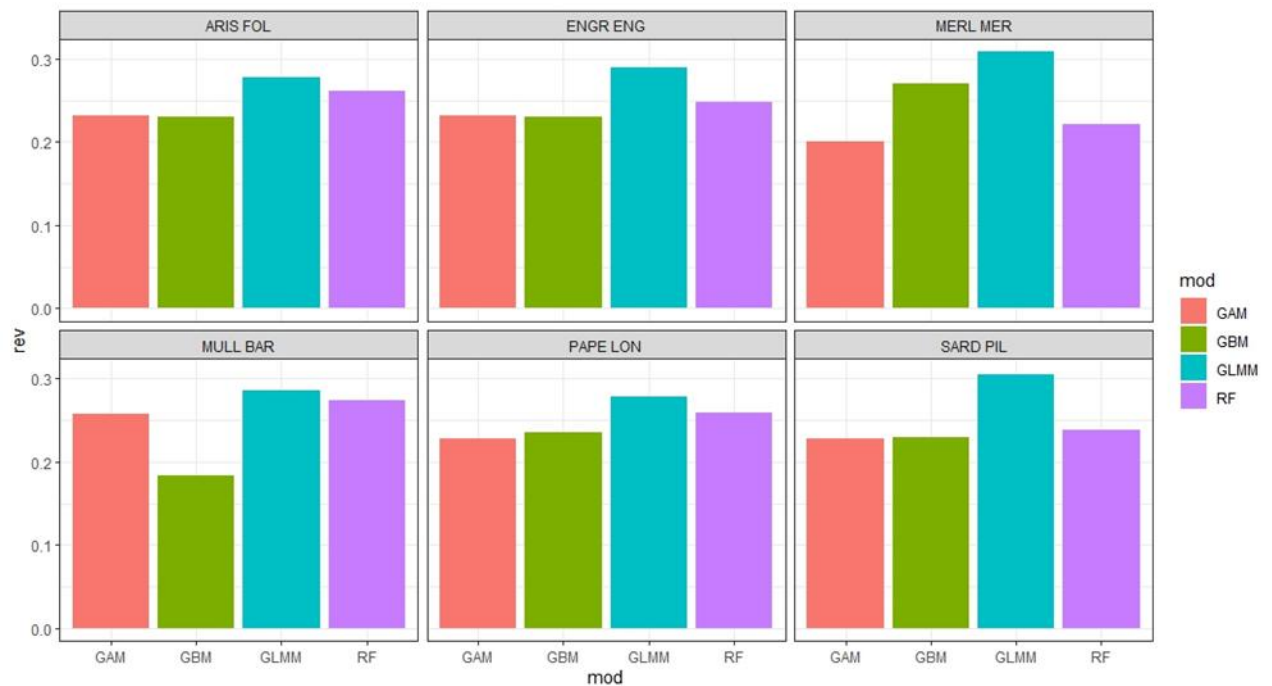


Figure 29: example of the percentage contribution of each approach to the ensemble model for the six species involved. The X-axis shows the name of the model, the Y-axis the percentage contribution (in decimals, e.g. 0.3 = 30%, 0.25=25% etc.)

### 3.9.2.3 Results

The best model, before being used as part of the ensemble, is evaluated as error and prediction uncertainty between observed and fitted values (example in Figure ) to assess the performance of each approach.



<b>Project</b>	NECTON No 101081273	<b>Deliverable</b>	D7.2
<b>Dissemination</b>	Public	<b>Nature</b>	Report
<b>Date</b>	14/10/2025	<b>Version</b>	1.0

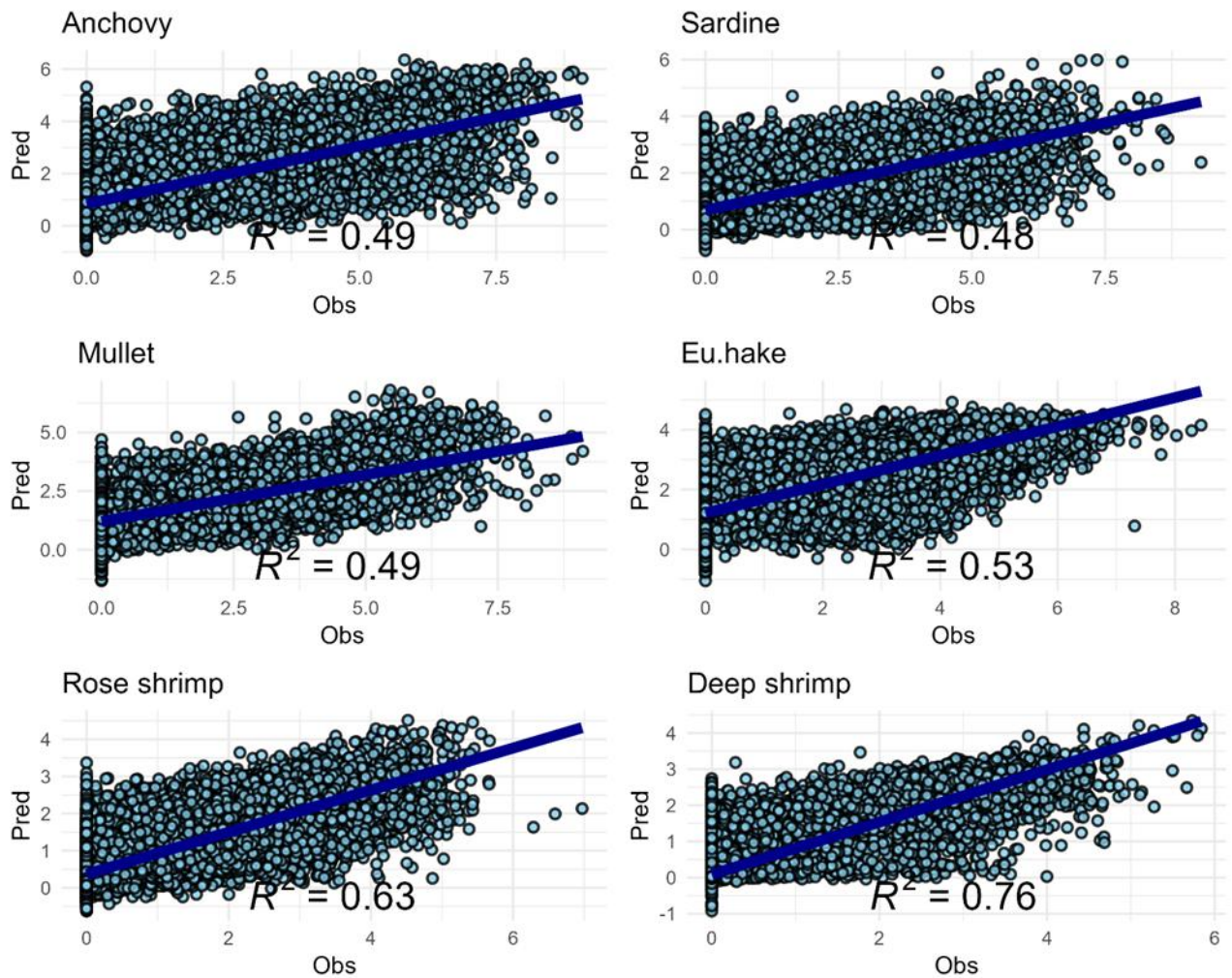


Figure 30. Example from the GBM model of predicted and observed values for each species.

We also evaluate the distribution of the spatial residuals of the models (example in Figure 31), which shows the difference between the predicted and observed value in the study area (taking all years into account).

<b>Project</b>	NECCTON No 101081273	<b>Deliverable</b>	D7.2
<b>Dissemination</b>	Public	<b>Nature</b>	Report
<b>Date</b>	14/10/2025	<b>Version</b>	1.0

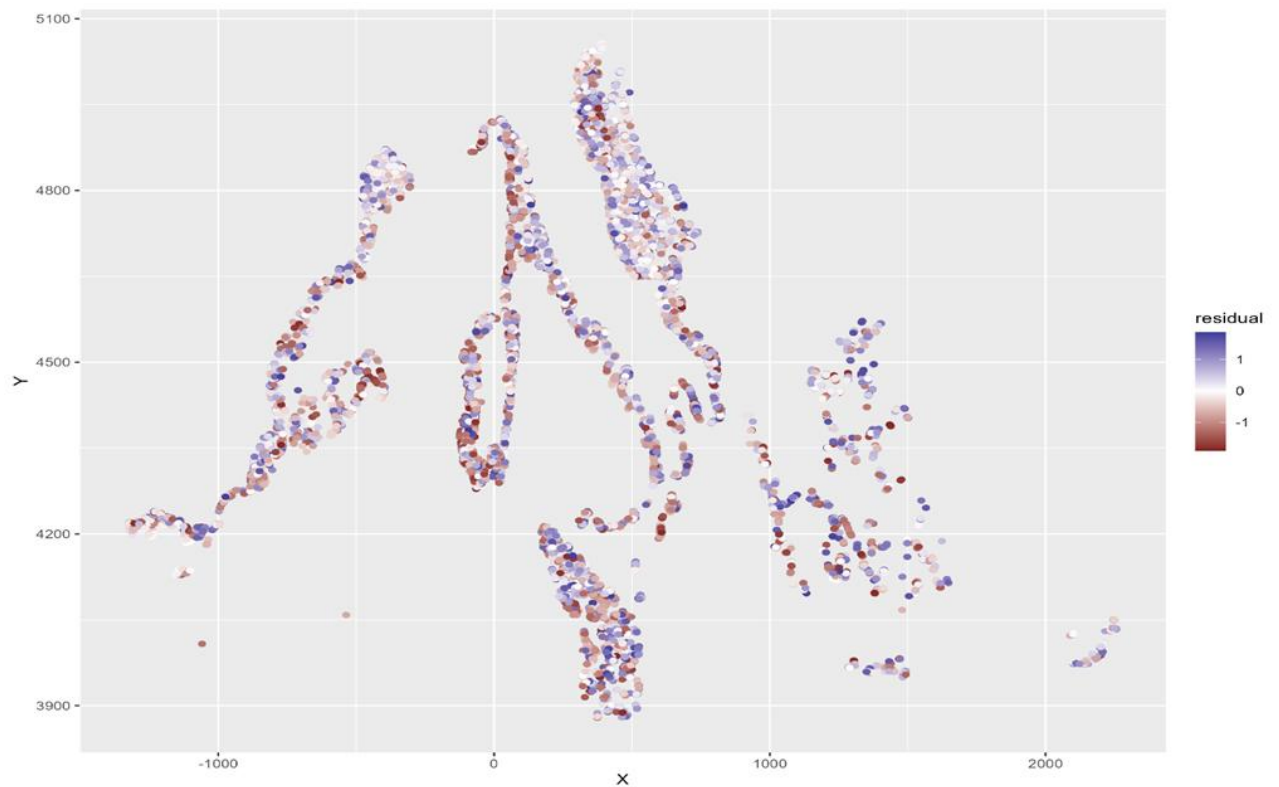


Figure 31. Map of spatial distribution of residuals (predicted – observed) for European hake and GBM model.

<b>Project</b>	NECCTON No 101081273	<b>Deliverable</b>	D7.2
<b>Dissemination</b>	Public	<b>Nature</b>	Report
<b>Date</b>	14/10/2025	<b>Version</b>	1.0

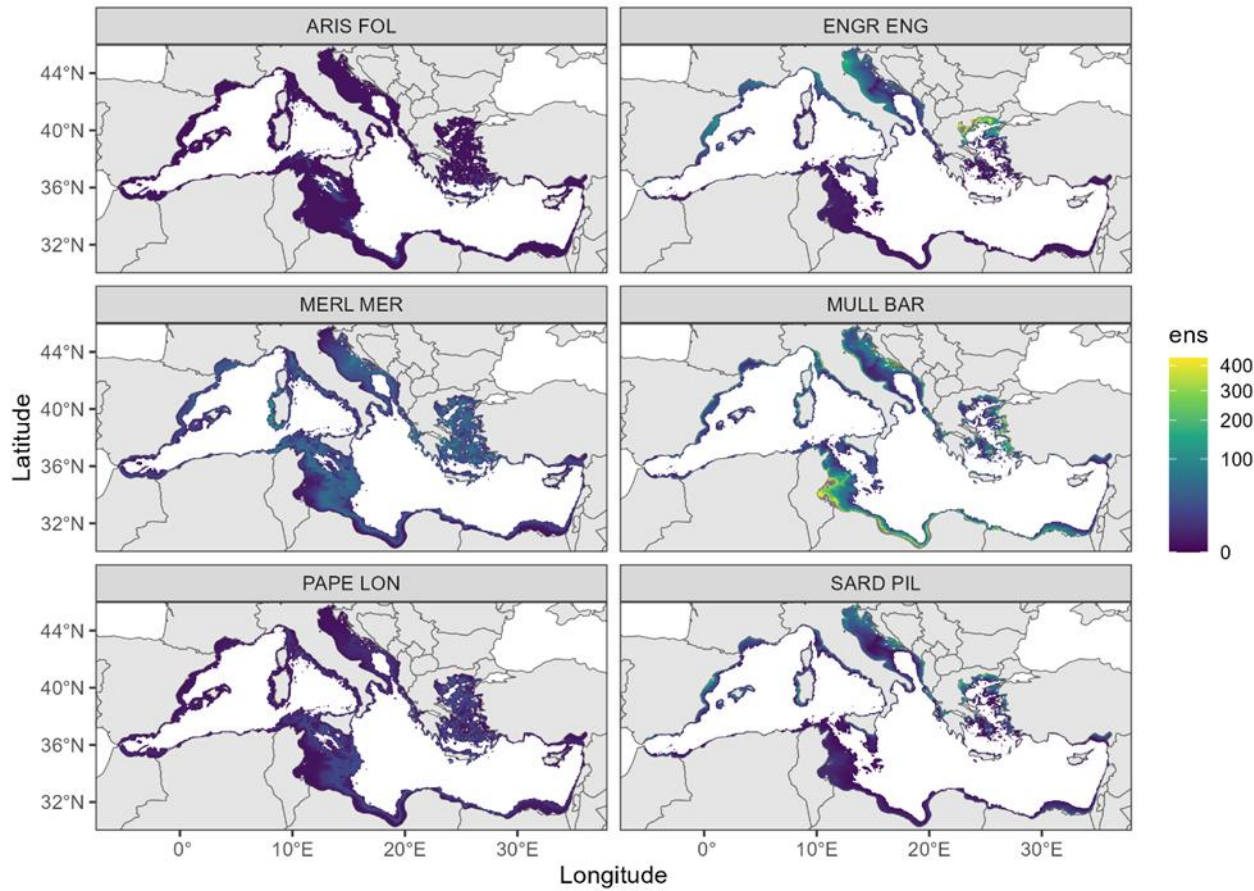


Figure 32. Distribution in kg/km<sup>2</sup> for each species for the ensemble model (averaged over the year 1999-2022)

<b>Project</b>	NECCTON No 101081273	<b>Deliverable</b>	D7.2
<b>Dissemination</b>	Public	<b>Nature</b>	Report
<b>Date</b>	14/10/2025	<b>Version</b>	1.0

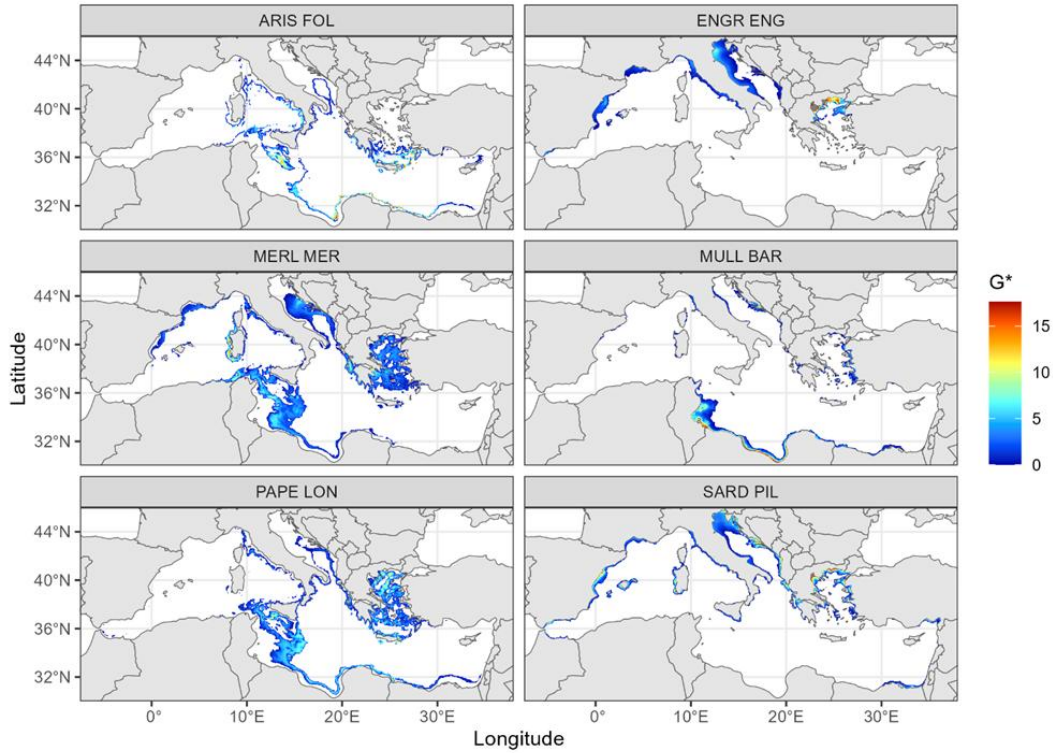


Figure 33. Map of the distribution of hot spots (legend =  $G^*$ , Getis ord  $G_i^*$  index) for each species, derived from the ensemble model and averaged over the year 1999:2022.

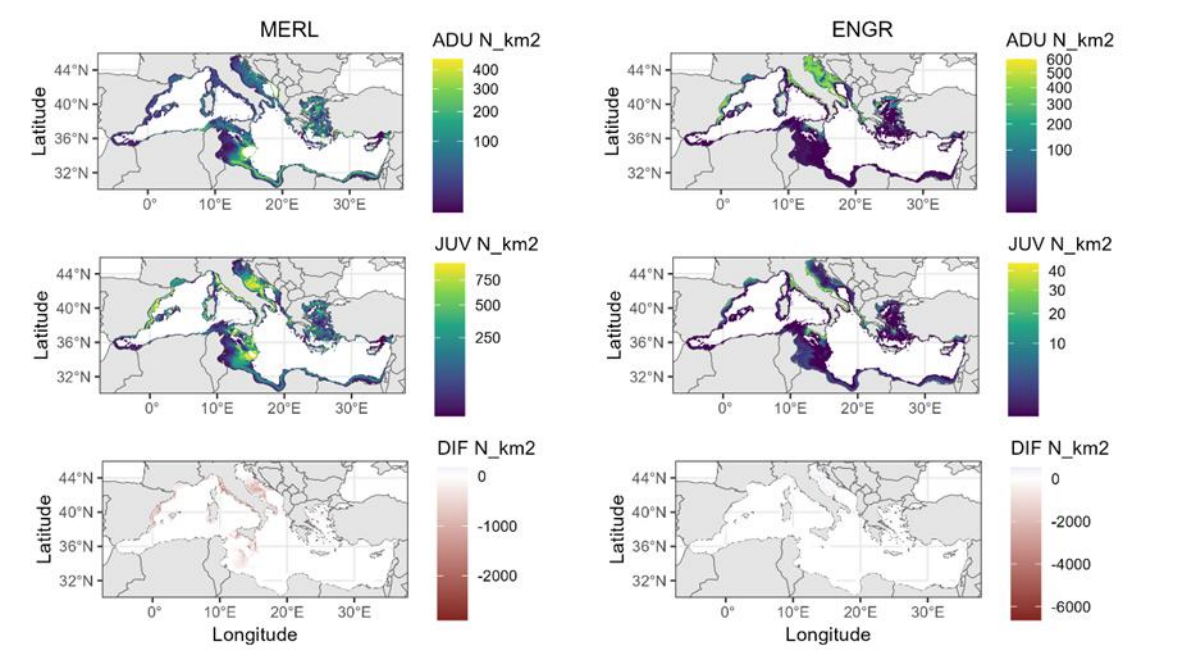


Figure 34. Map of the distribution of number of individuals (legend =  $N/km^2$ ) for European hake (left panel) and Anchovies (right panel), derived from the GLMM model and averaged over the year 1999:2022. Bottom row shows the difference in term of  $N/km^2$  between adults and juveniles (adults – juveniles).



<b>Project</b>	NECCTON No 101081273	<b>Deliverable</b>	D7.2
<b>Dissemination</b>	Public	<b>Nature</b>	Report
<b>Date</b>	14/10/2025	<b>Version</b>	1.0

### 3.9.3 NECCTON Products from the model

The ESD-MED produces the annual spatial distribution of the biomass index (kg/km<sup>2</sup>) for the following demersal species for NECCTON: European hake (*Merluccius merluccius*), red mullet (*Mullus barbatus*), deepwater red shrimp (*Aristaeomorpha foliacea*) and rose shrimp (*Parapenaeus longirostris*); as well as for two pelagic species such as European anchovy (*Engraulis encrasicolus*) and sardine (*Sardina pilchardus*).

In addition, for the same species, ESD-MED provides the abundance (N ind/km<sup>2</sup>) for juveniles and adults of the same species. In this case, we used the GLMM (Thorson et al., 2025), which also shows the best performance in the previous approach (see Figure 34), and we evaluated the difference in density (N ind/km<sup>2</sup>) between the two size classes (adult and juvenile fish) to determine the best potential area for spawning and nursery of the different species.

### 3.9.4 Discussion of pros and cons of the model

The ESD-MED has the advantage to provide a robust distribution of resources because it is based on a weighted average of different approaches (in the ensemble). This approach, however, implies the inclusion of poorly performing methods. As a result, the average error of the ensemble is not necessarily lower than that of some individual methods.

Another limitation of the approach is that current data come from scientific trawl survey which is carried out only once per year. This result in poor capabilities to represent the intra-annual dynamics that can change remarkably over the month for some species (e.g., red mullet). The approach, moreover, by relying on trawl survey data has the limitation to represent biomass index and not necessarily the absolute biomass at sea (because of net catchability).

## 3.10 NAWH-cetaceans (Leading partner: IMAR)

### 3.10.1 Model description

#### 3.10.1.1 Introduction and biological basis

The NAWH-cetaceans are species distribution models (SDMs) that relate occurrence data from two small delphinids (common dolphin (*Delphinus delphis*) and Atlantic spotted dolphins (*Stenella frontalis*)) and environmental variables to predict their spatio-temporal distribution. These SDM models, developed within the NECCTON project, predict the probability of occurrence of two of the most common delphinids species within the Azores (Central North Atlantic) (da Silva et al., 2025). To build the models, sightings data from the two dolphin species to build the NAWH-cetacean models were obtained from the Azores Fisheries Observer Program (POPA). Additionally, NAWH-cetaceans integrated fishing vessel tracking data to account for spatial and temporal biases due to uneven sampling effort. These models offer a significant advancement over previous SDM models for cetacean in the region by incorporating survey effort and by capturing complex and non-linear patterns (Tobeña et al., 2016).

<b>Project</b>	NECCOTON No 101081273	<b>Deliverable</b>	D7.2
<b>Dissemination</b>	Public	<b>Nature</b>	Report
<b>Date</b>	14/10/2025	<b>Version</b>	1.0

### 3.10.1.2 Model Formulations: State Variables, Equations, Parameters

#### *Parameterisation, sensitivity analysis*

The SDMs NAWH-cetaceans used two different statistical approaches, Generalized Additive Models (GAMs) and Boosted Regression Trees (BRTs), combined through a consensus method. GAMs are a non-parametric extension of generalized linear models (GLMs), with the advantage of being able to capture non-linear relationships between response and explanatory variables (Guisan et al., 2002). This ability is particularly valuable for modelling species-habitat relationships in marine ecosystems that have a very dynamic nature, implicating more complex nonlinear patterns. On the hand, BRTs combine tree-based statistical models and machine-learning methods to maximize the predictive performance of single regression models by fitting many models (Elith et al., 2008). The boosting algorithm is based on an iterative method which progressively adds trees to the model, while re-weighting the data to account for poorly predicted cases by the previous trees (Leathwick et al., 2006). These models are stochastic, which improves predictive performance by reducing the variance of the final model (Elith et al., 2008). Predictions from the individual models (GAMs and BRTs) were finally combined in an ensemble model, weighted according to the predictive performance of each method.

Dynamic and static environmental variables were included on the NAWH-cetaceans models. Dynamic variables were sea surface temperature (SST), Chlorophyll-a (CHL), spatial gradient of concentration of chlorophyll a (grad\_CHL), Chlorophyll-a of the previous two months (CHL\_2m), spatial gradient of concentration of chlorophyll a the previous two months (grad\_CHL\_2m), spatial gradient of eddy kinetic energy in the epipelagic layer (grad\_EKE\_L1), mass content of epipelagic micronekton (mnkc\_epi), mass content of highly migrant lower mesopelagic micronekton (mnkc\_hmlmeso) and spatial gradient of highly migrant lower mesopelagic micronekton (grad\_hmlmeso). Static variables included were water depth (depth), distance to the nearest 200 meters isobaths (dist\_200m) and bathymetric slope (slope).

For common dolphins, the best GAM and BRT identified SST, CHL and CHL\_2m, as the most important variables explaining the probability of occurrence of common dolphins. Other variables included in these models were month, depth, dist\_200m, slope, mnkc\_epi, mnkc\_hmlmeso, grad\_hmlmeso, grad\_EKE\_L1, grad\_CHL, and grad\_CHL\_2m. In the GAM, variables with effective degrees of freedom (edf) close to 1 (slope, dist\_200m, grad\_EKE\_L1 and grad\_hmlmeso) were included as linear predictors. This model also integrated the variables fisheries observer and fishing boat as random effects.

#### Common dolphin's best model (GAM):

$$p = \beta_0 + f(\text{SST}) + f(\text{CHL}) + f(\text{CHL\_2m}) + f(\text{depth}) + f(\text{grad\_hmlmeso}) + \text{dist\_200m} + \text{slope} + \text{grad\_EKE\_L1} + \text{mnkc\_hmlmeso} + \text{month} + b(\text{fisheries observer}) + b(\text{fishing boat}).$$

Where: p is the p: response variable (binary response on the presence of the dolphin species);  $f_i(x_i)$ : smooth functions of predictors;  $b_j$ : random effect on boat code and observer code;  $\beta_0$ : intercept

<b>Project</b>	NECCON No 101081273	<b>Deliverable</b>	D7.2
<b>Dissemination</b>	Public	<b>Nature</b>	Report
<b>Date</b>	14/10/2025	<b>Version</b>	1.0

#### Common dolphin's best model (BRT):

$$p = \sum_{m=1}^M \lambda_m * hm(SST, CHL, CHL_{2m}, depth, mnk_{epi}, mnk_{hlmeso}, grad_{CHL}, grad_{chl_{2m}}, dist_{200m}, slope, grad_{EKE_{L1}}, grad_{hlmeso}, month)$$

where: p is the predicted values for input (binary response on the presence of the dolphin species); M: number of boosting iterations (trees); hm(x):the predictions from the m<sup>th</sup> regression tree;  $\lambda_m$  : the learning rate for the mth tree.

For Atlantic spotted dolphins, the best GAM and BRT identified SST (with month as a grouping variable in the GAM) as the most important variable explaining the probability of occurrence of Atlantic spotted dolphins. The models also considered the dist\_200m, CHL, CHL\_2m, mnkc\_epi, mnkc\_hlmeso, grad\_CHL and grad\_SST. In the GAM, the variable month was added as a categorical variable, and fisheries observer and fishing boat as random effects. Both models indicated that the probability of occurrence of *Atlantic spotted dolphins* was strongly influenced by SST. The GAM suggested different relationships between the occurrence of this species and SST over the months, while the BRT showed a rapid increase in the presence of this species when water was warmer than 21°C.

#### Atlantic spotted dolphin's best model (GAM):

$p = \beta_0 + f(SST, \text{by month}) + f(CHL_{2m}) + f(grad_{CHL}) + f(grad_{SST}) + month + b(\text{fisheries observer}) + b(\text{fishing boat})$ .

where: p is the p: response variable (binary response on the presence of the dolphin species); f<sub>i</sub>(x<sub>i</sub>): smooth functions of predictors; b<sub>j</sub>: random effect on boat code and observer code;  $\beta_0$  : intercept

#### Atlantic spotted dolphin's best model (BRT):

$$p = \sum_{m=1}^M \lambda * hm(SST, CHL, CHL_{2m}, depth, mnk_{epi}, mnk_{hlmeso}, grad_{CHL}, grad_{chl_{2m}}, dist_{200m}, slope, grad_{EKE_{L1}}, grad_{hlmeso})$$

where: p is the predicted values for input (binary response on the presence of the dolphin species); M: number of boosting iterations (trees); hm(x):the predictions from the m<sup>th</sup> regression tree;  $\lambda_m$  : the learning rate for the mth tree.

#### *Model structure and required forcings and inputs; Implementation details*

The NAWH-cetaceans was written in R. The R code is available on the GitHub page: <https://github.com/AzWhaleLab/NECCON>

#### *Model specifics to HTL-LTL coupling*

This model does not require HTL-LTL coupling.



<b>Project</b>	NECCTON No 101081273	<b>Deliverable</b>	D7.2
<b>Dissemination</b>	Public	<b>Nature</b>	Report
<b>Date</b>	14/10/2025	<b>Version</b>	1.0

### 3.10.2 Application: Hindcast-Simulation

#### 3.10.2.1 Model configuration (Resolution, Boundary condition, Initial conditions, Model forcing)

Hindcast simulations for the NAWH-cetaceans model were conducted at a monthly resolution for the period 2001-2015, producing individual outputs for each of the two dolphin species. The models cover the Azores region (Central North Atlantic), with a spatial resolution of 0.1 degrees. Regarding environmental variables, depth and slope were derived from ETOPO-1 Global Relief Model. Distances to the 200 m were calculated using the geosphere package (Hijmans, 2024). SST and CHL were obtained from the CMEMS Global Ocean Physics Reanalysis and Global Ocean Colour, respectively. Mnk<sub>c</sub>\_epi and mnk<sub>c</sub>\_hmlmeso were obtained from the mid trophic level Spatial Ecosystem and Population Dynamics Model (SEAPODYM-MTL; Lehodey et al., 2010). The eastward and northward sea water velocity of the first layer of the SEAPODYM model were used to calculate the eddy kinetic energy (EKE\_L1).

#### 3.10.2.2 Results

##### Calibration and Validation of hindcast simulations

SDMs were compared and evaluated using the area under the receiver operating curve (AUC) and the percentage of deviance explained (Dev.Expl). The AUC gives the probability that a randomly selected presence will have a higher predicted value than a randomly selected absence. It ranges from 0 to 1, with 0.5 corresponding to a model with random discrimination (Jiménez-Valverde, 2012; Sillero et al., 2021). Low values (0.5-0.6) give a poor model performance, between 0.6-0.7 indicate a moderate predictive performance, 0.7-0.8 good, 0.8-0.9 very good and AUCs greater than 0.9 indicate a very high performance (Franklin, 2010).

Predictive performance of the models was tested on three training and testing dataset combinations: a) 75/25% data split, where the dataset was randomly divided with 75% of the observations being used to calibrate and the remaining 25% to evaluate the model; b) “Leave One Out” cross-validation (LOO) in which one year was iteratively left out from training and used for testing; and c) five folds cross-validation with a 75/25% training/testing data split, whereby the dataset was allocated in five equally distributed groups to which the 75/25% split was applied.

The same latitudinal spatial pattern was found on the habitat preference maps of the single models (GAM and BRT) and the ensemble across the months. In general, a good agreement was observed with reported sightings of the species each month. A consistent seasonal pattern was consistent throughout the years, however, a high inter-annual variability was identified in June and July.

Common dolphin SDMs had a moderately good predictive performance (AUC > 0.7), with deviance explained between 10.82% (BRT) and 12.49% (GAM) (da Silva et al., 2025). The ensemble outperformed the single models, scoring the highest AUC (0.73). Atlantic spotted dolphin models had a good performance (AUC > 0.77) with a deviance explained of 13.98% (GAM) and 14.64% (BRT). The ensemble outperformed the GAM but not the BRT, which had the highest AUC (0.8). The LOO had a lower predictive performance in comparison to the other validation method for both dolphin species (AUC=0.67 and AUC=0.72 for common and Atlantic spotted dolphin, respectively).

<b>Project</b>	NECCTON No 101081273	<b>Deliverable</b>	D7.2
<b>Dissemination</b>	Public	<b>Nature</b>	Report
<b>Date</b>	14/10/2025	<b>Version</b>	1.0

### 3.10.3 NECCTON Products from the model

The model provides probability of occurrence of two small delphinids by grid cell at a monthly scale (restricted to 4 months).

### 3.10.4 Discussion of pros and cons of the model

#### *Pros of NAWH-cetaceans:*

- These models predict the probability of occurrence of small delphinids taking into account survey sampling effort
- The modelling framework implemented can be replicated on other cetacean species and regions.
- Predictions capture relatively good the seasonal patterns of the target species, with a latitudinal pattern.

#### *Cons of NAWH-cetaceans:*

- Model only available from May to August (coverage of the existing dataset).
- High-interannual variability, as shown on the LOO performance.
- The model has a lack of validating through an independent dataset due to the lack of existing cetacean dataset having a similar spatio-temporal coverage.

## 3.11 FOIL-DEB (DEB-IBM for anchovy and sardine in the Bay of Biscay) (Leading partner: IFREMER)

### 3.11.1. Model description

FOIL-DEB (Fish On-or-Offline IBM with Lagrangian and DEB modules, Figure 35) is a model of population dynamics first developed for anchovy and sardine species. It is a mechanistic model build as an Individual Based Model (IBM) coupled to a Dynamic Energy Budget (DEB theory, Kooijman, 2010) model, to represent the many complex and detailed processes affecting fish life cycles. The IBM describes the life history trajectories of individuals in time and space (when in 3-D), and upscales to the population in a super-individual framework, while managing abundance based on reproduction and mortality processes. The DEB model is a bioenergetic model used to derive growth, reproduction and starvation mortality of individuals. Thus, population trajectories emerge from the interaction between individuals and their environment. To that end, FOIL-DEB requires temperature and food (plankton) as forcing, as well as velocity fields when run in 3-D for early life stages (eggs and larvae) transport.

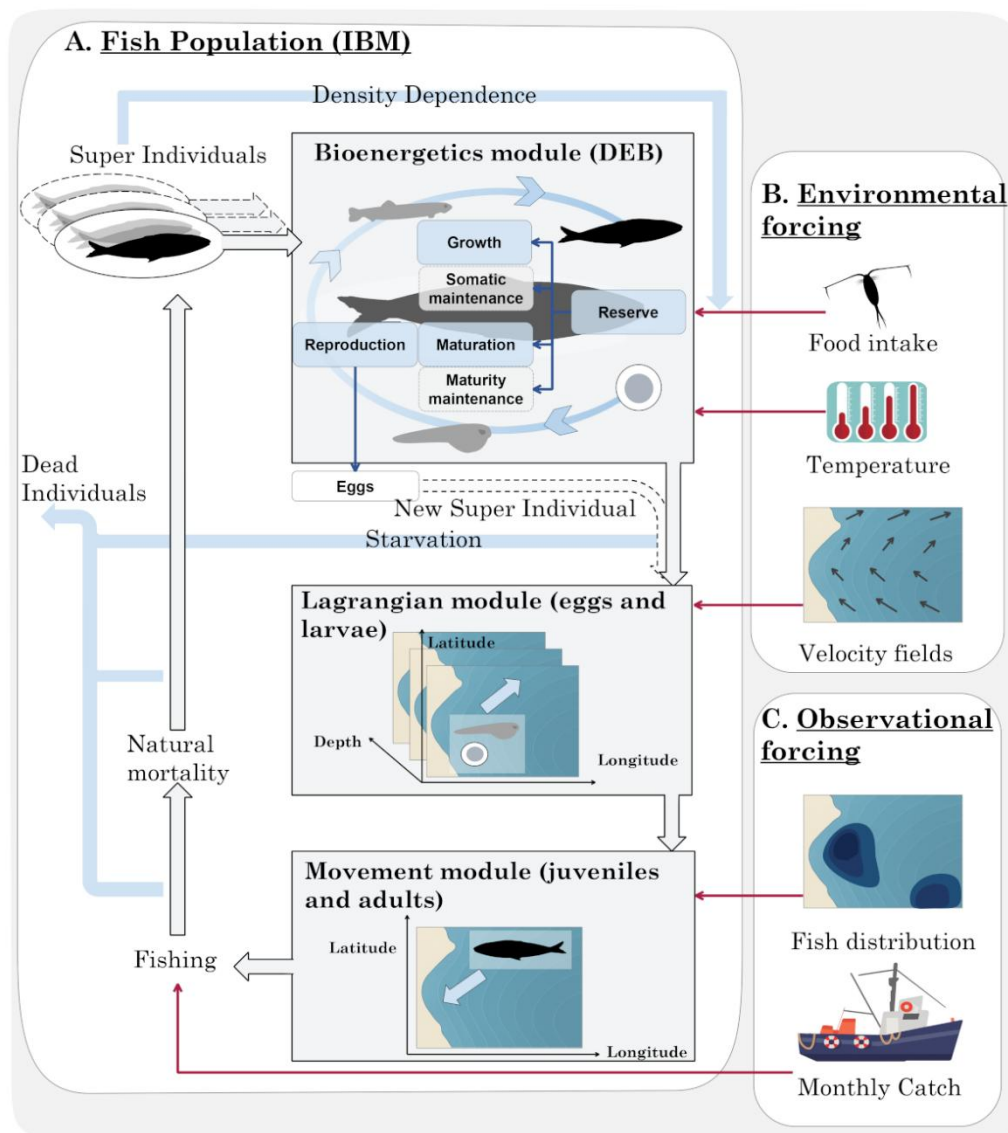
FOIL-DEB can be run online and in 3-D, in which case it is 1-way coupled to a physical-biogeochemical model that provides temperature, velocity and plankton fields. It was initially developed within the MARS hydrodynamic model framework but was recently integrated -and is now operational- within CROCO in NECCTON. It relies on a Lagrangian module (Huret et al., 2010), also integrated within

<b>Project</b>	NECCTON No 101081273	<b>Deliverable</b>	D7.2
<b>Dissemination</b>	Public	<b>Nature</b>	Report
<b>Date</b>	14/10/2025	<b>Version</b>	1.0

CROCO, for particle transport during the planktonic stages of fish, as well as on a fish movement module.

FOIL can also be run offline in one-way coupling mode when forcing are provided as external files, usually from a physical-biogeochemical model. This version is currently operational in 0-D in which case forcing variables are spatially averaged over the case-study domain (Bueno-Pardo et al., 2020; Menu et al., 2024). A 3-D off-line version would just require spatial fields of temperature, plankton and velocities to read, but is not developed yet.

For NECCTON, a combination of on-line and off-line versions is set up for the Bay of Biscay anchovy and sardine. FOIL-DEB is online coupled to CROCO but uses plankton fields from simulations of independent physical-biogeochemical models as provided by the project (WP 5). There are no direct or indirect interactions between both species.



<b>Project</b>	NECCON No 101081273	<b>Deliverable</b>	D7.2
<b>Dissemination</b>	Public	<b>Nature</b>	Report
<b>Date</b>	14/10/2025	<b>Version</b>	1.0

Figure 35. Schematic representation of the FOIL-DEB model, based on super individuals going through several modules and mortality sources (mechanistic processes are represented in blue), with the required inputs (environmental and observational forcing).

### 3.11.1.1 Model Formulations: State Variables, Equations, Parameters

#### Bioenergetics

Growth, maturation, reproduction and starvation mortality are handled by the DEB model (Kooijman, 2010) at the individual scale. The model considers five state variables: (E, J) - the amount of energy in reserve, (V, cm<sup>3</sup>) - the volume of structural mass, (ER, J) - the reproduction buffer, (EGam, J) - the gametes and (EH, J) - the level of maturity. Assimilated food goes to reserve (E), which is directly linked to food availability. The energy is then allocated to structure (V) and to maturation (EH) before the adult stage or reproduction (ER) when reaching the adult stage. Unlike reserve, structure and maturation require maintenance costs. The energy allocation within the organism is based on the kappa-rule. A fixed fraction  $\kappa$  is allocated to somatic maintenance and growth, whereas the remaining fraction  $(1 - \kappa)$  is allocated to maturity maintenance and maturation (juvenile) or reproduction (adult). Individuals become adults when they reach a particular maturity threshold which is species-specific. Our model refers to the standard DEB, except that energy can be reallocated from the reproduction buffer and/or gametes to somatic maintenance if the individual does not have enough energy for somatic maintenance. In case this additional supply remains insufficient, individuals die of starvation. The anchovy and sardine models were first developed by Gatti et al. (2017) and then applied to explore variability of traits across regions and periods (Huret et al., 2019 ; Menu et al., 2023). For parameter values please refer to Gatti et al. (2017) and Menu et al. (2023).

#### Inter-individual variability

Adding variability between individuals should increase the realism of our simulations as it allows various trajectories of life history, such as growth, to be represented as observed in our data, and because it allows selective processes to operate, depending on size for example. First, inter-individual variability arises as a plastic response to the environment. Individuals have different birth dates and locations within the same annual cohort, thus they will experience different environments. Second, to introduce genetic variability among individuals, we also considered variability on a limited number of DEB parameters. The number of parameters upon which variability is added is kept to a strict minimum for parsimony, but also to limit covariation issues. Each DEB parameter is calibrated as a single value. During this calibration process, parameter covariation was considered as all parameters were estimated together. Adding variability a posteriori on one or several parameters could lead to mathematical and/or biological mismatch. The zoom factor ( $z$ ) is a dimensionless parameter originally used for species comparison (Kooijman, 2010). This parameter is defined as the ratio of the maximum structural length of a species relatively to the structural length of a reference species. The assumption behind this parameter is that much of inter-specific variability can be explained by body size scaling relationships. In our model the zoom factor is used to model inter-individual variability based on the same assumptions. The variability on the zoom factor is fixed at birth by randomly choosing from a normal distribution as  $z \sim N(1, 0.066)$ , implying that 99.7% of the population has a zoom factor within  $\pm 20\%$  from the average (or calibrated) individual, whose zoom factor equals 1.

<b>Project</b>	NECCON No 101081273	<b>Deliverable</b>	D7.2
<b>Dissemination</b>	Public	<b>Nature</b>	Report
<b>Date</b>	14/10/2025	<b>Version</b>	1.0

### *Spawning strategy*

The spawning season corresponds to the period when energy is allocated to gametes from the reproduction buffer and their release in the environment. For the sake of parsimony and because no obvious trigger was found, the reproduction period is not triggered by any environmental variable, but instead constrained by the following periods. For anchovy, the spawning season runs from May to August as observed in Huret et al. (2018). For sardine, there are two spawning seasons. One is spanning from March to June and the second from October to November (Stratoudakis et al., 2007; Huret et al. 2018). Spawning distributions depend on the location of adults (see fish movement section below).

### *Transport*

For early life stages, we used the Lagrangian particle tracking module for 3-D advection and diffusion as described in Huret et al. (2010) and plugged into CROCO. For horizontal transport we use a random walk with a constant diffusivity coefficient ( $5\text{m}^2.\text{s}^{-1}$ ). In the vertical dimension, we use a non-naive random walk (Visser, 1997), with diffusivity coefficient provided by the hydrodynamic model. Four stages are distinguished, eggs, non-feeding larvae, feeding larvae without vertical migration and with vertical migration. Egg physical density is defined based on the relationship with local water density at spawning (Huret et al., 2016), and evolves throughout development (Ospina-Álvarez et al., 2012), which defines its vertical position in the water column and thus drift and development duration from current and temperature encountered. Vertical nycthemeral migration is initiated around the notochord flexion stage, i.e. at 6-7 mm SL, and occurs between the sea surface at night and the thermocline at day (unpublished data from the Bay of Biscay) with an increase of swimming speed with larval length.

### *Movement and migration*

For juvenile and adult movement, we have implemented a probabilistic approach in which displacement rules are constrained by acoustic survey-based maps of probability distribution by length and season. We have previously tried mechanistic rules for fish movement with some success in simulating seasonal reproduction migration (Politikos et al., 2015), but the environment triggers were not robust enough to explain the year-round fish behaviour. Thus, our objective is to constrain a realistic average distribution of the population, with individual variability dynamically represented within this population, as fish individually move within the observed distribution and have then their own life trajectory. We used these underlying population distribution maps to statistically constrain the movements of the individuals and their size-dependent locations. Movement is then not defined with behavioural rules but with a set of probabilistic rules, which constrain the displacement of the individuals to comply at each time step with a known underlying population spatial distribution. The underlying maps are an average over the observed time-series of the survey, without interannual variability so far.

The underlying map of probability distribution by size class is updated twice a year in our case since we only have seasonal maps of spring and autumn from surveys. We distinguish between random movements and migration. Individuals have random movements within spring observed distribution

<b>Project</b>	NECCON No 101081273	<b>Deliverable</b>	D7.2
<b>Dissemination</b>	Public	<b>Nature</b>	Report
<b>Date</b>	14/10/2025	<b>Version</b>	1.0

from winter and summer, and within autumn distribution from summer to winter, when migration is supposed to occur. The probabilistic movement is achieved using the Metropolis-Hasting (MCMC type) algorithm (Lantuéjoul, 2002). Applied to our IBM this gives the following algorithm:

For a given class length  $l$  :

For each individual in its grid cell  $i$ , with  $P(i,l)$  the probability to be in cell  $i$  for size  $l$  :

- Select a neighbouring cell  $j$  at random among the 4 neighbouring cells
- If  $P(j,l) > P(i,l)$  then move to cell  $j$ ,
- Otherwise ( $P(j,l) \leq P(i,l)$ ) move to  $j$  with probability  $P(j,l)/P(i,l)$ , otherwise stay in cell  $i$ .

This algorithm that makes fish move from one grid cell to the next one is applied every time step  $\Delta t$ . This time step controls that fish displacement is respectful of its swimming capacity, thus  $\Delta t > ds / v$ , with  $ds$  the length of the model grid cell and  $v$  the cruising speed set at 1.5 fish body length per second.

#### *Modelling abundance*

The IBM completes the individual's life cycle, as handled by the DEB, by turning spawned eggs into new individuals and is based on the work of Bueno-Pardo et al. (2020). Abundance results from the number of newborns minus those that die.

Numerically, it is impossible to simulate every individual of even a single population of small pelagic fish consisting of billions of organisms. To avoid this computational issue, the FOIL-DEB model represents a particle as  $N$  individuals having all the same properties, also called super-individuals (SI). The trade-off between the number of SI for representativeness and the computational cost converges towards few hundred thousand SI at any given time. The number of individuals in a SI then exponentially decreases from birth to death.

The numerical transcription of the reproduction process amounts to creating new particles or SI, and distributing eggs into the new SI while remaining conservative in numbers. During the spawning season of small pelagic fish, reproduction occurs every day (actually at night), although not all fish spawn every day depending on the spawning fraction or frequency. Users can play with the 'numerical' spawning frequency to regulate the number of SI created during the spawning season. Depending on the available computational capacity, the user knows approximately how much SI it can handle per annual cohort ( $SI_y$ ). Knowing the duration  $d$  of the spawning season and the spawning frequency  $f$  being set, the number of new SI per spawning event is then:  $SI_{sp} = SI_y * f / d$ , which can be modulated by a known temporal distribution of the egg abundance, usually gaussian over the spawning season. Then, the number of new SI in cell  $i$  is:

$$n_{SI}(i) = \text{round} (SI_{sp} * \text{eggs}(i) / \sum_i \text{eggs}(i)) ,$$

with  $\text{egg}(i)$  the number of eggs in cell  $i$  released since the last spawning event and stored in a buffer. Then the number of individuals in each SI of cell  $i$  at birth is defined as:

$$SI\text{Number} = \text{eggs}(i) / n_{SI}(i)$$

<b>Project</b>	NECCON No 101081273	<b>Deliverable</b>	D7.2
<b>Dissemination</b>	Public	<b>Nature</b>	Report
<b>Date</b>	14/10/2025	<b>Version</b>	1.0

Finally, new SI(i) are positioned randomly within the cell i.

### *Mortality*

Mortality sources are applied to each SI as an iterative process, rather than applying mortality on the total population directly. This allows mortality to scale with individual traits, with both natural and fishing mortality being a function of the length of individuals. Mortality sources are applied as follows:

$$SI(t+1)_{\text{number}} = SI(t)_{\text{number}} * e^{-Z_t} - N_{Ft}$$

With  $SI(t)_{\text{number}}$ , the number of individuals in SI à time t,  $Z_t$  the natural mortality, and  $N_{Ft}$  the number of individuals harvested by fishing. Note that some SI can also be removed from the population when dying from starvation based on the bioenergetic model. Here natural mortality  $Z_t$  can be interpreted as the proportion of natural mortality that is not related to starvation process. This mortality is a function of individual length and is applied continuously from eggs up to individual's death (Bueno-Pardo et al., 2020):

$$Z_t = Z_a + (Z_e - Z_a) * e^{-Z_L (L_t - L_{egg})}$$

with  $Z_e$  the egg mortality rate,  $Z_a$  the adult mortality rate when length tends to infinity (fixed at 0),  $Z_L$  a scaling coefficient of decreasing background mortality with length,  $L_t$  the individual length at a given time t,  $L_{egg}$  the size of an egg.

Unlike the previous mortality sources, fishing is considered as a forcing variable using raw monthly catch values as available from the assessment Working Group WGHANSA and is not spatialised so far. The catch biomass is distributed among the catchable part of the population, which excludes age-0 fish.

### *Density dependence*

To impact both growth and mortality, density dependence is introduced in the functional response for the intake rate of a consumer as a function of its prey density and linked to food availability. In the standard DEB model, the functional response is described as a Holling type II function expressed in the form of  $f = X/(X_K + X)$ , with X the zooplankton concentration and  $X_K$  the half saturation coefficient.

In the Holling type II function,  $X_K$  is a fixed parameter and is defined as proportional to the ratio of searching time and handling time. Following Beddington (1975) and DeAngelis et al. (1975), a density dependent factor is added in the functional response. The Beddington-DeAngelis functional response is similar to the Holling type II, yet the half saturation becomes  $X_K + B/b_K$  with B the biomass of predators. This additional factor represents mutual interference by competitors, i.e. more competitors lead to longer searching time when food availability is constant. In our model, density dependence scales to the total biomass of structure, encompassing life stages from exogenous feeding larvae to adults. The choice of structural biomass instead of total biomass allowed to limit seasonal variations



<b>Project</b>	NECCTON No 101081273	<b>Deliverable</b>	D7.2
<b>Dissemination</b>	Public	<b>Nature</b>	Report
<b>Date</b>	14/10/2025	<b>Version</b>	1.0

due to (i) food availability which results in seasonal variations in reserve, and (ii) spawning which results in seasonal variations in the reproduction buffer.

To allow density dependence to scale during individual's ontogeny, a weight effect is added similarly to David et al. (2019). This implies that density dependence starts at mouth opening, is the most effective at larval stage and then decreases through ontogeny according to individual weight.

$$f_i = X_t / (X + X_K + B_v / b_K * B_{vi}^\gamma)$$

where the functional response of individual  $i$  is affected by density dependence with  $B_v$ , the total population biomass of structure scaled by the parameter  $b_K$ ,  $B_{vi}$  the individual structural mass and  $\gamma$  a scaling factor decreasing density dependence intensity according to individual weight.

#### *3.11.1.2 Model structure and required forcings and inputs; Implementation details*

The FOIL-DEB model is coded in fortran 90 and coupled within the CROCO ocean modelling platform (<https://www.croco-ocean.org/>), with code available here: <https://gitlab.inria.fr/croco-ocean/croco>. The model is parallelised with MPI and can run on a HPC machine.

The CROCO hydrodynamic model requires typical inputs, such as boundary conditions, atmospheric forcing, and river runoff, and runs with a time-step of approximately 2mn.

For the calibration of FOIL-DEB, we use a global optimisation method, the Evolution Strategy from the family of the evolutionary algorithms (Baeck and Schwefel, 1993), with the Fortran library pCMALib (Müller et al. 2010). It is applied stepwise by first calibrating the parameters of the DEB on a single average individual representative of the population, then the population parameters of the IBM in 0-D.

#### *3.11.1.3 Model specifics to HTL-LTL coupling*

Within NECCTON, FOIL-DEB will be forced (one-way coupling) by outputs from NEMO-ERSEM. Total zooplankton is used as food for both sardine and anchovy that are mostly zooplanktivorous. Vertical averaging of the zooplankton biomass over the surface mixed layer (arbitrarily set to 50 m) is performed as a pre-process. Then daily forcing is used and interpolated to the time step of FOIL-DEB. The standard DEB uses a Holling Type 2 functional response. We rely on this standard (see density dependence section above). Within the 1-way forcing framework, food can be provided in any unit, then the half saturation coefficient needs to be calibrated accordingly.

### **3.11.2 Application Hindcast-Simulation**

#### *3.11.2.1 Model configuration (Resolution, Boundary condition, Initial conditions, Model forcing)*

The Bay of Biscay application of FOIL-DEB uses a CROCO configuration with a domain spanning from 40°N to 55°N, and 18°W to 10°E (Figure 36), using a grid of ~2.5 km and 40 sigma layers on the vertical. It runs in MPI with 441 processors. The meteorological forcing comes from the ERA5 ECMWF reanalysis. The oceanic boundary conditions come from the GLORYS reanalysis. We use daily river run-offs from national databases. CROCO provides the temperature and 3D velocity and diffusivity fields.

<b>Project</b>	NECCTON No 101081273	<b>Deliverable</b>	D7.2
<b>Dissemination</b>	Public	<b>Nature</b>	Report
<b>Date</b>	14/10/2025	<b>Version</b>	1.0

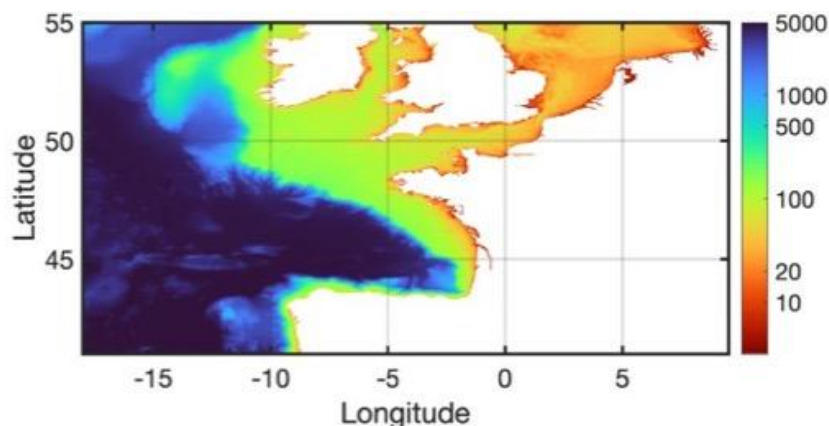


Figure 36. Model domain of the CROCO configuration to which FOIL-DEB-IBM) is coupled for the anchovy and sardine Bay of Biscay application.

Waiting for the complete NEMO-ERSEM run to become available in NECCTON, so far we have been using the zooplankton forcing from SEAPODYM available in CMEMS (GLOBAL\_MULTIYEAR\_BGC\_001\_033) for the model calibration and some first 3-D testing, that are presented below. The hindcast simulation will eventually cover the period 2000-2020. The initial condition for the populations of sardine and anchovy are taken from the observations (abundance-at-age) during the PELGAS survey in 2000.

#### *3.11.2.2 Calibration and validation of hindcast simulations*

The calibration of the DEB and population parameters can not be made on the multi-annual 3D simulations, because of computational limitations. Thus, we perform a multi-step calibration. First, the DEB parameters for each species are calibrated in 0-D based on an average representative individual (Figure 37), and using average population data from the Bay of Biscay from the PELGAS small pelagic survey occurring in May (Doray et al., 2018 ; Doray et al., 2020) : size- and weight-at-age, energy density-at-age, and reproduction quantitative information. Validation can be performed with growth and environmental data from other regions. Second, the population parameters (mortality, density-dependence) are calibrated in 0-D with a population simulation, using abundance, biomass and age structure data from the PELGAS survey (Figure 37).

Project	NECCTON No 101081273	Deliverable	D7.2
Dissemination	Public	Nature	Report
Date	14/10/2025	Version	1.0

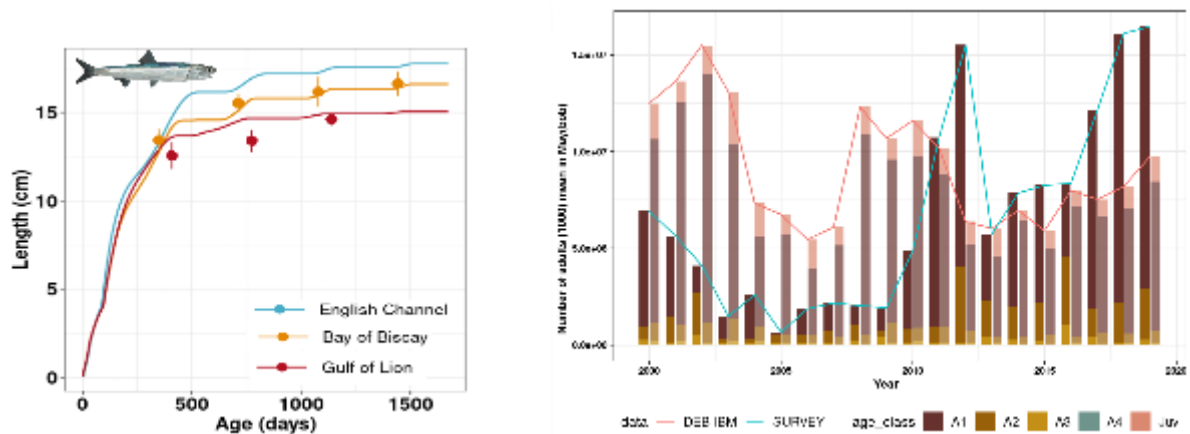


Figure 37. Calibration of the DEB (left panel) and then the IBM (right panel) modules of the FOIL-DEB model. Anchovy as an example. Left panel: Result of the calibration of the DEB model on size-at-age data of the Bay of Biscay (orange), and validation on data from the gulf of Lion (Mediterranean Sea, red). Predicted growth in the English Channel is also shown (blue). Right panel: Result of the calibration of the IBM model in 0-D. Number of adult per age class (barplots) as well as total abundance (curves) are represented for both model and survey data.

Within NECCTON the general validation will be performed based on the results of 3-D population hindcast simulations covering the period 2000-2020.

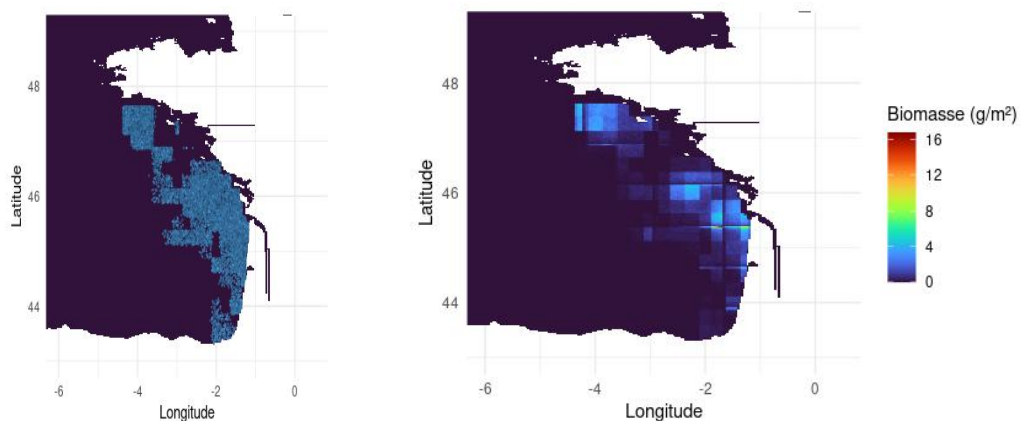


Figure 38. Snapshot of the model result for anchovy, with the location of super individuals (the left panel), and the corresponding biomass density as a NECCTON product (right panel).

### 3.11.3 NECCTON Products from the model

The outputs of the model are non-gridded netcdf files with all the attributes (position, size, energy, etc.) over time of all particles (or SI) of the model. A netcdf file gathers all SI of an annual cohort. For NECCTON, they are converted in 2D gridded netcdf files based on the CROCO model grid limited to the Bay of Biscay, with a daily or monthly temporal resolution (Figure 38). Biomass of anchovy and sardine will be provided.

<b>Project</b>	NECCON No 101081273	<b>Deliverable</b>	D7.2
<b>Dissemination</b>	Public	<b>Nature</b>	Report
<b>Date</b>	14/10/2025	<b>Version</b>	1.0

### 3.11.4 Discussions of pros and cons of the model

#### *Pros of FOIL-DEB:*

- Detailed representation of the successive life stages with their particularities, especially for early life stages.
- Short time step for consideration of detailed processes such as advection and diffusion (3D) for early life stages. Useful in connectivity studies.
- Species-specific population dynamics modelling, with potential management applications. Availability of relevant population scale data.
- The Fortran coding facilitates the coupling with CROCO, and potentially other hydrodynamic platform, as well as potentially 2-way coupling.
- Genericity of the modules (ex: DEB) and implemented processes for application to other fish species, particularly planktivorous species.
- Various versions (0-D/3-D, online/offline) for calibration purposes as well as flexibility regarding research and applied questions.

#### *Cons of FOIL-DEB:*

- Heavy to run in 3-D despite fortran base, especially when coupled online to the hydrodynamic model.
- The super-individual approach limits the realism in terms of inter-individual variability represented. There is a trade-off between the number of super-individuals we can simulate and the computational cost.
- Lack of explicit vertical processes for juvenile and adults due to lack of knowledge on their behaviour.
- No easy frontend for non-modellers, or those non familiar with fortran coding.
- Lack of interannual variability in the distribution of the adults, strongly constrained by observations in its current state.
- No explicit mortality by predation, i.e. natural mortality of the modelled populations is the closure term. No direct or indirect interaction between anchovy and sardine although this can be easily implemented.
- No explicit density-dependence (1-way coupling with LTL) but no structural limitation as soon as a biogeochemical model is coupled to the hydrodynamic model (in progress). Potential inconsistencies between physical and biogeochemical fields, the latter coming from an external model as forcing conditions.

<b>Project</b>	NECCON No 101081273	<b>Deliverable</b>	D7.2
<b>Dissemination</b>	Public	<b>Nature</b>	Report
<b>Date</b>	14/10/2025	<b>Version</b>	1.0

## 3.12 DEB-IBM European Anchovy BS (Leading partner: UoL)

### 3.12.1 Model description

#### 3.12.1.1 Introduction and biological basis

The DEB-IBM is an agent-based model (ABM) that offers a powerful computational platform for spatial and temporal modeling of population dynamics. ABMs operate from the bottom up by representing how individual entities (referred to as agents) interact with their localized environment that determines their growth, mortality, reproduction, and movement. Population-level predictions are then obtained by summing over all the individual entities, and enable population predictions in response to how environmental drivers and management actions influence individual behavior and vital rates (Bousquet and Le Page 2004).

Our DEB-IBM model is a three-dimensional (2D in the preliminary version whose results are reported here), agent-based model one-way coupled to a lower trophic level ecosystem model (NEMO-BAMHBI). It consists of several interconnected submodels: a Dynamic Energy Budget (DEB) model for individual growth and reproduction (Pethybridge *et al.* 2013, Gatti *et al.* 2017), a kinesis-based horizontal movement model (Watkins and Rose 2017), a particle tracking model (PTM) for transport of early life stages, a seasonal migration model, and with the 3D version, a vertical movement model. Our model is designed to simulate the full life cycle of European anchovy in the Black Sea. As of July 30, 2025, a fully functional preliminary version of the DEB-IBM model has been developed in a two-dimensional format and is currently undergoing calibration. We include below the planned steps for calibration and validation of the two-dimensional version of the model, with potential extension to the three-dimensional version.

The overall goal of our modeling is to mechanistically explore how environmental variables (e.g., temperature and food availability) influence the growth, mortality, reproduction, and movement of the anchovy population in the Black Sea. Our primary focus is on understanding interannual variability in spawning, life-stage dynamics, recruitment, and adult abundances and spatial distribution patterns. To achieve this, we develop a DEB-IBM model that integrates bioenergetic (growth), reproductive, mortality, and movement processes across life stages. By explicitly simulating the spatiotemporal dynamics of anchovies under varying environmental conditions, our model allows us to evaluate how environmental drivers influence population-level outcomes. This framework enables us to explore the mechanisms driving interannual variability and spatial dynamics at the population-level and provides insights into the sensitivity of the population to historical and projected future environmental conditions in the Black Sea.

European anchovy is a well-studied short-lived small pelagic species with a normal lifespan of five years (Pethybridge *et al.* 2013). The life cycle of the European anchovy in our model is divided into six developmental stages: egg, yolk-sac larva, early larva, late larva, juvenile, and adult. Anchovy is a typical oviparous species. During early development (i.e., egg and yolk-sac larva) individuals rely entirely on endogenous yolk reserves for energy. Temperature determined the development of the egg and yolk-sac larval stages, while the transitions between early larva, late larva, juvenile, and adult stages are based on individual body length. The early larval stage begins at 0.36 cm total length (TL)

<b>Project</b>	NECCON No 101081273	<b>Deliverable</b>	D7.2
<b>Dissemination</b>	Public	<b>Nature</b>	Report
<b>Date</b>	14/10/2025	<b>Version</b>	1.0

and extends up to 1 cm, with a reference duration of 12 days (Oguz *et al.* 2008). The late larval phase follows, with a reference duration of 22 days and a transition to juveniles at a length of 2.5 cm. Juveniles transition to adults at 7 cm, which is set based on reported maturity values in the literature (Akkuş and Gücü 2023). Adults progress to the next age on January 1 of each year. This is consistent with stock assessment reports and ensures that all potential newborn anchovies in the Black Sea are included prior to 1 June. As a result, early age-1 individuals can be immature or mature.

Temperature and prey availability are critical drivers shaping water column use across different life stages of anchovy in the Black Sea. Early life stages, including eggs and yolk-sac larvae, consistently inhabit the surface waters above the seasonal thermocline, typically within the upper 15–30 meters (Oguz *et al.* 2008). In contrast, juveniles and adults exhibit greater vertical mobility, often tracking the diel vertical migration of zooplankton prey and thus occupying a broader depth range within the euphotic zone (Güraslan *et al.* 2014). In the Black Sea, both the thermocline and euphotic zone depths exhibit minimal variation over shelf areas shallower than 50 meters, while deeper regions (50–100 m) are characterized by unimodal fluorescence profiles, indicating distinct vertical structuring of primary productivity (Finenko *et al.* 2005). Based on these hydrographic patterns, we define life–stage–specific vertical habitat ranges: 0–10 m for eggs and yolk-sac larvae, 0–30 m for early and late larvae, and up to 100 m for juveniles and adults.

The progression of anchovy early life stages is temperature-dependent and is modeled using daily time steps, based on the functions described by Gatti *et al.* (2017). According to observations of Black Sea anchovy, the combined duration of egg and yolk-sac stages is approximately 2 to 2.5 days at water temperatures above 20 °C (Lisovenko and Andrianov 1996). Detailed description of functions refers to Yu *et al.* (in prep.).

We used the Dynamic Energy Budget (DEB) model, following Pethybridge *et al.* (2013), to simulate growth and reproduction of individual anchovy from the onset of feeding (early-larvae). For each super-individual, the DEB model tracks reserves, structure, reproduction buffer, and gametes, with energy fluxes as described in Pethybridge *et al.* (2013) and Gatti *et al.* (2017). Assimilated energy supports maintenance, growth, maturation, and reproduction, with somatic and gamete-related maintenance prioritized. No explicit starvation thresholds are imposed; instead, stage-specific maximum durations and a low-worth threshold (<1) are used for removal. In the Black Sea, European anchovy spawns exclusively in the upper warm layer of the water column (0–10 m) above the thermocline (Niermann *et al.* 1994). Its spawning season typically extends from mid-May, when water temperature reaches approximately 16 °C, to mid-to-late August, when the temperature approaches 25–26 °C (Akkuş 2023). According to the literature, we define annual spawning windows based on sea temperature conditions in our model. The potential onset of spawning is identified as the earliest date when the maximum temperature averaged over the 0–10 m depth range exceed 16 °C in any grid cell. Conversely, the potential end of spawning was determined as the first date when the maximum 0–10 m average temperature drops below 26 °C in any grid cell. Following Pethybridge *et al.* (2013), we assume that 60% of energy for gametes supports final oocyte maturation (40% for earlier stages), with temperature-dependent development determining successful spawning. Therefore, the spawning period (180 days) is constrained by sea temperature conditions. Gamete development and fecundity

<b>Project</b>	NECCON No 101081273	<b>Deliverable</b>	D7.2
<b>Dissemination</b>	Public	<b>Nature</b>	Report
<b>Date</b>	14/10/2025	<b>Version</b>	1.0

followed temperature-dependent functions. We apply empirical calibration, which is defined as the adjustment of temperature-dependent oocyte development periods, relative batch fecundity, and associated reproduction rules. This ensures that simulated reproductive dynamics remain consistent with observed biological ranges under Black Sea conditions. Eggs release each day are aggregated by region, adjusted for a 50:50 sex ratio, and distribute across suitable spawning habitats (<200 m depth) (Yu et al., in prep.).

For eggs, yolk-sac larvae, and early larvae with limited swimming ability, we apply an hourly particle tracking model (PTM). The PTM simulates movement driven by surface currents, where temperature-, salinity-, and density-derived current fields are interpolated onto particle positions using bilinear interpolation (2D). In the planned 3D version, vertical movement will also be resolved bilinear and vertically linear interpolation, incorporating buoyancy effects (via Stokes' law), egg physical properties, and temperature–salinity dependent viscosity. Additionally, wave-induced Stokes drift will be included to adjust horizontal velocities with depth, while boundary conditions will be treated by setting velocities to zero at the grid edges. The horizontal movement of late-larvae, juveniles, and adults (age-1+) is modelled daily using the Kinesis approach (Watkins and Rose 2017), where movement velocities combine inertial and random components influenced by local temperature and food availability relative to individual preferences. When conditions are favorable, individuals tend to reduce movement and remain in suitable areas, whereas unfavorable conditions increase random movements. Movement at grid boundaries is randomized for moving direction to ensure individuals remained within the Black Sea domain, and vertical migration (planned for the 3D version) will be guided by depth-specific growth predictions from the DEB model (Yu et al., in prep.).

The overwintering migration of anchovy has been well documented (Panov and Chashchin 1990, Gücü *et al.* 2017), and is driven by ambient temperature dynamics in conjunction with coastal water current advection. Anchovies undertake migrations from their spawning and nursery grounds on the northern continental shelf to the southeastern Black Sea, following the basin-wide rim current (Gücü *et al.* 2017). Based on observations linking the initiation of this southward migration to seasonal cooling, which typically begins in early October or mid-November (Guraslan *et al.* 2017), we plan on implementing a temperature-based and vertical migration in the migration model. The model includes two daily mortality sources: natural and fishing. Natural mortality is stage-specific and is refined through calibration with plausible ranges defined by stock assessments and other literature. Juvenile natural mortality is modeled as density-dependent, with a multiplier (ZFAC) adjusting mortality based on local density, reflecting the likelihood of increased predation and/or competition at high densities. Fishing mortality is assumed spatially uniform due to limited data and applied daily to individuals >9 cm using rates from stock assessment reports (GFCM 2023 or GFCM 2024). Total daily mortality combines natural mortality (modulated by ZFAC) and fishing mortality (MF), and is applied directly to each super-individual's worth (Yu et al., in prep.).

### 3.12.1.2 Model Formulations: State Variables, Equations, Parameters

Each individual is characterized by a set of state and derived variables, including age, status (alive or dead), spatial location (continuous longitude and latitude, and corresponding cell number), depth, DEB state variables (Reserve, Reproduction buffer, Structural volume), total length (*TL*), body wet



Project	NECCTON No 101081273	Deliverable	D7.2
Dissemination	Public	Nature	Report
Date	14/10/2025	Version	1.0

weight ( $W_{ww}$ ), life stage, functional response to diet, experienced temperature, and fecundity. We describe the model, following the ODD (Overview, Design concepts, and Details) protocol (Grimm *et al.* 2006; Yu *et al.*, in prep.). Below we highlight several key features of the model.

We use a super-individual approach following the methodology described by Rose *et al.* (2015), where each super-individual represents multiple identical individuals and carries full biological and environmental attributes. Worth, indicating how many individuals it represents, is reduced by mortality over time and reassigned annually. Population-level metrics (e.g., abundance, mean length-at-age, egg production, spatial distribution) are computed by weighting individual outputs by worth. This approach allows efficient simulation of large populations with a fixed number of super-individuals (Scheffer *et al.* 1995; Rose *et al.* 2015).

### 3.12.1.3 Model structure and required forcings and inputs; Implementation details

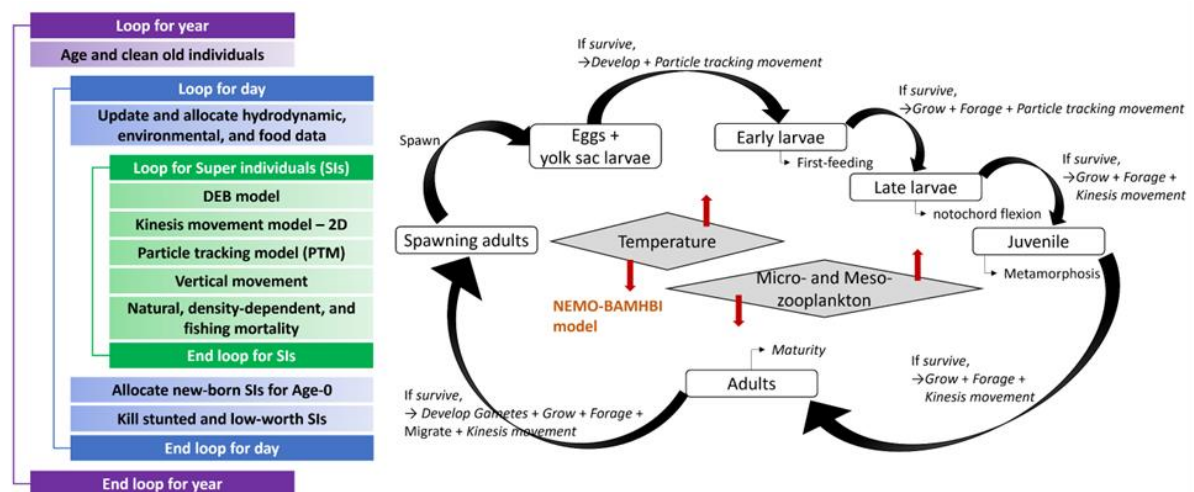


Figure 39. Model structure.

Our DEB-IBM model tracks the three-dimensional (2D in the preliminary version) spatial positions of each super-individual on a daily time step (Figure 39). The DEB-IBM uses the same 3D spatial grid used by NEMO-BAMHBI; the 2D version uses the average of grid cells for stage-specific layers. The calculations are structured with four nested loops: year, day, hour (necessary for particle tracking model), and individuals. Environmental variables derived from the NEMO-BAMHBI model are updated daily prior to running the submodels for growth, reproduction, and movement. Individuals in the egg, yolk-sac larval, and early-larval stages are advected using a particle tracking model with an hourly time step to capture finer-scale than daily hydrodynamic influences. For late-larvae, juveniles, and adults, growth (including early-larvae) and reproduction are simulated daily using the DEB, and movement is simulated daily using a kinesis algorithm for horizontal movement (vertical will be added) with temperature and food availability as movement cues. The total reproductive output of the super-individuals across the Black Sea grid is evaluated once per day. Juvenile and adult migratory behavior will be added by combining the particle tracking model with kinesis and vertical movement submodels.

<b>Project</b>	NECCON No 101081273	<b>Deliverable</b>	D7.2
<b>Dissemination</b>	Public	<b>Nature</b>	Report
<b>Date</b>	14/10/2025	<b>Version</b>	1.0

(will be incorporated in 3D version), triggered by a temperature threshold, following the approach of Guraslan *et al.* (2017).

The forcing variables derived from NEMO-BAMHBI include daily temperature, microzooplankton and mesozooplankton concentrations, horizontal ( $V_u$ ,  $V_v$ ) and vertical ( $V_w$ ) current velocities, water density, and salinity. In addition, the particle tracking model (PTM) requires additional daily surface Stokes drift velocity ( $u_s$  and  $v_s$ ), sea surface wave period ( $\omega_p$ ), and the significant wave height ( $H_s$ ), which are downloaded from E.U. Copernicus Marine Service Information (DOI: 10.25423/cmcc/blksea\_analysisforecast\_wav\_007\_003\_eas5). Although both the wave and hydrodynamic variables are available at a daily resolution, the PTM operates on an hourly timestep; therefore, temporal interpolation is applied to generate hourly values between successive days of all needed variables of PTM. All variables, except the velocity fields from the NEMO-BAMHBI model, are interpolated from the centers of the model grid cells, while the hydrodynamic velocity variables follow the Arakawa-C grid structure of the NEMO model. To accurately assign environmental conditions to each super-individual within the model, we employ bilinear interpolation in the horizontal plane (linear interpolation will be used in the vertical dimension) based on the specific spatial position of each super-individual.

Growth and reproduction of each super-individual are simulated daily using the DEB model, which is forced by temperature and food availability. The DEB model is activated at the onset of exogenous feeding (early-larvae stage) and tracks four state variables of each super-individual: reserves, structural volume, reproduction buffer, and gametes. Assimilated energy, determined by food intake and influenced by temperature effect, is first stored in reserves and then allocated to maintenance, structural growth, and reproductive development, with maintenance prioritized. Food intake is calculated from micro- and mesozooplankton concentrations using a multi-species Holling type II functional response (Rose *et al.* 2015), scaled between 0 and 1. In addition, the development of early stages (eggs to early larvae), which is not implemented in the DEB model, is determined by separate temperature-based functions (Gatti *et al.*, 2017).

Early stages (eggs to early larvae) are advected hourly using a particle tracking model driven by hydrodynamic currents and buoyancy. Late larvae to adults move daily using a kinesis algorithm, where movement depends on local temperature and food availability. Migration behavior for juveniles and adults is triggered by ambient temperature. Vertical movement will be added in the 3D model.

Daily mortality includes natural and fishing components. Natural mortality is stage-specific and calibrated, with juvenile mortality density-dependent via a multiplier (ZFAC) based on local juvenile density. Fishing mortality is assumed uniform across the Black Sea, applied daily to individuals > 9 cm. Total daily mortality reduces the worth of each super-individual.

Model parameters and definitions of all sub-models (super-individual, development of egg and yolk sac larvae, DEB, PTM, Kinesis, Migration, and Mortality) components are described in detail elsewhere (Yu *et al.*, in prep.). Our model is fully implemented in R (version 4.3.2). All submodels are independently integrated using the Euler method to solve the model's difference equations.

<b>Project</b>	NECCOTON No 101081273	<b>Deliverable</b>	D7.2
<b>Dissemination</b>	Public	<b>Nature</b>	Report
<b>Date</b>	14/10/2025	<b>Version</b>	1.0

#### 3.12.1.4 Model specifics to HTL-LTL coupling

We directly utilize the outputs from the high-resolution model NEMO-BAMHBI (Nucleus for European Modelling of the Ocean - Biogeochemical model for Hypoxic and Benthic Influenced areas, Grégoire et al., 2025, unpublished) as forcing variables in our DEB-IBM model. This implementation is a one-way coupling approach, with no feedback to the lower trophic level model. NEMO-BAMHBI is a three-dimensional, eddy-permitting model configured for the Black Sea at a spatial resolution of approximately 2.5 km (0.025° x 0.025°), encompassing 74068 horizontal grid cells and 59 sigma-coordinate depth layers. The BAMHBI component represents a moderate complexity marine biogeochemical model, simulating the cycling of carbon, nitrogen, phosphorus, silicon, and oxygen throughout the marine food web. It includes up to 35 state variables, ranging from bacteria to mesozooplankton, and has been previously applied in the Black Sea to investigate the eutrophication processes (Grégoire *et al.* 2008) and biogeochemical cycling (Grégoire and Soetaert 2010).

#### 3.12.2 Application: Hindcast-Simulation

##### 3.12.2.1 Model configuration (Resolution, Boundary condition, Initial conditions, Model forcing)

We plan on simulating January 1, 1990 to December 31, 2023 (34 years) with DEB-IBM using the outputs from the corresponding NEMO-BAMHBI simulation. To date, we perform a variety of shorter simulations to test the submodels (DEB, movement), ensure the solution methods are numerically accurate (convergence testing), and as part of model calibration. These shorter calibrations are part of building up confidence in the full model for use in the hindcast. When appropriate, all simulations use a 5-year spin-up period using 1990.

We calibrate growth and reproduction using zero-dimensional DEB models with two multi-year environmental datasets (1990-1994 and 2012-2017) from NEMO-BAMHBI. Environmental variables are averaged by life-stage depth ranges and spawning regions. Simulations begin at four spawning dates (June, July, August, and September) across ten regions, resulting in a total of 40 individuals per period. Growth calibration uses von Bertalanffy parameters (1954-2018) and fit period-specific curves. Field length-at-age data (2012-2018) are converted to weight and compared with model outputs. Reproduction calibration relies on empirical fecundity data and prior studies. Life-stage half-saturation constants are iteratively tuned to match realistic growth and reproduction.

We calibrate the Kinesis movement submodel using a simplified version with temperature and food cues on a 2D spatial grid from NEMO-BAMHBI. Artificial gradients of temperature and food are set with optimal values in different grid areas. We initialize 1000 adult individuals (TL = 13 cm) randomly and simulated movement only (no growth or mortality) for one year. Four scenarios are tested: (1) overlapping temperature and food gradients, expecting aggregation in the shared optimum; (2) opposing gradients, expecting mixed or no clear patterns; (3) adjacent but separate optima, expecting distribution around both zones; (4) opposite optima directions, expecting split distribution. Final positions and movement trajectories are analysed, and movement-related parameters are adjusted so that model predictions of spatial patterns match expected behaviours. The other movement-related submodel is the PTM, which uses standard formulations and is based on previously calibrated and validated outputs from the NEMO-BAMHBI model so further calibration is not needed.

<b>Project</b>	NECCTON No 101081273	<b>Deliverable</b>	D7.2
<b>Dissemination</b>	Public	<b>Nature</b>	Report
<b>Date</b>	14/10/2025	<b>Version</b>	1.0

The full DEB-IBM model is in the process of being calibrated. After calibrating the DEB and kinesis submodels, we integrate them into the full 2D DEB-IBM and focus on tuning mortality and density-dependence parameters. First, we run a 5-year simulation (1990–1994) without years that generate extreme conditions and adjust constant daily mortality rates for larvae, juveniles, and adults under density-independent conditions (ZFAC = 1) to achieve stable biomass. Next, we will fine-tune larval mortality using empirical data from GFCM stock assessments, which provide exploitable stock biomass and catch estimated by the State-space production model (SpiCT) in GFCM (2024) and spawning stock biomass, catch, and recruitment estimated by the state-space assessment model (SAM) in GFCM (2023). Then, we will introduce density-dependent mortality by calibrating reference density, slope, and maximum ZFAC to avoid unrealistic mortality spikes. Model-generated spawner-recruit relationships will be compared with historical assessment data and checked against a Beverton–Holt pattern. Our target is a steepness value of about 0.7, typical of values reported for anchovies and typical of other species with a similar opportunistic life history strategy (Rose *et al.* 2001).

### 3.12.2.2 Results

#### 3.12.2.2.1 DEB submodel calibration

Simulated total length and wet weight of individuals born in two distinct time periods (1990–1995 and 2012–2017) fell within the range of von Bertalanffy growth curves fitted to anchovy populations across the Black Sea from 1954 to 2018 (Figure 40 and Figure 41).). Spatial gradients in growth were evident, with individuals reaching total lengths of 12–15 cm and weights of 10–20 g across EEZs from the southern (e.g., Turkey) to the northwestern Black Sea (e.g., Ukraine\_1 and Romania). Notably, individuals born in Ukraine\_1 between 2012 and 2017 occasionally reached weights up to 30 g. For the 2012–2017 cohort, individuals born in Turkey\_1, Turkey\_2, and Turkey\_3 remained well within the observed ranges recorded in Turkish EEZ field surveys (Figure 40E–H and Figure 41E–H).

Temporally, individuals born during earlier spawning windows (June–July) consistently exhibited faster growth than those spawned later in the season (August–September), reflecting the biological peak of anchovy production in the Black Sea. Furthermore, individuals born in 2012 displayed larger body size than those from 1990, likely due to more favorable environmental conditions, including warmer temperatures and greater food availability (e.g., Figure 40E–H vs Figure 40A–D). Spatially, individuals born in the northwestern EEZs (Ukraine\_1 and Romania) attained the greatest lengths and weights, consistent with these regions being historically significant anchovy spawning grounds (Lisovenko and Andrianov 1996).

Patterns in spatial fecundity mirrored the trends in growth rates. Both cohorts (1990–1995 and 2012–2017) exhibited age-related increases in batch spawning, with older individuals producing more eggs. In the 1990–1995 cohort, individuals born in the Ukraine\_1 EEZ displayed the highest fecundity, with average total egg production ranging from 45,981 to 22,147 eggs from age-1 to age-4, followed by those in Romania and Bulgaria (Figure 42A–D). These outputs align with empirical estimates of an average 200,000 eggs per female per spawning season observed on the northwestern shelf in 1990 (Lisovenko and Andrianov 1996). In contrast, the 2012–2017 cohort exhibited a spatial shift in high-fecundity regions toward the southeastern Black Sea, particularly in Georgia and Turkey\_3, which was a transition previously documented by Gucu *et al.* (2016)(Figure 42E–H). The fecundity values were

<b>Project</b>	NECCTON No 101081273	<b>Deliverable</b>	D7.2
<b>Dissemination</b>	Public	<b>Nature</b>	Report
<b>Date</b>	14/10/2025	<b>Version</b>	1.0

consistent with age-dependent batch fecundity estimates for European anchovy in the Bay of Biscay (Pethybridge *et al.* 2013) and Turkish Aegean Sea (Taylan and Bayhan 2024), where batch fecundity ranged from 4,500-13,600 eggs and seasonal totals reached 133,270-302,040 eggs.

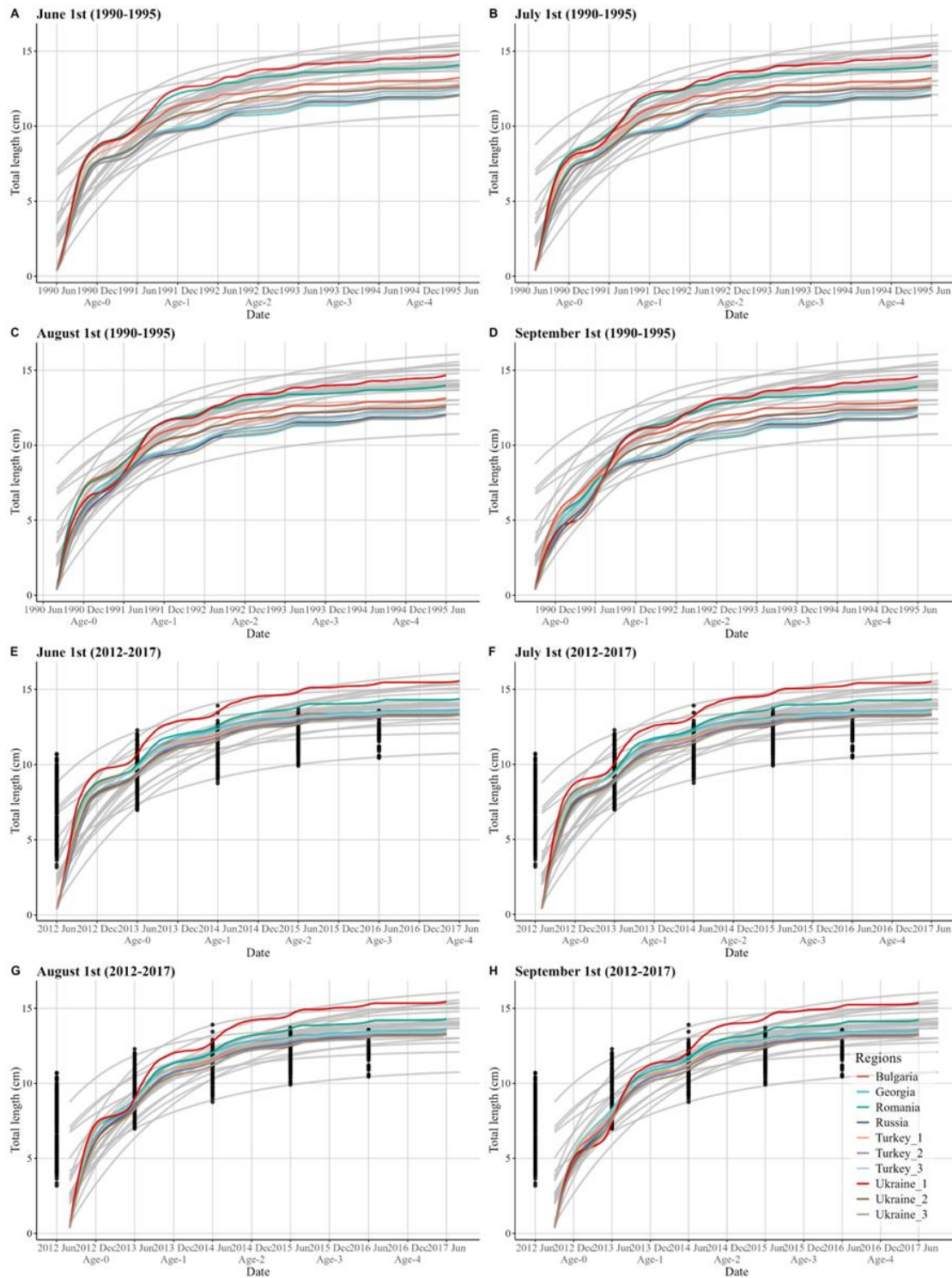


Figure 40. DEB model calibration of total length for individuals born on June 1st, July 1st, August 1st, and September 1st across 10 regions in two time periods: A–D (1990–1995) and E–H (2012–2017). Black dots



<b>Project</b>	NECTON No 101081273	<b>Deliverable</b>	D7.2
<b>Dissemination</b>	Public	<b>Nature</b>	Report
<b>Date</b>	14/10/2025	<b>Version</b>	1.0

represent age-length observations from field surveys in the Turkish EEZ. Grey lines show von Bertalanffy growth curves based on references (1954–2018).

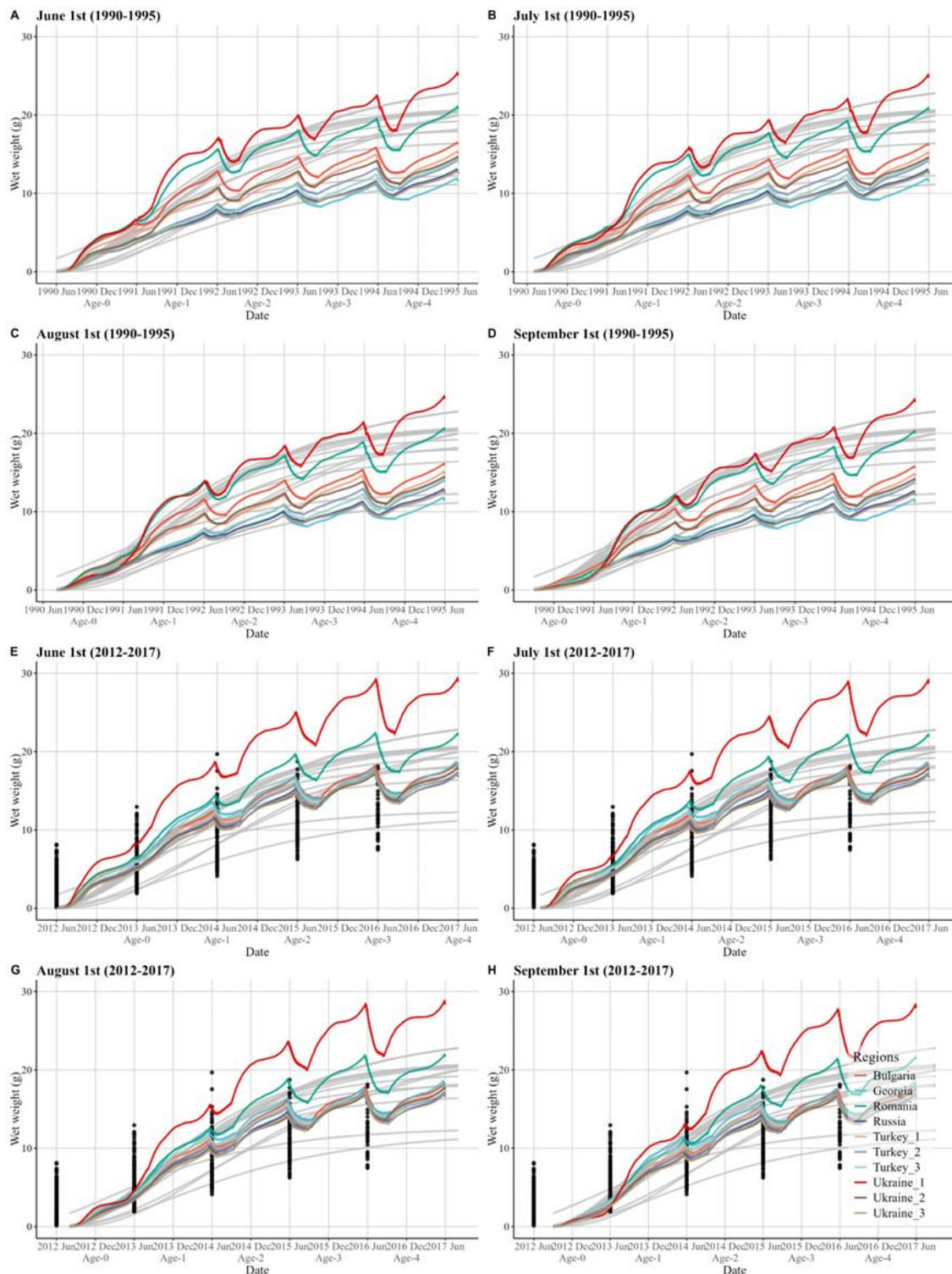


Figure 41. DEB model calibration showing wet weight for individuals born on June 1st, July 1st, August 1st, and September 1st across 10 regions in two time periods: A–D (1990–1995) and E–H (2012–2017). Black dots represent age-weight estimates derived from field survey length data using a length–weight relationship in the

<b>Project</b>	NECTON No 101081273	<b>Deliverable</b>	D7.2
<b>Dissemination</b>	Public	<b>Nature</b>	Report
<b>Date</b>	14/10/2025	<b>Version</b>	1.0

Turkish EEZ. Grey lines show fitted weight curves based on length–weight conversions from von Bertalanffy growth functions in the literature (1954–2018).

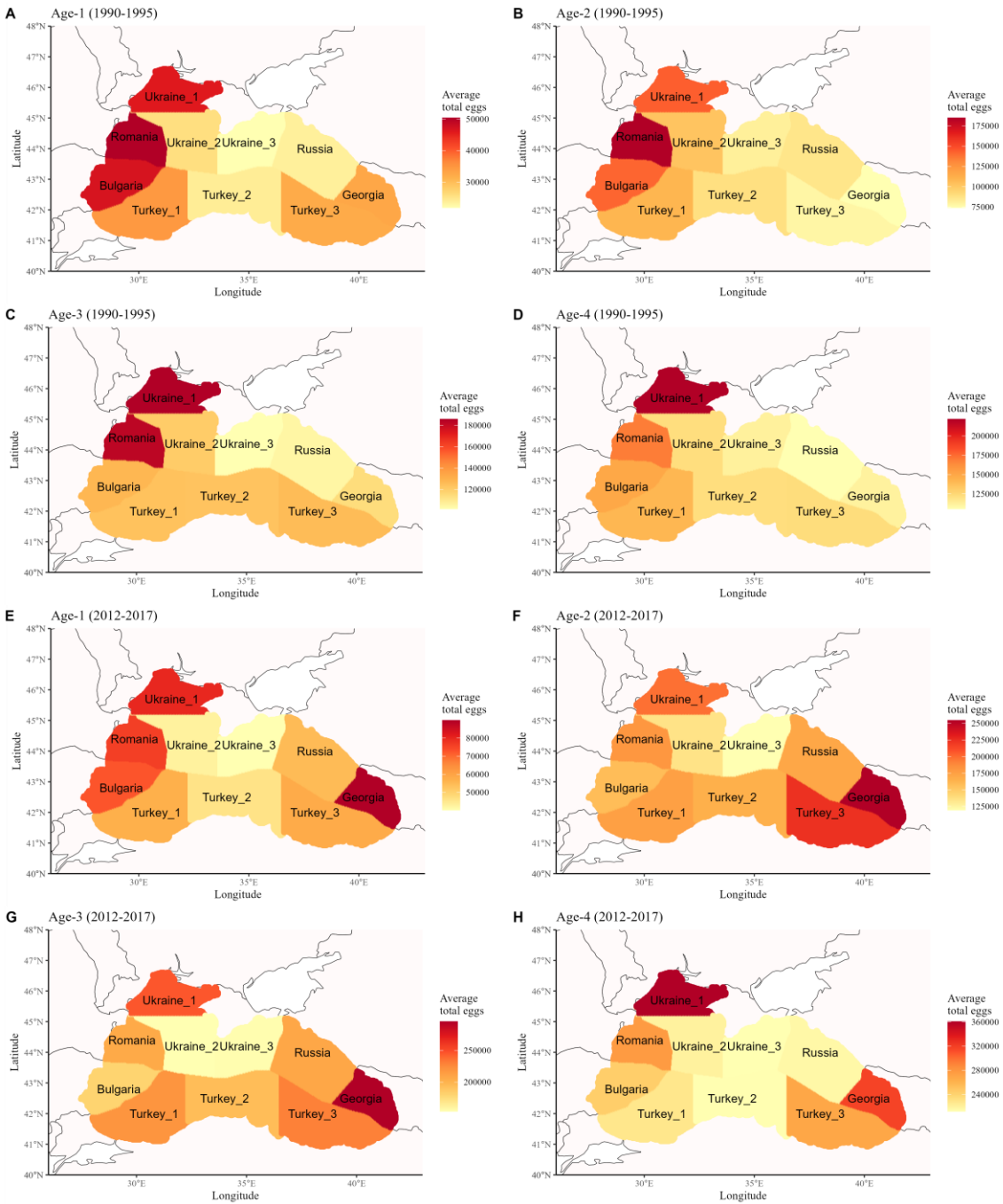


Figure 42. DEB model calibration results showing average fecundity by age class for individuals born on June 1st, July 1st, August 1st, and September 1st in two time periods: A–D (1990–1995) and E–H (2012–2017) in different regions.

#### Kinesis movement submodel calibration

The four scenarios produced movement patterns consistent with theoretical expectations. In scenarios where temperature and food cues were spatially aligned, individuals tended to aggregate in optimal areas, with only a few individuals scattered randomly outside these regions. This results from



<b>Project</b>	NECTON No 101081273	<b>Deliverable</b>	D7.2
<b>Dissemination</b>	Public	<b>Nature</b>	Report
<b>Date</b>	14/10/2025	<b>Version</b>	1.0

random movement dominating under poor conditions, with inertial component dominating when individuals get into good conditions (Figure 43 A-B, E-F). In contrast, scenarios with opposing gradients of temperature and food resulted in weak or no clear aggregation pattern, with individuals generally dispersing that resembled random distributions across the Black Sea (Figure 43C-D, G-H). There was a suggestion of weak avoidance of very poor temperatures and very low food areas.

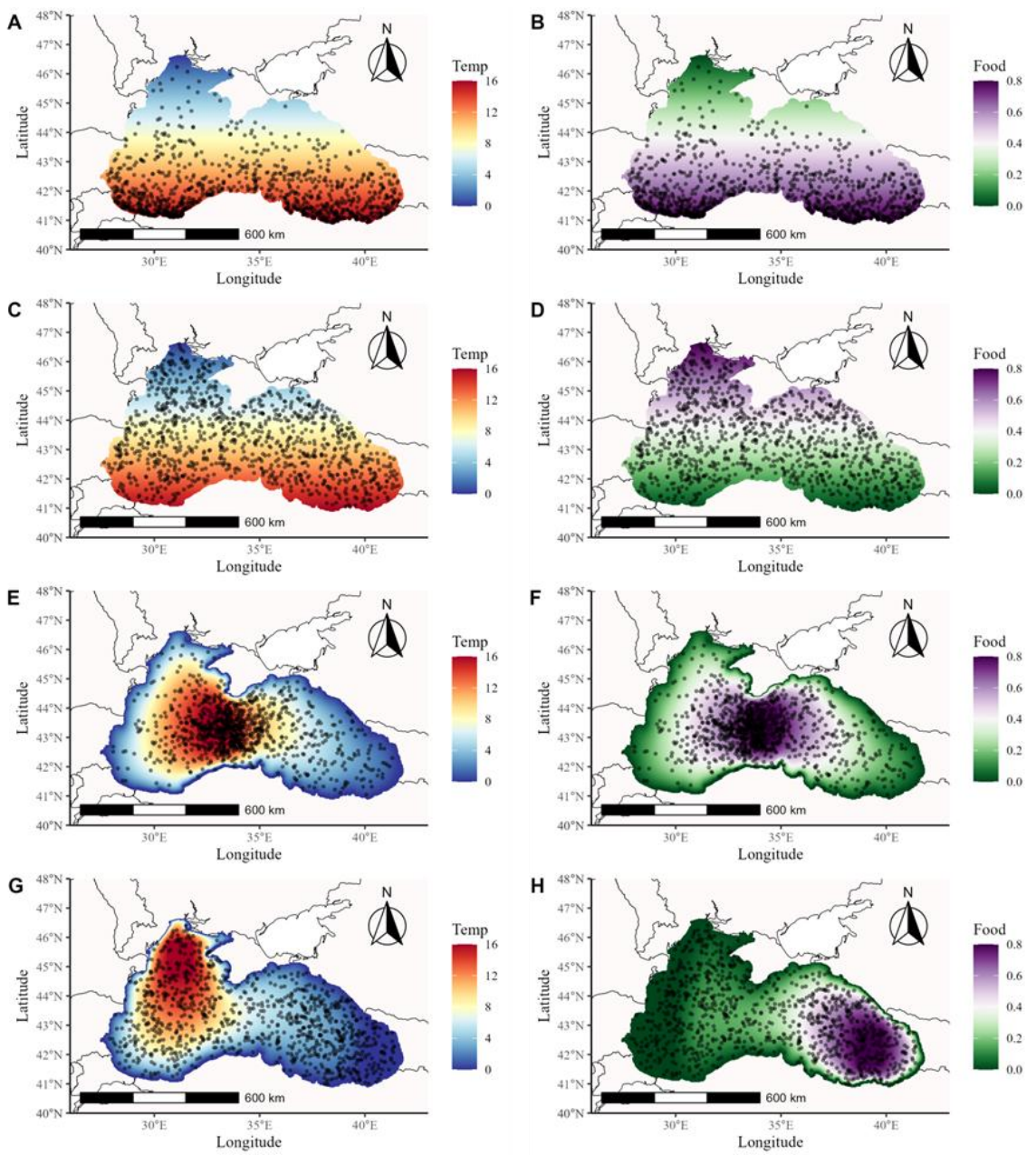


Figure 43. Kinesis model calibration of endpoint locations at the final day of a one-year simulation for 1,000 individuals tracking temperature cues (A, C, E, G) and food cues (B, D, F, H) under four artificial scenarios. A-B, overlapping gradients of temperature and food; C-D, opposing gradients of the two cues; E-F, adjacent but non-overlapping optimal regions; G-H, opposite directions of optimal regions.

<b>Project</b>	NECTON No 101081273	<b>Deliverable</b>	D7.2
<b>Dissemination</b>	Public	<b>Nature</b>	Report
<b>Date</b>	14/10/2025	<b>Version</b>	1.0

Movement trajectories further supported these findings. In aligned-cue scenarios, movement paths exhibited shorter and more constrained trajectories in optimal regions, reflecting effective inertia-driven behavior (Figure 44 A-B, E-F). In less favorable or ambiguous areas, trajectories were longer and lacked directionality, indicating dominance of the random component. In scenarios with opposing cues, trajectories were mostly random, with limited displacement and weak directional tendencies, particularly near zones of either optimal temperature or food availability (Figure 44 C-D, G-H).

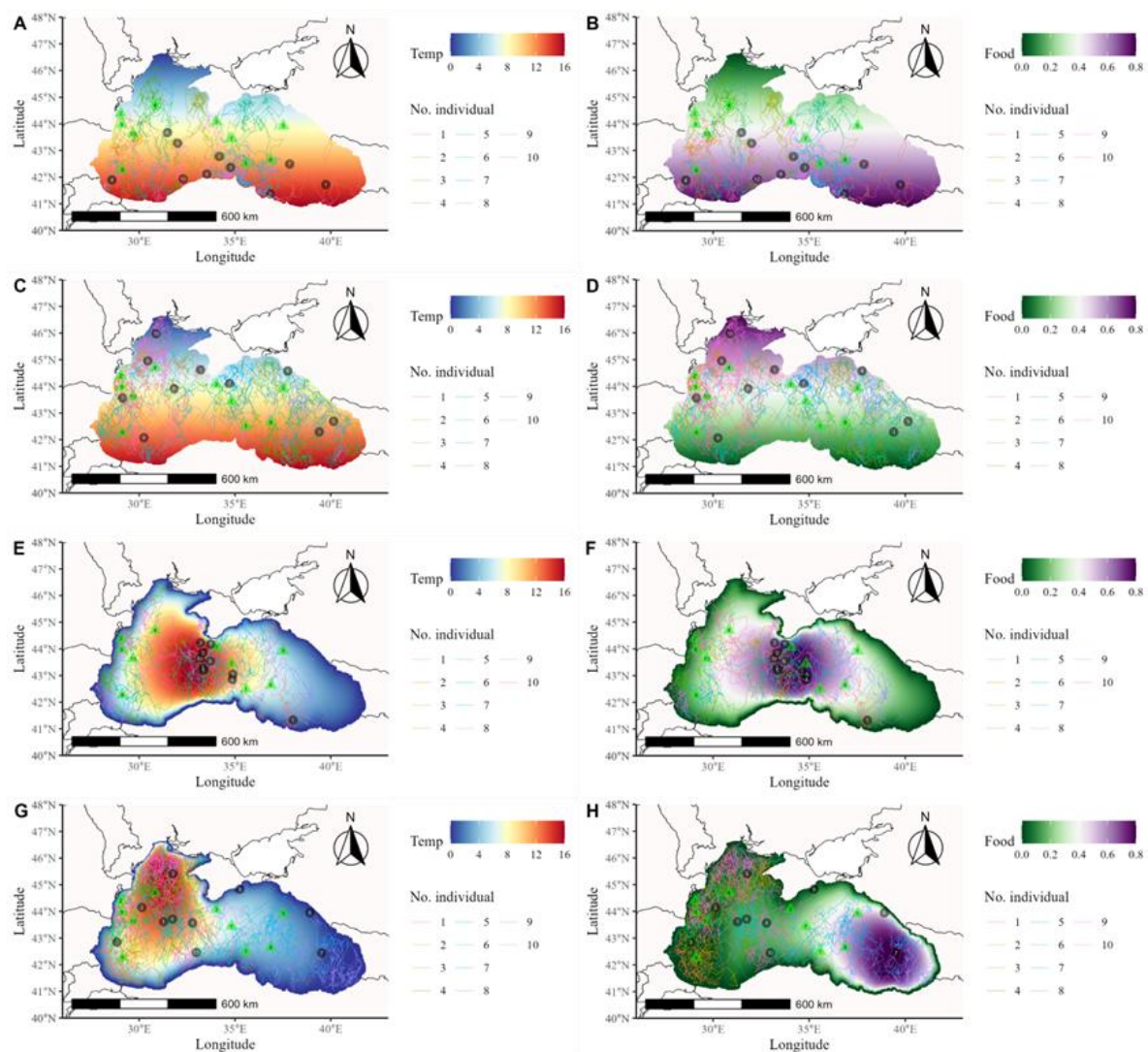


Figure 44. Kinesis model calibration of movement trajectories for 10 randomly selected individuals tracking temperature cues (A, C, E, G) and food cues (B, D, F, H) under four artificial scenarios. Green triangles mark the starting points; black dots indicate the endpoints. A-B, overlapping gradients of temperature and food; C-D, opposing gradients of the two cues; E-F, adjacent but non-overlapping optimal regions; G-H, opposite directions of optimal regions.

### 3.12.2.3 Calibration and Validation of hindcast simulations

We have completed the separate submodels calibration and validation, and we are currently performing the full model calibration. The full model will be used to generate the hindcast simulations of population dynamics and spatial distributions.

<b>Project</b>	NECCTON No 101081273	<b>Deliverable</b>	D7.2
<b>Dissemination</b>	Public	<b>Nature</b>	Report
<b>Date</b>	14/10/2025	<b>Version</b>	1.0

### 3.12.3 NECCTON Products from the model

We plan to generate seasonal spatial maps of European anchovy biomass in the Black Sea, at a 2.5 km resolution and stratified by age and stage structure, covering the hindcast period from 1990 to 2023 using the two-dimensional version of the calibrated full model. If the implementation of the three-dimensional model proves feasible, we will produce similar outputs in three dimensions. Depending on the results of the calibration, these spatial maps are likely best interpreted as relative distributions and as changes in biomass between years and between scenarios. Available survey data is limited in its ability to allow for rigorous evaluation of model prediction of spatial biomass distributions. Our approach enables mechanistic explanations of the spatial distributions and their changes and elucidation of the underlying processes that drove changes in spatial distributions.

Beyond spatial distributions, the DEB-IBM model also allows us to investigate the underlying biological and environmental drivers of anchovy population and recruitment dynamics. We will analyse individual-level energy allocation, growth, reproduction, and mortality processes to identify how environmental variability shapes population outcomes across time and space. This mechanistic insight is a core strength of the DEB-IBM approach and will be central to the interpretation of spatial distribution results and our understanding of drivers of population dynamics.

### 3.12.4 Discussion of pros and cons of the model

Advantages:

The DEB-IBM model has several key strengths:

- Enables the synthesis of diverse data types and modeling approaches (DEB, agent-based, movement, coupling to lower trophic model) to investigate the underlying processes driving temporal and spatial dynamics of an important fish species.
- Represents individual-level variability that is important to capturing what atypical individuals (not just the average individual) do under changing environmental conditions.
- Allows for conceptually straightforward representation of how and why individuals move and disperse through heterogeneous environments, making it suitable for studying spatial population dynamics. The model allows for incorporation of the advances occurring in the rapidly progressing field of Movement Ecology.
- Supports mechanistic representations of growth, mortality, reproduction, and movement responses to environmental forcing, making it particularly well-suited for climate change studies that push conditions to extremes. Applications include predicting shifts in spawning areas, changes in fecundity, altered timing of spawning, mis-matches between prey and predator, sizes-at-age, and availability of biomass available to harvest.
- Sets the stage for further development and application, such as evaluating the effects of fisheries management strategies or assessing the ecological impacts of invasive species (e.g., jellyfish).

Limitations:

<b>Project</b>	NECCON No 101081273	<b>Deliverable</b>	D7.2
<b>Dissemination</b>	Public	<b>Nature</b>	Report
<b>Date</b>	14/10/2025	<b>Version</b>	1.0

- The current R-based implementation is computationally demanding, especially at high spatial and temporal resolutions. This can limit scalability and efficiency, particularly for long-term simulations or when representing 10,000's of super-individuals.
- The high complexity of the model introduces challenges in model calibration and validation. The large number of parameters often leads to identifiability issues, and requires extensive data for proper calibration that is only partially available at present.
- Coupling the DEB-IBM model with lower trophic level models (e.g., biogeochemical or hydrodynamic models) is challenging due to differences in spatial/temporal scales, structural differences, and programming platforms. These challenges are especially critical in two-way coupling scenarios where dynamic feedbacks (fish consumption removes zooplankton) are resolved.
- The DEB-IBM model requires detailed biological and behavioural information and data at the individual and population levels. Such data are often unavailable at the necessary spatial and temporal resolutions, leading to uncertainty or the need for simplified assumptions.
- Classical validation (plots of predicted versus observed) of this kind of agent-based model is challenging and new methods (e.g., pattern-matching) are used that are under development. Quantifying uncertainty and ensuring reproducibility remain significant methodological challenges.

Next steps:

We will finalize the calibration and validation of the two-dimensional version of the model. It will be used to test hypotheses regarding the drivers of population dynamics and recruitment, and to generate seasonal spatial biomass maps by life stage over the hindcast period (1990–2023). These outputs will primarily be used for comparative analysis rather than for producing absolute estimates.

Then, we will proceed with the development, calibration, and validation of the three-dimensional model, and compare its outputs with those of the 2D model. Similar to the 2D implementation, the 3D model will be used to explore population and recruitment mechanisms and to produce spatial biomass distributions with a spatially-resolved vertical dimension.

### 3.13 OSMOSE (Leading partner: IFREMER)

#### 3.13.1 Model description

OSMOSE is a multispecies and individual-based model (IBM) which focuses on fish species. This model assumes opportunistic predation based on spatial co-occurrence and size suitability between a predator and its prey. It represents fish individuals grouped into schools, characterized by size, weight, age, taxonomy, and geographic location (2D model), that undergo the major processes of the fish life cycle (growth, reproduction, migration, and mortality from starvation, predation, and fishing). A number of developments in the OSMOSE framework provide a modular approach to the various processes, with several possible formulations according to the modelling objectives pursued.



<b>Project</b>	NECCTON No 101081273	<b>Deliverable</b>	D7.2
<b>Dissemination</b>	Public	<b>Nature</b>	Report
<b>Date</b>	14/10/2025	<b>Version</b>	1.0

Within NECCTON, an OSMOSE model is applied to the Bay of Biscay ecosystem, using the bioenergetics and evolutionary sub-modules, to account for evolutionary dynamics together with physiological and ecological dynamics in fish community.

#### *3.13.1.1 Model Formulations: State Variables, Equations, Parameters*

The main hypotheses and concepts of OSMOSE are described in the seminal papers of Shin and Cury (2001, 2004). Mostly focussing on fish dynamics, OSMOSE is coupled with a biogeochemical model, providing low trophic level (LTL) resources as well as abiotic conditions (Travers et al. 2009). The bioenergetics and evolutionary sub-modules allow to represent the fish individual physiological response to temperature and oxygen variations (Morell et al., 2023a), and to consider inter-individual phenotypic variability due to genotypic variability and plastic responses (Morell et al., 2023b). The main information extracted from these papers are only summarized here.

The biological unit of the model is a school (a super-individual in individual-based modeling terminology). It is formed by individuals from the same species that are biologically identical. The state variables characterizing a school  $i$  of a specific species at time step  $t$  are: i) its ontogenetic state described by its age, somatic mass and gonadic mass; ii) its abundance (the number of individuals in the school); and iii) its spatial location (the grid cell where the school is located).

In OSMOSE, the whole life cycle is modelled, from eggs to spawners, in a horizontal 2D grid. During each time step, super-individuals move in the grid, following either a random walk mimicking foraging or observed distribution maps in order to represent seasonal and/or age-based migrations. Based on the co-occurrence of available resources (both LTL and other super-individuals) in the cell and size adequacy between the super-individual and its prey, predation can occur and deplete the preys' pool (possibly up to a maximum ingested food amount). The assimilated proportion of ingested food is then partially mobilized depending on the environmental oxygen and temperature conditions. Once individual maintenance costs are covered, the resulting net energy can serve for production of new tissue, through somatic growth and eventually gonadal development depending of the individual maturity stage dependant on a maturation reaction norm. When mature, super-individuals can spawn during spawning seasons, thus releasing eggs (i.e., new super individuals) in the system. Mortality terms representing predation from other schools, fishing, starvation and an additional mortality term reduce the abundance of super-individuals.

The life cycle of each species is modeled using parameters related of life history traits: maximal food ingestion rate, coefficients of linear maturation reaction norm, gonado-somatic index. Other specific parameters are the minimal and maximal size ratios that limit the opportunistic predation, and longevity, egg size, mortality rates, temperature preference (see online documentation for a complete list of parameters). Information on species distribution and spawning seasonality is also required.

#### *3.13.1.2 Model structure and required forcings and inputs; Implementation details*

OSMOSE is open source and written in object-oriented java. A detailed documentation is available at <https://osmose-model.org/>. A dedicated R package allows to build a configuration and run simulations using OSMOSE (<https://github.com/osmose-model/osmose>). For NECCTON, the version 4.4.1 of OSMOSE was used, with the R package version 4.3.2.

<b>Project</b>	NECCTON No 101081273	<b>Deliverable</b>	D7.2
<b>Dissemination</b>	Public	<b>Nature</b>	Report
<b>Date</b>	14/10/2025	<b>Version</b>	1.0

### 3.13.1.3 Model specifics to HTL-LTL coupling

Within NECCTON, OSMOSE is forced (one-way coupling) by outputs from NEMO-ERSEM. Phytoplankton, zooplankton and zoobenthos prey fields, as well as temperature, salinity and oxygen modelled with NEMO-ERSEM are provided to OSMOSE at each time step. Temperature, salinity and oxygen are either considered at the surface, at the bottom, or averaged over the water column depending on fish species' habitat. For plankton prey fields, vertical integration is done over the first 200m. Finally, horizontal re-gridding and currency conversion are needed between the models. Furthermore, size ranges have been attributed to LTL groups (required for the size-based predation), as followed: micro-phytoplankton (0.002 – 0.02 mm), diatoms (0.01 – 0.2 mm), heterotrophic flagellates (0.002 – 0.02 mm), micro-zooplankton (0.02 – 0.2 mm), meso-zooplankton (0.2 – 2 mm), suspension feeders (2 – 5 cm), deposit feeders (0.1 – 2 cm) and meiobenthos (0.045 – 5 mm).

## 3.13.2 Application: Hindcast-Simulation

### 3.13.2.1 Model configuration (Resolution, Boundary condition, Initial conditions, Model forcing)

The Bay of Biscay (BoB) application of OSMOSE covers the French continental shelf from 43.3°N to 48°N, using a grid of 0.16° x 0.25°. It represents the ecological processes of the domain from the surface down to the sea bottom or 200m depths for cells outside the continental shelf. The time step was set to 15 days, a good compromise between fine scale process and computing time limitations. The selection of a set of HTL species was made following criteria of commercial fishing interest, data availability and food web dynamics. Finally, 18 pelagic, demersal, benthic, cephalopods and crustaceans species were explicitly represented, corresponding to a total of 73.8% of all catch volume (including Crustacea and except Seaweed, Bivalvia, Echinoidea, Maxillopoda and Gastropoda) in ICES area 8ab, between 2007 and 2021. These species are: European sardine (*Sardina pilchardus*), European anchovy (*Engraulis encrasicolus*), sprat (*Sprattus sprattus*), blue whiting (*Micromesistius poutassou*), whiting (*Merlangius merlangus*), European mackerel (*Scomber scombrus*), European horse mackerel (*Trachurus trachurus*), boarfish (*Capros aper*), pouting (*Trisopterus luscus*), European seabass (*Dicentrarchus labrax*), European hake (*Merluccius merluccius*), common sole (*Solea solea*), anglerfish (*Lophius piscatorius* and *Lophius budegassa*), Norway lobster (*Nephrops norvegicus*), cuttlefish (*Sepia officinalis*) squids (*Loligo vulgaris* and *Loligo forbesii*), lesser spotted dogfish (*Scyliorhinus canicula*) and albacore (*Thunnus alalunga*).

<b>Project</b>	NECCTON No 101081273	<b>Deliverable</b>	D7.2
<b>Dissemination</b>	Public	<b>Nature</b>	Report
<b>Date</b>	14/10/2025	<b>Version</b>	1.0

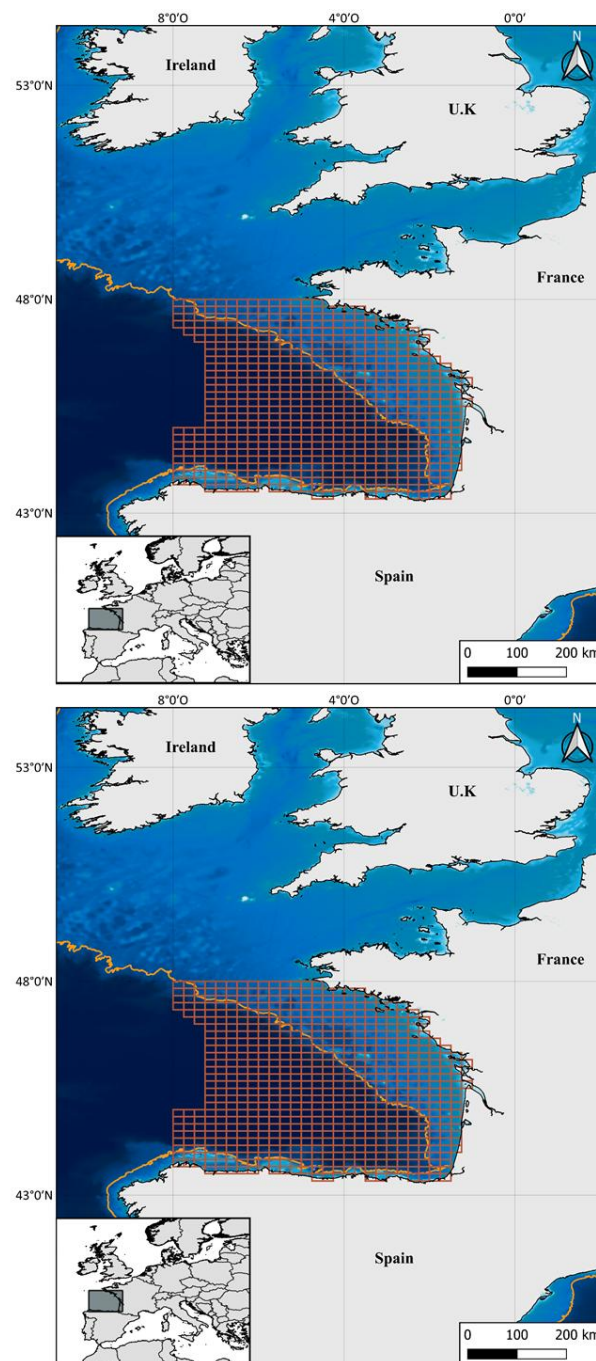


Figure 45. Location of the modelling domain, illustrated by the model cells in brown. The orange line represents the 200m isobath. Inset in the lower left corner: general location in Western Europe.

For this deliverable, the model has been forced by POLCOMS-ERSEM, and calibrated to fit the 2000-2022 time series of fish catch and biomass estimates when available. The model is initialized by distributing super-individuals of different sizes and abundances in the species distribution maps. From there, interannual deviates of fishing mortality and interannual forcing of LTL biomass as well as temperature and oxygen forcings are used to force the fish dynamics.



<b>Project</b>	NECTON No 101081273	<b>Deliverable</b>	D7.2
<b>Dissemination</b>	Public	<b>Nature</b>	Report
<b>Date</b>	14/10/2025	<b>Version</b>	1.0

### 3.13.2.2 Results

#### Calibration and Validation of hindcast simulations

Calibration is performed using the automatic evolutionary algorithm available in the calibrar R package. Parameters adjusted during this calibration are accessibilities to LTL resources, larval mortality rates of fish, additional and fishing mortality rates of fish, maximal ingestion rates of fish and initial total biomass. These parameters are tuned in order to fit observed catch per species, estimated biomass when available and size-at-age of each species.

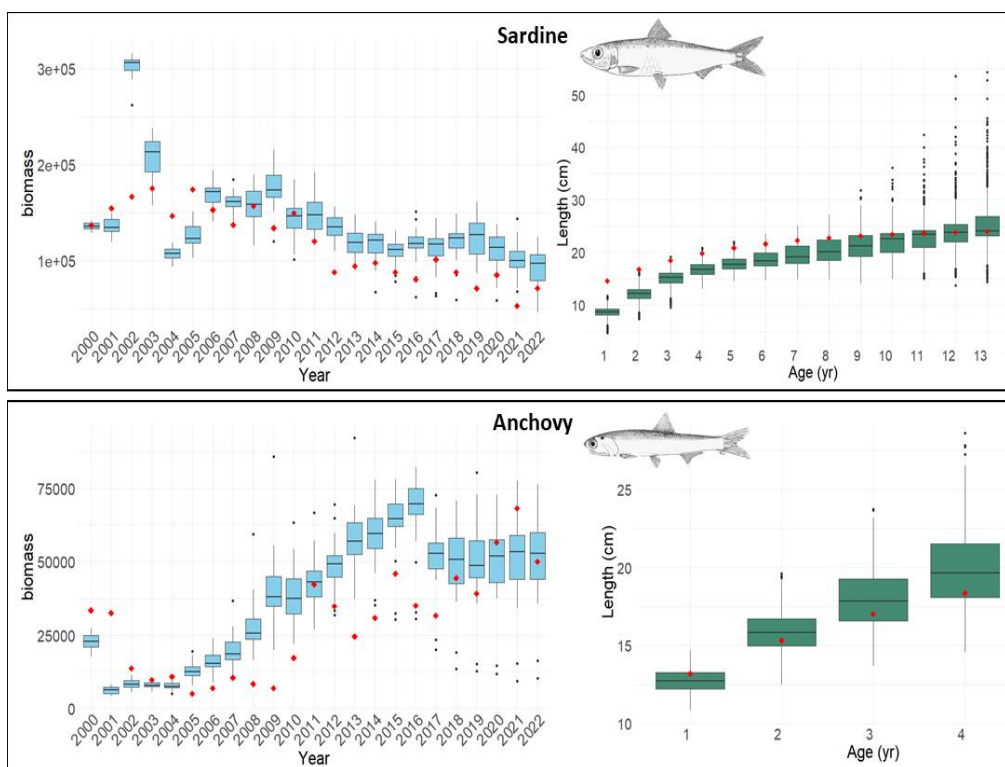


Figure 46. Preliminary fit of the model for sardine (top) and anchovy (bottom), showing the interannual dynamics of species total biomass summed over the area in tons (left) and the average size at age over the period 2000-2022. OSMOSE is a stochastic model, so 30 replicates were run and summarized through boxplots. Red dots correspond to observations.

Validation is performed by looking at the emerging diet of fish, which are not set a priori, and the size at maturity obtained in the simulation. A sensitivity analysis to forcings is under progress.

### 3.13.3 NECTON Products from the model

Biomass of small pelagic fish is available by time step, grid cell, age and species. For the NECTON project, total biomass of sardine and anchovy are provided by grid cell and time step.

<b>Project</b>	NECCTON No 101081273	<b>Deliverable</b>	D7.2
<b>Dissemination</b>	Public	<b>Nature</b>	Report
<b>Date</b>	14/10/2025	<b>Version</b>	1.0

### 3.13.4 Discussion of pros and cons of the model

Pros:

- By explicitly representing bioenergetic processes, OSMOSE allows for the simulation of environmental effects on fish dynamics (including temperature, oxygen levels and food availability). Its fundamental assumption of an opportunistic size-based predation results in a flexible food web structure that will adapt to changing conditions.
- By representing the main species of an ecosystem, OSMOSE relies on parameters easily available from observations, and can address specific concerns from stakeholders (in particular fisheries-related stakeholders).

Cons:

- Interannual simulations using OSMOSE is a recent feature of the model (previously only climatologies were run), thus the initialization and calibration procedures might be improved in the future.
- OSMOSE relies on some parameters for which there is no estimate available, therefore calibration is required and is time-consuming. Projections will require hypothesis regarding these parameters, especially for interannual runs

## 3.14 SEAPODYM-tuna (Leading partner: MOi)

### 3.14.1 Model description

In NECCTON, several fish population applications with SEAPODYM are considered. First, the application to large pelagic species, ie., tropical tunas, is focusing on the development of a fishing scenario tool (use case study 11 in WP9: lead MOi), using the SEAPODYM reference models achieved for Pacific tropical tunas and published in Bell et al. (2021) in collaboration with SPC. A second application is focusing on the anchovy in the Bay of Biscay (Lead: MOi; section 3.14), pursuing the initial work done on the Peruvian sardine and anchovy spawning habitat definition (Hernandez et al., 2014) and the applications to small pelagic species as the Pacific Jack Mackerel (Dragon et al, 2018). Finally, a third application concerns the North-East Atlantic mackerel (Lead: CLS; section 3.15).

The Spatial Ecosystem And Population Dynamics Model (SEAPODYM) is a numerical modelling framework developed initially for investigating population dynamics of tunas under the influence of environment and fishing. By using environmental forcing variables predicted from ocean physical models and satellite data or biogeochemical models (primary production; phytoplankton groups), SEAPODYM simulates first lower (zooplankton) and intermediate (micronekton) trophic functional groups in the vertical epipelagic and mesopelagic layers of the ocean (Lehodey et al., 2010 and section 3.5). Then, the detailed dynamics of commercial species and fisheries (Lehodey et al. 2008; Senina et al. 2021) is simulated in more detail, including animals' movements and spawning migrations. It discriminates changes due to fishing from those related to the environment (Figure 47).

<b>Project</b>	NECCON No 101081273	<b>Deliverable</b>	D7.2
<b>Dissemination</b>	Public	<b>Nature</b>	Report
<b>Date</b>	14/10/2025	<b>Version</b>	1.0

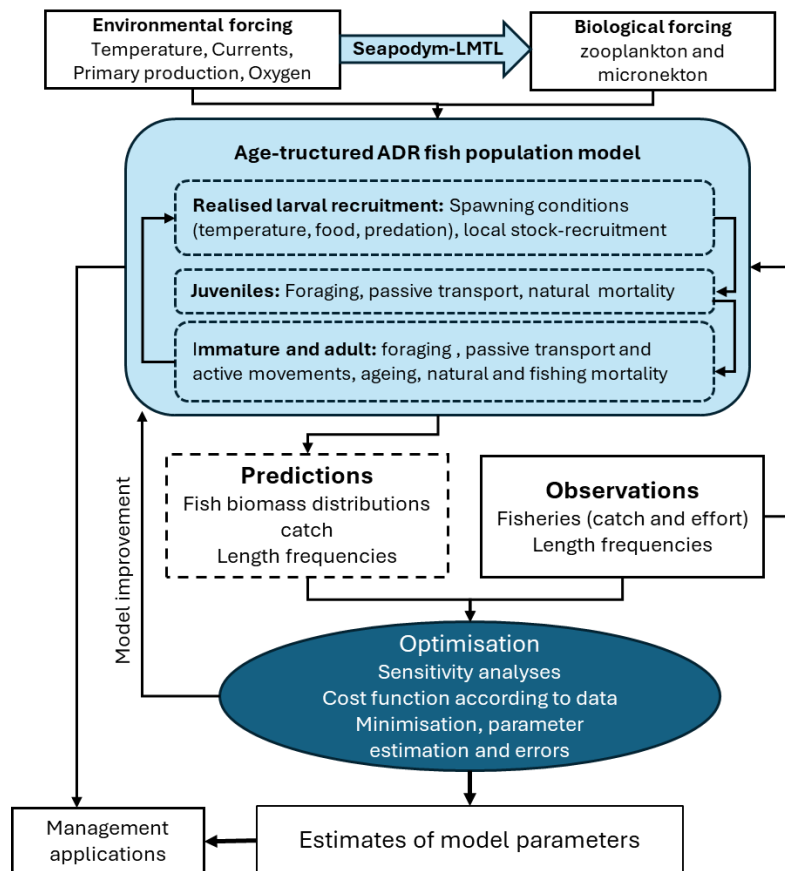


Figure 47. General scheme of SEAPODYM model structure.

#### 3.14.1.1 Introduction and biological basis

SEAPODYM considers several life stages of the target fish population, each being controlled by specific behavioral rules. The movements and key parameters of the life cycle are controlled by the definition of spawning and feeding habitats, which depend on the environment and species' preferences. The numerical system builds on advection-diffusion-reaction equations, which simulate changes in density distributions accounting for changes due to movements, natural and fishing mortality, growth and larval recruitment. This approach allows reducing the number of parameters and it facilitates the application of estimation methods for the parameters that are not directly observable (Senina et al 2008; 2021), subject to the accessibility of data that could be compared with predictions (e.g., larvae or juvenile densities, catch distributions, length frequencies, biomass acoustic estimations).

#### 3.14.1.2 Model Formulations: State Variables, Equations, Parameters

SEAPODYM model formulation is described in a user's manual available together with the code on a publicly accessible repository (<https://github.com/PacificCommunity/seapodym-codebase>). The model is continuously improved and model applications with underlying equations and parametrisation can be found in the scientific literature, e.g., for Pacific skipjack tuna (Lehodey et al., 2013; Senina et al., 2021), Pacific yellowfin tuna (Nicol et al., 2022), Pacific bigeye tuna (Hampton et

<b>Project</b>	NECCOTON No 101081273	<b>Deliverable</b>	D7.2
<b>Dissemination</b>	Public	<b>Nature</b>	Report
<b>Date</b>	14/10/2025	<b>Version</b>	1.0

al 2023), Atlantic albacore tuna (Dragon et al., 2015; Senina et al., 2020), and South Pacific albacore tuna (Lehodey et al., 2015; Senina et al., 2020).

#### *3.14.1.3 Parameterisation, sensitivity analysis*

SEAPODYM description of spatio-temporal dynamics of fish populations relies on parameters that provide links between environmental variability and intrinsic dynamic processes such as reproduction, survival and movement. These parameters can be estimated with quantitative methods fitting the model predictions to the observational data. This is done with a maximum likelihood estimation (MLE) method including geo-referenced catch and length frequency distributions. Before running simulations for achieving the best estimate of model parameters, sensitivity analysis can be conducted to reveal which parameters can be estimated from available data and which cannot. If model predictions are insensitive to some parameters, they should be removed from the optimization approach and fixed to values derived from scientific literature and expert judgment. Two types of sensitivity analyses can be performed in SEAPODYM – local and global sensitivity analyses (see Seapodym user’s manual and Senina et al. 2008; 2021).

#### *3.14.1.4 Model structure and required forcings and inputs; Implementation details*

SEAPODYM is written in C++ language and runs on Linux environment. It requires environmental and biological forcing variables that are used to simulate the key mechanisms driving the population dynamics (movements, foraging, spawning, mortality). Details are provided in the user reference manual and the scientific literature listed in section above.

When it is used for simulation runs with fixed (presumably optimal) parameters, there are no specific requirements for the computer configuration. In general, the computer power needs depend on the numerical model resolutions. However, the physical memory is the key requirement for the phase of optimal parameter estimation or other procedures involving the gradient computation. This is because the backward (adjoint) differentiation method stores all intermediate variables needed for the exact evaluation of a cost function gradient in the operational memory. If there is not enough RAM available, the program will dump all temporary data on the hard disk, which significantly increases the overall runtime. Compilation of the source code requires installation of two additional libraries: libxml2 (<ftp://xmlsoft.org/libxml2>) and Autodif included in the ADModel Builder software (<https://www.admb-project.org/>).

The species environment in SEAPODYM is defined by spatio-temporal fields of physical, biogeochemical, and biological variables. Physical variables include temperature and ocean currents; biogeochemical variables consist of dissolved oxygen, primary production, and euphotic depth; and the biological variables are biomasses of zooplankton and micronekton functional groups. Physical and biogeochemical variables are obtained from coupled physical-biogeochemical models and used by SEAPODYM-LMTL to simulate zooplankton and micronekton (cf. section 3.5). The model simplifies the ocean’s vertical structure into three pelagic layers: surface epipelagic, lower and upper mesopelagic, defined based on the euphotic depth. Three-dimensional variables are averaged or integrated (primary production) within these layers to create integrated environmental fields.

<b>Project</b>	NECCTON No 101081273	<b>Deliverable</b>	D7.2
<b>Dissemination</b>	Public	<b>Nature</b>	Report
<b>Date</b>	14/10/2025	<b>Version</b>	1.0

### 3.14.1.5 Model specifics to HTL-LTL coupling

The fish population dynamics in SEAPODYM relies on the definition of two types of habitats. The spawning habitat combines functional relationships to represent the optimal temperature window for spawning, the fish larvae-prey relationship (Holling type) and the fish larvae-predation relationship (Log-Normal) (Figure 48). Prey of fish larvae are the zooplankton that can be eventually replaced by primary production as a proxy. The predators of the fish larvae are the micronekton, and the relationship use the total biomass of micronekton in the epipelagic layer where are the larvae.

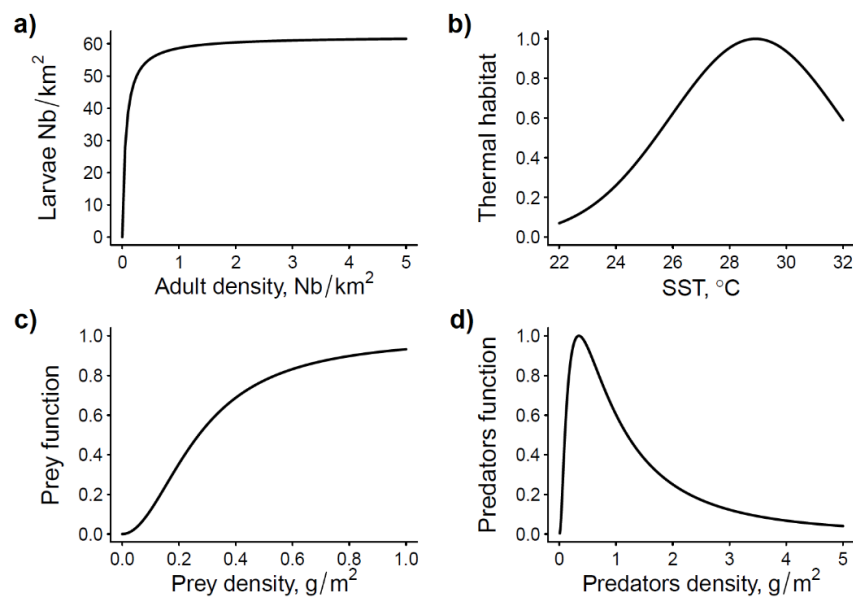


Figure 48. Functions used in the definition of spawning habitat and reproduction: (a) Beverton–Holt stock–recruitment function (Nb =numbers of individuals), (b)thermal function f1, (c) prey function f2, and(d) predator function f3, based on parameters estimated for bigeye tuna (Redrawn from SEAPODYM User’s manual).

The quality of feeding habitats is influenced by the availability of micronekton from the different vertical layers, which depends on both environmental conditions and the predator's tolerance to these conditions in each layer. The SEAPODYM model incorporates species’ thermal preferences and oxygen requirements to determine their accessibility to specific depths and locations in the ocean. For instance for tuna, the model uses two key functions: one for temperature preferences, represented by a Gaussian distribution, and one for oxygen levels, modeled by a sigmoid function that accounts for oxygen thresholds. Species vary in their oxygen tolerance, with low oxygen levels prompting behavioral changes, such as increased movement. As tuna grow larger, they seek colder habitats to offset their rising body temperature, but their tolerance for temperature variability also increases with size (Figure 49). This interplay of thermal and oxygen needs defines their movement and habitat choice, linked to prey availability, with tuna exhibiting both physiological and behavioral responses to environmental conditions.

The natural mortality of fish includes two mechanisms: population decay due to the predation process and population abundance decrease due to senescence of individuals with age. In addition, it is

<b>Project</b>	NECTON No 101081273	<b>Deliverable</b>	D7.2
<b>Dissemination</b>	Public	<b>Nature</b>	Report
<b>Date</b>	14/10/2025	<b>Version</b>	1.0

assumed that at any age, the natural mortality can be altered by local environmental conditions, such as temperature, availability of food and predators (Figure 49). Hence, we assume that total mortality rate can vary in space and time depending either on the spawning habitat index  $H_s$  (for larval and small juvenile stages) or feeding habitat index  $H_a$  for adult life stages.

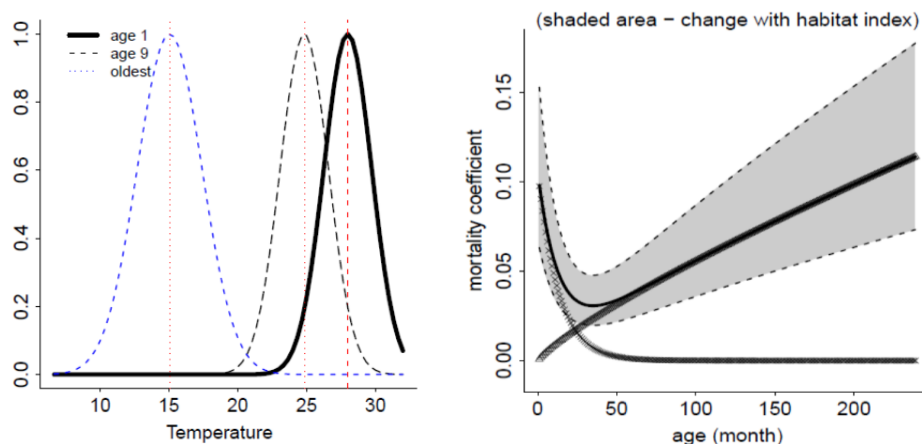


Figure 49. Left: Example of change (skipjack tuna) in thermal preferences function linked to species' growth: the optimal temperature decreases with increased body size, while standard deviation increases with increased body weight. This effect integrated in the feeding habitat, determines the accessibility to the available biomass of prey. Right: Functional relationships used to determine the natural mortality with shaded area corresponding to the variability allowed locally in relation to the feeding habitat.

### 3.14.2 Application to Pacific tropical tuna species

#### 3.14.2.1 Model configuration

The SEAPODYM model is used to investigate the combined impact of fisheries and climate change on Pacific tropical tuna species (skipjack, yellowfin, bigeye). A catch scenario tool is developed to project the future fishing impact. The model is driven by physical and biogeochemical variables generated by the coupled model NEMO-PISCES, using the scenario of high emission of greenhouse gases CMIP5 RCP8.5, close to the more recent CMIP6 SSP-8.5 scenario.

Before running the projections, the phase of model parameter optimisation over the historical period 1980-2010 provided the reference parameter estimates. It used NEMO-PISCES outputs generated with the ERA-INTERIM atmospheric reanalysis (ERAi) available from ECMWF. Once the optimal parameterization is achieved and validated by statistical fits to the historical fishing data, one more simulation is produced for the historical period but without fishing mortality. The structure of the unfished populations in December 2010, the last time step of the reanalysis, is saved to serve as the initial conditions for the projections starting in 2011, still without fishing and therefore highlighting the impact of climate change only.

All tuna species are voracious opportunistic predators feeding on micronekton organisms. The feeding habitat of immature and adult tuna is defined by their accessibility to the six functional groups of epi-

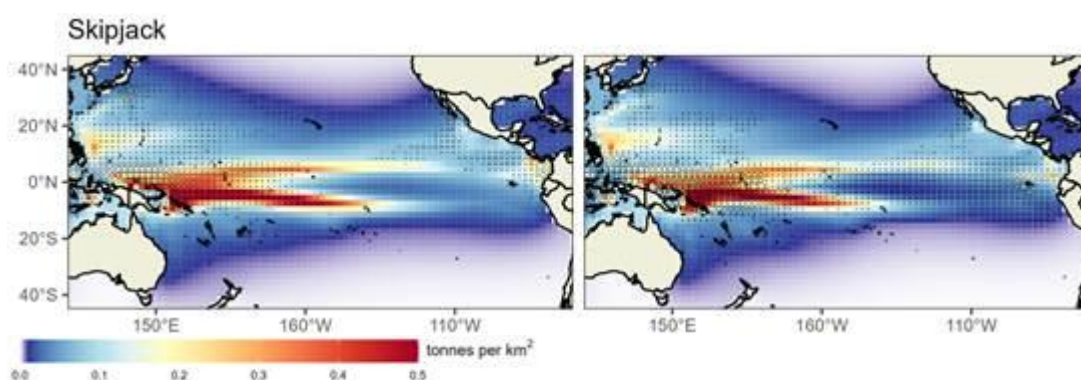
<b>Project</b>	NECCTON No 101081273	<b>Deliverable</b>	D7.2
<b>Dissemination</b>	Public	<b>Nature</b>	Report
<b>Date</b>	14/10/2025	<b>Version</b>	1.0

and mesopelagic micronekton included in the model. The accessibility of micronektonic prey depends on the tolerance of tuna to low oxygenated waters in subsurface waters, and the temperature preference of tuna species, which changes with age, and are estimated through the Maximum Likelihood Estimation approach.

#### 3.14.2.2 Model validation

This model configuration and its results have been described in detail for the historical fishing period in Senina et al. (2020a; 2020b); Hampton et al. (2022) and Nicol et al. (2022). The model optimizations provide realistic estimates of dynamics and distributions of the three species of tuna as known from historical fisheries and catch distributions (Figure 50) and general knowledge available on these species. With the narrowest estimated thermal habitat (26°- 28.5°C) and the lowest tolerance to low oxygenated waters (threshold value 3.8 mL L<sup>-1</sup>), skipjack tuna is mainly limited to epipelagic forage (i.e. either resident epipelagic or highly migrant mesopelagic micronekton species present in the surface layer at night). The thermal habitat of yellowfin is estimated to be wider (13.3°C – 32°C) and the model for this species shows a lack of sensitivity to oxygen. The habitat is known to be even wider for bigeye tuna. Adults of this species have well-developed thermoregulation mechanisms and physiological adaptation that confer good tolerance to low dissolved oxygen concentration (Brill 1994), allowing them to dive regularly to the deeper lower mesopelagic layer (> 400 m depth). In agreement with this knowledge, the model estimates a large thermal range for bigeye with the optimal value at age decreasing from 27°C for the youngest cohorts to 10°C for the oldest. There is also a low threshold oxygen value (0.5 mL L<sup>-1</sup>), and an increasing contribution of non-migrant lower-mesopelagic micronekton for bigeye tuna compared to the other species.

The model including micronekton and tuna variables and outputs are archived online and can be provided on demand.





<b>Project</b>	NECCTON No 101081273	<b>Deliverable</b>	D7.2
<b>Dissemination</b>	Public	<b>Nature</b>	Report
<b>Date</b>	14/10/2025	<b>Version</b>	1.0

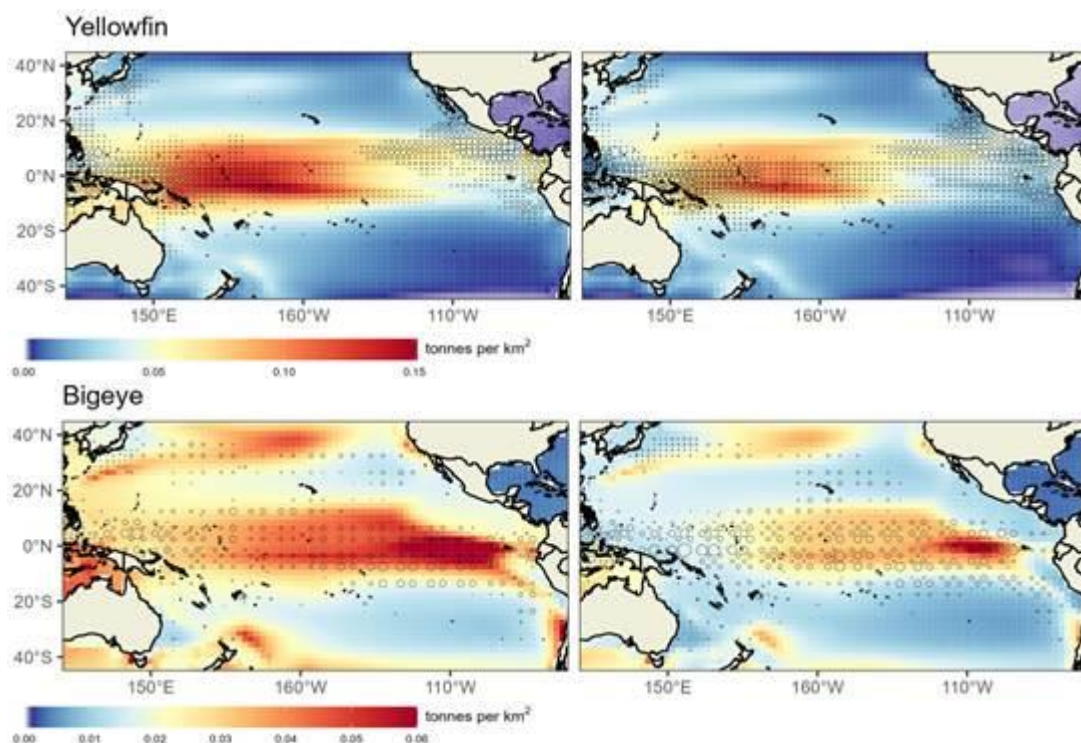


Figure 50. Comparison of predicted distributions of tuna total biomass (tonnes  $\text{km}^{-2}$ ) for 1<sup>st</sup> and last decade of the historical time series. Warmer and cooler colours indicate high biomass and low biomass levels, respectively. Total observed catches are shown, with catch proportional to the size of the circles (same scales between decades). Redrawn from Lehodey et al. (in press).

### 3.14.2.3 Development of the fishing scenario tool

To explore the combined effects of climate change and fishing in the future, a tool is developed to generate catch scenarios for the future (for application in use case 11 in WP9), starting from the reference models developed for the historical period and projected using IPCC greenhouse gas emission scenario.

Future mid-to-long-term fishing scenarios remain highly uncertain, as they depend on unpredictable economic drivers and policy decisions. Furthermore, the spatial distribution of fishing effort will certainly respond dynamically to changes in tuna stock distributions. To address these gaps, we develop a simple modeling tool for exploring changes in tuna stocks and fisheries under climate change and spatial management measures, i.e., marine protected areas and fishing closure areas. The fishing scenario simulation tool uses a catch extraction approach, suitable for use with SEAPODYM or any similar modeling approach. This tool allocates desired future catches, considering optional spatial measures and projected annual target catches. A few parameters allow testing different patterns of future desired catch distributions relative to fish density in absence of fishing. Then, the model will be run under selected IPCC climate change scenario and combining fishing and environmental effects. Depending on the scenarios chosen (fishing and climate), the target catches may or may not be achieved at the scale of the grid cells or achieved at the cost of unsustainable long-term objectives. The simulation results allow these different issues to be analyzed. The approach is validated through

<b>Project</b>	NECCTON No 101081273	<b>Deliverable</b>	D7.2
<b>Dissemination</b>	Public	<b>Nature</b>	Report
<b>Date</b>	14/10/2025	<b>Version</b>	1.0

counterfactual simulations that mimic the long-term trends of catches over the historical period. This is achieved by comparing the predicted and observed detailed catch distributions (Figure 51).

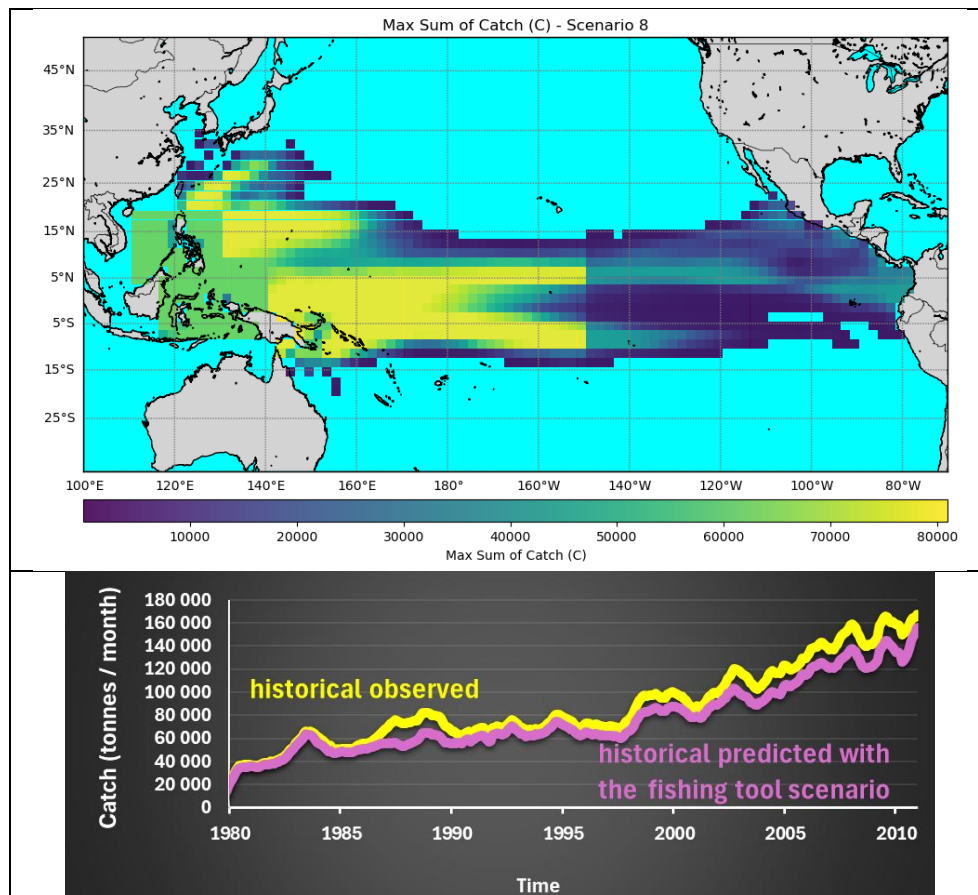


Figure 51. Example of catch distribution of skipjack tuna in the Pacific Ocean proposed by the fishing tool and validation using only 3 super fisheries (South-East Asia; Western Central Pacific and Eastern Pacific) of the method by comparison with observed catch.

### 3.14.3 NECCTON Products from the model

SEAPODYM model predicts the spatial abundance distribution of each age cohort from the first larval cohort to the last age cohort (classically defined as an age+ cohort accumulating all the oldest individual after a fixed limit in the number of cohorts). In standard outputs the cohorts are aggregated by life stages (Table 11). An option needs to be activated to get the detail of density for all cohorts. The model uses a native binary format that can be easily converted to NetCDF standards with a python or R library. Outputs regarding the fisheries include the predicted catch by fishery either from the fishing effort or the catch removal methods at the spatial and temporal resolution used by the model.

Once the reference model has been achieved with the best fit to fishing data (cf above), it is possible to run a second simulation without fishing to compare the two simulations and assess the fishing

<b>Project</b>	NECCOTON No 101081273	<b>Deliverable</b>	D7.2
<b>Dissemination</b>	Public	<b>Nature</b>	Report
<b>Date</b>	14/10/2025	<b>Version</b>	1.0

impact. Similarly, as long as appropriate environmental forcings are available longer simulation can be run by extending the time series in the past or in the future, eg with climate change projections.

Table 10. Standard outputs of the SEAPODYM model applied to a given species and its fisheries. The ‘.dym’ format is a native binary format that can be converted to NetCDF format with R or Python routines.

File	File description	Unit
sp_larvae.dym	Mean biomass of tuna larvae, i.e. first cohort of the population age structure.	Nb indiv. m <sup>-2</sup>
sp_juvnl.dym	Mean biomass of juvenile tuna, i.e. sum of cohorts > 1 until age “juvenile” (3 months)	Nb indiv. m <sup>-2</sup>
sp_recru.dym	Mean number of recruits at age of recruitment	Nb indiv. m <sup>-2</sup>
sp_young.dym	Mean biomass of young immature tuna, i.e. sum of cohorts older than juvenile up to age at maturity.	g m <sup>-2</sup> (equivalent to tonne km <sup>-2</sup> )
sp_adult.dym	Mean biomass of adult tuna, i.e. sum of all cohorts older than the age at maturity.	g m <sup>-2</sup> (equivalent to tonne km <sup>-2</sup> )
sp_totbm.dym	Mean total biomass of young and adult tuna cohorts.	g m <sup>-2</sup> (equivalent to tonne km <sup>-2</sup> )
sp_age1.dym ... sp_ageN.dym	Mean number of individuals by tuna cohort	Nb indiv. m <sup>-2</sup>
sp_Ha_first_maturity.dym	Habitat index for the species at age of maturity	-
sp_Ha_oldest.dym	Habitat index for the species at oldest age	-
sp_diffusion.dym	Mean diffusion for the oldest cohort	naut.mil. <sup>2</sup> mon <sup>-1</sup>
sp_Utot_x.dym	Zonal component of total advection (currents + swimming) for the oldest cohort	naut.mil. mon <sup>-1</sup>
sp_Vtot_y.dym	Meridional component of total advection (currents + swimming) for the oldest cohort	Naut.mil.mon <sup>-1</sup>
sp_speed.dym	Velocity field (currents + swimming) for the oldest cohort	naut.mil. mon <sup>-1</sup>

#### 3.14.4 Discussion of pros and cons of the model

Modelling ocean pelagic ecosystems is a complex task that requires simplification due to the challenges of capturing species interactions and environmental variability. SEAPODYM was developed to incorporate spatial and environmental dimensions missing from traditional population dynamics models. While SEAPODYM includes functional relationships with physical and biological factors, it does not explicitly parameterise energy fluxes between the various species groups and assemblages that make up the entire pelagic ecosystem. Instead, the model focuses on creating new management tools that integrate climate variability, fishing pressure, and spatial regulation. The use of advection–diffusion–reaction (ADR) equations in SEAPODYM offers a valuable approach for simulating large-scale movement patterns of pelagic species. By accounting for environmental drivers, these equations reduce the complexity of parameterisation and facilitate integration with observational data.

Because the model includes detailed representation of the biophysical environment of the species, the complete spatially explicit population dynamics can be described with a small number of parameters. In return, such a model depends strongly on the quality of environmental forcing variables. Once the optimal parameterisation is achieved, the model can be run in simple (and fast) simulation mode either without fishing mortality to measure the impact of fishing by difference, or with any desired fishing scenario.

*Pros of SEAPODYM:*

<b>Project</b>	NECCON No 101081273	<b>Deliverable</b>	D7.2
<b>Dissemination</b>	Public	<b>Nature</b>	Report
<b>Date</b>	14/10/2025	<b>Version</b>	1.0

- Simulates detailed spatial population dynamics and fisheries of target species, with fish movements and migrations explicitly driven by environmental cues.
- Integrates environmental functional relationships directly into fish population dynamics.
- Accounts for 3D variations in physical (e.g., temperature, currents), biogeochemical (e.g., primary production, euphotic depth, dissolved oxygen), and biological (e.g., zooplankton, micronekton) factors.
- Employs a robust optimization approach to estimate model parameters, limited in number thanks to the Eulerian framework used and the incorporation of diverse and spatially disaggregated data sources.
- Model outputs distinguish variability arising from climate and fishing impacts.
- The spatially explicit framework supports the evaluation of spatial planning and fisheries management scenarios.
- Applicable as an operational forecasting tool and for projecting future environmental changes on fish population dynamics.

*Cons of SEAPODYM:*

- Developed in C++ by a small team of experts; currently supported by a relatively small user community.
- Focuses on target species and fisheries, not designed for the entire ecosystem or to achieve mass-balance objectives.
- The optimisation method targeting massive use of various sources of data requires expertise and is computationally intensive.

### 3.15 SEAPODYM-anchovy (Leading partner: MOi)

#### 3.15.1 Model description

The general description of the model SEAPODYM is presented in section 3.14 of this document, in its application to tuna species. Below, we focus on its adaptation to the anchovy population in the Bay of Biscay.

The anchovy population in the Bay of Biscay has experienced a collapse in its population at the beginning of the 21st century, which led to the closure of its fishery between 2006 and 2010 (ICES, 2011). This moratorium, coupled with strict management measures, including total allowable catch limits and monitoring programs, and likely more favorable environmental conditions, facilitated the recovery of the anchovy stock. By 2010, the population had sufficiently recovered, allowing the fishery to reopen under sustainable management practices.

Most studies devoted to the anchovy in the Bay of Biscay highlight a favourable range of temperature for spawning, within which the productivity and food (zooplankton) would control the juvenile recruitment success and subsequent life stages. This is shown directly or indirectly in statistical models, with significant relationships between catch, or observed densities of eggs or juvenile fish with proxies of productivity such as up-welling, stratification index, wind regimes and climate indices (e.g., Motos et al 1996; Planque et al 2007; Irigoien et al, 2007; Borja et al 2008; Erauskin-Extramania

<b>Project</b>	NECCTON No 101081273	<b>Deliverable</b>	D7.2
<b>Dissemination</b>	Public	<b>Nature</b>	Report
<b>Date</b>	14/10/2025	<b>Version</b>	1.0

et al 2019). The role of river flow is also highlighted and often included in these statistical models using sea surface salinity to account for the general observation of a close association of anchovy (*Engraulis* sp.) with river estuaries. The variability in the flow of the Gironde and Loire rivers has been positively correlated to the mesozooplankton productivity and nutritional condition of anchovy (Bergeron et al 2010; 2013). However, environmental conditions only do not necessarily explain stock recruitment, which is also dependent on the reproductive biomass, particularly for short-lived species. Recruitment of the Bay of Biscay anchovy is associated with the one-year age class and the reproductive biomass consists mainly of individuals aged 2 and 3 years (Ibaibarriaga et al., 2008). Therefore, anchovy reproductive biomass each year depends also on the fishing mortality of the previous 2 years. SEAPODYM offers an ideal framework to analyse these different mechanisms together. This requires preparing a realistic ensemble of environmental forcing variables for the Bay of Biscay domain, and to reconstruct the history of anchovy fishing in the Bay since the 1990s, with detailed (i.e., spatially - disaggregated) catch, effort and length frequency data that can be used in the Maximum Likelihood Estimation approach.

### 3.15.2 Application: hindcast simulation

#### 3.15.2.1 Model configuration

With the model parameter estimation approach used in SEAPODYM, it is particularly important to use the most realistic environmental dataset. The first one used for the hindcast (historical period) simulation and optimisation use temperature and currents from the Ocean reanalysis GLORYS12 and the satellite ocean-colour derived primary production and euphotic depth. These variables are provided in the catalogue of CMEMS products at daily resolution and 1/12th degree together with the SEAPODYM-LMTL zooplankton and micronekton biomass ([https://data.marine.copernicus.eu/viewer/expert?view=dataset&dataset=GLOBAL\\_MULTIYEAR\\_BG\\_C\\_001\\_033](https://data.marine.copernicus.eu/viewer/expert?view=dataset&dataset=GLOBAL_MULTIYEAR_BG_C_001_033)). Given the high computational cost of optimisation method, the resolution for the phase of parameter estimation was degraded at 1/4 deg x month.

The interannual variability of environmental conditions has been analysed. It was shown that winter meteorological conditions over the North Atlantic have a strong impact on the main rivers flow in spring, that then influence the dynamics of primary production in the Bay of Biscay. This analysis was shared with colleagues working on the biogeochemical operational models to ask for a better representation of the rivers flow interannual variability (represented by a mean climatological conditions). In the meantime, it was decided to continue the optimisation phase with the satellite derived primary production product covering the time series 1998-present.

The model requires some population dynamics parameters that have been obtained from scientific literature. These are the age-growth (size and weight) functions and the age at maturity. An initial total adult biomass estimated by stock assessment studies was provided in the cost function to limit the tendency of the model to quickly increase the biomass to get better fit to catch data. The initial conditions of the fish population have also been created based on the stock-assessment studies conducted by the ICES ad-hoc group for this species (ICES 2024). This consisted in redistributing the total biomass of anchovies by age cohort in each cell of the grid domain. Note that these initial population conditions are improved by several iterations through the optimisation process.

<b>Project</b>	NECCTON No 101081273	<b>Deliverable</b>	D7.2
<b>Dissemination</b>	Public	<b>Nature</b>	Report
<b>Date</b>	14/10/2025	<b>Version</b>	1.0

The Biscay anchovy has been exploited mostly by Spain and France fishing fleets. The fisheries data for the historical period since the early 1990s have been obtained from different sources. Fisheries are defined in SEAPODYM by a unique selectivity function, which does not depend on space and time, and by a unique catchability coefficient, which can only change linearly with time. The linear trend may be necessary to account for technological advances, affecting the time of searching and volumes of fish being caught. Spatial and temporal variability in catch is assumed to be driven by the spatial distributions of fish that are explicitly described by the model. There are two catch prediction methods in SEAPODYM. The first method is based on the spatially distributed fishing effort, following the catch equation including catchability and selectivity of the fishing gear. The second method consists of removal of total catch in number of fish of a given age class directly from the predicted fish density.

The model optimisation phase used two sources of information to reconstruct fishing history based on catch effort and length frequencies data. The ICES WGHANSA reports provide total catch in the entire domain of Biscay on a quarterly basis and size frequencies of catch aggregated by quarter in regions 27.8.a-b and 27.8.b-c. The EU Fisheries Dependent Information (FDI) database gives access to the fishing effort (time spent fishing in days) and landings for the 3 main fishing gears (purse seine; pelagic pair trawl and midwater otter trawl) used to catch anchovy. Data are provided on a quarterly and 0.5 degrees resolution. From these data, a total of 8 fisheries was defined with the first 4 (S1, S2, T3, T4) of them being used in the cost function by predicting catch from using the fishing effort. The 4 others without fishing effort data were used with the catch removal method to simply account for fishing mortality (Table 11). To match the computational needs in the optimization process, effort and catch data were evenly redistributed on a monthly basis and 0.5 or 1/12 degrees (Table 11; Figure 52). The common time period for these two sources of data is 2013-2018. It is used to run the model parameter estimation phase.

Table 11. Description of fisheries targeting anchovy in the Bay of Biscay used in SEAPODYM. PS= purse seine; OTM = midwater otter trawl; PTM = pelagic pair trawl.

<b>Fishery code</b>	<b>Fishing gear</b>	<b>Flag</b>	<b>Fishing area (ICES rectangles)</b>	<b>Time period and resolution</b>	<b>Resolution after disaggregation</b>	<b>Associated length frequencies range (bin) and sampling area</b>
S1	PS	Es	27.8.b-c	2013-2018;	Month x 0.5°	6.5-19.5 cm (0.5) 27.8.b-c
S2	PS	Es	27.8.a	2013-2018	Month x 0.5°	9.0-19.5 cm (0.5) 27.8.a-b
T3	OTM	Fr	27.8.a-b	2013-2018	Month x 0.5°	9.0-19.5 cm (0.5) 27.8.a-b
T4	PTM	Fr	27.8.a-b	2013-2018	Month x 0.5°	9.0-19.5 cm (0.5) 27.8.a-b
S5	PS	Es	27.8.b-c	2013-2018	Month x 1/12°	6.5-19.5 cm (0.5) 27.8.b-c
S6	PS	Fr	27.8.a	2013-2018	Month x 1/12°	9.0-19.5 cm (0.5) 27.8.a-b
T7	OTM	Fr	27.8.a-b	2013-2018	Month x 1/12°	9.0-19.5 cm (0.5)



<b>Project</b>	NECCOTON No 101081273	<b>Deliverable</b>	D7.2
<b>Dissemination</b>	Public	<b>Nature</b>	Report
<b>Date</b>	14/10/2025	<b>Version</b>	1.0

						27.8.a-b
T8	PTM	Fr	27.8.a-b	2013-2018	Month x 1/12°	9.0-19.5 cm (0.5) 27.8.a-b

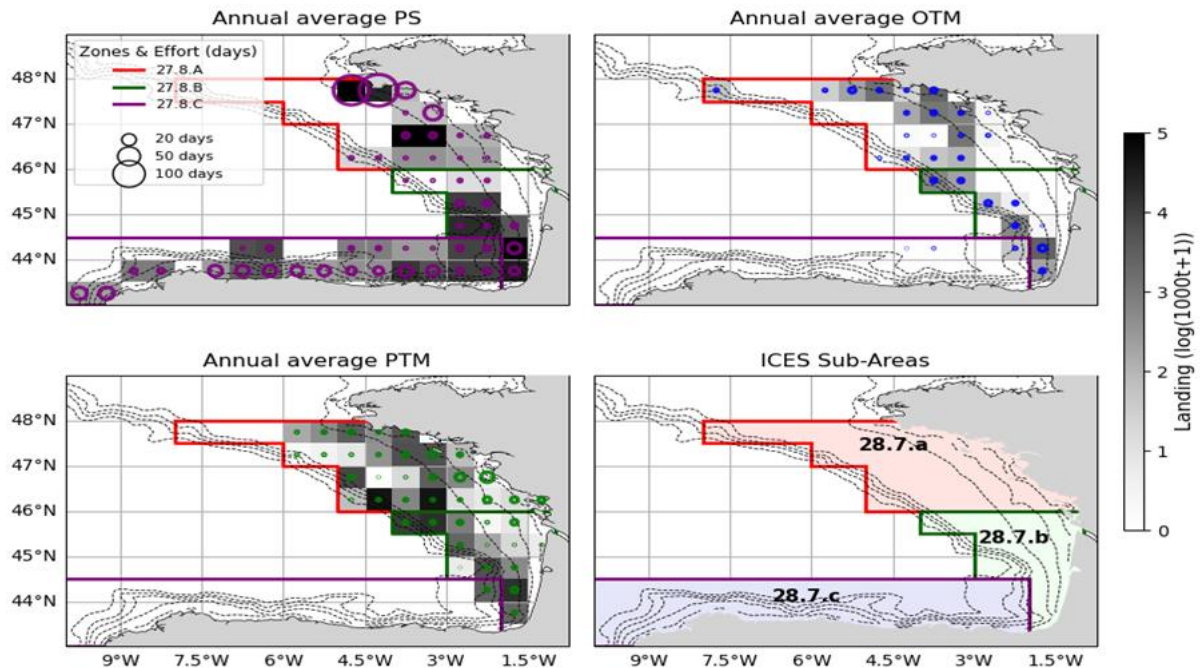


Figure 52. Distribution of annual averages of anchovy catch (2013-2018) by the three main fishing gears.

### 3.15.2.2 Results

A long series of anchovy egg density and zooplankton abundance observations provided by IFREMER with the regular PELGAS monitoring cruises allowed to make a first statistical analysis using the forcing variables of SEAPODYM (temperature, primary production, zooplankton, micronekton, bathymetry) to which the adult stock of the previous year estimated by stock assessment was added to account for the spawning biomass effect. A bias in the predicted zooplankton biomass distribution was quickly detected and corrected using a relationship to the bathymetry. The correction was validated independently with the zooplankton time series collected in the Channel by the Plymouth Marine Laboratory.

Then a delta-GAM statistical model was used to predict egg density observations using these variables. Briefly the results indicate that the best descriptors were the temperature, either Sea Surface Temperature (SST) or bottom temperature in shallow waters, bathymetry, micronekton and spawning biomass from previous year. The zooplankton had limited effect. Once they are released anchovy eggs typically develop and hatch within 2 to 4 days, depending on water temperature. During this period, the embryos rely entirely on their own yolk reserves for nourishment. It is thus coherent that the egg density is more correlated to temperature, predation by micronekton and spawning biomass of adults than to the zooplankton abundance. This one becoming likely more critical for the older stages. This first analysis provided confidence in the forcing variables and the following steps using SEAPODYM. In



<b>Project</b>	NECCTON No 101081273	<b>Deliverable</b>	D7.2
<b>Dissemination</b>	Public	<b>Nature</b>	Report
<b>Date</b>	14/10/2025	<b>Version</b>	1.0

fact, SEAPODYM simulates the survival of larvae using temperature, predation and prey abundance, but does not account for mortality of eggs before larval recruitment.

#### *3.15.2.3 Validation of hindcast simulations*

The model parameters are estimated with the Maximum Likelihood Estimation approach using the spatially disaggregated catch, effort and length frequencies data from the 4 fisheries S1, S2, T3 and T4. A series of simulations is needed to estimate all the parameters, starting from initial values defined according to the knowledge of the species and existing stock assessment studies. The best statistical scores are researched in terms of catch, and size frequency distributions over time and space. Once the best score is achieved, the model is run without fishing to measure the fishing impact on the population structure (Figure 53) and biomass (Figure 54).

Additional validation is conducted by comparing the model outputs with independent data such as the anchovy acoustic biomass estimate from the JUVENA research cruises (Boyra et al., 2013) and the recruitment, adult and total biomass time series from stock assessment studies (ICES 2021). Finally, a simulation without fishing is run over the extended time series (1998-2024) to check if the model with its parametrization can reproduce a decline in the population due to unfavorable environmental conditions.

<b>Project</b>	NECCON No 101081273	<b>Deliverable</b>	D7.2
<b>Dissemination</b>	Public	<b>Nature</b>	Report
<b>Date</b>	14/10/2025	<b>Version</b>	1.0

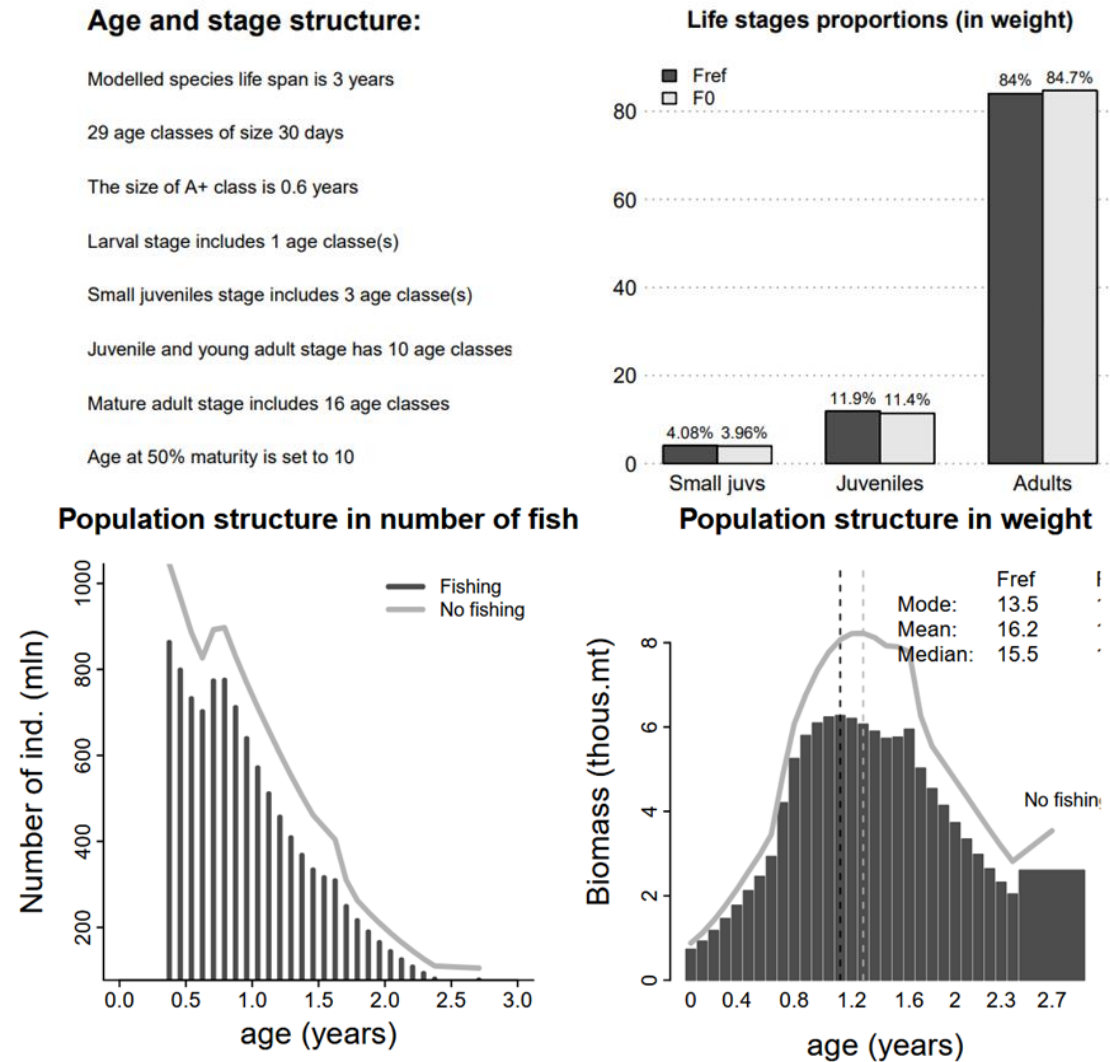


Figure 53. Summary of the population structure for the Biscay anchovy as predicted by SEAPODYM

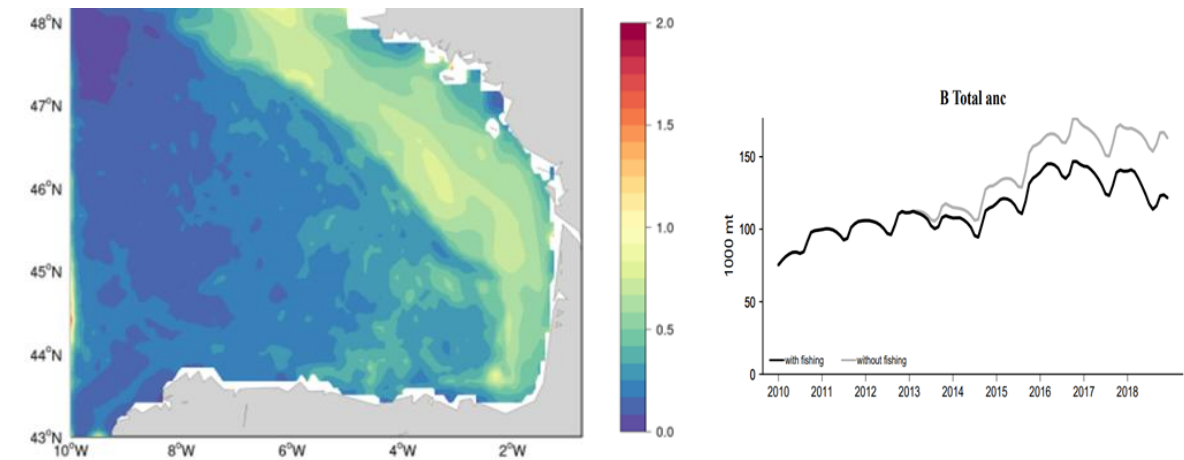


Figure 54. Predicted mean distribution of anchovy total biomass in the Bay of Biscay (left: t/km2) and evolution of biomass over time with fishing (black) and in absence of fishing (grey).

<b>Project</b>	NECCTON No 101081273	<b>Deliverable</b>	D7.2
<b>Dissemination</b>	Public	<b>Nature</b>	Report
<b>Date</b>	14/10/2025	<b>Version</b>	1.0

### 3.15.3 NECCTON Products from the model

The model outputs are like those listed for the tuna application (Table 10), with differences in the definition of the duration of life stages described in section above.

### 3.15.4 Discussion of pros and cons of the model

In addition to pros and cons listed for the application SEAPODYM-tuna (section 3.14.4), it should be noted the need for high quality forcings in very coastal areas, and the need to start including interactions (energy flux) with the benthos system when using zooplankton, due to the coastal nature of the target species. On the other side, the model is sufficiently generic to be adapted to a small pelagic species without requiring code modification, allowing the use of the maximum likelihood estimation approach to estimate the anchovy population and fisheries parameters. It would be possible and desirable to use higher resolution fishing data.

## 3.16 SEAPODYM-Mackerel (Leading partner: CLS)

### 3.16.1 Model description

The SEAPODYM model, described in section 3.5.1, has been adapted to the North-East Atlantic mackerel *Scomber scombrus*.

Mackerel is a widely distributed species found throughout the North Atlantic, forming diffuse aggregations and feeding offshore, beyond the continental shelf (Trenkel et al., 2014). Its spawning areas are located along the continental slope from the north of the Iberian Peninsula to the west of Scotland (Brunel et al., 2018). The peak spawning period occurs from March to May in the Bay of Biscay and west of Ireland, but diffuse spawning takes place from February to July along the continental slope between 36°N and 72°N (Dos Santos Schmidt et al., 2024).

Mackerel undertake annual migrations. After spawning, they migrate northward (North Sea, Norwegian Sea, Barents Sea) to feed during the high-latitude production season. In autumn, they reverse this migration, returning to lower latitudes, offshore of the British Isles and even further south (Jansen et al., 2012). There is no evidence of daily vertical migration (Jansen et al., 2019).

In 2014, the Northeast Atlantic mackerel stock reached a historically high level due to rising temperatures and a succession of strong recruitment years since 2000. This increase in biomass may have intensified intraspecific competition for food, resulting in a northward and westward expansion (respectively by about 400km and 1600km) of the stock's distribution into new productive areas to meet the species' bioenergetic needs (Dos Santos Schmidt et al., 2024; Olafsdottir et al., 2019).

Mackerel is one of the most heavily exploited fish stock in the North East Atlantic, ranging between 500,000-1,000,000 tonnes landed per year over the last 40 years (ICES, 2024c). Stock assessments works have emphasised the complexity and uncertainty in modelling that species. Succeeding to model the significant stock displacements would therefore provide useful information for stock management.

<b>Project</b>	NECCOTON No 101081273	<b>Deliverable</b>	D7.2
<b>Dissemination</b>	Public	<b>Nature</b>	Report
<b>Date</b>	14/10/2025	<b>Version</b>	1.0

### 3.16.2 Application to North-East Atlantic mackerel: Hindcast-Simulation

#### 3.16.2.1 *Model configuration*

To adapt the SEAPODYM model to mackerel modelling, the parameters were checked and updated. In addition, the forage matrix was modified to account for the mackerels feeding on zooplankton.

#### Forcings

The SEAPODYM model for mackerel was forced with Net Primary Productivity (NPP) computed from chlorophyll a concentration observation provided by the Copernicus Marine Service OCEANCOLOUR\_GLO\_BGC\_L4\_MY\_009\_104 product. When these observations are not available (ie, at latitudes  $>60^{\circ}$  during boreal and austral winters), NPP comes from the Copernicus Marine Service biogeochemical reanalysis (PISCES model, Aumont et al., 2015). A relaxation technique is used to smoothly adjust the data at the frontier of the two fields. Temperature and currents forcings come from GLORYS12V1 which corresponds to the Copernicus Marine Service product GLOBAL\_REANALYSIS\_PHY\_001\_030. Oxygen originated from the climatology Levitus WOA13 (NOAA). Zooplankton and micronekton biomass were taken from the Copernicus Marine Service GLOBAL\_MULTIYEAR\_BGC\_001\_033 provided by CLS. The zooplankton and micronekton biomass in this product were computed using the above mentioned NPP, temperature and currents forcings.

The mackerel simulations were conducted at the spatial resolution of  $\frac{1}{4}^{\circ}$  and temporal resolution of the month (for the parameter optimisation part).

#### Fisheries

Catch data were retrieved from the ICES catch and length-frequency (LF) database. In the SEAPODYM model, these data serve a dual purpose: they inform the estimation of fishing mortality and are used to calibrate the model. Catch data were aggregated according to ICES Division 27 subareas. Catch by statistical rectangle data is monthly from 2010 and quarterly before. LF data was not available for some of the fisheries, as it is specified in the table below. When LF data was available, the selectivity of the fishery was computed.

Table 12: Description of fisheries targeting mackerels in the North-East Atlantic.

<b>Fishery code</b>	<b>Fishing gear</b>	<b>Flag</b>	<b>Time period</b>	<b>Temporal and spatial resolution the data was aggregated in</b>	<b>LF data associated (Yes/No)</b>	<b>Selectivity function type</b>	<b>Associated mean length (cm)</b>
PT1	Pelagic trawl	Denmark, Canary Island, Ireland, Russia, UK, North Ireland, Scotland, Faroe Islands	1998-2018	Month x ICES stat rect ( $1^{\circ} \times 0.5^{\circ}$ )	Yes	asymmetric Gaussian	34.6
PT2	Pelagic trawl	Greenland	1998-2018	Month x ICES stat rect ( $1^{\circ} \times 0.5^{\circ}$ )	Yes	asymmetric Gaussian	34.6

<b>Project</b>	NECCON No 101081273	<b>Deliverable</b>	D7.2
<b>Dissemination</b>	Public	<b>Nature</b>	Report
<b>Date</b>	14/10/2025	<b>Version</b>	1.0

PT3	Pelagic trawl	Iceland	1998-2018	Month x stat (1°x0.5°)	ICES rect	Yes	asymmetric Gaussian	34.6
PT4	Pelagic trawl	Germany, Netherlands	1998-2018	Month x stat (1°x0.5°)	ICES rect	Yes	asymmetric Gaussian	34.35
PT5	Pelagic trawl	England	1998-2018	Month x stat (1°x0.5°)	ICES rect	Yes	asymmetric Gaussian	32.6
PT6	Pelagic trawl	Estonia, Lithuania, Sweden	1998-2018	Month x stat (1°x0.5°)	ICES rect	No	-	34.6
S7	Bottom trawl	Portugal	1998-2018	Month x stat (1°x0.5°)	ICES rect	Yes	asymmetric Gaussian	32.6
S8	Bottom trawl	Jersey, Belgium	1998-2018	Month x stat (1°x0.5°)	ICES rect	No	-	34.6
PS9	Purse seine	Norway	1998-2018	Month x stat (1°x0.5°)	ICES rect	Yes	asymmetric Gaussian	34.6
O10	Other	Bonaire, Sint Eustatius and Saba	1998-2018	Month x stat (1°x0.5°)	ICES rect	Yes	asymmetric Gaussian	34.6
O11	Other	Spain	1998-2018	Month x stat (1°x0.5°)	ICES rect	Yes	asymmetric Gaussian	34.75
O12	Other	Man, France, Guernsey, Poland	1998-2018	Month x stat (1°x0.5°)	ICES rect	No	-	34.75

### Age and life stage parameters

To model the mackerel population structure, the maximum age (31 years from ICES, 2022) and the time resolution (month in the optimisation version) are used to determine the number of cohorts. The first cohort correspond to the larval stage. Juvenile's cohorts correspond to an age of approximately 3 months, which aligns with the recruitment age defined in ICES stock assessment reports. From the fourth cohort onward (13<sup>th</sup> cohort in weeks), individuals are considered young adults and adult. The difference between young adults and adults is that only adults are mature. The maturity in SEAPODYM is coded as the percentage of the population that contributes to the recruitment and was taken from ICES WGWIDE reports (ICES, 2022).

The length at age and weight at age relationships are used to inform the age and weight structure of the model. Those relationships have to be discretized to inform the length and weight of the different cohorts of the 4 life stages represented by the model (larvae, juveniles, young and adults). Length function of age and weight function of length were taken from ICES stock assessment reports (ICES, 2024c) and used to inform the length and weight parameters of the table below.

<b>Project</b>	NECCON No 101081273	<b>Deliverable</b>	D7.2
<b>Dissemination</b>	Public	<b>Nature</b>	Report
<b>Date</b>	14/10/2025	<b>Version</b>	1.0

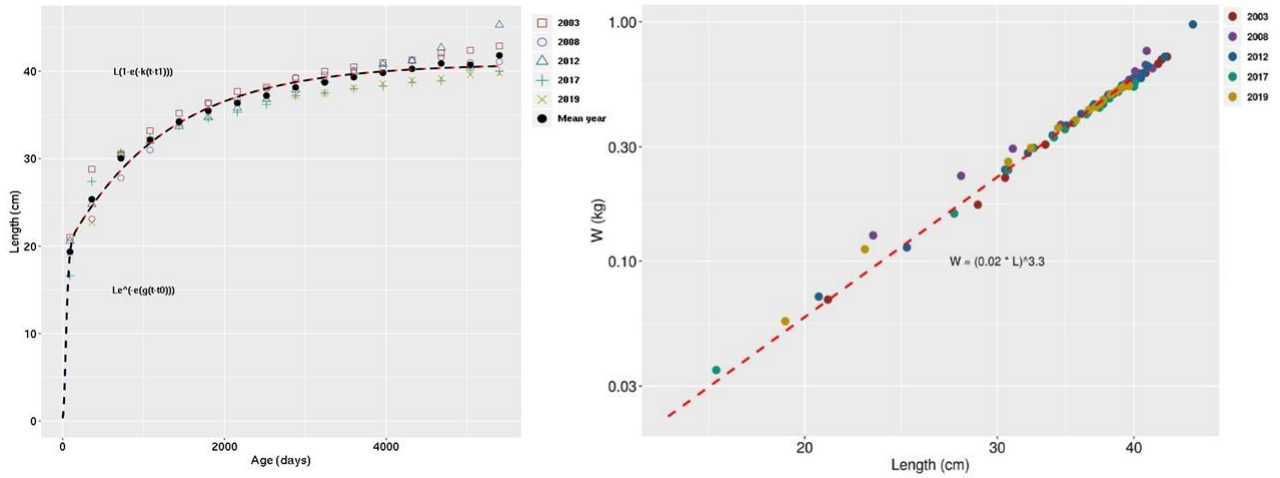


Figure 55: Length at age (left) and weight at length (right) from ICES stock assessment reports.

Table 13: Age and life stage parameters estimated from bibliography.

Parfile name	Description	Value
nb_life_stages	The number of the species life stages to be considered in the model	3
life_stage	List of names of the life stages	larvae juvenile adult
nb_cohort_life_stage	A vector of size 3 giving the number of age classes by life stage (in weeks)	4, 8, 359
sp_unit_cohort	A vector of the size of age class in days of length nb_cohorts_life_stage (356)	
maturity_age	The vector of maturity-at-age estimates of length nb_cohorts_life_stage. The values between 0 and 1 give the proportion of mature adults in each age class.	-
length	A vector of mean fork lengths of fish of length nb_cohorts_life_stage (356), estimated in the middle of each age class.	-
weight	A vector of mean weights of fish of length nb_cohorts_life_stage (356), estimated in the middle of each age class.	-

Recruitment (Beverton Holt function parameters) and mortality parameters were estimated from stock assessment data (ICES, 2024c).

<b>Project</b>	NECCTON No 101081273	<b>Deliverable</b>	D7.2
<b>Dissemination</b>	Public	<b>Nature</b>	Report
<b>Date</b>	14/10/2025	<b>Version</b>	1.0

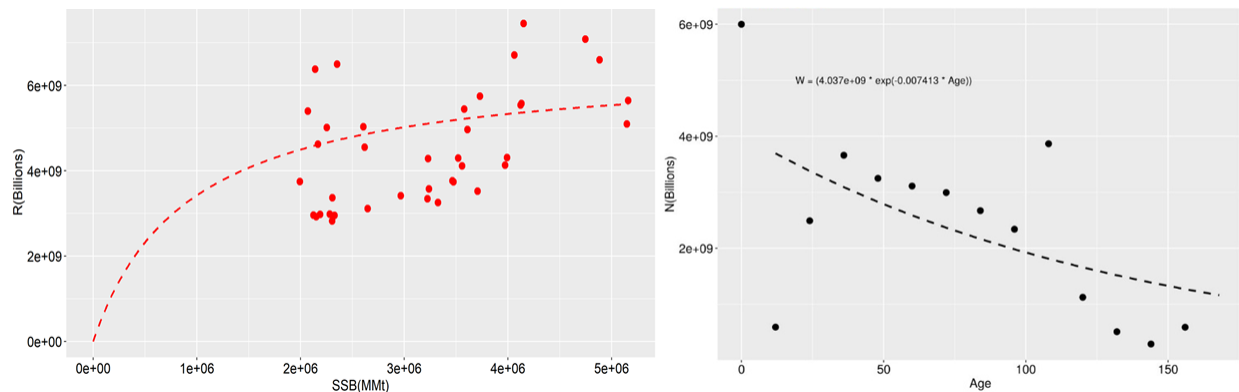


Figure 56: Beverton Holt function (recruitment function of stock standing biomass) (left) and abundance at age (right) from stock assessment reports.

Table 14: Demographic parameters estimated from stock assessment data and previous SEAPODYM studies

Parfile name	Description	Unit	Estimated value
<i>Recruitment</i>			
nb_recruitment	Reproduction rate in Beverton–Holt function	month <sup>-1</sup>	0.02
a_adult_spawning	Slope parameter in Beverton–Holt function	Nb/km <sup>2</sup>	0.001
<i>Natural mortality</i>			
Mp_mean_max	Predation mortality rate at age 0	month <sup>-1</sup>	0.56
Mp_mean_exp	Slope coefficient in predation mortality		0.51
Ms_mean_max	Senescence mortality rate at age 0	month <sup>-1-βs</sup>	0.002
Ms_mean_slope	Slope coefficient in senescence mortality		0.34
M_mean_range	Variability of mortality rate with habitat index		0.27

### Habitat parameters

Preferred temperature at length related parameters were estimated from RFID data downloaded from the Norwegian Marine Data Center (<http://metadata.nmdc.no/metadata-api/landingpage/f9e8b1cff4261cf6575e70e56c4c3b3e>), under the guidance of Aril Slotte (IMR) and Anna Ólafsdóttir (MFRI). Preferred temperature for larvae was computed from Eggs and Larvae database (<https://eggsandlarvae.ices.dk/Download.aspx>). Regarding oxygen, there is no study indicating a critical threshold value. Values of the oxygen parameters are set so that it does not constrain habitat.

The hypothesis is made that mackerel only feed in epipelagic layer, which seems realistic according to Diaz, 2013 and Jansen et al., 2019.



<b>Project</b>	NECCTON No 101081273	<b>Deliverable</b>	D7.2
<b>Dissemination</b>	Public	<b>Nature</b>	Report
<b>Date</b>	14/10/2025	<b>Version</b>	1.0

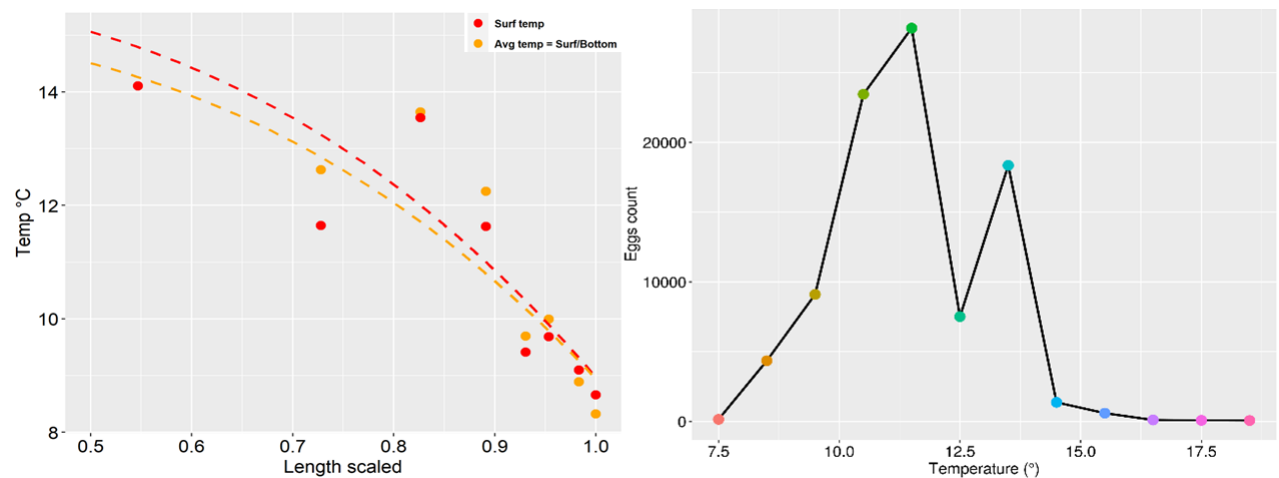


Figure 57: Temperature function of length (from RFID tag data) (left) and egg count function of temperature (right) from ICES Eggs and larvae database.

Table 15: Habitat parameters, estimated from RFID tag data, Eggs and Larvae ICES data, bibliography as well as previous SEAPODYM studies.

Parfile name	Description	Unit	Estimated value
<i>Spawning habitat index</i>			
a_sst_larvae	Standard deviation in temperature Gaussian function of spawning habitat	°C	0.97
b_sst_larvae	Optimal water temperature for larvae survival	°C	13.94
alpha_hsp_pre	Prey encounter rate in Holling type III function	day <sup>-1</sup>	0.86
alpha_hsp_predator	Log-normal mean parameter in predator-dependent function	g/m <sup>2</sup>	1.24
beta_hsp_predator	Log-normal shape parameter in predator-dependent function.		2.82
<i>Thermal accessibility and age-dependance</i>			
a_sst_spawning	Standard deviation in temperature Gaussian function for age 0	°C	See optimisation section
a_sst_habitat	Standard deviation in temperature Gaussian function at age A+	°C	See optimisation section
b_sst_spawning	Preferred temperature for age 0	°C	See optimisation section
b_sst_habitat	Preferred temperature for the oldest adult class A+	°C	See optimisation section
T_age_size_slope	Allometric power coefficient for thermal preferences at age		See optimisation section

<b>Project</b>	NECCON No 101081273	<b>Deliverable</b>	D7.2
<b>Dissemination</b>	Public	<b>Nature</b>	Report
<b>Date</b>	14/10/2025	<b>Version</b>	1.0

<i>Oxygen limitation of accessibility to prey</i>			
a_oxy_habitat	Slope in the oxygen accessibility function		0.05
b_oxy_habitat	Minimal threshold oxygen value, required by the predator to access the habitat for foraging	ml/L	1
<i>Food selection parameters</i>			
eF_habitat_epi	Contribution of epipelagic forage to the feeding habitat index	-	1
eF_habitat_meso	Contribution of mesopelagic forage to the feeding habitat index	-	0
eF_habitat_mmeso	Contribution of migrant mesopelagic forage to the feeding habitat index	-	0
eF_habitat_bathy	Contribution of lower mesopelagic forage to the feeding habitat index	-	0
eF_habitat_mbathy	Contribution of migrant lower mesopelagic forage to the feeding habitat index	-	0
eF_habitat_hmbathy	Contribution of highly migrant lower mesopelagic forage to the feeding habitat index	-	0

#### Movement and migration parameters

The spawning season start and peak were taken from WGWIDE 2022 report, figure 3.4.2.1.1 (ICES, 2022). The velocity at maximal habitat gradient was estimated from the RBIF tag data. The  $c\_diff\_fish$  parameter, that controls the decrease of diffusion with increasing habitat index, was taken from Dragon et al., (2018).

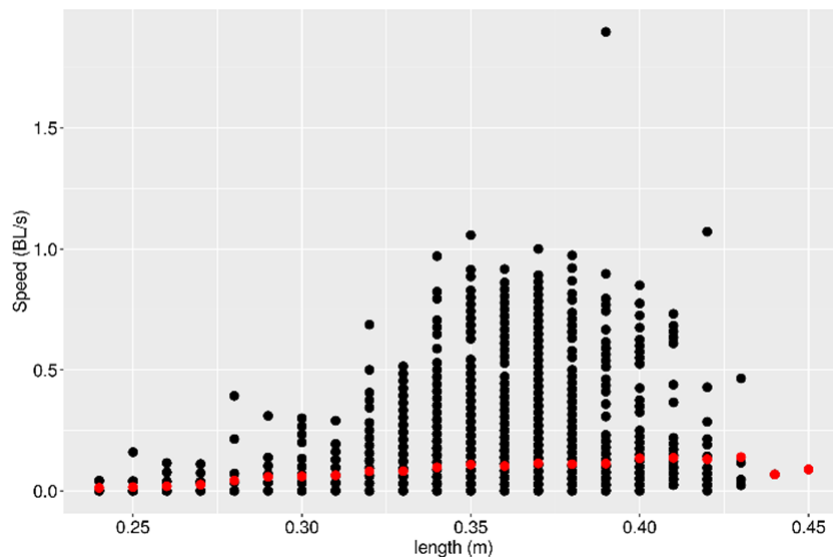


Figure 58: Velocity at maximal habitat gradient function of body length, from RBIF data.

Table 16: Movement and migration parameters, estimated from RBIF data and taken from previous SEAPODYM studies.

Parfile name	Description	Unit	Value
--------------	-------------	------	-------

<b>Project</b>	NECCON No 101081273	<b>Deliverable</b>	D7.2
<b>Dissemination</b>	Public	<b>Nature</b>	Report
<b>Date</b>	14/10/2025	<b>Version</b>	1.0

spawning_season_peak	Mid-date (day of the year) of seasonal spawning migrations of adults	day	130
spawning_season_start	Critical value of day–night ratio (or day length gradient), % triggering seasonal migrations. It also controls the duration of spawning season at each latitude	%	1.25
MSS_size_slope	Slope coefficient in allometric function for velocity		4.19e-8
MSS_species	Velocity at maximal habitat gradient and MSS_size_slope = 1.	Body length/s	9.34
sigma_species	Multiplier for the theoretical diffusion rate $V^{-2}\Delta T^4$	s	See optimisation section
c_diff_fish	Coefficient of diffusion variability with habitat		6.3e-7

### Parameter optimisation with the SEAPODYM-TAG model

The SEAPODYM-TAG model is a simplified version of the SEAPODYM model, designed to simulate the movement of tagged fish densities over time and space. It uses the same transport equation as the one embedded in the SEAPODYM population dynamics model. Movement parameters are linked to the habitat characteristics of individuals. Since tagged fish are primarily adults, the model provides insights into the spatio-temporal dynamics of adult fish and their habitats.

Before calibration, a sensitivity analysis is performed to identify which parameters can be estimated, i.e. those to which the model is sensitive. If the model's predictions are insensitive to variations in a given parameter, that parameter can be excluded from the optimization process. This sensitivity analysis is conducted globally over the 2015–2019 period, for computational efficiency, to determine which parameters can be estimated from the available data.

To perform this analysis, Sobol indices are used to measure the relative contribution of each parameter to the total variance in the likelihood function. Two types of experiments are conducted:

- AAT (All-At-a-Time): all parameters are randomly sampled in each model run.
- OAT (One-At-a-Time): only one parameter is randomly varied across a series of model runs, while the others are held constant.

Both approaches are based on 10,000 Monte Carlo iterations. The resulting likelihood profiles help visualize the parameter values at which global minima of the likelihood function occur. These are the values we aim to identify for model calibration. Parameters leading to the lowest likelihood values in AAT experiments are selected for further exploration in OAT experiments.

In the case of mackerel, the model is sensitive to only 10 parameters, significantly fewer than the ~40 parameters influencing the full SEAPODYM model. Moreover, these parameters are the same as those used in the full model. The RFID tag data were used to inform the tag model. This approach also eliminates the need for predefined initial conditions, as data from the first captures are used instead.

<b>Project</b>	NECCTON No 101081273	<b>Deliverable</b>	D7.2
<b>Dissemination</b>	Public	<b>Nature</b>	Report
<b>Date</b>	14/10/2025	<b>Version</b>	1.0

Additionally, it allows for faster computations due to the reduced number of processes involved and the use of a single data source and likelihood function.

As a result, calibrating the tag model helps reduce the number of parameters to optimize when transitioning to the full SEAPODYM model. The calibration of the tag model parameters is performed using a maximum likelihood estimation approach.

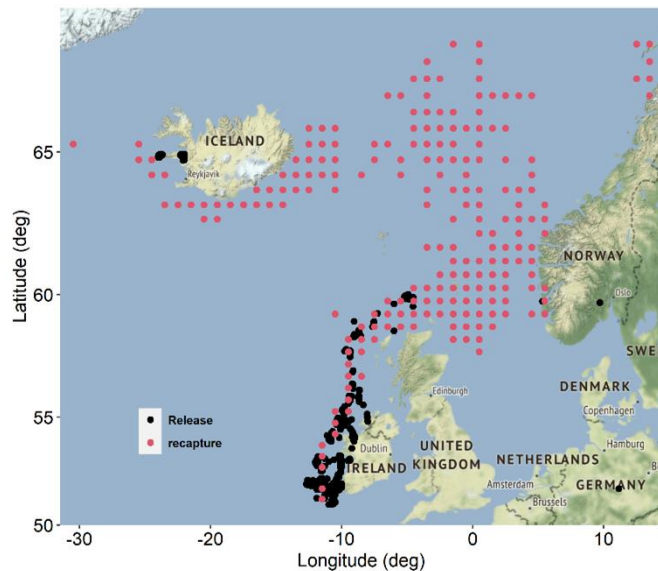


Figure 59: Catch and release positions used in the SEAPODYM-TAG optimisation.

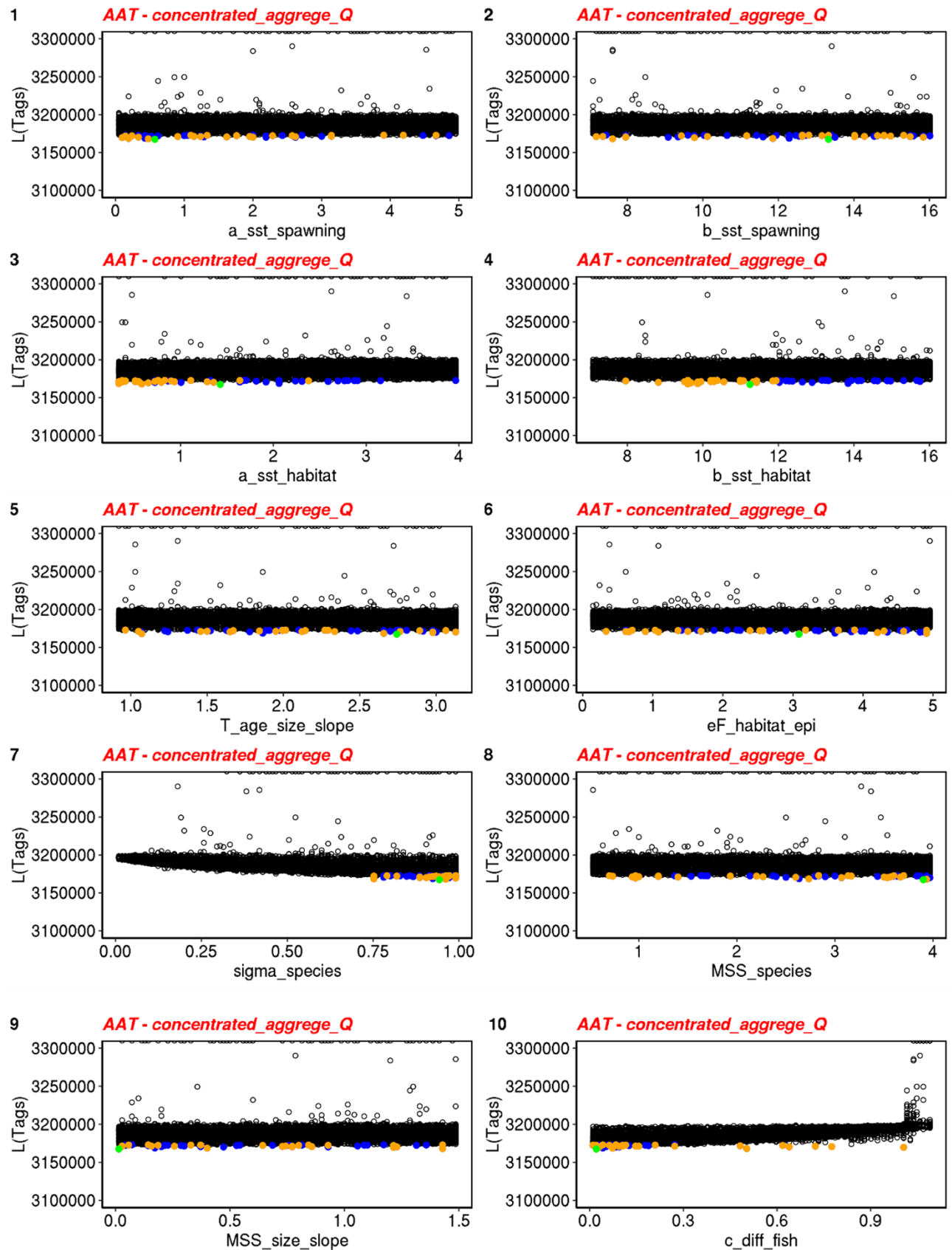
### 3.16.2.2 Results

#### Parameter optimization results

##### All At Time experiments

The AAT experiments rely on Monte Carlo simulations in which all model parameters are simultaneously varied across their predefined ranges.

Project	NECCTON No 101081273	Deliverable	D7.2
Dissemination	Public	Nature	Report
Date	14/10/2025	Version	1.0



<b>Project</b>	NECCTON No 101081273	<b>Deliverable</b>	D7.2
<b>Dissemination</b>	Public	<b>Nature</b>	Report
<b>Date</b>	14/10/2025	<b>Version</b>	1.0

Figure 60: Likelihood values of 10,000 independent configurations as a function of each SEAPODYM-TAG model parameter. Black dots represent arbitrary configurations. The green dot corresponds to the configuration with the lowest likelihood value among all points. Blue and orange dots represent the 50 best configurations, with the orange ones being those with a temperature below 12 degrees.

### One At Time experiments

The 50 simulations with the lowest likelihood values from the AAT (All-At-a-Time) experiments were selected. Starting from a previously identified configuration, each of the 10 parameters was individually varied: for each parameter, its value was randomly changed 25 times within its defined bounds, while all other parameters were held constant.

The graphs resulting from the OAT (One-At-a-Time) analysis represent slices through the parameter space in different directions, centred around the minima identified during the AAT phase. Since OAT explores the likelihood function while keeping other parameters fixed, the absolute global minimum may not appear in all plots. However, if the conditioned likelihood reveals multiple clusters, each can serve as a potential starting point for the global optimization process. Conversely, if the likelihood surface shows broad minima, it suggests that the corresponding parameter has limited influence on the model's output.

<b>Project</b>	NECTON No 101081273	<b>Deliverable</b>	D7.2
<b>Dissemination</b>	Public	<b>Nature</b>	Report
<b>Date</b>	14/10/2025	<b>Version</b>	1.0

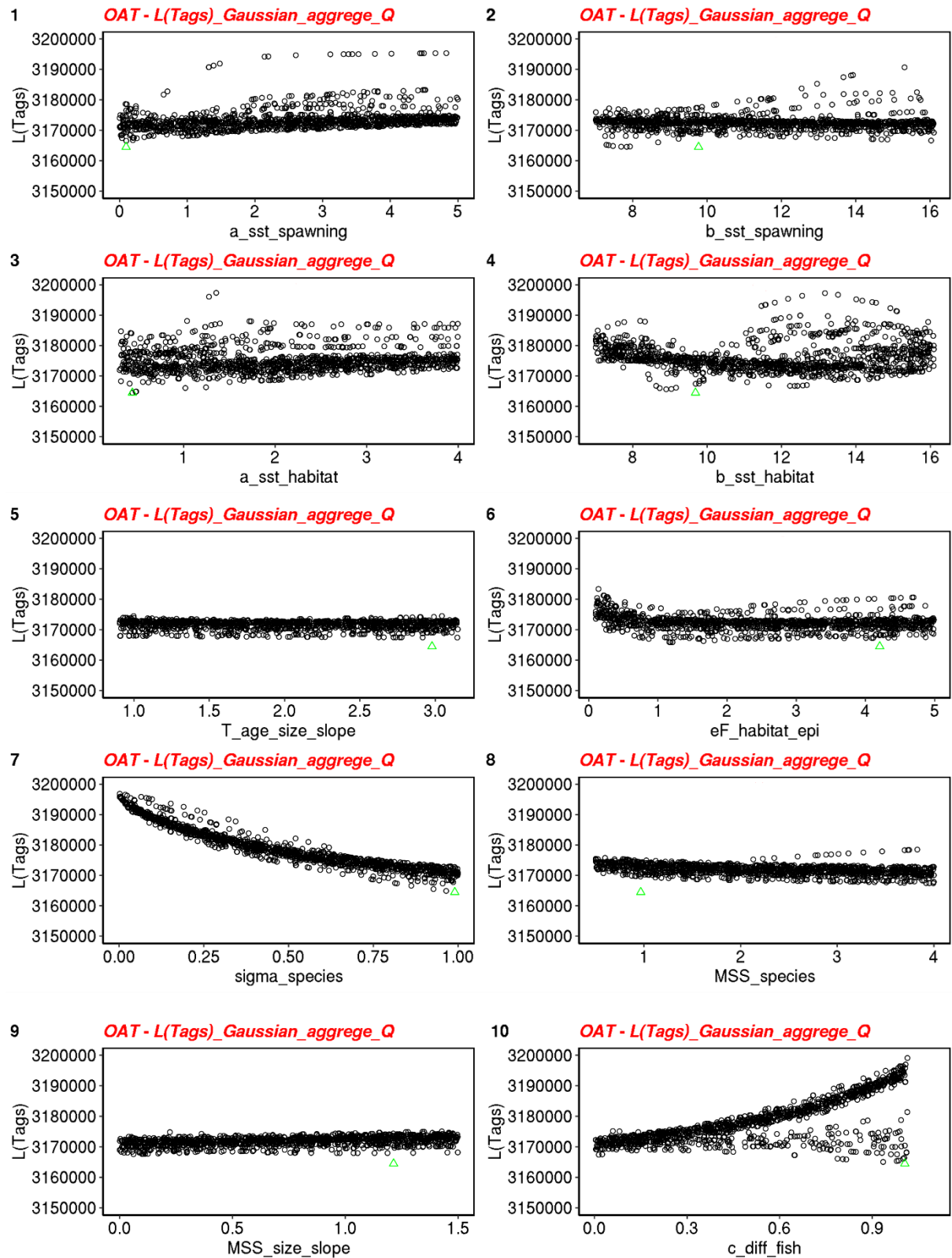


Figure 61: Likelihood values function of the parameters of the SEAPODYM-TAG model, conditioned by the value of the other parameters.



<b>Project</b>	NECCON No 101081273	<b>Deliverable</b>	D7.2
<b>Dissemination</b>	Public	<b>Nature</b>	Report
<b>Date</b>	14/10/2025	<b>Version</b>	1.0

That sensitivity analysis enabled us to better understand the link between a data type (tag data here) and the variables. The OAT graphs 2,4,6 and 8 suggest that the model is sensitive to the parameter and that the range is well fixed. The OAT graphs 5 and 9 show that the model is not very sensitive to the variation of these parameters. The OAT graphs 1,3,7 and 10 indicate that the range should be adapted for those parameters, since the value of the parameter leading to the minimum of the likelihood function is close to the minimum or maximum boundary of the interval explored. Graph 10 suggests the *c\_diff\_fish* parameter is in interaction with another parameters whose value is poorly fixed, probably the *sigma\_species* parameters since they interact together in the definition of the active random movement. This relationship has to be further investigated.

Below are provided the estimated value of the parameters from SEAPODYM-TAG model optimisation. Those parameters were used in the first run. At the exception of the *c\_diff\_fish* parameters whose optimised values is unrealistic. Its value from Dragon et al., (2018) has been used in the first run.

Table 17: Estimated values of the parameters obtained after optimisation.

<b>Parameter name</b>	<b>Description</b>	<b>Value Optimized</b>
a_sst_spawning	Standard deviation in temperature Gaussian function for age 0	4.76
b_sst_spawning	Preferred temperature for age 0	7.78
a_sst_habitat	Standard deviation in temperature Gaussian function at age A+	2.49
b_sst_habitat	Preferred temperature for the oldest adult class A+	9.86
T_age_size_slope	Allometric power coefficient for thermal preferences at age	1.86
eF_habitat_epi	Contribution of epipelagic forage to the feeding habitat index	1
sigma_species	Multiplier for the theoretical diffusion rate	0.63
MSS_species	Velocity at maximal habitat gradient and MSS_size_slope = 1	1.67
MSS_size_slope	Multiplier for the theoretical diffusion rate $V^{-2}\Delta T^4$	1.2
C_diff_fish	Coefficient of diffusion variability with habitat	0.08

### First simulations

Using the updated parameters described above, initial simulations of the mackerel model were conducted. The resulting time series of biomass for larvae, juveniles, young, and adult mackerel is shown below.

The increase in adult biomass from 2005 aligns with trends documented in stock assessment reports (ICES, 2024c). However, the biomass peak in our simulation occurs earlier than indicated by the stock recruitment assessments: 2007–2008 instead of 2014–2015. The decline in biomass after 2015 is consistent with the patterns observed in the recruitment assessments. Larvae biomass peaks in 2008 and 2010 in the simulation, leading to increased juvenile biomass those years.

<b>Project</b>	NECCTON No 101081273	<b>Deliverable</b>	D7.2
<b>Dissemination</b>	Public	<b>Nature</b>	Report
<b>Date</b>	14/10/2025	<b>Version</b>	1.0

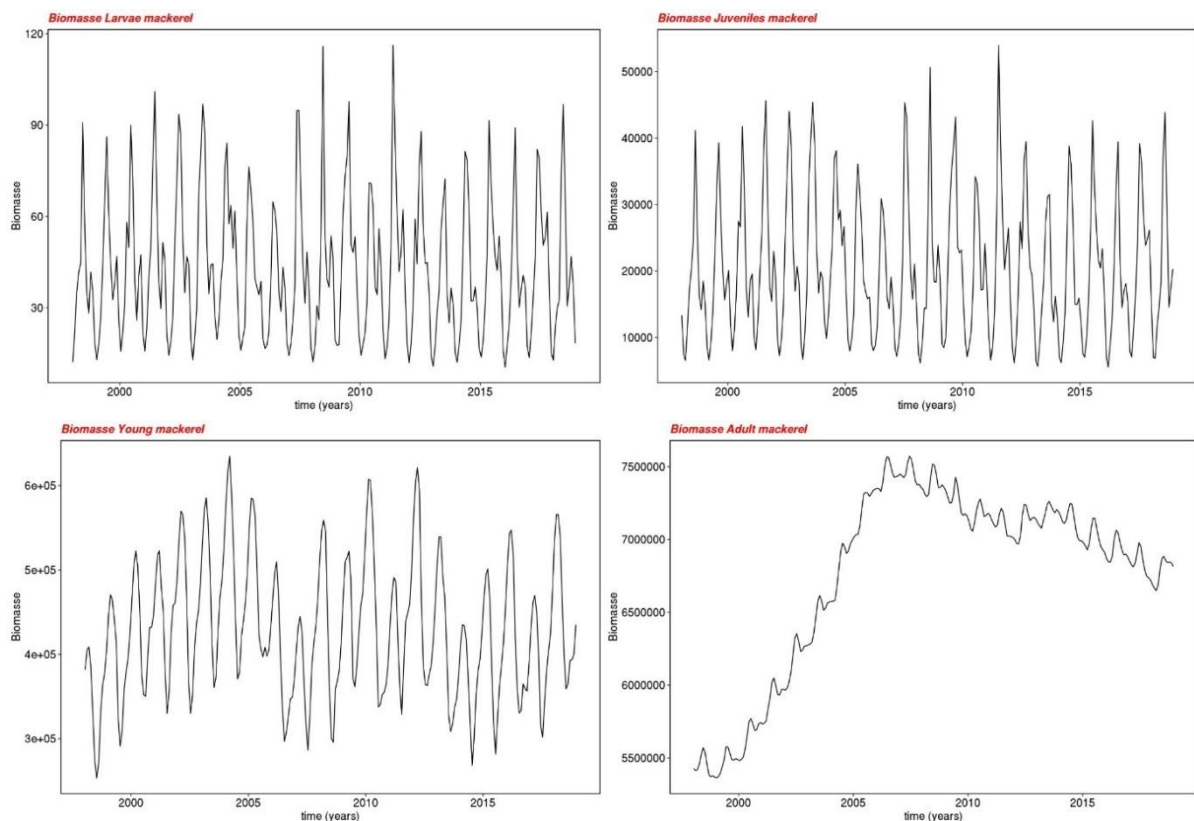
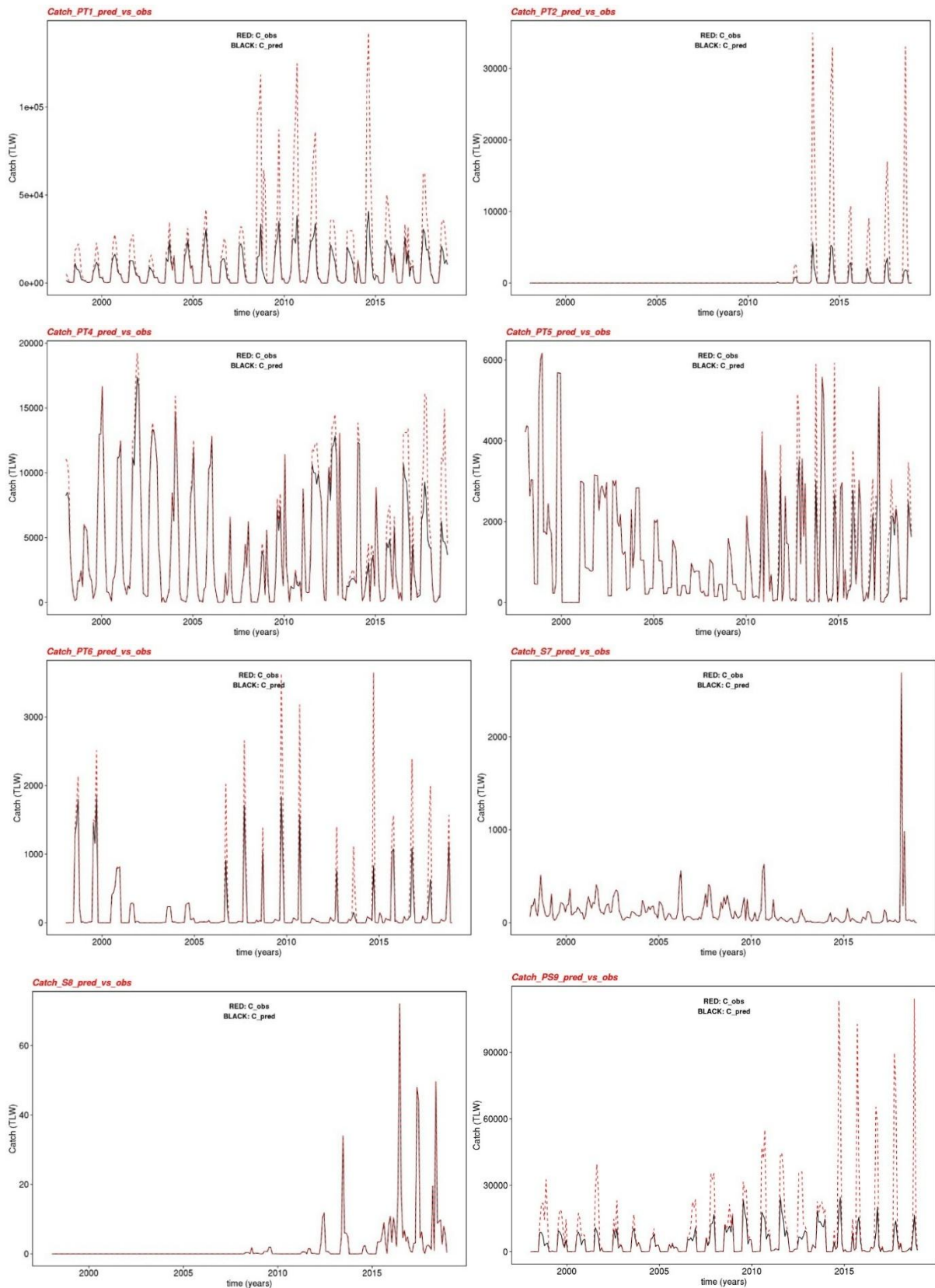


Figure 62: Outputs from the SEAPODYM-TAG model.

### 3.16.2.3 Validation of hindcast simulations

For the SEAPODYM-TAG data simulations, observed catches were compared to model predictions. For all fisheries included in the optimization process (ie those with associated length-frequency data) the visual agreement between observations and predictions is very good, as illustrated in the figure below.

<b>Project</b>	NECTON No 101081273	<b>Deliverable</b>	D7.2
<b>Dissemination</b>	Public	<b>Nature</b>	Report
<b>Date</b>	14/10/2025	<b>Version</b>	1.0



<b>Project</b>	NECCTON No 101081273	<b>Deliverable</b>	D7.2
<b>Dissemination</b>	Public	<b>Nature</b>	Report
<b>Date</b>	14/10/2025	<b>Version</b>	1.0

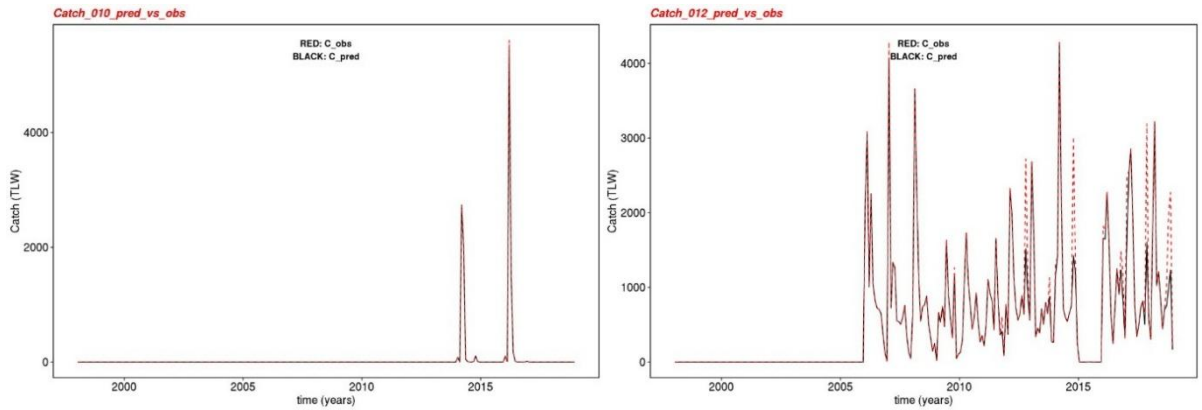


Figure 63: Observed catch (dotted red line) and predicted (black line) for each of the fisheries with length frequency data (used in the optimisation).

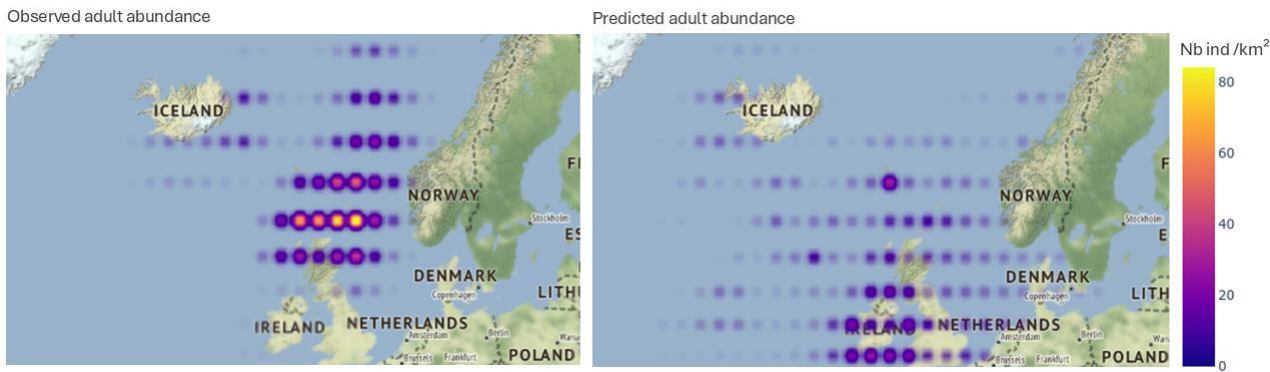


Figure 64: Observation and prediction from the SEAPODYM TAG model

Regarding the spatial distribution of the adult biomass, it seems that the large biomass north of Scotland is not reproduced by the model, that tend to predict more biomass in the Celtic Sea than observed. Overall, this first hindcast is not satisfactory since the spatial distribution is poorly modelled. Feeding and spawning habitats, that control notably the movements, should be more investigated to improve this first run. In addition, the full SEAPODYM model should now be used to conduct simulations.

### 3.16.3 NECCTON Products from the model

As with other SEAPODYM models, the SEAPODYM mackerel model provides spatial abundance estimates for each life stage (larvae, juvenile, young, and adult). Given the well-known challenges in modelling the spatial dynamics and biomass of North-East Atlantic mackerel, these outputs offer valuable opportunities for comparison with other models, contributing to ensemble modelling approaches for this species.

Since the effects of fishing can be assessed by running the final model without fishing mortality, it becomes possible to disentangle the impacts of fishing from those of climate variability. By using

<b>Project</b>	NECCTON No 101081273	<b>Deliverable</b>	D7.2
<b>Dissemination</b>	Public	<b>Nature</b>	Report
<b>Date</b>	14/10/2025	<b>Version</b>	1.0

climate projections as forcings, the model can be applied to test various exploitation scenarios under climate change conditions, thereby informing sustainable management strategies.

#### 3.16.4 Discussion of pros and cons of the model

In addition to the ones already listed in the SEAPODYM model application to Pacific tropical tuna and anchovy, the following pro and cons specific to the mackerel model can be added:

Pros:

- Provide spatial modelling of a species that experienced large shifts in its spatial distribution since 2007 (shift westward and northward).
- Help the ensemble modelling effort conducted for that species by the WGWIDE.

Cons:

- The model is not fully calibrated yet and has to be further validated.

## 4. Synthesis

### 4.1 Summary of Key model developments in NECCTON

The NECCTON project has achieved significant advances in end-to-end marine ecosystem modelling by integrating higher trophic level (HTL) dynamics with lower trophic level (LTL) and biogeochemical models, while also refining the representation of fishing and environmental variability.

A key development has been the move towards improved coupling between trophic levels. Some models now either feature two-way coupling, constrain fish consumption to primary and secondary production, incorporate benthic–pelagic interactions, or explicitly link fish predation to benthic fauna. This ensures more realistic energy transfer across food webs and incorporates processes that were previously missing. At the same time, models have improved spatial and temporal variability: horizontal resolutions have been refined for several models, migration schemes and movement modules have been implemented, and seasonal, interannual to decadal variability is increasingly represented.

Another major achievement is the integration of fishing dynamics. Several frameworks now include spatially variable fishing pressure, parameter estimation based on catch and effort data, and new fishing modules to test management strategies under climate change. This opens the way for scenario testing that combines ecological, environmental, and socioeconomic drivers.

<b>Project</b>	NECCTON No 101081273	<b>Deliverable</b>	D7.2
<b>Dissemination</b>	Public	<b>Nature</b>	Report
<b>Date</b>	14/10/2025	<b>Version</b>	1.0

The project has also improved model calibration and validation by leveraging long-term datasets such as MEDITS trawl surveys, fisheries-dependent data, and observations of biomass, egg production, and juvenile distributions. Parameter estimation methods and ensemble modelling approaches, including machine learning, have further increased model skill and reliability.

From a functional perspective, NECCTON has broadened the scope of models to include small pelagic fishes, demersal fishes, invertebrates, and marine mammals across diverse regions such as the Mediterranean, Black Sea, Arctic Ocean, the Azores region and Bay of Biscay. These developments have produced outputs ranging from biomass distribution maps to decision-support tools for spatial management of tuna and small pelagic fisheries.

Taken together, NECCTON has advanced the field towards fully integrated, spatially explicit, and management-relevant ecosystem models. By embedding ecological realism (through trophic coupling, benthic-pelagic interactions, and migration), environmental variability (climate drivers, river inputs, zooplankton corrections), and anthropogenic pressures (fishing scenarios, spatial effort distribution), the project provides a new generation of tools capable of providing management relevant HTL products, in the frame of Copernicus Marine Service.

## 4.2 Summary of pros and cons

This report provides an overview of model concepts and performances to systematically guide the use of the proposed new HTL products (see D7.1). It also aims to highlight the strengths and weaknesses of the different model approaches and the respective products to allow contextualizing of the latter regarding the user needs.

The models discussed in this report are grouped into three main categories (Table 1): ecosystem biomass models (EcoBM), species distribution models (SpDM), and species population models (SpPM). All three types are useful for addressing ecosystem questions related to management, spatial planning, long-term scenarios, and short-term forecasting, however on different levels of aggregation along the dimensions of biology (individuals, populations, communities), time and space. Questions may also arise from users about the scalability of different models across species and regions, the types of data required for model setup and validation, computational demands, and the extent to which model outputs are reliable for short-term forecasting versus long-term scenario analysis. This report addresses these questions in detail, and readers are encouraged to consult the individual sections dedicated to each model category for specific explanations and guidance. A synthesis of the pros and cons sections of the different modelling approaches is provided in Table 18 for convenience.

<b>Project</b>	NECCTON No 101081273	<b>Deliverable</b>	D7.2
<b>Dissemination</b>	Public	<b>Nature</b>	Report
<b>Date</b>	14/10/2025	<b>Version</b>	1.0

Table 18. Pros and cons of the NECCTON higher-trophic-level models

<b>Model</b>	<b>Pros</b>	<b>Cons</b>
<b>EcoBM</b>	Fast runtime; Fortran base allows FABM coupling; R and Shiny frontend easy for ecologists; Simulates entire fish community; Mass-balanced, no artificial production; Globally valid parameterization for flexible applications	Cannot simulate specific species; No horizontal movement/migration; Current offline coupling means no feedback to LTL model; Same parameters everywhere limit regional precision
<b>1 FEISTY</b>		
<b>2 Ecospace</b>	Builds on Ecopath/Ecosim calibration; Facilitates ecosystem modelling from phytoplankton to fish; Flexible biological resolution; Graphical user interface with large community; Produces spatial outputs useful for managers	Requires large amount of input data; Reduced flexibility when modifying data input; Calibration is difficult; Relies on mass-balance assumptions; Full spatio-temporal features only in Pro version
<b>3 EcoOcean</b>	Explicit interactions within of food web, species movement, climate and fishing; Useful for broad-scale cumulative impact studies; Spatial validation tools for calibration	Too coarse for local case studies; Unsuitable at fine scales; Downscaling challenges in coastal areas
<b>4 MIZER-ERSEM</b>	Two-way coupling includes top-down/bottom-up feedback; Represents whole ecosystem from photons to fisheries; Covers whole fish community. MIZER can be easily be coupled to other FABM-BGC models	No horizontal migration; Cannot provide species-level insights; Recruitment tied only to planktonic size spectrum; Cannot calculate MSY
<b>5 SEAPODYM-LMTL</b>	Links LTL drivers to mid-trophic prey; Represents diel vertical migration (DVM) groups; Physics-aware transport; Robust parameter optimization; Operational global gridded outputs	Biological simplifications (few groups, layers); Large-scale assumptions; Sensitive to forcing accuracy; Acoustic calibration biases; Limited coastal fidelity
<b>6 ECOSMO E2E</b>	Two-way coupling with FABM-BGC models (ECOSMO, ERSEM, ERGOM); Modular, Fortran/ based; Migration scheme included; Simple parameterization; Works regionally and globally	biological simplification (few functional groups); Juveniles/adults may split between groups; Hard to compare with species-level data
<b>7 Small Pelagic Fish Model (SPF-ERSEM)</b>	Two-way coupled (providing feedback to the ecosystem) to a well-established, operational and thoroughly validated ecological model. Species-specific (anchovy, sardine); Can also be upgraded to include more species; Captures bioenergetics & population dynamics; Customizable for regional peculiarities	Demanding calibration; Heavy and slow, memory-intensive; Long-term simulations costly
<b>SpDM 8 SS-DBEM</b>	Uses theoretical/empirical data; Avoids complexity of explicit species interactions; Size-based processes capture trophic patterns	Assumes equilibrium distribution; Ignores phenotypic/evolutionary adaptation; Simplifies trophic interactions; No transient dynamics



<b>Project</b>	NECCON No 101081273	<b>Deliverable</b>	D7.2
<b>Dissemination</b>	Public	<b>Nature</b>	Report
<b>Date</b>	14/10/2025	<b>Version</b>	1.0

<b>Model</b>	<b>Pros</b>	<b>Cons</b>
<b>9 ESD-MED</b>	Robust distribution using ensemble of approaches; Represents biomass from survey data	Ensemble may retain poor models; Trawl survey data only yearly → poor intra-annual resolution; Biomass indices not absolute biomass
<b>10 NAWH-cetaceans</b>	Predicts occurrence probability of small delphinids; Replicable to other cetaceans/regions; Captures seasonal and latitudinal patterns	Limited to May–August; High interannual variability; No independent validation dataset available No independent sightings dataset with associated effort estimates was available for validation.
<b>SpPM</b>	Species-specific population dynamics; Coupled to hydrodynamics; Detailed life-stage representation (esp. early stages);	Computationally heavy in 3D; Calibration demanding (time and data); Super-individual approach reduces realism; No explicit vertical behavior for adult fish; No GUI; No explicit predation mortality; Limited interannual variability
<b>11 FOIL-DEB</b>	Fine time step for advection/diffusion; Species-specific population dynamics; Flexible modules; Fortran code facilitates coupling	
<b>12 DEB-IBM Anchovy (Black Sea)</b>	Synthesizes diverse modelling approaches; Captures individual variability; Suitable for movement ecology; Mechanistic representation of growth, mortality, reproduction; Good for climate change/extremes	Computationally demanding (R implementation); Complex calibration/validation; Coupling with LTL models challenging; Needs detailed data, often unavailable; Validation and uncertainty quantification difficult
<b>13 OSMOSE</b>	Straightforward forcing by LTL models; Bioenergetics and environmental drivers included; Size-based opportunistic predation leading to flexible trophic structure; Species-based, parameterized from observations; High flexibility in number of species considered; Useful for fisheries management	Two-ways coupling possible but with code development of the LTL model; Stochasticity of the model requires replicates; Recent developments (e.g. evolutionary dynamics, interannual variability) with limited feedback on these modules simulations still developing; PRequires parameter calibration can be difficult; Some parameters lack estimates; and tTime-consuming calibration,
<b>14 SEAPODYM-Tuna</b>	Generic framework SEAPODYM adapted to tuna life cycle. Simulates detailed spatial population dynamics and fisheries; Movements driven by environmental cues; Integrates environmental factors directly; Optimization method robust; Outputs distinguish climate vs fishing impacts; Supports spatial planning/management	Focused on target species, not entire ecosystem; Strong dependence on forcing quality; Computationally intensive; Small user base
<b>15 SEAPODYM-Anchovy</b>	Generic framework SEAPODYM adaptable to anchovy life cyclesmall pelagics; Allows maximum likelihood estimation of population/fisheries parameters; Can use higher-resolution fishing data	Needs high-quality forcings in coastal zones; Model is mMissing benthic interactions; Forcings and resolution critical
<b>16 SEAPODYM-Mackerel</b>	Generic framework SEAPODYM adapted to mackerel life cycle. Models recent	Not fully calibrated; Requires further validation

<b>Project</b>	NECCTON No 101081273	<b>Deliverable</b>	D7.2
<b>Dissemination</b>	Public	<b>Nature</b>	Report
<b>Date</b>	14/10/2025	<b>Version</b>	1.0

<b>Model</b>	<b>Pros</b>	<b>Cons</b>
	spatial shifts in distribution; Supports ensemble modelling efforts	

Across the sixteen models in Table 18, several **strengths** emerge consistently (Table 18). Many of the approaches are designed to represent **the marine ecosystem as whole**, often spanning from primary production through to fish and, in some cases, higher predators. This capacity to capture the broader food web, seen for example in FEISTY, EcoSpace, EcoOcean, MIZER, and ECOSMO E2E, makes them well suited to studying large-scale dynamics and trophic interactions. A subset of models goes further by implementing **two-way coupling**, meaning they account not only for bottom-up effects of food availability on fish but also for top-down feedback from fish onto lower trophic levels. This is a notable feature of (1) ECOSMO E2E, which, through FABM, has been coupled to several biogeochemical models (namely, ERSEM, ERGOM and ECOSMO); (2) MIZER-ERSEM, (3) SPF-ERSEM.

**Flexibility** is another recurring advantage. Many models, particularly the SEAPODYM family, FEISTY, and DEB-based frameworks, are designed with generic structures or parameterizations that make them transferable across regions, species, and scenarios. This adaptability allows them to be applied both in climate-change studies and in diverse regional contexts. At the same time, certain models stand out for their ability to capture biological realism at the level of **individual species or life stages**. The FOIL-DEB, the DEB-IBM, OSMOSE and SEAPODYM include detailed representations of early life stages, individual variability, or movement behaviours, and focus on selected ecologically and economically important stocks (including tuna, mackerel and anchovy)

Despite their strengths, the models also share several **limitations** (Table 18). A frequent drawback is the **lacking representation of species-specific dynamics**. Models based on functional groups or size spectra, such as FEISTY, Mizer, ECOSMO E2E, and SS-DBEM, inevitably lose resolution at the species level, limiting their applicability for fisheries management that requires stock-specific insights. Even those focused on particular species, such as SEAPODYM applications or FOIL-DEB, inevitably **simplify** certain ecological processes or interactions of the species, with implications for management and operational applications

Another recurring issue is the **demand for calibration and data**. Ecospace, EcoOcean, OSMOSE, FOIL-DEB, and DEB-IBM in particular require large datasets covering diet, catch, distribution, or biological traits, and the calibration of these parameters is often time-consuming, uncertain, or constrained by data availability. Where models are heavily parameterized, calibration may also face **identifiability** problems.

**Computational burden** is also a common theme, especially for two-way coupled models (SPF, MIZER, E2E), as well as individual-based and DEB approaches such as the FOIL-DEB, and DEB-IBM Anchovy, which can be very heavy to run at realistic scales. Even OSMOSE and SEAPODYM, though conceptually simpler, rely on optimization methods that are computationally intensive.

<b>Project</b>	NECCTON No 101081273	<b>Deliverable</b>	D7.2
<b>Dissemination</b>	Public	<b>Nature</b>	Report
<b>Date</b>	14/10/2025	<b>Version</b>	1.0

A further limitation lies in **simplifications and assumptions**, which is intrinsic in modelling, but fundamental in some approaches. Ecosystem biomass models, in particular, **group species** into broad categories that can mask ecological diversity, while **equilibrium assumptions** or the exclusion of evolutionary and adaptive processes, as seen in SS-DBEM and ESD-MED, may limit realism under changing conditions. **Absent migration and oversimplified behavioural processes** are also limiting factors, as for example in FEISTY, Mizer, and FOIL-DEB.

Finally, all models depend strongly on the **quality of their environmental forcings**. This is highlighted in models that include quantitative methods to estimate their parameters. The SEAPODYM family and the DEB-IBM Anchovy model in particular are highly sensitive to physical and biogeochemical drivers, meaning that their reliability is only as strong as the input data available. In practice, this dependence can make them less robust in poorly observed regions or under scenarios where forcing data are uncertain.

<b>Project</b>	NECCTON No 101081273	<b>Start / Duration</b>	2023-2026
<b>Dissemination</b>	Public	<b>Nature</b>	Report
<b>Date</b>	14/10/2025	<b>Version</b>	1.0

### 4.3 Model choice and user needs

Choosing the right model depends on scientific use needs in focus, while considering their pros and cons. Below are a few key points to consider when choosing a model or interpreting the hindcast simulation from the NECCTON project.

SpPM models are most appropriate when the aim is to study a specific species and its population dynamics. These models simulate life-cycle processes such as growth, reproduction, mortality, and early-stage connectivity under environmental forcing from physics and food availability from NPZD biogeochemistry models. For example, FOIL-DEB, DEB-IBM, and the SPF-HCMR capture Lagrangian transport, while SEAPODYM uses a Eulerian framework and represents horizontal migration. When interactions between species and size-based predation are important, multi-species individual-based models can be applied: OSMOSE for instance incorporates opportunistic, size-based predation.

SpDM models are designed to map habitat suitability and predict species ranges using environmental parameters, biogeochemical data, fishing pressure, or species sightings. These models rely on statistical modelling and can also be forced with future scenarios, making them useful for projecting species distributions under changing conditions. ESD-MED is well suited for demersal and pelagic fish, SS-DBEM can address multiple fish species simultaneously, and NAWH-Cetaceans focuses on marine mammals.

EcoBM models with one-way coupling are more suitable for studying functional group responses and bottom-up control within food webs. The FEISTY model, for example, uses globally valid parameters that can be adapted to different regions with minimal tuning, while EcoSpace and EcoOcean include intuitive graphical user interfaces. Where more complex dynamics are important at functional-group level, EcoBM models with two-way coupling can capture top-down feedback between fish and lower trophic levels as well as benthic-pelagic interactions. ECOSMO-E2E and ERSEM-MIZER are examples of this category, with functional fish groups that feed on both plankton and benthic fauna.

## 5. Concluding remarks

This report provides a complete standardised documentation of the state-of-the-art HTL models developed in WP7 and their coupling with LTL models used in the Copernicus Marine Service. Regional applications, for the Adriatic Sea, Bay of Biscay, Northwest European Shelf, North Sea, Baltic Sea, Arctic Ocean, and Mediterranean Sea, are presented to evaluate the performance of these models. Collectively, these applications cover the entire European seas, demonstrating the broad scope and applicability of the model developments in WP7. Overall, the report offers a comprehensive reference for understanding and applying HTL models within the Copernicus Marine Service framework.



<b>Project</b>	NECCTON No 101081273	<b>Deliverable</b>	D7.2
<b>Dissemination</b>	Public	<b>Nature</b>	Report
<b>Date</b>	14/10/2025	<b>Version</b>	1.0

## 6. References

- Acuña, J. L., López-Urrutia, Á., & Colin, S. (2011). Faking giants: The evolution of high prey clearance rates in jellyfishes. *Science*, 333(6049), 1627–1629. <https://doi.org/10.1126/science.1205134>
- Ahrens, R.N.M., Walters, C.J., Christensen, V., 2012. Foraging arena theory. *Fish and Fisheries* 13, 41–59. <https://doi.org/10.1111/j.1467-2979.2011.00432.x>
- Akkuş G. The Effects of The Environment on The Black Sea Anchovy-Signals on The Growth. In: Middle East Technical University, 2023
- Akkuş G., Gücü A.C. First maturity size of the Black Sea anchovy and its implications on the age-based stock assessment models. 2023.
- Albernhe, Sarah & Gorgues, Thomas & Lehodey, Patrick & Menkes, Christophe & Titaud, Olivier & Giclais, S. & Conchon, Anna. (2024). Global characterization of modelled micronekton in biophysically defined provinces. *Progress in Oceanography*. 229. 103370. 10.1016/j.pocean.2024.103370.
- Andersen, K. H., Berge, T., Gonçalves, R. J., Hartvig, M., Heuschele, J., Hylander, S., Jacobsen, N. S., Lindemann, C., Martens, E. A., Neuheimer, A. B., Olsson, K., Palacz, A., Prowe, A. E. F., Sainmont, J., Traving, S. J., Visser, A. W., Wadhwa, N., & Kiorboe, T. (2016). Characteristic Sizes of Life in the Oceans, from Bacteria to Whales. *Annual Review of Marine Science*, 8. <https://doi.org/10.1146/annurev-marine-122414-034144>
- Anderson, S.C., Ward, E.J., English, P.A. and Barnett, L.A., 2022. sdmTMB: an R package for fast, flexible, and user-friendly generalized linear mixed effects models with spatial and spatiotemporal random fields. *BioRxiv*, pp.2022-03.
- Anonymous. 2017. MEDITS Handbook, Version n. 9. MEDITS Working Group, 106 pp. <http://www.sibm.it/MEDITS%202011/principaledownload.htm>
- Aumont, O., Éthé, C., Tagliabue, A., Bopp, L., Gehlen, M., 2015. PISCES-v2: an ocean biogeochemical model for carbon and ecosystem studies. *Geoscientific Model Development Discussions* 8 (2), 1375–1509.
- Baeck, T. and Schwefel, H.-P. 1993. An overview of evolutionary algorithms for parameter optimization. *Evol. Comput.* 1, 1–23, <http://dx.doi.org/10.1162/evco.1993.1.1.1>.
- Barbin, L., Lebourges-Dhaussy, A., Allain, V., Receveur, A., Lehodey, P., Habasque, J., Menkes, C., 2024. Comparative analysis of day and night micronekton abundance estimates in west Pacific between acoustic and trawl surveys. *Deep Sea Research Part I: Oceanographic Research Papers* 204, 104221.
- Baretta, J., Ebenhö, W. and Ruardij, P., 1995. The European regional seas ecosystem model, a complex marine ecosystem model. *Netherlands Journal of Sea Research*, 33 (3-4), 233-246.
- Beddington, J. R. 1975. Mutual Interference Between Parasites or Predators and its Effect on Searching Efficiency. *The Journal of Animal Ecology* 44.1, p. 331. doi: 10.2307/3866.
- Behrenfeld, M.J., Falkowski, P.G., 1997. A consumer's guide to phytoplankton primary productivity models. *Limnology and Oceanography* 42 (7), 1479–1491.
- Bell J.D., Senina I., Adams T., Aumont O., Calmettes B., Clark S., Dessert M., Hampton J., Hanich Q., Harden-Davies H., Gehlen M., Gorgues T., Holmes G., Lehodey P., Lengaigne M., Mansfield B., Menkes C., Nicol S., Pasisi

<b>Project</b>	NECCON No 101081273	<b>Deliverable</b>	D7.2
<b>Dissemination</b>	Public	<b>Nature</b>	Report
<b>Date</b>	14/10/2025	<b>Version</b>	1.0

C., Pilling G., Ota Y., Reid C., Ronneberg E., Sen Gupta A., Seto K., Smith N., Tai S., Tsamenyi M., Williams P. (2021). Pathways to sustaining tuna-dependent Pacific Island economies during climate change. *Nature Sustainability* <https://doi.org/10.1038/s41893-021-00745-z>

Benoit-Bird, K.J., 2009. The effects of scattering-layer composition, animal size, and numerical density on the frequency response of volume backscatter. *ICES Journal of Marine Science* 66 (3), 582–593.

Bergeron J.P., (2013). Interannual fluctuations in spring pelagic ecosystem productivity in the Bay of Biscay (northeast Atlantic) measured by mesozooplankton aspartate transcarbamylase activity and relationships with anchovy population dynamics. *Fisheries Research*,143: 184-190. <https://doi.org/10.1016/j.fishres.2013.02.006>

Bergeron, J.P., Delmas, D. & Koueta, N. (2010). Do river discharge rates drive the overall functioning of the pelagic ecosystem over the continental shelf of the Bay of Biscay (NE Atlantic)? A comparison of two contrasting years with special reference to anchovy (*Engraulis encrasicolus* L.) nutritional state. *J Oceanogr* 66, 621–631. <https://doi.org/10.1007/s10872-010-0051-7>

Bianchi, D., C. Stock, E. D. Galbraith, and J. L. Sarmiento (2013), Diel vertical migration: Ecological controls and impacts on the biological pump in a one-dimensional ocean model, *Global Biogeochem. Cycles*, 27, 478–491, doi:10.1002/gbc.20031.

Blanchard, J. L., Andersen, K. H., Scott, F., Hintzen, N. T., Piet, G., & Jennings, S. (2014). Evaluating targets and trade-offs among fisheries and conservation objectives using a multispecies size spectrum model. *Journal of Applied Ecology*, 51(3), 612–622. <https://doi.org/10.1111/1365-2664.12238>

Blanchard, J. L., Jennings, S., Holmes, R., Harle, J., Merino, G., Allen, J. I., Holt, J., Dulvy, N. K., & Barange, M. (2012). Potential consequences of climate change for primary production and fish production in large marine ecosystems. *Philosophical Transactions of the Royal Society B: Biological Sciences*, 367(1605), 2979–2989. <https://doi.org/10.1098/rstb.2012.0231>

Blanchard, J. L., Jennings, S., Law, R., Castle, M. D., McCloghrie, P., Rochet, M. J., & Benoît, E. (2009). How does abundance scale with body size in coupled size-structured food webs? *Journal of Animal Ecology*, 78(1), 270–280. <https://doi.org/10.1111/j.1365-2656.2008.01466.x>

Blumberg, A., Mellor, G., 1983. Diagnostic and prognostic numerical circulation studies of the South Atlantic Bight. *Journal of Geophysical Research: Oceans*, 88 (C8), 4579-4592.

Boot, A.A., Steenbeek, J., Coll, M., Von Der Heydt, A.S., Dijkstra, H.A., 2025. Global Marine Ecosystem Response to a Strong AMOC Weakening Under Low and High Future Emission Scenarios. *Earth's Future* 13, e2024EF004741. <https://doi.org/10.1029/2024EF004741>

Borja A., Fontan A., Saenz J., Valencia V. (2008). Climate, oceanography, and recruitment: the case of the Bay of Biscay anchovy (*Engraulis encrasicolus*), *Fish. Oceanogr.* 17:6, 477–493.

Boudreau, P. R., & Dickie, L. M. (1992). Biomass Spectra of Aquatic Ecosystems in Relation to Fisheries Yields. *Can. J. Fish. Aquat. Sci.* 49, 1528–1538.

Bousquet F., Le Page C. Multi-agent simulations and ecosystem management: a review. *Ecological Modelling* 2004; 176: 313-332. <https://doi.org/10.1016/j.ecolmodel.2004.01.011>

<b>Project</b>	NECCTON No 101081273	<b>Deliverable</b>	D7.2
<b>Dissemination</b>	Public	<b>Nature</b>	Report
<b>Date</b>	14/10/2025	<b>Version</b>	1.0

Boyra G., Martínez U., Cotano U., Santos M., Irigoien X., Uriarte A., (2013). Acoustic surveys for juvenile anchovy in the Bay of Biscay: abundance estimate as an indicator of the next year's recruitment and spatial distribution patterns, *ICES Journal of Marine Science*, 70 (7): 1354–1368, <https://doi.org/10.1093/icesjms/fst096>

Brey, T., Müller-Wiegmann, C., Zittier, Z.M.C., Hagen, W., 2010. Body Composition in Aquatic Organisms — a Global Data Bank of Relationships Between Mass, Elemental Composition and Energy Content. *Journal of Sea Research* 64, 334–340. <https://doi.org/10.1016/j.seares.2010.05.002>

Brown, J. H., Gillooly, J. F., Allen, A. P., Savage, V. M., & West, G. B. (2004). Toward a metabolic theory of ecology. *Ecology*, 85(7). <https://doi.org/10.1890/03-9000>

Bruggeman, J. (2021). FABM-Mizer (0.8.1). Zenodo. <https://doi.org/10.5281/zenodo.5575152>

Bruggeman, J., & Bolding, K. (2014). A general framework for aquatic biogeochemical models. *Environmental Modelling & Software*, 61, 249–265. <https://doi.org/10.1016/j.envsoft.2014.04.002>

Brunel, T., van Damme, C. J. G., Samson, M., & Dickey-Collas, M. (2018). Quantifying the influence of geography and environment on the northeast Atlantic mackerel spawning distribution. *Fisheries Oceanography*, 27(2), 159–173. <https://doi.org/10.1111/fog.12242>

Bueno-Pardo, J. Petitgas, P., Kay, S. and Huret, M. 2020. Integration of bioenergetics in an individual-based model to hindcast anchovy dynamics in the Bay of Biscay. *ICES Journal of Marine Science*, 77(2):655–667.

Butenschön, M., Clark, J., Aldridge, J. N., Allen, J. I., Artioli, Y., Blackford, J., ... & Torres, R. (2016). ERSEM 15.06: a generic model for marine biogeochemistry and the ecosystem dynamics of the lower trophic levels. *Geoscientific Model Development*, 9(4), 1293-1339.

Carlucci, R., Capezzuto, F., Cipriano, G., D’Onghia, G., Fanizza, C., Libralato, S., et al., 2020. Assessment of cetacean-fishery interactions in the marine food web of the Gulf of Taranto (Northern Ionian Sea, Central Mediterranean Sea). *Rev. Fish Biol. Fish.* 10.1007/s11160-020-09623-x

Catucci, E., Panzeri, D., Libralato, S., Cossarini, G., Garofalo, G., Maina, I., Kavadas, S., Quattrocchi, F., Cipriano, G., Carlucci, R. and Vitale, S., 2025. Modeling the spatial distribution and abundance of deep-water red shrimps in the Mediterranean Sea: a machine learning approach. *Fisheries Research*, 281, p.107257.

Christensen, V., Coll, M., Buszowski, J., Cheung, W.W.L., Frölicher, T., Steenbeek, J., Stock, C.A., Watson, R.A. and Walters, C.J. (2015), Modelling life and fisheries in the global ocean. *Global Ecology and Biogeography*, 24: 507-517. <https://doi.org/10.1111/geb.12281>

Christensen, V., Coll, M., Steenbeek, J., et al., 2014. Representing variable habitat quality in a spatial food web model. *Ecosystems* 17, 1397–1412. <https://doi.org/10.1007/s10021-014-9803-3>

Christensen, V., Pauly, D., 1993. Trophic Models of Aquatic Ecosystems. WorldFish.

Christensen, V., Walters, C.J., Pauly, D., Forrest, R., 2008. Ecopath with Ecosim version 6: User guide. Vancouver: Fisheries Centre, University of British Columbia

Clark, J., Samuelson, A., Yumruktepe, Ç., Albernhe, S., Lindenthal, A., Hahn, J., Belharet, M., Millington, R., Bonino, G., Choblet, M., Powley, H., Galli, G., Cossarini, G., Lazzari, P., Alvarez, E., Macé, L., & Skakala, J. (2025). NECCTON Integrated pelagic model developments (D5.2). Zenodo.



<b>Project</b>	NECCON No 101081273	<b>Deliverable</b>	D7.2
<b>Dissemination</b>	Public	<b>Nature</b>	Report
<b>Date</b>	14/10/2025	<b>Version</b>	1.0

Clarke, A., & Johnston, N. M. (1999). Scaling of metabolic rate with body mass and temperature in teleost fish. *Journal of Animal Ecology*, 68, 893-905. doi:<https://doi.org/10.1046/j.1365-2656.1999.00337.x>

Coll M, Steenbeek J, Pennino MG, Buszowski J, Kaschner K, Lotze HK, Rousseau Y, Tittensor DP, Walters C, Watson RA and Christensen V (2020) Advancing Global Ecological Modeling Capabilities to Simulate Future Trajectories of Change in Marine Ecosystems. *Front. Mar. Sci.* 7:567877. doi: 10.3389/fmars.2020.567877

Colléter, M., Valls, A., Guitton, J., et al., 2015. Global overview of the applications of the Ecopath with Ecosim modeling approach using the EcoBase models repository. *Ecological Modelling* 302, 42–53. <https://doi.org/10.1016/j.ecolmodel.2015.01.025> .

Conchon, A., 2016. Modélisation du zooplancton et du micronecton marins, Université de La Rochelle (2016), Doctoral dissertation.

Copernicus Marine Service (CMEMS) - <http://marine.copernicus.eu/> accessed on September, 9th 2024.

Copernicus Marine Service (CMEMS) - MEDSEA\_MULTIYEAR\_PHY\_006\_004. [https://data.marine.copernicus.eu/product/MEDSEA\\_MULTIYEAR\\_PHY\\_006\\_004/description](https://data.marine.copernicus.eu/product/MEDSEA_MULTIYEAR_PHY_006_004/description) . accessed on September, 9th 2024

Copernicus Marine Service (CMEMS) - MEDSEA\_MULTIYEAR\_PHY\_006\_008. [https://data.marine.copernicus.eu/product/MEDSEA\\_MULTIYEAR\\_BGC\\_006\\_008/description](https://data.marine.copernicus.eu/product/MEDSEA_MULTIYEAR_BGC_006_008/description). accessed on September, 9th 2024.

da Silva, M.I.P., Tobeña, M., Machete, M., Silva, M.A. and Pérez-Jorge, S., 2025. Water temperature drives the segregation between common and Atlantic spotted dolphins in Azorean waters. *Global Ecology and Conservation*, 2025, e03769. <https://doi.org/10.1016/j.gecco.2025.e03769>

Daewel, U., Hjøllø, S.S., Huret, M., Ji, R., Maar, M., Niiranen, S., Travers-Trolet, M., Peck, M.A., van de Wolfshaar, K.E., 2014. Predation control of zooplankton dynamics: a review of observations and models. *ICES Journal of Marine Science* 71, 254–271. <https://doi.org/10.1093/icesjms/fst125>

Daewel, U., Samuelsen, A., Schrum, C., Vijayakumaran, V., Yumruktepe, C., 2025 (in preparation). Zooplankton dynamics as a key driver for large scale-fish migration pattern: A modelling study in the North Atlantic/Arctic Ocean.

Daewel, U., Schrum, C., & Macdonald, J. I. (2019). Towards end-to-end (E2E) modelling in a consistent NPZD-F modelling framework (ECOSMO E2E\_v1.0): application to the North Sea and Baltic Sea. *Geosci. Model Dev.*, 12(5), 1765-1789. doi:10.5194/gmd-12-1765-2019

David, V., Joachim, S., Tebby, C., Porcher, J.-M., and Beaudouin, R. (2019). Modelling population dynamics in mesocosms using an individual-based model coupled to a bioenergetics model. *Ecological Modelling* 398, pp. 55–66.

de Mutsert, Kim, Coll, Marta, Steenbeek, Jeroen, Ainsworth, Cameron, Buszowski, Joe, Chagaris, David, Christensen, Villy, Heymans, Sheila J.J., Lewis, Kristy A., Libralato, Simone, Oldford, Greig, Piroddi, Chiara, Romagnoni, Giovanni, Serpetti, Natalia, Spence, Michael A. and Walters, Carl (2024) Advances in spatial\_temporal coastal and marine ecosystem modeling using Ecospace. In: Baird, Daniel and Elliott, Michael (eds.) *Treatise on Estuarine and Coastal Science*, 2nd Edition, vol. 5, pp. 122–169. Oxford: Elsevier.

<b>Project</b>	NECCTON No 101081273	<b>Deliverable</b>	D7.2
<b>Dissemination</b>	Public	<b>Nature</b>	Report
<b>Date</b>	14/10/2025	<b>Version</b>	1.0

DeAngelis, D. L., Goldstein, R. A., and O'Neill, R. V. 1975. A Model for Tropic Interaction. *Ecology*. 56.4, pp. 881–892. doi: 10.2307/1936298.

Delpech, A., Conchon, A., Titaud, O., and Lehodey, P. 2020. Influence of oceanic conditions in the energy transfer efficiency estimation of a micronekton model, *Biogeosciences*, 17, 833–850, <https://doi.org/10.5194/bg-17-833-2020>

Denderen, P. Daniël van, Colleen M. Petrik, Charles A. Stock, and Ken H. Andersen. 2021. “Emergent Global Biogeography of Marine Fish Food Webs.” *Global Ecology and Biogeography* 30 (9): 1822–34.

Diaz, J. E. (2013). Schooling dynamics of summertime migrating northeast atlantic mackerel (*scomber scombrus*) in the norwegian sea using multibeam sonar. Master 2 thesis.

Dolan, T.E., Patrick, W.S., Link, J.S., 2016. Delineating the continuum of marine ecosystem-based management: a US fisheries reference point perspective. *ICES Journal of Marine Science* 73, 1042–1050. <https://doi.org/10.1093/icesjms/fsv242>.

Doray, M., Duhamel, E., Huret, M., Petitgas, P., Masse J. 2000. PELGAS, <https://doi.org/10.18142/18>

Doray, M., Petitgas, P., Romagnan, J-B., Huret, M., Duhamel, E., Dupuy, C., Spitz, J., Authier, M., Sanchez, F., Berger, L., Doremus, G., Bourriau, P., Grellier, P., Masse, J. 2018. The PELGAS survey: ship-based integrated monitoring of the Bay of Biscay pelagic ecosystem. *Progress In Oceanography*. 166. 15-29. <https://doi.org/10.1016/j.pocean.2017.09.015>

Dos Santos Schmidt, T. C., Slotte, A., Olafsdottir, A. H., Nøttestad, L., Jansen, T., Jacobsen, J. A., Bjarnason, S., Lusseau, S. M., Ono, K., Hølleland, S., Thorsen, A., Sandø, A. B., & Kjesbu, O. S. (2024). Poleward spawning of Atlantic mackerel (*Scomber scombrus*) is facilitated by ocean warming but triggered by energetic constraints. *ICES Journal of Marine Science*, 81(3), 600–615. <https://doi.org/10.1093/icesjms/fsad098>

Dragon A-C., Senina, Hintzen N.T., Lehodey P., (2018). Modelling South Pacific Jack Mackerel spatial population dynamics and fisheries. *Fisheries Oceanography*, 27 (2): 97-113, <http://onlinelibrary.wiley.com/doi/10.1111/fog.12234/full>

Dragon AC, Senina I., Conchon A., Titaud O., Arrizabalaga H. and Lehodey P. (2015). An ecosystem-driven model for spatial dynamics and stock assessment of North Atlantic albacore. *Canadian Journal of Fisheries and Aquatic Sciences*, 72(6): 864-878, <https://doi.org/10.1139/cjfas-2014-0338>

Dunic, J. C., & Baum, J. K. (2017). Size structuring and allometric scaling relationships in coral reef fishes. *Journal of Animal Ecology*, 86(3). <https://doi.org/10.1111/1365-2656.12637>

Elith, J., Leathwick, J. R., & Hastie, T. (2008). A working guide to boosted regression trees. *Journal of Animal Ecology*, 77(4), 802–813. <https://doi.org/10.1111/j.1365-2656.2008.01390.x>

Erauskin-Extramiana M., Alvarez P., Arrizabalaga H., Ibaibarriaga L., Uriarte A., Cotano U., Santos M., Ferrer L., Cabré A., Irigoien X., Chust G. (2019). Historical trends and future distribution of anchovy spawning in the Bay of Biscay. *Deep Sea Research Part II*, 159: 169-182. <https://doi.org/10.1016/j.dsr2.2018.07.007>

FAO. 2023. *The State of Mediterranean and Black Sea Fisheries 2023 – Special edition*. General Fisheries Commission for the Mediterranean. Rome.

<b>Project</b>	NECCTON No 101081273	<b>Deliverable</b>	D7.2
<b>Dissemination</b>	Public	<b>Nature</b>	Report
<b>Date</b>	14/10/2025	<b>Version</b>	1.0

Fao.org (no date) Report of the Working Group on Stock Assessment of Small Pelagic Species (WGSASP) | General Fisheries Commission for the Mediterranean (GFCM) | Food and Agriculture Organization of the United Nations. Available at: <https://www.fao.org/gfcm/technical-meetings/detail/en/c/1634928/> (Accessed: 11 July 2025).

Finenko Z, Churilova TY, Lee R. Dynamics of the vertical distributions of chlorophyll and phytoplankton biomass in the Black Sea. *OCEANOLOGY C/C OF OKEANOLOGIJA* 2005; 45: S112.

Gatti P, Petitgas P, Huret M. Comparing biological traits of anchovy and sardine in the Bay of Biscay: A modelling approach with the Dynamic Energy Budget. *Ecological Modelling* 2017; 348: 93-109. <https://doi.org/https://doi.org/10.1016/j.ecolmodel.2016.12.018>

Gatti, P., Petitgas, P. and Huret M. 2017. Comparing biological traits of anchovy and sardine in the Bay of Biscay: a modelling approach with the dynamic energy budget. *Ecological Modelling*, 348:93–109.

GFCM 2030 Strategy for Sustainable Fisheries and aquaculture in the Mediterranean and the Black Sea [Preprint]. doi:10.4060/cb7562en.

GFCM. Stock Assessment Form Small Pelagics (Reference Year: 2021, Reporting Year: 2023). In, 2023

GFCM. Stock Assessment Form Small Pelagics (Reference Year: 2023, Reporting Year: 2024). In, 2024

Gibin, Maurizio; Zanzi, Antonella; Hekim, Zeynep; Adamowicz, Maciej; Kavsars, Maksims (2024): Fisheries landings & effort: data by c-square. European Commission, Joint Research Centre (JRC) [Dataset] PID: <http://data.europa.eu/89h/00ae6659-ddde-4314-a9da-717bb2e82582>

Gillooly, J. F., Brown, J. H., West, G. B., Savage, V. M., & Charnov, E. L. (2001). Effects of Size and Temperature on Metabolic Rate. *Science*, 293, 2248-2251. doi:doi: 10.1126/science.1061967

Gkanasos, A. et al. (2021) A three dimensional, full life cycle, Anchovy and Sardine model for the North Aegean Sea (Eastern Mediterranean): Validation, sensitivity and climatic scenario simulations, *Mediterranean Marine Science*, 22(3), p. 653. doi:10.12681/mms.27407.

Gregg, W.W., Casey, N.W., 2007. Sampling biases in MODIS and SeaWiFS ocean chlorophyll data. *Remote Sensing of Environment* 111 (1), 25–35.

Grégoire M., Raick C., Soetaert K. Numerical modeling of the central Black Sea ecosystem functioning during the eutrophication phase. *Progress in Oceanography* 2008; 76: 286-333. <https://doi.org/https://doi.org/10.1016/j.pocean.2008.01.002>

Grégoire M., Soetaert K. Carbon, nitrogen, oxygen and sulfide budgets in the Black Sea: A biogeochemical model of the whole water column coupling the oxic and anoxic parts. *Ecological Modelling* 2010; 221: 2287-2301. <https://doi.org/https://doi.org/10.1016/j.ecolmodel.2010.06.007>

Grimm V., Berger U, Bastiansen F., et al. A standard protocol for describing individual-based and agent-based models. *Ecological Modelling* 2006; 198: 115-126. <https://doi.org/https://doi.org/10.1016/j.ecolmodel.2006.04.023>

Gücü A.C, Genç Y., Dağtekin M., et al. On Black Sea anchovy and its fishery. *Reviews in Fisheries Science & Aquaculture* 2017; 25: 230-244.

<b>Project</b>	NECCOTN No 101081273	<b>Deliverable</b>	D7.2
<b>Dissemination</b>	Public	<b>Nature</b>	Report
<b>Date</b>	14/10/2025	<b>Version</b>	1.0

Gucu A.C, Inanmaz Ö.E., Ok M., et al. Recent changes in the spawning grounds of Black Sea anchovy, *Engraulis encrasicolus*. *Fisheries Oceanography* 2016; 25: 67-84. <https://doi.org/https://doi.org/10.1111/fog.12135>

Guisan, A., Edwards, T. C., & Hastie, T. (2002). Generalized linear and generalized additive models in studies of species distributions: setting the scene. *Ecological Modelling*, 157(2–3), 89–100. [https://doi.org/10.1016/S0304-3800\(02\)00204-1](https://doi.org/10.1016/S0304-3800(02)00204-1)

Güraslan C., Fach B.A., Oguz T. Modeling the impact of climate variability on Black Sea anchovy recruitment and production. *Fisheries Oceanography* 2014; 23: 436-457. <https://doi.org/https://doi.org/10.1111/fog.12080>

Guraslan C., Fach B.A., Oguz T. Understanding the Impact of Environmental Variability on Anchovy Overwintering Migration in the Black Sea and its Implications for the Fishing Industry. *Frontiers in Marine Science* 2017; 4. <https://doi.org/10.3389/fmars.2017.00275>

Halpin, P., et al., (2009). OBIS-SEAMAP: the world data center for marine mammal, sea bird and sea turtle distributions. *Oceanography*, 22(2), 104–115.

Hampton J., Lehodey P., Senina I., Nicol S., Scutt Philipps J., Tiamere K., (2022). Limited conservation efficacy of large-scale marine protected areas for Pacific skipjack and bigeye tunas. *Frontiers in Marine Sciences*. 9:1060943. <https://doi.org/10.3389/fmars.2022.1060943>

Handbook of Ecological Parameters and Ecotoxicology, Edited by L.A. Jørgensen, S.E. Jørgensen and S.N. Nielsen, Elsevier, Amsterdam, 2000, First Electronic Edition

Haris, K., Kloser, R.J., Ryan, T.E., Downie, R.A., Keith, G., Nau, A.W., 2021. Sounding out life in the deep using acoustic data from ships of opportunity. *Scientific Data* 8 (1), 23.

Hernandez O., Lehodey P., Senina I., Echevin V., Ayon P., Bertrand A., Gaspar P., (2014). Understanding mechanisms that control fish spawning and larval recruitment: Parameter optimization of an Eulerian model (SEAPODYM-SP) with Peruvian anchovy and sardine eggs and larvae data. *Progress in Oceanography* 123, 105-122. <http://dx.doi.org/10.1016/j.pocean.2014.03.001>

Hersbach, H. et al. (2020) ‘The ERA5 global reanalysis’, *Quarterly Journal of the Royal Meteorological Society*, 146(730), pp. 1999–2049. doi:10.1002/qj.3803.

Heymans, J. J., Coll, M., Link, J. S., Mackinson, S., Steenbeek, J., Walters, C., & Christensen, V. (2016). Best practice in Ecopath with Ecosim food-web models for ecosystem-based management. *Ecological modelling*, 331, 173-184.

Hijmans, R. (2024a). *geosphere: Spherical Trigonometry* (R package version 1.5-20). <https://github.com/rspatial/geosphere>

Holsman, K., Samhouri, J., Cook, G., et al., 2017. An ecosystem-based approach to marine risk assessment. *Ecosystem Health and Sustainability* 3, e01256. <https://doi.org/10.1002/ehs2.1256>

Huret, M., Bourriau P., Gatti P., Dumas F., Petitgas, P. 2016. Size, permeability and buoyancy of anchovy (*Engraulis encrasicolus*) and sardine (*Sardina pilchardus*) eggs in relation to their physical environment in the Bay of Biscay. *Fisheries Oceanography*, 25(6), 582-597. <https://doi.org/10.1111/fog.12174>

<b>Project</b>	NECCTON No 101081273	<b>Deliverable</b>	D7.2
<b>Dissemination</b>	Public	<b>Nature</b>	Report
<b>Date</b>	14/10/2025	<b>Version</b>	1.0

Huret, M., Bourriau, P., Doray, M., Gohin, F. and Petitgas, P. 2018. Survey timing vs. ecosystem scheduling: Degree-days to underpin observed interannual variability in marine ecosystems. *Progress in Oceanography* 166, pp. 30–40. doi : 10.1016/j.pocean.2017.07.007.

Huret, M., Petitgas, P. and Woillez, M. 2010. Dispersal kernels and their drivers captured with a hydrodynamic model and spatial indices: a case study on anchovy (*Engraulis encrasicolus*) early life stages in the Bay of Biscay. *Progress in Oceanography*, 87(1-4):6–17.

Huret, M., Tsiaras, K., Daewel, U., Skogen, M.D., Gatti, P., Petitgas, P. and Somarakis, S. 2019. Variation in life-history traits of European anchovy along a latitudinal gradient: a bioenergetics modelling approach. *Marine Ecology Progress Series*, 617:95–112.

Huse, G., MacKenzie, B. R., Trenkel, V., Doray, M., Nøttestad, L., and Oskarsson, G. 2015a. Spatially explicit estimates of stock sizes, structure and biomass of herring and blue whiting, and catch data of bluefin tuna. *Earth System Science Data*, 7: 35–46.

Ibaibarriaga L., Fernández C., Uriarte A., Roel B.A. (2008). A two-stage biomass dynamic model for Bay of Biscay anchovy: a Bayesian approach, *ICES Journal of Marine Science*, 65 (2): 191–205, <https://doi.org/10.1093/icesjms/fsn002>

ICES (2011). "Report of the Working Group on Anchovy and Sardine (WGANSA)." ICES CM 2011/ACOM:16. Copenhagen, Denmark.

ICES (2021). Working Group on Southern Horse Mackerel, Anchovy and Sardine (WGHANSA). ICES Scientific Reports. Report. <https://doi.org/10.17895/ices.pub.8138>

ICES. (2022). Working Group on Widely Distributed Stocks (WGWIDE). ICES Scientific Reports, 4:73(73), 922 pp. <http://doi.org/10.17895/ices.pub.21088804>

ICES (2024a). Working Group on Southern Horse Mackerel, Anchovy and Sardine (WGHANSA). ICES Scientific Reports. Report. <https://doi.org/10.17895/ices.pub.26003356.v2>

ICES, (2024b) Official Nominal Catches 2006-2022. Version 30-08-2024. Accessed via <http://ices.dk/data/dataset-collections/Pages/Fish-catch-and-stock-assessment.aspx> ICES, Copenhagen.

ICES. (2024c). Mackerel (*Scomber scombrus*) in subareas 1–8 and 14 and division 9.a (the Northeast Atlantic and adjacent waters). In ICES Advice on fishing opportunities, catch, and effort Ecoregions in the Northeast Atlantic and the Arctic Ocean (Issue September). <https://doi.org/10.17895/ices.advice.21856533>

Irigoién X., Fiksen Ø., U. Cotano U., Uriarte A., Alvarez P., H. Arrizabalaga, Boyra G., Santos M., Sagarminaga Y., Otheguy P., Etxebeste E., Zarauz L., Artetxe I., Motos L. (2007). Could Biscay Bay Anchovy recruit through a spatial loophole? *Progress in Oceanography* 74: 132–148

Irigoién, X., T.A. Klevjer, A. Røstad, U. Martinez, G. Boyra, J.L. Acuña, S. Kaartvedt, 2014. Large mesopelagic fishes biomass and trophic efficiency in the open ocean. *Nature Communications*, 5 (1) (2014), p. 3271. DOI: 10.1038/ncomms4271

Iverson, R.L. 1990. Control of marine fish production. *Limnology and Oceanography*, 35 (7) (1990), pp. 1593-1604. <https://doi.org/10.4319/lo.1990.35.7.1593>

<b>Project</b>	NECCTON No 101081273	<b>Deliverable</b>	D7.2
<b>Dissemination</b>	Public	<b>Nature</b>	Report
<b>Date</b>	14/10/2025	<b>Version</b>	1.0

Jansen, T., Kristensen, K., Payne, M., Edwards, M., Schrum, C., & Pitois, S. (2012). Long-term retrospective analysis of mackerel spawning in the North Sea: A new time series and modeling approach to CPR data. *PLoS ONE*, 7(6). <https://doi.org/10.1371/journal.pone.0038758>

Jansen, T., Post, S., Olafsdottir, A. H., Reynisson, P., Óskarsson, G. J., & Arendt, K. E. (2019). Diel vertical feeding behaviour of Atlantic mackerel (*Scomber scombrus*) in the Irminger current. *Fisheries Research*, 214, 25–34. <https://doi.org/10.1016/j.fishres.2019.01.020>

Jordi, A., Wang, D.P., 2012. A parallel implementation of Princeton Ocean model. *Environ. Model. Software* 38, 59–61.

Kalaroni, S., Tsiaras, K., Petihakis, G., Economou-Amilli, A., Triantafyllou, G., 2020. Modelling the mediterranean pelagic ecosystem using the POSEIDON ecological model. Part II: Biological dynamics. *Deep Sea Research Part II: Topical Studies in Oceanography*, 171.

Kaschner, K., Kesner-Reyes, K., Garilao, C., Rius-Barile, J., Rees, T., and Froese, R. (2016). AquaMaps: Predicted Range Maps for Aquatic Species. World Wide Web Electronic Publication. Available online at: [www.aquamaps.org](http://www.aquamaps.org).

Kooijman, S.A.L.M. 2010. Dynamic Energy Budget Theory for Metabolic Organisation. Cambridge University Press.

Korres, G., Hoteit, I., and Triantafyllou, G. (2007). Data assimilation into a Princeton Ocean Model of the Mediterranean Sea using advanced Kalman filters. *J. Mar. Syst.* 65, 84–104. doi: 10.1016/j.jmarsys.2006.09.005

Lantuéjoul, C., 2002. Chap. 8.2. Metropolis Algorithm, in: *Geostatistical Simulation: Models and Algorithms*. pp. 71–73.

Lazzari P., Solidoro C., Salon S., Bolzon G., Spatial variability of phosphate and nitrate in the Mediterranean Sea: A modeling approach, *Deep Sea Research Part I: Oceanographic Research Papers*, 108, 2016, 39-52, ISSN 0967-0637, <https://doi.org/10.1016/j.dsr.2015.12.006>

Lazzari, P., Solidoro, C., Ibello, V., Salon, S., Teruzzi, A., Béranger, K., Colella, S., and Crise, A.: Seasonal and inter-annual variability of plankton chlorophyll and primary production in the Mediterranean Sea: a modelling approach, *Biogeosciences*, 9, 217–233, <https://doi.org/10.5194/bg-9-217-2012>, 2012

Learmonth, J. A., MacLeod, C. D., Santos, M. B., Pierce, G. J., Crick, H. Q. P., & Robinson, R. A. (2006). Potential effects of climate change on marine mammals. In R. N. Gibson, R. J. A. Atkinson, & J. D. M. Gordon (Eds.), *Oceanography and Marine Biology: An Annual Review* (Vol. 44, pp. 431–464). CRC Press. <https://doi.org/10.1201/9781420006391>

Lehodey P., Murtugudde R., Senina I. (2010). Bridging the gap from ocean models to population dynamics of large marine predators: a model of mid-trophic functional groups. *Progress in Oceanography*, 84: 69–84 <https://doi.org/10.1016/j.pocean.2009.09.008>

Lehodey P., Senina I., Calmettes B, Hampton J, Nicol S. (2013). Modelling the impact of climate change on Pacific skipjack tuna population and fisheries. *Climatic Change*, 119 (1): 95-109. <https://doi.org/10.1007/s10584-012-0595-1>

<b>Project</b>	NECCTON No 101081273	<b>Deliverable</b>	D7.2
<b>Dissemination</b>	Public	<b>Nature</b>	Report
<b>Date</b>	14/10/2025	<b>Version</b>	1.0

Lehodey P., Senina I., Murtugudde R. (2008). A Spatial Ecosystem And Populations Dynamics Model (SEAPODYM) - Modelling of tuna and tuna-like populations. *Progress in Oceanography*, 78: 304-318. <https://doi.org/10.1016/j.pocean.2008.06.004>

Lehodey P., Senina I., Nicol S., Bell J., Calmettes B., Forestier R., Gorgues T., Menkes C., Hampton J., Lengaigne M., Sen Gupta A., Williams P. (in press). The implications of climate change for oceanic fisheries in the tropical Pacific Islands region. In Pacific regional climate change vulnerability assessment. SPC book.

Lehodey P., Senina I., Nicol S., Hampton J. (2015). Modelling the impact of climate change on South Pacific albacore tuna. *Deep Sea Research*. 113: 246–259. <https://doi.org/10.1016/j.dsr2.2014.10.028>

Lehodey, P., Conchon, A., Senina, I., Domokos, R., Calmettes, B., Jouanno, J., Hernandez, O., and Kloser, R. (2015) Optimization of a micronekton model with acoustic data. – *ICES Journal of Marine Science*, 72(5): 1399-1412. <https://doi.org/10.1093/icesjms/fsu233>

Lehodey, P., Murtugudde, R., & Senina, I. (2010). Bridging the gap from ocean models to population dynamics of large marine predators: A model of mid-trophic functional groups. *Progress in Oceanography*, 84(1–2), 69–84. <https://doi.org/10.1016/j.pocean.2009.09.008>

Lellouche Jean-Michel, Bourdalle-Badie Romain, Greiner Eric, Garric Gilles, Melet Angelique, Bricaud Clement, Legalloudec Olivier, Hamon Mathieu, Candela Tony, Regnier Charly, Drevillon Marie (2021). The Copernicus global 1/12° oceanic and sea ice reanalysis. <https://doi.org/10.5194/egusphere-egu21-14961>

Leonori, I. et al. (2021) ‘History of hydroacoustic surveys of small pelagic fish species in the European Mediterranean Sea’, *Mediterranean Marine Science*, 22(4), p. 751. doi:10.12681/mms.26001.

Lessin, G., Mudde, Q., Millington, R., Soetaert, K. (2025). (in prep) D6.3 “Report on benthic process model developments”. Report of the Horizon Europe NECCTON project (grant 101081273).

Libralato, S., Coll, M., Tempesta, M., Santojanni, A., Spoto, M., Palomera, I., ... & Solidoro, C. (2010). Food-web traits of protected and exploited areas of the Adriatic Sea. *Biological Conservation*, 143(9), 2182-2194.

Libralato, S., Solidoro, C., 2009. Bridging biogeochemical and food web models for an End-to-End representation of marine ecosystem dynamics: The Venice lagoon case study. *Ecological Modelling* 220, 2960–2971. <https://doi.org/10.1016/j.ecolmodel.2009.08.017>

Link J.S., 2010. Adding rigor to ecological network models by evaluating a set of pre-balance diagnostics: A plea for PREBAL. *Ecological Modelling*, 221, 12, 1580-1591, ISSN 0304-3800, <https://doi.org/10.1016/j.ecolmodel.2010.03.012>

Link, J.S., Marshak, A.R., 2022. *Ecosystem-Based Fisheries Management: Progress, Importance, and Impacts in the United States*. Oxford University Press.

Lisovenko L.A., Andrianov D.P. Reproductive biology of anchovy (*Engraulis encrasicolus ponticus* Alexandrov 1927) in the Black Sea. *Scientia Marina* 1996; 60: 209-218.

Ludwig, W. et al. (2009) ‘River discharges of water and nutrients to the Mediterranean and Black Sea: Major drivers for ecosystem changes during past and future decades?’ *Progress in Oceanography*, 80(3-4), pp.199-217. doi:10.1016/j.pocean.2009.02.001



<b>Project</b>	NECCTON No 101081273	<b>Deliverable</b>	D7.2
<b>Dissemination</b>	Public	<b>Nature</b>	Report
<b>Date</b>	14/10/2025	<b>Version</b>	1.0

Mackinson S. and Daskalov G. (2007) An ecosystem model of the North Sea for use in research supporting the ecosystem approach to fisheries management: Description and parameterisation. Cefas Science Series Technical Report, pp 142

McEvoy, A. J., Atkinson, A., Airs, R. L., Brittain, R., Brown, I., Fileman, E. S., ... & Widdicombe, S. (2023). The Western Channel Observatory: a century of physical, chemical and biological data compiled from pelagic and benthic habitats in the western English Channel. *Earth System Science Data*, 15(12), 5701-5737.

Menu, C. 2024. Population dynamics and evolution of biological traits of anchovy and sardine in the Bay of Biscay : a coupled DEB-IBM approach. Université de Bretagne occidentale, Brest, PhD Thesis.

Menu, C. Pecquerie, L., Bacher, C., Doray, M., Hattab, T., van der Kooij J. and Huret M. 2023. Testing the bottom-up hypothesis for the decline in size of anchovy and sardine across european waters through a bioenergetic modeling approach. *Progress in Oceanography*, 210:102943.

Morell, A., Shin, Y. J., Barrier, N., Travers-Trolet, M., & Ernande, B. (2023b). Ev-OSMOSE: An eco-genetic marine ecosystem model. *BioRxiv*.

Morell, A., Shin, Y. J., Barrier, N., Travers-Trolet, M., Halouani, G., & Ernande, B. (2023a). Bioen-OSMOSE: A bioenergetic marine ecosystem model with physiological response to temperature and oxygen. *Progress in Oceanography*, 216, 103064.

Morello E.B. , Frogli C. , Atkinson R.J.A. , Moore P.G. (2005). Hydraulic dredge discards of the clam (*Chamelea gallina*) fishery in the western Adriatic Sea, Italy. *Fisheries Research*, 76, 3, 430-444, ISSN 0165-7836, <https://doi.org/10.1016/j.fishres.2005.07.002>

Motos L., Uriarte A., Valencia V. (1996). The spawning environment of the Bay of Biscay anchovy (*Engraulis encrasicolus* L.). *Scientia Marina.*, 60 (Supl. 2): 117-140

Müller, C.L., Ofenbeck, G., Baumgartner, B., Sbalzarini, I.F. 2010. pCMALib - Manual for version 1.0.

Nguyen, H. T. T., Daewel, U., Banas, N., and Schrum, C.: Parameterisation toolbox for physical-biogeochemical model compatible with FABM. Case study: the coupled 1D GOTM-ECOSMO E2E for the Sylt-Romo Bight, North Sea, *EGUsphere* [preprint], <https://doi.org/10.5194/egusphere-2024-2710> , 2024.

Nicol S., Lehodey P., Senina I., Bromhead D., Frommel A.Y., Hampton J., Havenhand J., Margulies D., Munday P.L., Scholey V., Williamson J.E. and Smith N. (2022). Ocean Futures for the World's Largest Yellowfin Tuna Population Under the Combined Effects of Ocean Warming and Acidification. *Front. Mar. Sci.* 9:816772. doi:10.3389/fmars.2022.816772, <https://www.frontiersin.org/articles/10.3389/fmars.2022.816772/full>

Niermann U., Bingel F., Gorban A., et al. Distribution of anchovy eggs and larvae (*Engraulis encrasicolus* Cuv.) in the Black Sea in 1991–1992. *ICES Journal of Marine Science* 1994; 51: 395-406. <https://doi.org/10.1006/jmsc.1994.1041>

Oddo, P., Adani, M., Pinardi, N., Fratianni, C., Tonani, M., and Pettenuzzo, D.: A nested Atlantic-Mediterranean Sea general circulation model for operational forecasting, *Ocean Sci.*, 5, 461–473, <https://doi.org/10.5194/os-5-461-2009> , 2009.

Oguz T., Salihoglu B., Fach B. A coupled plankton–anchovy population dynamics model assessing nonlinear controls of anchovy and gelatinous biomass in the Black Sea. *Marine Ecology Progress Series* 2008; 369: 229-256.

<b>Project</b>	NECCTON No 101081273	<b>Deliverable</b>	D7.2
<b>Dissemination</b>	Public	<b>Nature</b>	Report
<b>Date</b>	14/10/2025	<b>Version</b>	1.0

Olafsdottir, A. H., Utne, K. R., Jacobsen, J. A., Jansen, T., Óskarsson, G. J., Nøttestad, L., Elvarsson, B., Broms, C., & Slotte, A. (2019). Geographical expansion of Northeast Atlantic mackerel (*Scomber scombrus*) in the Nordic Seas from 2007 to 2016 was primarily driven by stock size and constrained by low temperatures. *Deep-Sea Research Part II: Topical Studies in Oceanography*, 159, 152–168. <https://doi.org/10.1016/j.dsr2.2018.05.023>

Ospina-Álvarez, A., Palomera, I., Parada, C., 2012. Changes in egg buoyancy during development and its effects on the vertical distribution of anchovy eggs. *Fish. Res.* 117-118, 86–95. doi:10.1016/j.fishres.2011.01.030 .

Panov B., Chashchin A. Aspects of the water structure dynamics in the southeastern Black Sea as prerequisites for the formation of winter aggregations of Black Sea anchovy off the coast of Georgia. *Oceanology* 1990; 30: 242-247.

Panzeri, D., Libralato, S., Carlucci, R., Cipriano, G., Bitetto, I., Spedicato, M.T., Masnadi, F., Ricci, P., Scarcella, G., Russo, T. and Zupa, W., 2021, October. Defining a procedure for integrating multiple oceanographic variables in ensemble models of marine species distribution. In 2021 International Workshop on Metrology for the Sea; Learning to Measure Sea Health Parameters (MetroSea) (pp. 360-365). IEEE.

Panzeri, D., Russo, T., Arneri, E., Carlucci, R., Cossarini, G., Isajlović, I., Krstulović Šifner, S., Manfredi, C., Masnadi, F., Reale, M., Scarcella, G., Solidoro, C., Spedicato, M. T., Vrgoč, N., Zupa, W., & Libralato, S. (2024). Identifying priority areas for spatial management of mixed fisheries using ensemble of multi-species distribution models. *Fish and Fisheries*, 25, 187–204. <https://doi.org/10.1111/faf.12802>

Pauly, D., Christensen, V. Primary production required to sustain global fisheries. *Nature* **374**, 255–257 (1995). <https://doi.org/10.1038/374255a0>

Pérez-Jorge, S., Tobeña, M., Prieto, R., et al. (2020). Environmental drivers of large-scale movements of baleen whales in the mid-North Atlantic Ocean. *Diversity and Distributions*, 26(8), 1013–1032. <https://doi.org/10.1111/ddi.13038>

Pethybridge H., Roos D., Loizeau V., et al. Responses of European anchovy vital rates and population growth to environmental fluctuations: An individual-based modeling approach. *Ecological Modelling* 2013; 250: 370-383. <https://doi.org/https://doi.org/10.1016/j.ecolmodel.2012.11.017>

Petrik, Colleen M., Charles A. Stock, Ken H. Andersen, P. Daniël van Denderen, and James R. Watson. 2019. “Bottom-up Drivers of Global Patterns of Demersal, Forage, and Pelagic Fishes.” *Progress in Oceanography* 176:102124.

Pinti, J., T. DeVries, T. Norin, C. Serra-Pompei, R. Proud, D.A. Siegel, A.W. Visser 2021. Metazoans, migrations, and the ocean’s biological carbon pump BioRxiv. <https://scholar.archive.org/work/vzsaz2iqmzgkdpikzivexe5gpe/access/wayback/https://www.biorxiv.org/content/biorxiv/early/2021/03/22/2021.03.22.436489.full.pdf>

Piroddi, C., Akoglu, E., Andonegi, E., et al., 2021. Effects of nutrient management scenarios on marine food webs: A pan-European assessment in support of the marine strategy framework directive. *Front. Mar. Sci.* 8. <https://doi.org/10.3389/fmars.2021.596797>

Piroddi, C., Bearzi, G., Christensen, V. (2010). Effects of local fisheries and ocean productivity on the northeastern Ionian Sea ecosystem. *Ecol. Model.*, 221:1526–1544.

<b>Project</b>	NECCON No 101081273	<b>Deliverable</b>	D7.2
<b>Dissemination</b>	Public	<b>Nature</b>	Report
<b>Date</b>	14/10/2025	<b>Version</b>	1.0

Planque B., Bellier E., Lazure P. (2007). Modelling potential spawning habitat of sardine (*Sardina pilchardus*) and anchovy (*Engraulis encrasicolus*) in the Bay of Biscay. *Fish. Oceanog.* 16, Issue 1: <http://dx.doi.org/10.1111/j.1365-2419.2006.00411.x>

Politikos D., Huret M., Petitgas P. 2015. A coupled movement and bioenergetics model to explore the spawning migration of anchovy in the Bay of Biscay. *Ecological Modelling* , 313, 212-222. <https://doi.org/10.1016/j.ecolmodel.2015.06.036>

Politikos, D., Somarakis, S., Tsiaras, K.P., Giannoulaki, M., Petihakis, G., *et al.* 2015. Simulating anchovy's full life cycle in the northern Aegean Sea (eastern Mediterranean): A coupled hydro-biogeochemical-IBM model. *Progress in Oceanography*, 138: 399-416.

Powley, H.R., Millington, R., Artioli, Y., Wilson, R.J., Bruggeman J., (in review) Challenging One-Way Fish Modelling: Two-Way Coupling Reveals Critical Marine Ecosystem Dynamics. *Progress in Oceanography*

Proud, P., N.O. Handegard, R.J. Kloser, M.J. Cox, A.S. Brierley, 2019. From siphonophores to deep scattering layers: uncertainty ranges for the estimation of global mesopelagic fish biomass. *ICES Journal of Marine Science*, 76 (3) (2019), pp. 718-733. doi:10.1093/icesjms/fsy037

Raicevich, S. 2008. Discard in the Northern Adriatic Sea multi-gear fishing activities: ecological consequences and implications for mitigation strategies. Presented at “Workshop on discards organized by DGMARE”, Brussels, 27–28 May 2008.

Ricci, P., Serpetti, N., Cascione, D., Cipriano, G., D’Onghia, G., de Padova, D., Fanizza, C., Ingrosso, M., Carlucci, R. (2023). Investigating fishery and climate change effects on the conservation status of odontocetes in the Northern Ionian Sea (Central Mediterranean Sea). *Ecological Modelling*, 485. <https://doi.org/10.1016/j.ecolmodel.2023.110500>

Romagosa, M., Lucas, C., Pérez-Jorge, S., et al. (2019). Differences in regional oceanography and prey biomass influence the presence of foraging odontocetes at two Atlantic seamounts. *Marine Ecology Progress Series*, 617, 155–170. DOI: 10.1111/mms.12626

Rose K.A., Cowan Jr J.H., Winemiller K.O., et al. Compensatory density dependence in fish populations: importance, controversy, understanding and prognosis. *Fish and Fisheries* 2001; 2: 293-327. <https://doi.org/https://doi.org/10.1046/j.1467-2960.2001.00056.x>

Rose K.A., Fiechter J., Curchitser E.N., et al. Demonstration of a fully-coupled end-to-end model for small pelagic fish using sardine and anchovy in the California Current. *Progress in Oceanography* 2015; 138: 348-380. <https://doi.org/https://doi.org/10.1016/j.pocean.2015.01.012>

Scheffer, M., Baveco, J.M., DeAngelis, D.L., Rose, K.A. and van Nes, E., 1995. Super-individuals a simple solution for modelling large populations on an individual basis. *Ecological modelling*, 80(2-3), pp.161-170. [https://doi.org/10.1016/0304-3800\(94\)00055-M](https://doi.org/10.1016/0304-3800(94)00055-M)

Scott, F., Blanchard, J. L., & Andersen, K. H. (2014). mizer: An R package for multispecies, trait-based and community size spectrum ecological modelling. *Methods in Ecology and Evolution*, 5(10), 1121–1125. <https://doi.org/10.1111/2041-210X.12256>

Senina I., Lehodey P., Hampton J., Sibert J. (2020). Quantitative modeling of the spatial dynamics of South Pacific and Atlantic albacore tuna populations. *Deep Sea Res.* 175, 104667 <https://doi.org/10.1016/j.dsr2.2019.104667>

<b>Project</b>	NECCON No 101081273	<b>Deliverable</b>	D7.2
<b>Dissemination</b>	Public	<b>Nature</b>	Report
<b>Date</b>	14/10/2025	<b>Version</b>	1.0

Senina I., Lehodey P., Sibert J., Hampton J., (2021) Integrating tagging and fisheries data into a spatial population dynamics model to improve its predictive skills. *Canadian Journal of Aquatic and Fisheries Sciences*, 77(3): 576-593, <https://doi.org/10.1139/cjfas-2018-0470>

Senina I., Sibert J., Lehodey P. (2008). Parameter estimation for basin-scale ecosystem-linked population models of large pelagic predators: application to skipjack tuna. *Progress in Oceanography*, 78: 319-335. <https://doi.org/10.1016/j.pocean.2008.06.003>

Shin, Y.-J., Cury, P., 2001. Exploring fish community dynamics through size-dependent trophic interactions using a spatialized individual-based model. *Aquatic Living Resources* 14, 65–80.

Shin, Y.-J., Cury, P., 2004. Using an individual-based model of fish assemblages to study the response of size spectra to changes in fishing. *Can. J. Fish. Aquat. Sci.* 61, 414–431.

Sillero, N., Arenas-Castro, S., Enriquez-Urzelai, U., Vale, C. G., Sousa-Guedes, D., Martínez-Freiría, F., Real, R., & Barbosa, A. M. (2021). Want to model a species niche? A step-by-step guideline on correlative ecological niche modelling. *Ecological Modelling*, 456, 109671. <https://doi.org/10.1016/j.ecolmodel.2021.109671>

Spedicato, M.T., Massutí, E., Mérigot, B., Tserpes, G., Jadaud, A. and Relini, G., 2019. The MEDITS trawl survey specifications in an ecosystem approach to fishery management. *Sci. Mar*, 83(S1), pp.9-20.

Steenbeek, J (2024) DOI: 10.5821/dissertation-2117-417801

Steenbeek, J., Buszowski, J., Christensen, V., Akoglu, E., Aydin, K., Ellis, N., Felinto, D., Guitton, J., Lucey, S., Kearney, K., Mackinson, S., Pan, M., Platts, M., Walters, C., 2016. Ecopath with Ecosim as a model-building toolbox: Source code capabilities, extensions, and variations. *Ecol. Model.* 319, 178–189.

Stratoudakis, Y., Coombs, S., Lanzas, A. L. de, Halliday, N., Costas, G., Caneco, B., Franco, C., Conway, D., Santos, M. B., Silva, A., and Bernal, M. 2007. Sardine (*Sardina pilchardus*) spawning seasonality in European waters of the northeast Atlantic. *Marine Biology* 152.1, pp. 201–212. doi : 10.1007/s00227-007-0674-4.

Taylan B, Bayhan B. Reproductive biology of the European anchovy *Engraulis encrasicolus* (Linnaeus, 1758) in the Turkish Aegean Sea. *Oceanological and Hydrobiological Studies* 2024; 53: 7-15. <https://doi.org/10.26881/oahs-2024.1.02>

Thorson, J.T., Anderson, S.C., Goddard, P. and Rooper, C.N., 2025. tinyVAST: R Package With an Expressive Interface to Specify Lagged and Simultaneous Effects in Multivariate Spatio-Temporal Models. *Global Ecology and Biogeography*, 34(4), p.e70035.

Tittensor, D. P., Eddy, T. D., Lotze, H. K., Galbraith, E. D., Cheung, W., Barange, M., Blanchard, J. L., Bopp, L., Bryndum-Buchholz, A., Büchner, M., Bulman, C. M., Carozza, D. A., Christensen, V., Coll, M., Dunne, J. P., Fernandes, J. A., Fulton, E. A., Hobday, A. J., Huber, V., Jennings, S., Jones, M. C., Lehodey, P., Link, J. S., Mackinson, S., Maury, O., Niiranen, S., Oliveros-Ramos, R., Roy, T., Schewe, J., Shin, Y.-J., Silva, T., Stock, C. A., Steenbeek, J., Underwood, P. J., Volkholz, J., Watson, J. R., Walter, N. D. (2018). A protocol for the intercomparison of marine fishery and ecosystem models: Fish-MIP v1.0. *Geosci. Model Dev.*, 11: 1421-1442.

Travers, M., Shin, Y.-J., Jennings, S., Machu, E., Huggett, J.A., Field, J.G., Cury, P.M., 2009. Two-way coupling versus one-way forcing of plankton and fish models to predict ecosystem changes in the Benguela. *Ecological Modelling*, 220, 3089–3099.

<b>Project</b>	NECCTON No 101081273	<b>Deliverable</b>	D7.2
<b>Dissemination</b>	Public	<b>Nature</b>	Report
<b>Date</b>	14/10/2025	<b>Version</b>	1.0

Travers, M., Shin, Y.-J., Jennings, S., Machu, E., Huggett, J.A., Field, J.G., Cury, P.M., 2009. Two-way coupling versus one-way forcing of plankton and fish models to predict ecosystem changes in the Benguela. *Ecological Modelling* 220, 3089–3099. <https://doi.org/10.1016/j.ecolmodel.2009.08.016>

Trenkel, V. M., Huse, G., MacKenzie, B. R., Alvarez, P., Arrizabalaga, H., Castonguay, M., Goñi, N., Grégoire, F., Hátún, H., Jansen, T., Jacobsen, J. A., Lehodey, P., Lutcavage, M., Mariani, P., Melvin, G. D., Neilson, J. D., Nøttestad, L., Óskarsson, G. J., Payne, M. R., ... Speirs, D. C. (2014). Comparative ecology of widely distributed pelagic fish species in the North Atlantic: Implications for modelling climate and fisheries impacts. *Progress in Oceanography*, 129(PB), 219–243. <https://doi.org/10.1016/j.pocean.2014.04.030>

Trenkel V. et al (2023). D7.1 “Technical specification of the HTL products”. Report of the Horizon Europe NECCTON project (grant 101081273). DOI: 10.5281/zenodo.10057558

Van Denderen, P. D., N. Jacobsen, K. H. Andersen, J. L. Blanchard, C. Novaglio, C. A. Stock, and C. M. Petrik. 2024. “Estimating Fishing Exploitation Rates to Simulate Global Catches and Biomass Changes of Pelagic and Demersal Fish.” *Earth’s Future* 12 (10). <https://doi.org/10.1029/2024ef004604>

Vijayakumaran, V., Daewel, U., Millington, R., Bruggeman, J., Powley, H., Lessin, G., Lindenthal, A., and Schrum, C.: The effect of coupling higher trophic level modules on the dynamics of three models of lower trophic level , EGU General Assembly 2025, Vienna, Austria, 27 Apr–2 May 2025, EGU25-7123, <https://doi.org/10.5194/egusphere-egu25-7123> , 2025.

Visser, A., 1997. Using random walk models to simulate the vertical distribution of particles in a turbulent water column. *Marine Ecology Progress Series* 158, 275–281

Von Schuckmann, K., Le Traon, P.Y., Smith, N., Pascual, A., Djavidnia, S., Gattuso, J.P., Grégoire, M., Aaboe, S., Alari, V., Alexander, B.E. and Alonso-Martirena, A., 2021. Copernicus marine service ocean state report, issue 5. *Journal of Operational Oceanography*, 14(sup1), pp.1-185.

Walters, C., 2000. Impacts of dispersal, ecological interactions, and fishing effort dynamics on efficacy of marine protected areas: how large should protected areas be? *Bulletin of Marine Science* 66, 745–757.

Watkins KS, Rose KA. Simulating individual-based movement in dynamic environments. *Ecological Modelling* 2017; 356: 59-72. <https://doi.org/https://doi.org/10.1016/j.ecolmodel.2017.03.025>

Wilson, R. J., Kay, S., Fernandes, J. A., et al. (2021). Large projected reductions in marine fish biomass for Kenya and Tanzania in the absence of climate mitigation. *Ocean & Coastal Management*, 215, 105921. <https://doi.org/10.1016/j.ocecoaman.2021.105921>

Yumruktepe, V. Ç., Samuelsen, A., & Daewel, U. (2022). ECOSMO II(CHL): a marine biogeochemical model for the North Atlantic and the Arctic. *Geosci. Model Dev.*, 15(9), 3901-3921. doi:10.5194/gmd-15-3901-2022

Zhao, Yixin, Daniel van Denderen, Rémy Denéchère, Jonathan E. Falciani, Nis Sand Jacobsen, Themistoklis Konstantinopoulos, Daniel Ottmann, Colleen M. Petrik, Karline Soetaert, and Charles A. Stock. 2025. “FEISTY Fortran Library and R Package to Integrate Fish and Fisheries with Biogeochemical Models.” *Methods in Ecology and Evolution* 16 (1): 40–48.